



HAL
open science

Effect of process operational factors on *Chlorella vulgaris* biofilms : from cell mechanisms to process optimization

Sufang Li

► To cite this version:

Sufang Li. Effect of process operational factors on *Chlorella vulgaris* biofilms : from cell mechanisms to process optimization. Chemical and Process Engineering. Université Paris-Saclay, 2022. English. NNT : 2022UPAST005 . tel-03596436

HAL Id: tel-03596436

<https://theses.hal.science/tel-03596436v1>

Submitted on 3 Mar 2022

HAL is a multi-disciplinary open access archive for the deposit and dissemination of scientific research documents, whether they are published or not. The documents may come from teaching and research institutions in France or abroad, or from public or private research centers.

L'archive ouverte pluridisciplinaire **HAL**, est destinée au dépôt et à la diffusion de documents scientifiques de niveau recherche, publiés ou non, émanant des établissements d'enseignement et de recherche français ou étrangers, des laboratoires publics ou privés.

Effect of process operational factors on
Chlorella vulgaris biofilms: from cell
mechanisms to process optimization

Thèse de doctorat de l'université Paris-Saclay

Préparée à CentraleSupélec

École doctorale n° 579, sciences mécaniques et énergétiques, matériaux
et géosciences (SMEMAG)

Spécialité de doctorat : Génie des procédés

**Thèse présentée et soutenue à Gif-Sur-Yvette, le
20 Janvier 2022, par**

Sufang LI

Composition du Jury

M. Antoine SCIANDRA

Directeur de recherche,
Laboratoire d'Océanographie de Villefranche,
Sorbonne Universités, CNRS

Rapporteur

M. Olivier BERNARD

Directeur de recherche, INRIA Sophia Antipolis

Rapporteur

M. Gaël BOUGARAN

Directeur de recherche,
IFREMER-PBA

Examineur

M. Romain BRIANDET

Directeur de recherche,
Micalis Institute, Inra, AgroParisTech,
Université Paris-Saclay

Président

Direction de la thèse

Mme Filipa LOPES

Professeur, Université Paris-Saclay
GS Sciences de l'ingénierie et des systèmes

Directrice de thèse

M. Andrea FANESI

Post doctorant, Université Paris-Saclay
GS Sciences de l'ingénierie et des systèmes

Co-Encadrant de thèse

Titre : Effet des facteurs opératoires du procédé sur les biofilms de *Chlorella vulgaris* : des mécanismes cellulaires à l'optimisation des procédés

Mots clés : Acclimatation, Biofilm, *Chlorella vulgaris*, Croissance, Facteurs opératoires, Propriétés physiologiques

Résumé : La technologie de culture de microalgues sous forme de biofilm est présentée aujourd'hui comme une alternative prometteuse à la culture en suspension. Cependant, une meilleure compréhension de l'impact des facteurs opératoires du procédé sur le développement du biofilm et sur la productivité du système de culture est nécessaire pour confirmer pleinement le potentiel de cette technologie pour la production de biomasse/composés d'intérêt à grande échelle. Cela permettra d'identifier des facteurs limitants/inhibiteurs, d'optimiser ce type de procédés, et apportera également de nouvelles connaissances sur le comportement des cellules immobilisées, qui reste encore mal compris.

L'objectif de cette thèse est d'évaluer l'effet des facteurs opératoires tels que la lumière, le type de support et l'inoculum sur la croissance du biofilm, la productivité et la physiologie des cellules sessiles. Pour ce faire, *C. vulgaris* a été immobilisé sur des matériaux poreux comprenant des supports en tissu et des membranes. Le comportement des cellules immobilisées (croissance, composition, activité photosynthétique) a été étudié dans différentes conditions d'intensité lumineuse, de matériaux et de densité d'inoculum/physiologie. Les résultats montrent que les cellules se sont acclimatées en seulement 3 jours pour un biofilm développé dans un réacteur continu. Cependant, des productivités faibles ont été obtenues, ce qui peut être lié à un détachement élevé ou aux propriétés du support en coton. Par conséquent, la capacité de rétention cellulaire de cinq tissus a été testée par la suite afin de trouver des supports prometteurs. Le matériau Terrazzo avec la plus petite taille de pores et

la plus faible densité des mailles (micro-texture) a présenté la capacité de rétention la plus élevée, ce qui en fait ainsi un support prometteur pour la culture à grande échelle. La distribution des cellules immobilisées sur les tissus, le développement et l'activité du biofilm se sont avérés fortement affectés par le type de support. De plus, un autre système de culture, où les cellules sont immobilisées sur une membrane, a été utilisé par la suite pour étudier l'effet combiné de l'intensité lumineuse et de la densité de l'inoculum sur le développement du biofilm dans des conditions plus contrôlées. Les résultats ont montré qu'une densité d'inoculum élevée sur les supports (tissus et membranes) affecte négativement la productivité, ce qui peut être lié à une limitation de la lumière et des nutriments. Des conditions combinées de lumière et de densité de l'inoculum favorisant la production de biomasse ou de lipides ont également été identifiées. Par ailleurs, les résultats montrent que l'acclimatation de l'inoculum à 350 et 500 $\mu\text{mol m}^{-2} \text{s}^{-1}$ a bénéficié à la production de biomasse et a évité le mécanisme de photo-inhibition, respectivement. Cela suggère l'importance de prendre en compte la photo-acclimatation des cultures dans la conduite des technologies à biofilm. Enfin, pour la première fois, le processus d'acclimatation des cellules passant de l'état planctonique à l'état immobilisé a été étudié : au cours des premières heures, les cellules ont augmenté leur taille, accumulant des glucides et diminuant leur teneur en Chl *a*. Il est très probable que ce comportement soit lié à un changement au niveau des conditions environnementales, permettant aux cellules de s'acclimater au nouveau mode de vie sous forme sessile.

Title: Effect of process operational factors on *Chlorella vulgaris* biofilms: from cell mechanisms to process optimization

Keywords: Acclimation, Biofilm, *Chlorella vulgaris*, Growth, Process operational factors, Physiological properties

Abstract: Microalgae biofilm-based technology has been pointed out as a promising alternative to suspended cells cultivation. However, a better understanding of the impact of process operational factors on biofilm development and productivity is actually needed to fully confirm the potential of biofilm-based processes for biomass/compounds production at large-scale. This will help identifying stressful factors and optimizing this kind of processes, and it will also provide new knowledge on immobilized cell behavior, which remains poorly understood.

The aim of this thesis is to assess the effect of operational factors like light, support and inoculum on growth, productivity, and physiological properties of sessile cells during biofilm development. To do so, *C. vulgaris* was immobilized on porous materials including fabric supports and membranes. Immobilized cell behavior (growth, composition, photosynthetic activity) was investigated under different conditions of light intensity, supports and inoculum density /physiology. In a continuously submerged reactor, cells acclimated within only 3 days to the new biofilm lifestyle. Low productivities were though obtained, which may be related to high detachment or support properties. Consequently, cell retention capability on five fabrics was tested afterwards in order to find promising supports. Accordingly, Terrazzo with the smallest pore size and mesh density exhibited the highest

cell retention capability, representing thus a potential support for large-scale biofilm cultivation. Immobilized cells distribution on fabrics, biofilm development and activity were found to be strongly affected by the support material. Another biofilm-based system (perfused system) where cells are immobilized on a membrane was then used to study the combined effect of light intensity and inoculum density on biofilm development under more controlled conditions. Results showed that high cell density affects negatively the productivity on fabrics and membranes which may be linked to limitation in light and nutrients. Combined conditions of light and cell density which promote either biomass or lipids production were also identified. Inoculum acclimation to 350 and 500 $\mu\text{mol m}^{-2} \text{s}^{-1}$ benefited biomass production and avoided photo-inhibition, respectively, suggesting the importance of considering photo-acclimation on biofilm-based systems set-up. For the first time, the acclimation process of cells switching from planktonic to the immobilized state was lastly studied. Unexpectedly, within the first hours, cells increased their size, accumulating carbohydrates, and decreasing the Chl *a* content. It is likely that changes in environmental conditions trigger this behaviour, allowing the cells to acclimate to the new lifestyle.

Acknowledgements

This 3-year studying life in France brings me precious wealth and I will remember this special period forever wherever I am in the future. This thesis is a long-long journey but full of encouragements and cares. It wouldn't have been completed without the supports from my dear supervisors, family and friends.

First of all, I want to deeply thank my supervisor, prof. Filipa LOPES. In the past three years, she gave me great guidance from the subject selection, materials preparation, experimental operation, data analysis, to the writing of this thesis. Prof. Filipa LOPES always took time out of her busy schedule to carefully revise my thesis, checking word by word with huge patience. Her rigorous academic researching spirit will inspire me forever. In life, she always makes me feel warm because of her great enthusiasm and considerateness. Herein, I would like to express my deep gratitude to her.

Secondly, I would like to express my most sincere thanks to Dr. Andrea FANESI who has also made great contributions in my work from experimental design to the revision of my thesis. He gave me many valuable guidance and suggestions in my study and routine life. It is my greatest luck to meet him on the academic road.

I'm also grateful to Thierry MARTIN, H el ene SANTIGNY, Cyril BRETON, Nathalie RUSCASSIER, C edric GUERIN and Vincent BUTIN for helping me in the design of systems, medium sterilization, biofilm structure observation, nutrients and CHNS analysis. Their precious work lay the foundation for this thesis. In addition, a very special acknowledgement for Magali DUPUY, thanks for her earnest help in technical support.

Thousands of thanks to my motherland for the financial support. Finally, my parents and my elder brothers, they give me the endless loves. Thanks to them.

General preamble

The manuscript was written using an article-based formatting, and composed of one published submitted article (chapter IV) and additional unpublished information. The articles' title:

- **Biomass production and physiology of *Chlorella vulgaris* during the early stages of immobilized state are affected by light intensity and inoculum cell density.** Su Fang Li, Andrea Fanesi, Thierry Martin, Filipa Lopes. Algal research, Volume 59, July 2021, 102453. <https://doi.org/10.1016/j.algal.2021.102453>
- **Effect of textile supports, inoculum cell density and inoculum physiological properties on the immobilized growth of *Chlorella vulgaris*** (submitted manuscript, part of data from chapter III)

This work was also the subject of a poster communication at a national and international scientific conference:

- **Light and initial cell density affect the physiological transition of *Chlorella vulgaris* from planktonic to immobilized growth** (chapter V). Su Fang Li, Andrea Fanesi, Thierry Martin, Filipa Lopes. (AlgaEurope, 01 – 04, December, 2020)

Résumé en français

Introduction

La crise alimentaire/énergétique et le réchauffement climatique associés à l'augmentation de la population mondiale suscitent des préoccupations considérables. Dans ce contexte, la recherche de ressources alimentaires/énergétiques renouvelables et durables devient un enjeu majeur.

Les microalgues sont des organismes photosynthétiques qui fixent le CO₂ en présence de lumière, en produisant des composés d'intérêt, dont des sucres, des protéines et des lipides. Par conséquent, elles sont aujourd'hui largement reconnues comme une source potentielle de biocarburants, de biomasse pour l'alimentation humaine et animale, et de produits à haute-valeur ajoutée pour la cosmétique et l'industrie pharmaceutique.

Les systèmes de culture en suspension sont largement utilisés pour la culture de microalgues pour la production de biomasse et de biocarburants, pour le traitement des eaux usées et la capture du CO₂. Cependant, les coûts de production élevés, notamment associés à une forte consommation énergétique, constituent une entrave à l'utilisation industrielle des cultures à microalgues. Récemment, la technologie de culture sous forme de biofilm a suscité un grand intérêt en raison d'une productivité plus importante, d'une utilisation moindre d'énergie et d'eau, et d'une récolte plus efficace par rapport aux systèmes classiques.

Un biofilm est un assemblage de microorganismes associés à une surface et insérés dans une matrice de substances polymériques (EPS). Des nombreux facteurs affectent le développement des biofilms de microalgues, entre autres, la disponibilité de la lumière/des nutriments, le pH, la température, l'espèce, la densité cellulaire de l'inoculum, le design du photobioréacteur et la fréquence de la récolte. La plupart de ces paramètres de culture peuvent être contrôlés ; ils sont par conséquent nommés facteurs opératoires du procédé dans cette thèse.

Plusieurs études ont été menées pour évaluer l'effet de ces facteurs sur le développement du biofilm et la productivité du système de culture. Cependant, une étude approfondie permettant de lier le comportement des cellules dans le biofilm à la productivité du système reste à faire.

Parmi les facteurs opératoires, la lumière est un paramètre majeur. Des nombreuses études ont élucidé l'effet de l'intensité de la lumière sur la croissance des microalgues en suspension. Cependant, contrairement aux cellules en suspension qui sont cultivées dans un microenvironnement relativement stable et homogène (en milieu à faible concentration cellulaire), les cellules sessiles (immobilisées) des biofilms peuvent être exposées à des conditions de culture assez différentes en raison de l'atténuation de la lumière et des gradients de concentration en nutriments, en particulier pour celles cultivées dans un biofilm épais/mature. Comme attendu, certaines études ont confirmé que l'intensité de la lumière diminue fortement en profondeur en raison du phénomène de photo-ombrage. Par conséquent, afin de mieux évaluer l'effet de l'intensité de la lumière sur le développement des biofilms photosynthétiques, différentes densités cellulaires initiales peuvent être utilisées afin de simuler des biofilms avec différentes épaisseurs ou à différentes phases de formation.

A notre connaissance, l'effet combiné de la lumière et de la densité de l'inoculum sur le développement des biofilms de microalgues a rarement été discuté. D'autre part, il a été largement démontré que le support affecte l'attachement des cellules en raison de leurs propriétés physico-chimiques dont la micro-texture, affectant par conséquent la densité de l'inoculum et ainsi la productivité globale. Par conséquent, l'inoculum en tant que facteur opératoire a également été étudié dans cette thèse.

Plus précisément, **trois facteurs opératoires** : l'intensité lumineuse, l'inoculum et le type de support ont été sélectionnés dans ce travail afin de comprendre comment ces facteurs affectent la croissance et la productivité des biofilms de *C. vulgaris*. De plus, la physiologie des cellules immobilisées (morphologie, activité photosynthétique, composition), qui est rarement étudiée, a également été caractérisée. Cela aidera à mieux comprendre les mécanismes associés à la formation du biofilm, et en particulier ceux d'acclimatation des cellules sessiles. Il s'agit également à identifier en amont les paramètres inhibiteurs, en aidant les opérateurs à faire des choix opératoires raisonnés pour maximiser les productions de biomasse et de composés d'intérêt.

Objectifs

Les objectifs généraux de cette thèse sont les suivants :

1. Évaluer l'effet des facteurs opératoires, intensité de lumière, densité/propriétés physiologiques de l'inoculum et type de support sur le développement du biofilm de *C. vulgaris*. Pour ce faire, la croissance du biofilm, sa composition chimique et son activité photosynthétique ont été suivies. L'objectif est également d'identifier les paramètres qui impactent négativement la productivité à un stade précoce du développement du biofilm. Cela permettrait à un opérateur de réagir rapidement en changeant les conditions de culture afin de maximiser la productivité.

2. Identifier et comprendre la réponse des cellules immobilisées aux différentes conditions de culture testées et en particulier, décrire les mécanismes d'acclimatation des cellules sessiles. Décrire la transition physiologique de l'état planctonique à l'état immobilisé. Enfin, il s'agit de mieux appréhender les mécanismes impliqués dans la formation du biofilm.

3. Sélectionner des supports prometteurs qui pourront être testés par la suite dans des systèmes de culture à biofilm à l'échelle pilote.

Méthodologie

Afin d'évaluer l'effet des facteurs opératoires sur le développement des biofilms de *C. vulgaris*, des suspensions cellulaires ont été inoculées sur différents types de supports (tissus et membranes), à différentes concentrations initiales (inoculum) puis exposées à des intensités lumineuses variées. La croissance des biofilms de microalgues et la productivité ont été évaluées par la suite. La physiologie des cellules (morphologie, activité photosynthétique, composition) a été également déterminée.

La croissance et la productivité du biofilm ont été évaluées par comptage cellulaire (cytométrie en flux) et/ou par la détermination du poids sec. La taille des cellules, la distribution des cellules et du biofilm sur les supports et la micro-texture des derniers ont été évalués à l'aide des outils d'imagerie (microscopie optique, microscopie confocale à balayage laser, CLSM, microscopie électronique à balayage environnemental, ESEM, tomographie optique, OCT). Les propriétés physico-chimiques des supports ont été mesurées, entre autres, en utilisant la spectroscopie FTIR (Fourier Transform InfraRed) et la microscopie. L'activité photosynthétique des cellules planctoniques et sessiles a été déterminée avec un fluoromètre portable (PAM). Enfin, la composition biochimique, y compris la teneur en Chl *a*, carbone et en azote, ainsi que les pools relatifs de carbohydrates

et lipides, a été quantifiée avec la spectrométrie visible, l'analyse élémentaire et la spectroscopie FTIR, respectivement.

Principaux résultats et conclusions

La revue bibliographique est présentée dans le **Chapitre I**. Parmi les sujets abordés, le métabolisme algal, les différents types de cultures à microalgues, dont les systèmes à biofilm, et les facteurs impactant le développement des biofilms photosynthétiques sont présentés.

Des nombreuses études ont montré l'intérêt d'utiliser le coton comme support pour la formation des biofilms de microalgues. Par conséquent, dans le **chapitre II**, la dynamique de formation des biofilms de *C. vulgaris* cultivés sur un support en coton a été suivie dans un réacteur continu.

L'effet combiné de l'intensité lumineuse et de la densité/physiologie de l'inoculum sur le développement du biofilm et la physiologie des cellules sessiles (composition chimique) a été évalué. Les biofilms avec une densité cellulaire initiale de 4.54×10^6 cellules cm^{-2} et exposés à $100 \mu\text{mol photons m}^{-2} \text{s}^{-1}$ ont présenté le taux de croissance et la productivité en biomasse ($0.65 \text{ g m}^{-2} \text{d}^{-1}$) les plus élevés. Cependant, la productivité en biomasse s'est révélée assez faible par rapport à celle d'autres études de la littérature. Des hypothèses ont été ainsi émises pour expliquer ce résultat : entre autres, un fort taux de détachement et une faible concentration en inoculum, peut-être associé aux propriétés du support, auraient pu expliquer ce résultat. Il est également à souligner une réduction de la teneur en Chl *a* entre 1 à 3 jours, suggérant une acclimatation rapide des cellules sessiles. Les résultats de ce chapitre ont démontré que la densité cellulaire de l'inoculum, la physiologie de celui-ci (teneur en chlorophylle *a*) et l'intensité lumineuse affectent fortement la dynamique et la composition du biofilm de *C. vulgaris*. L'acclimatation des cellules sessiles, qui reste très mal connue, a été mise également en évidence

Afin de vérifier l'impact du type de support sur la productivité en biomasse, cinq supports en tissu ont été étudiés en **Chapitre III**. La capacité de rétention cellulaire, leurs propriétés physico-chimiques et leur micro-texture ont été caractérisés dans un premier temps.

Le support Terrazzo, avec la plus petite taille de pore/densité de maille, a présenté la meilleure performance. Ainsi, dans un deuxième temps, le coton (étudié en Chapitre II) et le Terrazzo ont été sélectionnés pour étudier l'interaction cellule/biofilm-support de manière

approfondie, en utilisant différents outils d'imagerie (CLSM, ESEM, OCT). Les résultats suggèrent que la rétention cellulaire plus importante sur le Terrazzo serait liée à sa microtexture (fibres étroitement connectées) et à la chimie de surface (présence de certains groupes fonctionnels qui auraient pu interagir avec la cellule).

Enfin, l'impact du type de support, de la densité de l'inoculum/de ses propriétés physiologiques sur la croissance, l'activité et la composition du biofilm a été étudié. Une réduction significative de la croissance du biofilm avec la densité de l'inoculum a été observée, ce qui a été attribué à la limitation en lumière et/ou nutriments. De plus, les résultats montrent que la pré-acclimatation des cellules de l'inoculum a un impact sur la productivité en biomasse à trois jours. Ce paramètre semble donc important à prendre en compte dans la conduite des systèmes de culture à biofilm. En conclusion, le Terrazzo semble être un support prometteur et son utilisation combiné à celle d'un inoculum de faible densité ($\sim 1.5 \times 10^6$ cells cm^{-2}) et pré-acclimaté à une lumière plutôt élevée ($350 \mu\text{mol m}^{-2} \text{s}^{-1}$), permettrait d'améliorer significativement la culture à biofilm de *C. vulgaris*.

Dans le **Chapitre IV**, un système perfusé (type *Twin-Layer reactor*, voir Chapitre I) a été mis au point pour étudier de manière plus contrôlée l'effet de l'intensité lumineuse et de la densité de l'inoculum sur la croissance, la composition et l'activité du biofilm de *C. vulgaris*. Ici, une membrane en nitrate de cellulose a été choisie comme support pour le développement du biofilm. En effet, la difficulté de récupération de la totalité de la biomasse des tissus de coton et de Terrazzo a été mise en évidence en Chapitre III. Les résultats montrent que, après 3 jours de culture, la photo-limitation a affecté la croissance des biofilms exposés à une faible intensité lumineuse ($50 \mu\text{mol m}^{-2} \text{s}^{-1}$). Des conditions permettant de maximiser la production de biomasse et de lipides ont été déterminées, respectivement : $250 \mu\text{mol m}^{-2} \text{s}^{-1}$, densité d'inoculum faible ($4,8 \times 10^6$ cellules cm^{-2}) ou élevée ($28,8 \times 10^6$ cellules cm^{-2}). De plus, les biofilms cultivés à une intensité lumineuse élevée ($500 \mu\text{mol m}^{-2} \text{s}^{-1}$) ont la plus forte capacité de transport d'électrons ($r\text{ETR}_{\text{max}}$) et la plus faible teneur en chlorophylle, sans que le taux de croissance soit affecté, ce qui pourrait être attribué à un mécanisme d'adaptation pour éviter l'endommagement de la cellule à forte intensité en lumière. Cette étude a permis de mieux comprendre les mécanismes de photosynthèse dans les biofilms de *C. vulgaris*. Ce type d'approche qui évalue la croissance, l'activité et la composition un biofilm, à un stade précoce de son développement, pourra être utilisé dans le contexte de la conduite et l'optimisation des systèmes de culture de microalgues à biofilm.

D'après les chapitres III et IV, il est à remarquer que le processus d'acclimatation de *C. vulgaris* peut affecter le développement du biofilm et la productivité du système. Cependant, à notre connaissance, la manière dont les microalgues planctoniques s'acclimatent à un mode de vie en biofilm n'a jamais été décrite. Par conséquent, dans le **chapitre V**, les changements en termes de concentration cellulaire, morphologie et physiologie ont été suivis au cours de la transition (premières 24 heures) des cellules de l'état planctonique à l'état immobilisé. Cette étude a mis en évidence l'augmentation significative de la taille des cellules, accompagnée de l'augmentation du *pool* relatif de carbohydrates et de la réduction de la teneur en Chl a au cours des 3 à 6 premières heures. Les résultats ont démontré que les microalgues répondent rapidement aux nouvelles conditions environnementales par un ajustement physiologique. De plus, ce comportement semble spécifique aux cellules à l'état immobilisé.

Perspectives

A partir de ce travail, différentes perspectives peuvent être émises et d'autres études portant sur les biofilms photosynthétiques et, en particulier, les cultures de microalgues à biofilm pourront être réalisées pour approfondir nos résultats.

D'autres recherches pourront porter sur :

- L'optimisation d'autres facteurs opératoires comme la qualité de la lumière, l'apport de nutriments, la température, le régime hydrodynamique, le temps de colonisation, etc. (facteurs seules et combinés) dans la production de biofilms ;
- L'identification de supports et des souches permettant d'obtenir de fortes productivités en biomasse/produit ciblé à grande échelle. Dans ce contexte, la méthodologie mise en œuvre dans cette thèse de caractérisation des propriétés du support et de l'inoculum pourra être utilisée.

Par ailleurs, notre approche consistant à suivre la physiologie et l'activité photosynthétique des cellules sessiles permet d'identifier rapidement des facteurs limitants/inhibiteurs de la culture. Elle pourrait ainsi être utilisée pour la conduite du bioprocédé et ainsi aider l'opérateur à adapter/reformuler les conditions de culture. L'approche présentée permettrait d'améliorer la productivité et, ainsi de réduire les coûts de production.

- L'identification du/des facteur(s) déclencheur(s) qui induisent les modifications physiologiques observées dans le Chapitre V. En particulier, la pénétration de la lumière, la concentration en nutriments, ainsi que la disponibilité de l'eau sur la profondeur du biofilm doivent être étudiées. Peu d'études décrivent et discutent les profils de ces paramètres dans les biofilms photosynthétiques, ce qui est en partie dû à la complexité de ces communautés microbiennes. En effet, peu de travaux appliquent des micro-électrodes pour caractériser l'activité photosynthétique *in situ* des biofilms de microalgues (Gieseke et de Beer, 2004 ; Li et al., 2016). L'utilisation de tels outils pourra fournir des nouvelles informations permettant de mieux comprendre les changements physiologiques des cellules de l'état planctonique à celui immobilisé.

- L'utilisation des outils de biologie moléculaires (par exemple, les approches basées sur la génomique et la protéomique) pour vérifier si le quorum sensing est l'un des mécanismes intervenant dans la transition du mode de vie planctonique à celui sessile. Ces outils combinés à d'autres approches chimiques et d'imagerie aideront certainement à élucider les mécanismes biologiques responsables du développement et de l'activité des biofilms photosynthétiques.

Content

Résumé en français	v
List of figures	xvii
List of tables	xxi
Abbreviations	xxiii
Symbols	xxv
General introduction	1
CHAPTER I Literature review	5
A- Overview of microalgae	6
1. Microalgae.....	6
1.1. What are microalgae?	6
1.2. Microalgae mechanism.....	6
1.2.1. Cell cycle	6
1.2.2. Photosynthesis	9
1.2.2.1. Light-dependent reaction and dark reaction	9
1.2.2.2. P-I curve	12
1.2.3. Photo-acclimation.....	13
1.3. Microalgae lifestyle	16
1.3.1. Planktonic and immobilized lifestyle	16
1.3.2. Lifestyle transition.....	17
1.4. Interest of microalgae	18
1.5. Why <i>Chlorella vulgaris</i> ?	21
B- Microalgae cultivation systems	23
2. Suspended cultivation systems	23
1.1. Open systems.....	23
1.2. Closed systems	23
3. Immobilized cultivation systems	25
2.1. Constantly submerged biofilm systems.....	26
2.2. Intermittently submerged biofilm systems	27
2.3. Perfused biofilm system	28
2.4. Other sorted biofilm systems.....	29
4. Advantages of biofilm-based culture systems compared to suspension systems.....	34
C- Process operational factors impacting biofilm development and productivity ...	37
1. Operational factors - Support	37
1.1. Surface micro-texture	38
1.2. Surface roughness.....	40
1.3. Surface hydrophobicity	40
1.4. Chemical composition	41

2.	Operational factors – Microalgae/inoculum	42
2.1.	Inoculum density	42
2.2.	Inoculum/colonization time	43
2.3.	Microalgae species	43
2.4.	Microalgae properties	44
3.	Operational factors - culture conditions control	46
3.1.	Light availability	46
3.2.	Nutrients concentration.....	48
3.3.	Hydrodynamic regime	48
3.4.	CO ₂ supplement.....	49
3.5.	pH	50
4.	Other operational factors	50
5.	Conclusion	51
	Knowledge gap.....	53
	CHAPTER II <i>Chlorella vulgaris</i> biofilm dynamics in a continuous photo-bioreactor	55
	Preamble	56
	Abstract.....	57
1.	Introduction	58
2.	Materials and Methods	61
2.1.	Planktonic culture maintenance.....	61
2.2.	Biofilm inoculation and dynamics.....	63
2.3.	Biomass recovery from the support.....	64
2.4.	Specific growth rate.....	65
2.5.	Biomass productivity.....	65
2.6.	Cellular compounds.....	65
2.7.	Nutrients concentration in the bulk water.....	66
2.8.	Statistical analysis	67
3.	Results and discussion	67
3.1.	Biofilm dynamics	67
3.2.	Biomass productivity.....	70
3.3.	Biofilm chemical composition dynamics	71
4.	Conclusion.....	76
	Supplementary data	79
	CHAPTER III. Effect of textile supports, inoculum cell density and inoculum physiological properties on the immobilized growth of <i>Chlorella vulgaris</i>	85
	Preamble	86
	Abstract.....	88
1.	Introduction	89
2.	Materials and Methods	90
2.1.	Planktonic culture maintenance.....	90
2.2.	Microalgae inoculation.....	91

2.3. Selection of textile supports	92
2.4. Immobilization and growth of <i>C. vulgaris</i> on two textile supports (Cotton and Terrazzo).....	93
2.5. Relative biomass increase and cell areal density on textile supports and percentage of unattached biomass	93
2.6. Micro-texture and physical-chemical properties of textile supports	94
2.6.1. Mesh size and mesh areal density	94
2.6.2. Roughness of surface.....	95
2.6.3. Hydrophobicity.....	95
2.6.3. Chemical properties (FTIR spectroscopy).....	95
2.7. Physiological characterization of pre-acclimated cells and sessile cells.....	95
2.7.1. Cell morphology	95
2.7.2. Variable chlorophyll <i>a</i> fluorescence measurements and relative electron transport rate (rETR) estimation.....	96
2.7.3. Cellular composition: Chlorophyll <i>a</i> and macromolecules	96
2.8. Biofilm imaging.....	96
3. Results and discussion.....	97
3.1. Support selection for microalgae immobilized growth	98
3.2. Understanding the interaction between Terrazzo/Cotton and <i>C. vulgaris</i> at different scales.....	101
3.3. Does the support and inoculum density affect sessile cells growth, activity, composition and biofilm productivity?	106
3.4. Does the light history of inoculum cells affect biofilm growth and productivity?.	109
4. Conclusions	112
Supplementary data	115
CHAPTER IV. Biomass production and physiology of <i>Chlorella vulgaris</i> during the early stages of immobilized state are affected by light intensity and inoculum cell density	119
Preamble	120
Abstract.....	121
1. Introduction	122
2. Materials and Methods	124
2.1. Planktonic culture maintenance.....	124
2.2. Immobilization and growth of <i>C. vulgaris</i> on membranes.....	125
2.3. Microscopic observation of initially immobilized cultures.....	126
2.4. Relative biomass increase.....	126
2.5. Variable chlorophyll <i>a</i> fluorescence measurements and relative electron transport rate (rETR) estimation.....	126
2.6. Determination of cellular compounds	127
2.7. Statistics analysis.....	128
3. Results and discussion.....	129
3.1. Biomass production as a function of light intensity and initial inoculum density .	129
3.2. Monitoring the physiological state of cells in order to improve biomass and energy-rich compounds production	130
4. Conclusion.....	135

Supplementary data	137
CHAPTER V. Physiological transition of <i>Chlorella vulgaris</i> from planktonic to immobilized conditions	139
Preamble	140
Abstract.....	141
1. Introduction	141
2. Materials and Methods	143
2.1. Inoculum - Planktonic culture maintenance	143
2.2. Immobilized growth of <i>C. vulgaris</i> on filter membranes	143
2.3. Suspended versus immobilized cultures.....	144
2.4. Cell number	145
2.5. Cell volume	145
2.6. Photosynthetic performance	145
2.7. Cell components: Chlorophyll <i>a</i> , macromolecular and elemental composition....	145
2.8. Light measurements in the biofilm and suspended cultures.....	146
2.9. Relative air humidity for immobilized culture	147
2.10. Statistics.....	147
3. Results and discussion.....	148
3.1. Short term physiological changes of immobilized cells.....	148
3.2. Are the short-term physiological changes biofilm specific?	154
4. Conclusion.....	155
Supplementary data	157
CHAPTER VI. General conclusions and perspectives	161
1. General conclusion	162
2. Perspectives	164
Supplementary data	166
Reference:.....	167

List of figures

Figure i. Outline of the main content of the manuscript.....	4
Figure 1-1. Different types of cell-cycle phases of binary fission cell cycle model and the multiple fission found in the alga <i>Scenedesmus</i> (or <i>Chlorella</i>) dividing into two (a, b), four (c), and eight (d) daughter cells.....	8
Figure 1-2. Schematic representation of the mechanism of photosynthesis consisting of biophysical and biochemical processes.....	11
Figure 1-3. Light absorption spectra for photosynthetic pigments.....	11
Figure 1-4. Schematic representation of the photosynthetic light-response curve.....	13
Figure 1-5. Model of saturation curves.....	16
Figure 1-6. Biofilm structure and composition.....	17
Figure 1-7. Schematic representation of microbial biofilm development, adapted from bacterial biofilm.....	18
Figure 1-8. Bio-products acquired from algal biomass and their applications.....	19
Figure 1-9. Schematic ultrastructure of <i>C. vulgaris</i> representing different organelles.....	22
Figure 1-10. Suspended systems for microalgae cultivation.....	25
Figure 1-11. Biofilm-based systems for microalgae cultivation.....	26
Figure 1-12. Schematic illustration of bacterial adhesion and the effects of material properties on cells adhesion and biofilm formation.....	38
Figure 1-13. Schematic representation of cell attachment to different surface features.....	39
Figure 2-1. Schematic representation of light profiles through an algae biofilm at various light intensities.....	56
Figure 2-2. Schematic model for the chlorophyll and light distribution inside the microalgae biofilm.....	61
Figure 2-3. Experimental protocols for biofilm cultivation and experimental analysis.....	63
Figure 2-4. Dynamics of <i>C. vulgaris</i> biofilms under different conditions.....	67
Figure 2-5. pH (a), nitrate (b) and phosphate (c) ions concentration in aqua-medium over time.....	68
Figure 2-6. Dynamics of cellular Chl <i>a</i> content (green bars), carbohydrates (Car/Pro, white bars) and lipids to proteins ratio (Lip/Pro, yellow bars) with regard to the changes in immobilized cell concentration (aligned dots) under combined conditions.....	73
Figure 2-7. Growth rate of sessile cell concentration and Chl <i>a</i> concentration for biofilms under different conditions.....	74
Figure 2-8. The relationship between cellular Chl <i>a</i> content and cell concentration on cotton support under combined conditions.....	75
Figure S2-1. Configuration of flow-lane system for microalgae biofilm cultivation.....	81
Figure S2-2. Oscillation recovery capability as a function of vortexing time during harvesting process.....	81
Figure S2-3. Dynamics of biomass areal density of <i>C. vulgaris</i> biofilms under different conditions.....	82
Figure S2-4. Logarithm of cell concentration of <i>C. vulgaris</i> biofilms under different conditions at exponential phase.....	82
Figure S2-5. Cell detachment percentage of immobilized <i>C. vulgaris</i> on cotton support in the first 24 h.....	83
Figure 3-1. Flowchart of the main contents of Chapter III.....	87
Figure 3-2. Suspended cultures (before dilution) (a), cell concentration (b), cellular chl <i>a</i>	

content and maximum quantum yield (F_v/F_m) (c) over time under 50 (low light, LL) and 350 $\mu\text{mol m}^{-2} \text{s}^{-1}$ (high light, HL) in the pre-acclimated process	91
Figure 3-3. Micro-texture of textile materials observed with 30 \times magnification	92
Figure 3-4. Cell areal density and cell detachment percentage on different textile materials after 6-h incubation.....	98
Figure 3-5. FTIR spectra of Cotton and Terrazzo supports.....	102
Figure 3-6. Microscopic structural observation of supports (Control) and cells attached on their fibers at day 3	104
Figure 3-7. OCT images of LC-inoculated biofilm on Terrazzo support during 3-days cultivation	105
Figure 3-8. Cell areal density of biofilms (with the pre-acclimated inoculum at 50 $\mu\text{mol m}^{-2} \text{s}^{-1}$) on Cotton and Terrazzo after 3-days cultivation	106
Figure 3-9. Effect of support and initial cell density (pre-acclimated to 50 $\mu\text{mol m}^{-2} \text{s}^{-1}$) on relative biomass increase and detachment percentage (a) and biomass productivity (b) after 3-days cultivation of <i>C. vulgaris</i> biofilms	107
Figure 3-10. Chl <i>a</i> content (a), relative maximum electron transport rate ($rETR_{\text{max}}$, b) and carbohydrates to proteins ratio (c) of <i>C. vulgaris</i> biofilms (with the pre-acclimated inoculum at 50 $\mu\text{mol m}^{-2} \text{s}^{-1}$) grown on Cotton and Terrazzo after 3-days cultivation at LC condition	108
Figure 3-11. Relative biomass increase (a), biomass productivity (b) and relative carbohydrates pool size (c) of 3-day <i>C. vulgaris</i> biofilms (inoculated with the pre-acclimated cells to 50 and 350 $\mu\text{mol m}^{-2} \text{s}^{-1}$) grown on Terrazzo at LC-conditions	110
Figure 3-12. Average cell volume (a, c) and cellular Chl <i>a</i> content (b, d) of pre-acclimated cells at 50 and 350 $\mu\text{mol m}^{-2} \text{s}^{-1}$ light intensities and sessile cells on Terrazzo at day 3 at LC-condition.....	111
Figure 3-13. Photosynthetic parameters (F_v/F_m , α , $rETR_{\text{max}}$ and E_k) of pre-acclimated cells at 50 and 350 $\mu\text{mol m}^{-2} \text{s}^{-1}$ light intensities (above) and sessile cells on Terrazzo at day 3 (below) at LC-condition	112
Figure S3-1. Relative biomass increase of <i>C. vulgaris</i> biofilms grown on Cotton and Terrazzo after 3-days cultivation as a function of inoculation approaches	115
Figure S3-2. Images of <i>C. vulgaris</i> growing on Cotton and Terrazzo supports at day 3..	115
Figure S3-3. Roughness profile of the texted textile materials	116
Figure S3-4. Cells retention capability of textile materials as a function of the surface mesh areal density.....	117
Figure S3-5. Effect of support and initial cell density on relative biomass increase and detachment percentage after 3-days cultivation of <i>C. vulgaris</i> biofilms that pre-acclimated to 350 $\mu\text{mol m}^{-2} \text{s}^{-1}$	117
Figure 4-1. Graphical abstract of Chapter IV.....	122
Figure 4-2. Schematic representation of the cultivation system used for the immobilized culture of <i>C. vulgaris</i> (NC membrane represents cellulose nitrate membrane filter).....	125
Figure 4-3. Effect of light intensity and initial cell density on the relative biomass increase of <i>C. vulgaris</i> biofilms after 3-days cultivation.....	129
Figure 4-4. Effect of light intensity and initial cell density on Chl <i>a</i> content of <i>C. vulgaris</i> biofilms after 3-days cultivation.....	132
Figure 4-5. Effect of light intensity and initial cell density on photosynthetic parameters (a, F_v/F_m ; b, $rETR_{\text{max}}$; c, α ; d, E_k) of <i>C. vulgaris</i> biofilms after 3-days cultivation.....	133
Figure 4-6. Effect of light intensity and initial cell density on carbohydrates (a) or lipids (b) to proteins ratio of <i>C. vulgaris</i> biofilms after 3-days cultivation	134
Figure S4-1. CLSM images of initially immobilized cultures with low and high cell densities originating from the pre-acclimated cultures which were exposed to 50, 250 and	

500 $\mu\text{mol m}^{-2} \text{s}^{-1}$ light intensities	137
Figure S4-2. Normalized FTIR spectra of early-stage biofilms illuminated with three light intensities	137
Figure S4-3. Effect of light intensity and initial cell density on cellular C/ N ratio of <i>C. vulgaris</i> biofilms after 3-days cultivation.....	138
Figure 5-1. Schematic representation of the cultivation system used for the immobilized culture of <i>C. vulgaris</i> (NC membrane represents cellulose nitrate membrane filter) (a), photos of immobilized cells at the beginning (b) and end (c) of cultivation.....	144
Figure 5-2. Scores plot of PCA (a) and heatmap (b) depicting the similarity between planktonic and immobilized cells and the patterns of the physiological parameters during the transition (24 hours), respectively	149
Figure 5-3. Changes in average cell volume (a), relative carbohydrates content (b), Chl <i>a</i> quota (c) and relative lipids content (d) over time.....	150
Figure 5-4. Evolution of cell areal density on membrane over time	151
Figure 5-5. Carbon and nitrogen content at the beginning and end of cultivation	153
Figure 5-6. Changes of cell concentration (a), average cell volume (b) and Chl <i>a</i> quota ($\text{fg } \mu\text{m}^{-3}$) of planktonic culture over time.....	154
Figure S5-1. Linear correlation between the suspension absorbance and cell concentration. Points were from actual measurement of suspended cultures under 250 $\mu\text{mol m}^{-2} \text{s}^{-1}$	157
Figure S5-2. Image of the combined temperature/air humidity sensor (embedded in a Petri dish cover) used in this work.....	158
Figure S5-3. Changes in rETR/PFD curves (a), maximal relative electron transport rate (b), and photo-saturation irradiance (c) over time	158
Figure S5-4. Changes of normalized FTIR spectra for <i>C. vulgaris</i> after a transition from planktonic to immobilized growth over time	159
Figure S5-5. Cellular Chl <i>a</i> content (pg cell^{-1}) and cell volume in relation to the levels in inoculum	159
Figure S5-6. Changes in relative air humidity over time	160
Figure S5-7. Carbon and nitrogen content by cell dry weight, and their ratio at the beginning and end of cultivation	160

List of tables

Table 1-1. Constantly submerged systems	31
Table 1-2. Intermittently submerged systems.....	32
Table 1-3. Perfused systems	33
Table 1-4. Comparison of suspended and biofilm-based cultivations.....	35
Table 2-1. Experimental design with different conditions in terms of inoculum density, light intensity, and cellular Chl <i>a</i> content and relative carbohydrates/lipids contents in immobilized cultures at day 0.....	64
Table 2-2. Maximum biomass production and productivity of <i>C. vulgaris</i> biofilms inoculated with different cell density under different light intensity	70
Table S2-1. Productivity of <i>C. vulgaris</i> biofilms under different conditions.....	84
Table 3-1. Physical-chemical properties of textile materials	100
Table S3-1. Morphology, photosynthetic activity and cellular composition of immobilized <i>C. vulgaris</i> (pre-acclimated to 50 $\mu\text{mol m}^{-2} \text{s}^{-1}$) after 3-days cultivation	117
Table S6-1. Biomass productivities of immobilized cultures in each chapter	166

Abbreviations

C	Carbon
CBB	Calvin-benson-bassham cycle
CCS	CO ₂ capture and storage
Chl	Chlorophyll
Chl*	Excited chlorophyll
CLSM	Confocal laser scanning microscopy
CO ₂	Carbon dioxide
CP	Commitment point
DHA	Docosahexaenoic acid
DMSO	Dimethyl sulfoxide
EPA	Eicosapentaenoic acid
EPS	Extracellular polymeric substances
ESEM	Environmental scanning electron microscopy
ETR/PFD curve	Electron transport rate versus photon flux density curve
Fd	Carrier ferredoxin
FTIR	Fourier-transform infrared spectroscopy
FNR	Ferredoxin NADP reductase
GHG	Greenhouse gases
GRAS	Generally recognized as safe state
G3P	Glyceraldehyde 3-phosphate
HC	High inoculum density
HL	High light intensity
IUPAC	International union of pure and applied chemistry
LC	Low inoculum density
LC-PUFAs	long-chain polyunsaturated fatty acids
LL	Low light intensity
LHC	Light harvesting complex
ML	Moderate light intensity
P	Phosphorus
P _{max}	Photosynthesis attains the maximum
PBRs	Photo-bioreactors
PC	Plastocyanin
PCA	Principal component analysis
PDF	Photon flux density
P-I curve	Photosynthesis-irradiance curve
PSI	Photosynthetic system I
PSII	Photosynthetic system II
PSUs	Photosynthetic units
PVC	Polyvinyl chloride
R _a	Surface roughness
R _b	Relative biomass increase with respect to the initial biomass
R _c	Relative biomass increase to the initial cell population
RC	Reaction center
RFC	Radial Flow Chamber

Abbreviations

ROS	Reactive oxygen species
Rubisco	Ribulose-1,5-bisphosphate carboxylase/oxygenase
RuBP	Ribulose phosphate
3D	Three dimensional
3-PGA	3-phosphoglyceric acid
N	Nitrogen
NPQ	Non-photo-chemical excitation energy quenching
WWT	Wastewater treatment

Symbols

A	Cross-sectional area of the flow chamber (m^2)
ΔA	Change of support surface area
A_{biofilm}	Light attenuation in the biofilm
A_{ξ}	Suspension light absorbance
b	Biofilm extinction coefficient (m^{-1})
C_0	Cell number on supports at the beginning
C_1	Cell areal density day t_1 (cell m^{-2})
C_2	Cell areal density at day t_2 (cell m^{-2})
C_v	Cell numbers obtained by mechanically harvesting after 3 days
C_{chl}	Cell numbers normalized by residual Chl <i>a</i> -content on coupons after 3 days
$C_{\text{unattached}}$	Total cell number unattached to the support
C_t	Cell areal density at time t (cell m^{-2})
D_c	Cell areal density at day 3 (cell m^{-2})
D_h	Hydraulic diameter of the chamber (m)
D_p	Cell detaching percentage (%)
E_{area}	Apparent area of the support (cm^2)
E_k	Photosynthetic saturation irradiance ($\mu\text{mol m}^{-2} \text{s}^{-1}$)
ETR	Electron transport rate
ETR_{max}	Maximal relative electron transport rate
$rETR$	Relative electron transport rate
$rETR_{\text{max}}$	Relative maximal relative electron transport rate
E_k	Photo-saturation irradiance
f	Friction factor
F_0	Minimum chlorophyll fluorescence after 10 min dark-adaptation
F	Minimum chlorophyll fluorescence during illumination
F'_m	Max chlorophyll fluorescence during illumination
F_m	Maximum chlorophyll fluorescence from dark-adapted cells
F_v/F_m	Maximum quantum yield
$\Delta F/F'_m$	Effective quantum yield
h	Biofilm thickness at 0h (μm)
I_0	Income light ($\mu\text{mol m}^{-2} \text{s}^{-1}$)
I_{bottom}	Light intensity in the bottom of biofilm ($\mu\text{mol m}^{-2} \text{s}^{-1}$)
I_z	Light intensities at the depth of z for biofilm ($\mu\text{mol m}^{-2} \text{s}^{-1}$)
t_1	Beginning exponential growth phase (d)
t_2	End of exponential growth phase (d)
R_b	Relative biomass increase with respect to the initial level
R_c	Relative biomass increase to the initial population
Re	Reynold's number
P	Wetter perimeter (m)
P_X	Maximal biomass productivity at exponential growth phase ($\text{g m}^{-2} \text{d}^{-1}$)
V_s	Flow velocity (m s^{-1})
X	Cell concentration in suspension (cells mL^{-1})
X_0	Biomass areal density at the beginning of the immobilization (g m^{-2})
X_1	Biomass areal density at day t_1 (g m^{-2})

Symbols

X_2	Biomass areal density at day t_2 (g m^{-2})
X_t	Biomass areal density after 3 days (g m^{-2})
W	Energy required to realize the adhesion
z	Depth of suspension (mm)

Greek letters

α	Initial slope of photosynthetic light-response curve
γ	Support surface free energy
μ	Specific growth rate (d^{-1})
μ_{Chla}	Specific growth rate calculated by areal Chl a concentration (d^{-1})
μ_{Cell}	Specific growth rate calculated by sessile cell concentration (d^{-1})
μ_v	Viscosity of the fluid ($\text{kg m}^{-1} \text{s}^{-1}$)
ξ	Suspension absorption coefficient
ρ	Density of the fluid (kg m^{-3})
τ_w	Wall shear stress (N m^{-2})

General introduction

Introduction

With the increase of world population, food/energy crisis and global warming have become major challenges and attracted considerable concerns. In this context, searching for renewable and sustainable food/energy resources is becoming a vital issue. Microalgae, photosynthetic organisms, can capture photons and CO₂ to produce biomass and valuable compounds, such as carbohydrates, proteins and lipids. Therefore, they have been widely recognized as a potential source for clean biofuels and food raw materials.

Suspension-based methods have been extensively applied for microalgae cultivation for biomass and biofuels production, wastewater treatment, CO₂ fixation, etc., however, limitations presented in currently suspended methods such as low biomass productivity and high operation costs (e.g., mixing, harvesting and dewatering processes) hinder the microalgae commercial values and industrial use. Recently, microalgae biofilm-based cultivation technology has gained an increasing interest due to their advantages compared to suspended cultures in terms of lower water demand, more efficient harvesting and higher biomass productivity. It has been therefore proposed as a potential alternative to suspension-based technology for microalgae production.

A biofilm is an assemblage of microbial cells that are associated with a surface and enclosed in a matrix of extracellular polymeric substance (EPS). There are many factors affecting microalgae biofilm development, including: light/nutrients availability, pH, temperature, inoculum density/method/time/species, systems design/supports applied and harvesting frequency, etc. Most of these cultivation parameters can be controlled by researchers or producers, therefore, they are collectively referred to as operational factors in this thesis. Currently, extensive studies have been carried out to assess the effect of those factors on biofilm development and overall productivity. However, the underlying mechanisms leading to different cell behaviors and productivities of microalgae biofilms are seldom studied.

Among them, light is a major parameter and many studies have elucidated the effect of light on microalgae growth and physiological properties. However, compared to the cells in a relative stable and homogenous micro-environment in well-mixed and low-cell-

concentration suspension, the sessile (immobilized) cells in biofilms might be exposed to quite different conditions due to light attenuation and/or mass transfer resistance, in particular for those grown in a thick/mature biofilm. Some studies have reported that the light availability decreases sharply with the increase of biofilm thickness owing to self-shading. Therefore, in order to better assess the effect of light, different initial densities could be inoculated on the support to mimic biofilms with different thicknesses or those grown on different phases. In fact, to the best of our knowledge, the topic on the synergistic effect of light and inoculum density on microalgae biofilm development has been seldom discussed. Besides, support materials have been widely demonstrated to affect the initial cell attachment because of their various physical-chemical properties and micro-textures, consequently affecting the inoculum density and ultimately impacting the overall productivity. Therefore, the inoculum as an operational factor was also investigated in this thesis.

Specifically, **three operational factors**: light intensity, inoculum and support were selected to study how they affect growth and productivity of *C. vulgaris* biofilms in this work. Additionally, the physiological properties of immobilized cells (morphology, photosynthetic activity, composition), rarely investigated, were also characterized in this work. This will help understanding the underlying mechanisms of biofilm formation, and in particular the sessile cells acclimation mechanisms. It will also help identifying stressful parameters in advance, allowing the operators to take reasoned operation choices for maximizing biomass or targeted compounds productions.

Overall objectives

The overall aims of this thesis were to:

1. Assess the effect of the operational factors light intensity, inoculum density/properties and support material on microalgae biofilm development. To do so, biofilm growth, composition and photosynthetic activity were monitored. The goal is also to identify parameters that impact negatively productivity at early stage of biofilm development through our approach. This would allow to react quickly by changing cultivation conditions/production strategies in order to maximize process productivity.

2. Understand the responses of immobilized cells to the tested conditions and in particular, describe the acclimation mechanisms of sessile cells. Track the physiological transition from planktonic to immobilized state. On the whole, the goal is to get a better insight into the underlying mechanisms involved in biofilm formation.

3. Select potential supports which demonstrate high cell retention capability and that could be further tested in pilot-scale microalgae biofilm cultivation systems.

Manuscript outline

Chapter I summarizes the current knowledge on microalgae, biofilms and systems used for microalgae cultivation. It also identifies the operational factors affecting microalgae biofilm development and the underlying mechanisms of formation.

Chapter II describes the dynamics of *C. vulgaris* biofilms on a continuous biofilm submerged reactor under different light and inoculum conditions. In this chapter, a rapid acclimation process within 3 days was observed, which provided a theoretical basis for the following chapters.

Chapter III confirms the hypothesis proposed in chapter II that support nature affects cell retention (detachment) capability. In this chapter, the impact of support, light intensity and inoculum density/properties on biofilm growth, activity and composition was assessed.

In **chapter IV**, a perfused cultivation system was used for biofilm development in order to overcome some challenges encountered in chapter III (partial harvesting of the cells from the support) and develop biofilms in more controlled conditions. Further studies on the impact of light intensity and inoculum density on biofilm growth and physiological profiles at the early stage (3 days) of biofilm formation were carried out.

In **chapter V**, for the first time, the characterization of the physiological transition of *C. vulgaris* cells from planktonic to immobilized lifestyle is investigated.

Lastly, general conclusions were drawn in **chapter VI**, and some suggestions for further work are proposed.

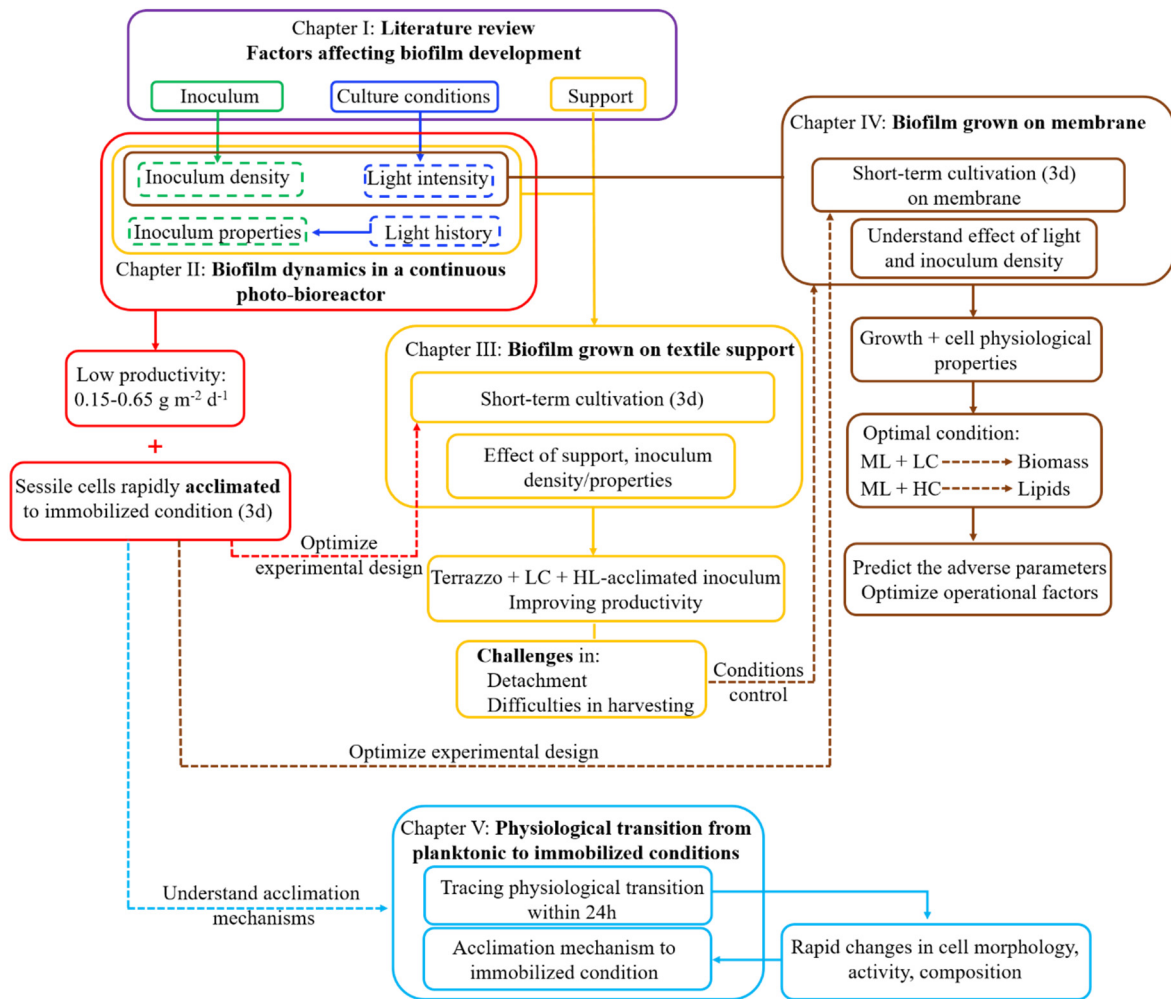


Figure i. Outline of the main content of the manuscript. LL, ML, and HL represent low, middle and high light intensity, respectively; LC and HC are low and high inoculum cell density, respectively (the corresponding light density and inoculation density are detailed in each chapter).

CHAPTER I Literature review

A- Overview of microalgae

1. Microalgae

1.1. What are microalgae?

Microalgae are a large group of prokaryotic or eukaryotic phototrophic microorganisms which are capable of using light energy and nutrients (CO₂, nitrogen, phosphorus and silicon, etc.) to produce biomass and interesting commercial products. It is unclear how many algae species exist, but according to conservative estimates, around 72500 species, and ~ 44000 species have been described in publications (Guiry, 2012).

Microalgae range in size from several to hundreds of microns (µm) and can be found in both terrestrial and aquatic ecosystems (including waste water, fresh, brackish and marine water) (Rodríguez-Palacio et al., 2012). They can grow in form of individuals or consortia.

The taxonomic classification of microalgae is usually based on their pigments (type, content or proportion), cell structure and life cycle. Among them, green algae (*Chlorophyta*), red algae (*Rhodophyta*), diatoms (*Bacillariophyta*) and blue-green algae (*Cyanophyta*) are the species mostly concerned.

Microalgae present some advantages over traditional agricultural crops, such as the high photosynthesis efficiency, growth rate, and productivity. Microalgae cultivation can be carried out on non-arable land and many algal species are salt and pollutants tolerant. They are thus able to grow in sea and polluted waters (Ahmad et al., 2021; Shetty et al., 2019).

1.2. Microalgae mechanism

1.2.1. Cell cycle

Generally, cell cycle is defined as a sequence of events repeatedly occurring in mother and daughter cells (Bišová and Zachleder, 2014). With this process, algae can constantly reproduce new daughter cells, maintaining species or thriving their communities. In addition to a broad diversity in terms of morphology and structural organization (like unicellular microalgae and multicellular macro-algae), algae also show variations in reproductive patterns: from binary fission to multiple fission, which is based on the fact that cells are

typically divided into 2^n (n is an integer) (Howard and Pelc, 1953; Setlik, 1984; Zachleder et al., 2016; Zachleder and Van Den Ende, 1992). When $n = 1$, mother cell is divided into two daughter cells with a binary fission pattern (C_1 cell cycle). This classical cell cycle model is commonly observed in microalgae, especially in those filamentously organized (Fig. 1-1a and b). When $n \geq 2$, cell cycle pattern is multiple fission where mother cell is divided into four to thousands of daughter cells (C_n cell cycle). This process is a general cell cycle pattern that occurs in green algae, such as *Chlorella*, *Scenedesmus*, *Desmodesmus* and *Chlamydomona*. It should be noted that both binary and multiple fission can be observed in the same algal species though cells are in different growth conditions or at different growth phase.

A cell cycle normally includes two coordinated processes: growth (G1 phase), and the DNA replication-division sequence which consists of synthesis phase (S phase), second growth phase (G2 phase), nuclear division (M phase) and cytokinesis (C) (Fig. 1-1, Bišová and Zachleder, 2014; Mitchison, 1971). In the growth stage, algal cells build up functional structures, synthesize essential constituents (including energy reserves) and increase their volume. At the end of this event, cells reach to a critical size and enter into a commitment point (CP), that is, a critical point/threshold size through which cells are committed to divide. After that, cells can be competent to start DNA replication and cellular division; these latter events that take place after the CP are collectively termed as DNA replication-division sequence (Zachleder et al., 2016).

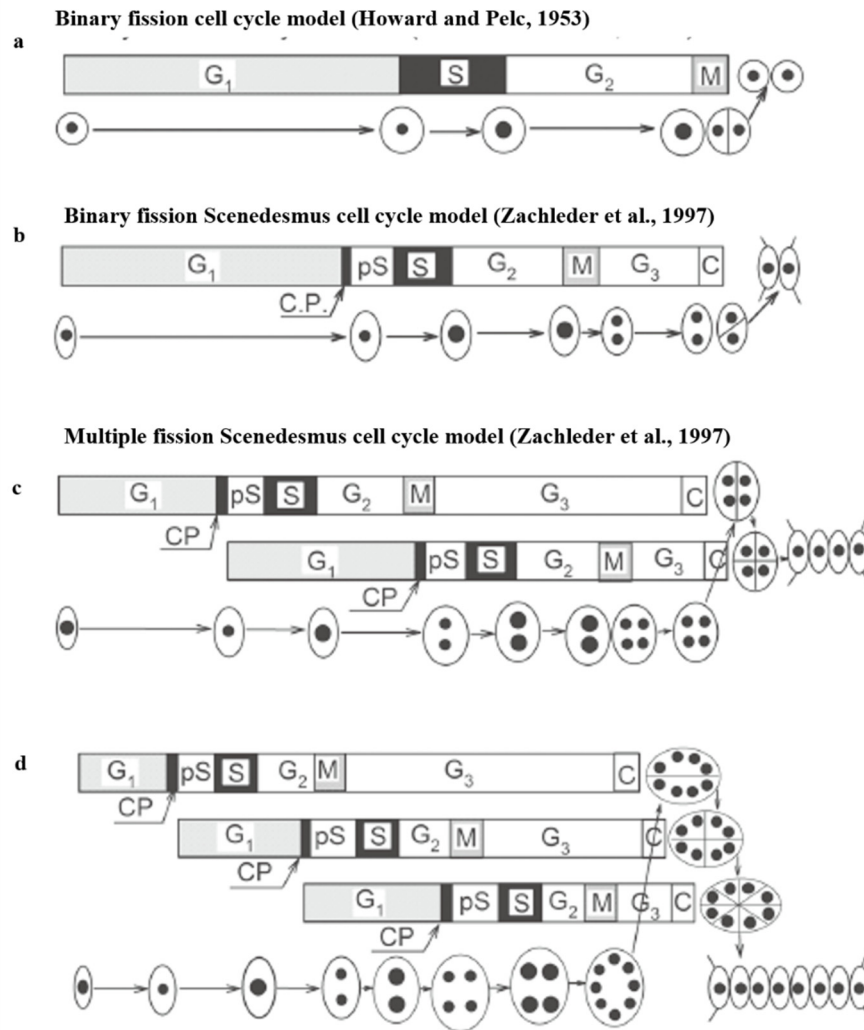


Figure 1-1. Different types of cell-cycle phases of binary fission cell cycle model and the multiple fission found in the alga *Scenedesmus* (or *Chlorella*) dividing into two (a, b), four (c), and eight (d) daughter cells. (a) binary fission cell cycle model proposed by (Howard and Pelc, 1953); (b), (c) and (d) *Scenedesmus*-type binary and multiple fission cell cycle models proposed by (Zachleder et al., 1997); Individual bars show the sequence of cell-cycle phases during which growth and the DNA replication-division sequence take place. Two bars (c) and three bars (d) illustrate mother cell undergoes two and three times CP, respectively, consecutively starting sequences of growth and reproductive events. G₁, the phase during which the critical cell size is attained; it can be called a pre-commitment period because it is terminated when the commitment point (CP) is reached. CP, the stage in the cell cycle at which the cell becomes committed to triggering and terminating the DNA replication-division sequence. pS, the pre-replication phase between the CP and the beginning of DNA replication; the processes required for the initiation of DNA replication are assumed to happen during this phase. S, the phase during which DNA replication takes place. G₂, the phase between the termination of DNA replication and the start of mitosis; processes leading to the initiation of mitosis are assumed to take place during this phase. M, the phase during which nuclear division occurs. G₃, the phase between nuclear division and cell division; the processes leading to cellular division are assumed to take place during this phase. C, the phase during which cell cleavage occurs (Bišová and Zachleder, 2014).

Compared to the binary fission, multiple fission shows multiple commitment points and consecutively overlaps sequences of growth and reproductive events during a single cell cycle (Fig. 1-1). At each commitment point, an approximately twofold cell size that of the previous one is attained (Šetlík et al., 1972; Zachleder et al., 2016). As stated by Zachleder et al. (2016), commitment point studies may provide crucial information for the field of cell cycle research. While cell attaining CP is highly affected by environmental factors such as light, nutrients availability (e.g., N, P, Si) and temperature (Bišová and Zachleder, 2014). Under adverse conditions, a mother cell will divide into two daughter cells, while in favorable conditions it will reproduce more cells. For instance, with the improvement of light intensity (under optimum temperature), the same culture will increase commitment points and transfer the cell cycle pattern from b to c to d (Fig. 1-1).

In the case of *Chlorella*, the cell cycle is similar to that of *Scenedesmus* cells (Fig. 1-1) and thus can be described similarly. *Chlorella* is one of the first microalgae successfully grown in synchronous cultures and used for analyzing cell-cycle regulation (Senger and Bishop, 1966; Tamiya et al., 1953). They were observed to grow only in light period (under 12h L:12h D regime), while cellular division (or the separation of mother cells) occurred during the dark (Bišová and Zachleder, 2014; Hase et al., 1959; Morimura et al., 1961). When daughter cells are exposed to light, they can enter G1 phase. After a period, cells increase their volume (roughly 2- fold) and attain the CP, then the first DNA replication-division sequence is followed. This series of events can be repeated for second, third, fourth, n^{th} growth sequences, along with doubling cell volumes and producing four, eight,, 2^n daughter cells.

1.2.2. Photosynthesis

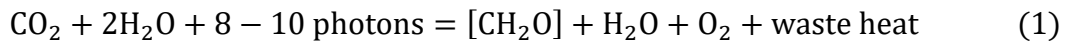
1.2.2.1. Light-dependent reaction and dark reaction

Photosynthesis is the most important biological process on earth. It emerged more than 2.5 billion years ago and transform life in our planet by supplying oxygen. Briefly, it consists in the biological conversion of light energy and inorganic carbon into organic molecules, and produces O_2 required for plants and animals (see Eq. (1)) (Masojídek et al., 2021).

Like in plants, microalgae photosynthesis takes place in chloroplasts (cytoplasm for cyanobacteria) and can be mainly divided into two steps:

1) the light-dependent reaction, that occurs on photosynthetic membranes and in which light energy is converted into chemical energy and reducers factors (NADPH₂ and ATP), and

2) the dark reaction, which is carried out in the stroma. The generated NADPH₂ and ATP are here used to reduce CO₂ to organic compounds.



As shown in Fig. 1-2 (Yang et al., 2020), the light-dependent reaction begins with the absorption of photons by pigments, such as Chl *a*, *b* and carotenoids (the photosynthetic pigments and their light absorption spectra are shown in Fig. 1-3). Chl passes then from a stable to an excited state (e.g., Chl → Chl^{*}). A large amount of excited energy is transferred to the specialized Chl dimers in the reaction centers (RCs) of PSII (called P680) and PSI (called P700), which triggers charge separation and water splitting. After charge separation, P680^{*} releases two electrons for every two photons absorbed to plastoquinone Q_A, and then to the mobile carrier plastoquinone Q_B. Combined with two protons from the stroma, Q_B can be reduced. At the same time, the lost electrons of P680 can be replenished from the splitting of H₂O. Afterwards, the reduced Q_B can be oxidized by Cytb₆f. During this process, two protons are released into the lumen of thylakoid, forming a proton gradient with the protons derived from H₂O. This proton gradient is used to drive the ATP synthase to produce ATP. One of the electron absorbed by Cytb₆f is shuttled onto plastocyanin (PC) in the lumen through the high potential chain (Rochaix, 2011). Then PC is oxidised by PSI complex, and the electron is transferred through RC of PSI to the mobile carrier ferredoxin (Fd), which consequently pass the electron to the Ferredoxin NADP reductase (FNR) complex. When two electrons are transferred to FNR, NADPH is generated by the two electrons, one proton and NADP⁺. Meanwhile, ATP is also produced by ATP synthase driven by the proton gradient which is created by the electron transport chain (Mitchell, 1966).

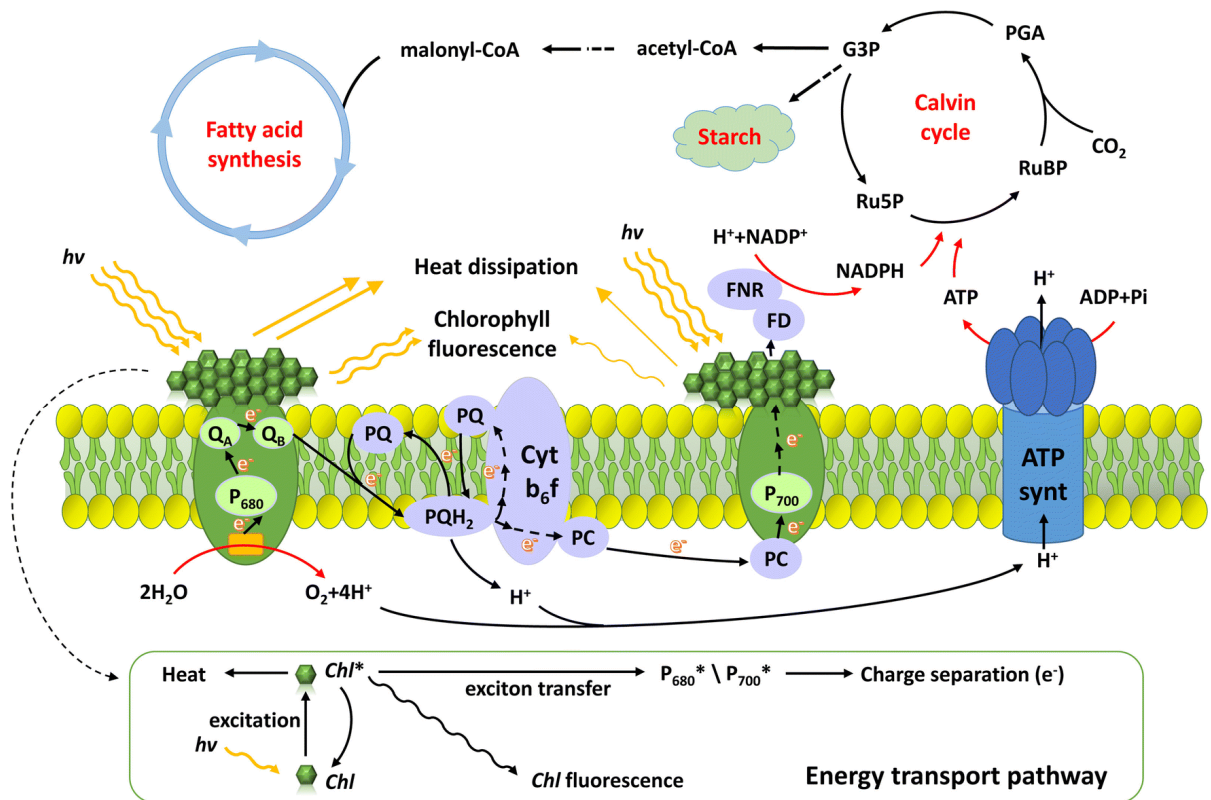


Figure 1-2. Schematic representation of the mechanism of photosynthesis consisting of biophysical and biochemical processes (Yang et al., 2020).

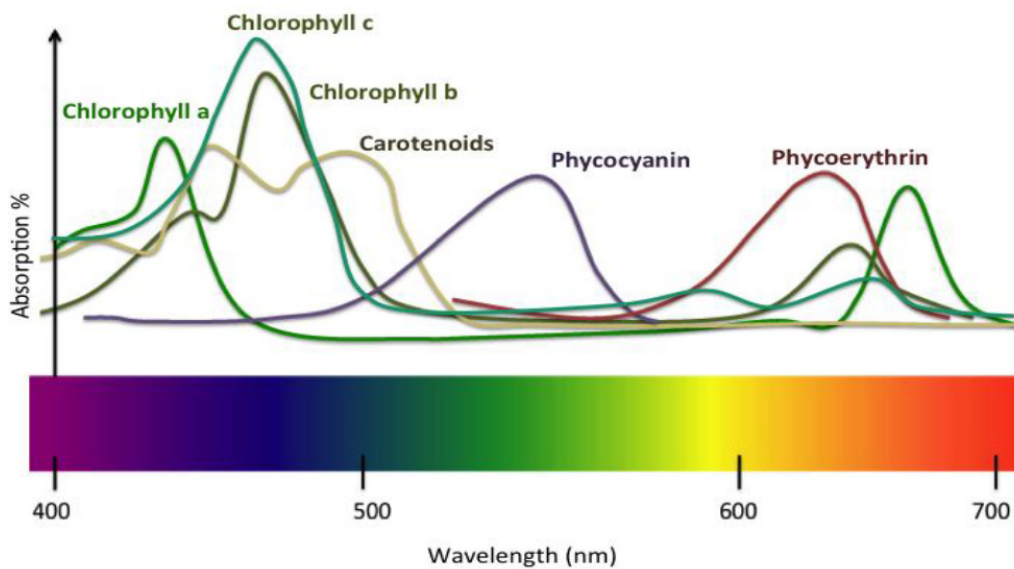


Figure 1-3. Light absorption spectra for photosynthetic pigments (Yarish et al., 2012).

Dark reactions involve the reduction of CO₂ into organic matters with ATP and NADPH produced in light-dependent reactions. This carbon fixation process is carried out by the Calvin-Benson-Bassham (CBB), mainly via four reaction steps (Masojídek et al., 2021):

1) Carboxylation, in this step the enzyme ribulose-1,5-bisphosphate carboxylase/oxygenase (Rubisco) catalyzes the reaction between ribulose phosphate (RuBP) and CO₂ to form two molecules of 3-phosphoglyceric acid (3-PGA);

2) Reduction, a step where 3-PGA is reduced to glyceraldehyde 3-phosphate (G3P);

3) Regeneration, RuBP is regenerated for another CO₂ fixation in the series of reactions;

4) Production, primary end-products of photosynthesis, carbohydrates, are biosynthesized.

1.2.2.2. P-I curve

Light is one of the most important factor impacting microalgae photosynthesis and growth. When plotting the photosynthesis rate, which can be characterized by the rate of CO₂ assimilation or O₂ evolution, over light intensity, we can obtain the so-called photosynthesis-irradiance (P-I) curve, as shown in Fig. 1-4 (Malapascua et al., 2014).

Typically, the P-I curve can be divided into four regions: 1) respiratory region, in which light is lower than the compensation point, and the organic matter produced by photosynthesis cannot compensate that consumed by respiration; 2) photo-limited region, in which microalgae show a high light utilization efficiency and their photosynthesis rate increases with the rising irradiance; 3) photo-saturated region, in which photosynthesis is saturated and microalgae show the highest photosynthesis rate; 4) photo-inhibited region, in which photosynthesis rate slows down with a further increase of light intensity (Malapascua et al., 2014; Torzillo and Vonshak, 2013).

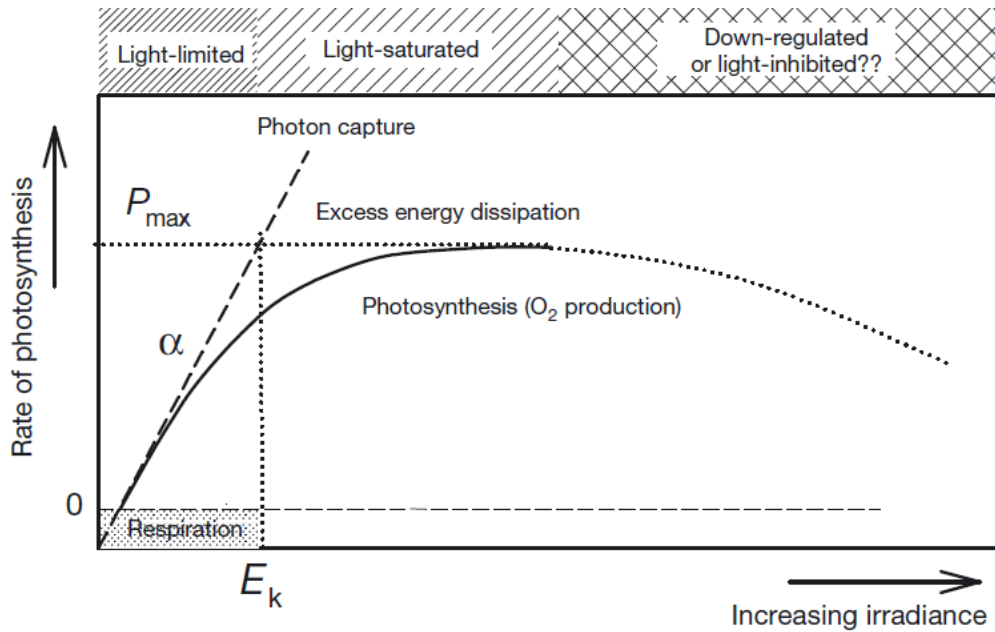


Figure 1-4. Schematic representation of the photosynthetic light-response curve (solid line), i.e. the dependency of photosynthesis on irradiance (Malapascua et al., 2014).

Several important photosynthetic parameters can be estimated from the P-I curve (Fig. 1-4).

Under very low light, the photosynthesis rate linearly increases with the increasing irradiance and the electron transport rate is determined by the photons absorption rate. In this range, the initial slope of P-I curve, α , can be considered as a direct measurement of the maximum quantum yield (Torzillo and Vonshak, 2013).

Then, the photosynthesis rate is not proportional to irradiance with the further increase of irradiance and the quantum yield decreases. In the photo-saturated region, photosynthesis attains the maximum (P_{max}). The maximum electron transport rate (ETR_{max}) through PSII complex can be thus estimated. The derived parameter E_k ($E_k = P_{max} / \alpha$) denotes the photo-saturation irradiance, and it is often taken as an indicator of the photo-acclimation state of microalgae (Torzillo and Vonshak, 2013). When the irradiance is less than E_k , the main chlorophyll fluorescence-quenching mechanism is photochemical, whereas above E_k , it also involves the non-photochemical quenching, the excess energy will be thermally dissipated (Malapascua et al., 2014; Torzillo and Vonshak, 2013).

1.2.3. Photo-acclimation

As suggested by (Raven and Geider, 2003), microalgae do respond to changes in environmental conditions through several cellular processes occurring at different time scales: **regulation** is described as the adjustment of catalytic efficiency (enzyme activity) and energetic dissipation efficiency occurring in a short period of time (seconds to minutes), **acclimation** refers to changes of macromolecular composition within hours to days, and **adaptation** is considered as an outcome of evolution, involving adjustments in the gene pool of a specie, which requires a relatively long periods of time (from days up to thousands of millions of years).

These processes are all typically thought to optimize cellular performance (fitness) when microalgae encounter variations in environmental conditions. Acclimation process is the mostly investigated and well-studied mechanism. It consists in a strategy to optimize light energy absorption (light harvesting) and utilization, and avoid photo-inhibition. It can progressively improve the tolerances of photo-organisms to adverse conditions, like stresses due to light (Nymark et al., 2009; Torzillo et al., 2012) and nutrients availability (Xiang et al., 2021), salinity (Shetty et al., 2019), dehydration (Aigner et al., 2020; Karsten and Holzinger, 2014) and presence of heavy metals (Kumar et al., 2020), etc.

Generally, **photo-acclimation** involves coordinated variations in the composition and function of photosynthetic apparatus, e.g., abundance of pigments and light-harvesting complexes (LHCs), and PSI:PSII ratio, catalysts within electron transfer chain, as well as the abundance of CBB enzymes (mainly focus on Rubisco) in response to the environmental changes in light availability (light quantity and/or quality) (Raven and Geider, 2003; Sukenik et al., 1987). However, the most important and distinct phenotype of photo-acclimation is associated with light harvesting capacity that involves the antenna pigment-protein complex.

There is evidence indicating that the occurrence of photo-acclimation is highly related to a signal transition mechanism which is driven by the redox state of components of photosynthetic apparatus (Escoubas et al., 1995; Raven and Geider, 2003). Up to now, most studies focused on the effect of redox state of plastoquinone pool on the transcriptional control of LCHs genes that govern the generation of the antenna pigment-protein complex (Escoubas et al., 1995; Kana et al., 1997; Lepetit et al., 2013; Raven and Geider, 2003). For instance, a high PQH₂/PQ ratio (ratio of reduced and oxidized plastoquinone) under high irradiance triggers the transcriptional systems to down-regulate light-harvesting apparatus and restrict the excitation energy input to PSII. Conversely, low reduction state of PQ pool (with a low PQH₂/PQ ratio) typically reflects a low excitation energy flux to PSII and then

to the downstream events (e.g., electron transport chain and CO₂ fixation), signals to improve the antennae light-harvesting pigment are thus generated. This process has long been recognized as an acclimation response for improving the light-harvesting efficiency of photo-organisms under light-limited conditions.

Microalgae can also change the composition of pigments of the xanthophyll cycles to deal with high light. This acclimation mechanism involves the de-epoxidation of violaxanthin to antheraxanthin and to ultimate zeaxanthin, or that of diadinoxanthin to diatoxanthin (Raven and Geider, 2003; Sun et al., 2020). Xanthophyll cycles are indeed associated with non-photo-chemical excitation energy quenching (NPQ) in LHCs for safely dissipating energy to heat, and adjusting the quantity of excitation energy reaching to PS II and to downstream events. Therefore, this mechanism can be considered as a photo-protective strategy of microalgae that are subjected to excess irradiance, protecting cellular plastids from over-excitation of the photosynthetic units (PSUs) and over-reduction of electron transport chain which may induce the accumulation of reactive oxygen species (ROS) (Lacour et al., 2020; Raven and Geider, 2003).

It has been proved that ROS accumulation may lead to damages in the PsbA (D1) protein due to over-oxidative stress, resulting in a non-functionalization of PSII reaction center (Lacour et al., 2020). It should be noted that D1 protein is a crucial component of PSII that is associated with charge separation.

Notably, the timescale for accomplishing the regulation of pigmentation through photo-acclimation is species-specific, from hours to days. Literature has demonstrated that cellular Chl content in microalgae rapidly decreases after transition from low (LL) to high light (HL) due to the pigment dilution in the course of cell division but not as a result from the pigment degradation (Anning et al., 2000; Berner et al., 1989; Post et al., 1984). By contrast, photo-acclimation process of microalgae during the light shift from HL to LL is consistent with an increase in pigmentation (Fisher et al., 1996).

Kana et al. (1997) also proposed a dynamic theory described by a dynamic balance between the PSUs synthesis and loss in response to the alteration of light conditions. These opposing forces will ultimately reach a balance point for the PSUs number or size (under low or high light, see Fig. 1-5) where cellular energy input just balances with the demand for cellular energy.

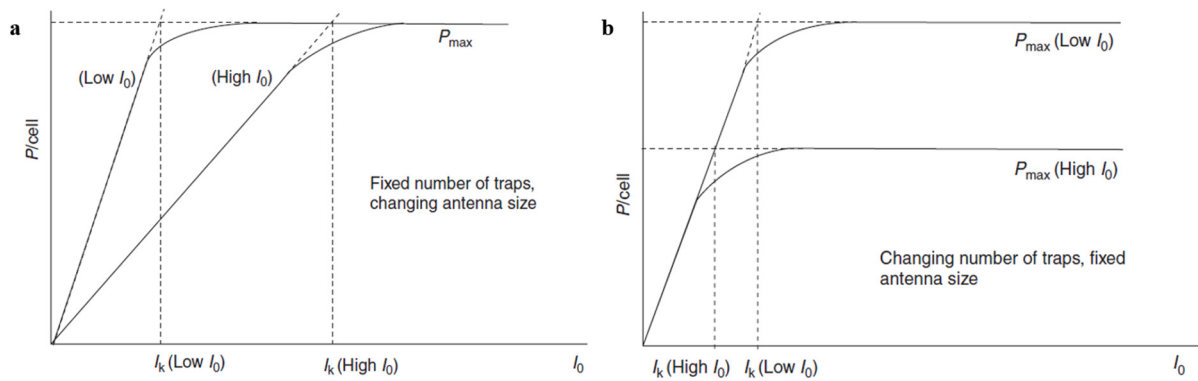


Figure 1-5. Model of saturation curves. (a) Model of adjustment to low and high light irradiances by changing the size of a fixed number of PSUs. (b) Model of adjustment of the photosynthesis unit to low and high light by changing the number of PSUs and not their size (Ramus, 1981; Torzillo and Vonshak, 2013).

1.3. Microalgae lifestyle

1.3.1. Planktonic and immobilized lifestyle

Microalgae are capable of living in the bulk water column, where cells freely swim in suspension (planktonic state), or in complex communities attached to substrates (biofilms) or entrapped in polymers (e.g., alginate, carrageenan, chitosan) with non-motile modes. In nature, planktonic and biofilm-stated microalgae are both ubiquitous.

The surface-associated lifestyle of microalgae has obtained increasing interest in recent years, as it provides new ideas and insights for cost-efficient cultivation of algal biomass. As defined by the IUPAC (International Union of Pure and Applied Chemistry), biofilms are “aggregates of microorganisms in which cells, that are embedded within a self-produced matrix of extracellular polymeric substance (EPS, a network of water, polysaccharides, proteins, nucleic acids, etc.), adhere to each other and/or to a surface” (Vert et al., 2012).

According to the previous studies that characterized the biofilm architecture and composition (Boudarel et al., 2018; Fanesi et al., 2019; Flemming and Wingender, 2010), there are many features distinguishing algal biofilms from their planktonic counterparts: the high cell concentration (the order can reach up to 10^{10} cells mL^{-1}), the associated solid surface, the increased EPS matrix and physical-chemical heterogeneity (Fig. 1-6).

Micro-environmental conditions to which algal cells are exposed in a biofilm remarkably differ from those in suspension. For instance, the free-floating cells in a well-mixed water environment generally are exposed to uniform nutrient concentration, whereas nutrient gradients across the 3D structure of a algal biofilm may occur due to the reaction-

diffusion/convection mechanisms (Fig. 1-6), leading to local heterogeneities in pH, metabolites, and O_2 concentration (Boudarel et al., 2018; Karygianni et al., 2020; Murphy and Berberoglu, 2014).

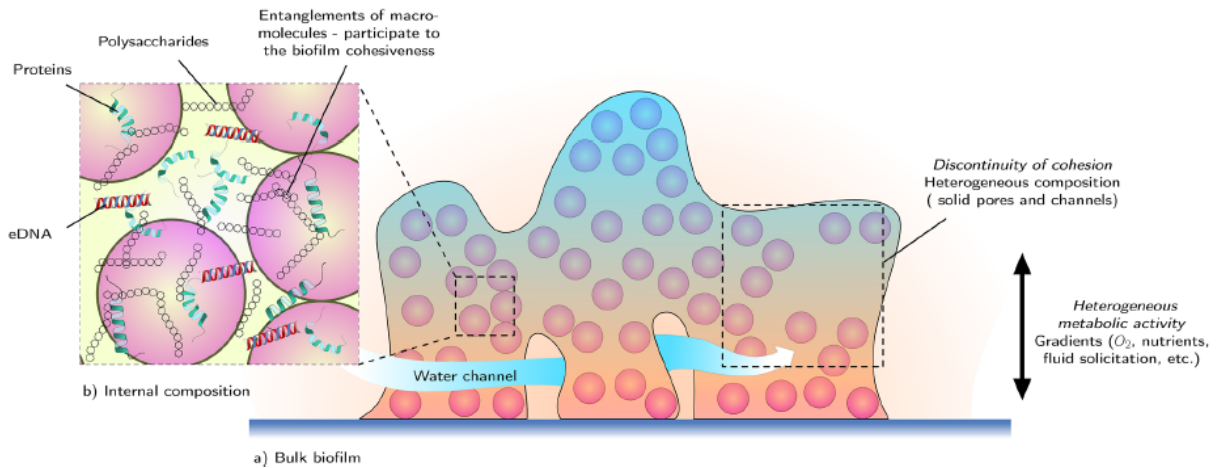


Figure 1-6. Biofilm structure and composition (bacterial biofilm, Boudarel et al., 2018).

1.3.2. Lifestyle transition

Like bacterial biofilms, algal biofilm development can also be divided into four stages (Fig. 1-7): 1) initial attachment 2) micro-colonies formation and active growth, 3) maturation, and 4) and dispersion (Achinas et al., 2019; Guzmán-Soto et al., 2021; Irving and Allen, 2011; Tolker-Nielsen, 2015). At the latter stage, cells detachment occurs linked to nutrients, light depletion (Matthiessen et al., 2010; Muylaert et al., 2009; Tesson et al., 2016). The dispersal cells enter into the floating water phase and can further attach to the biofilm.

Similar to bacteria, microalgae can therefore undergo a transition from planktonic to biofilm lifestyle (planktonic cells attaching to solid surface) or vice versa (dispersal cells into liquid) (Fig. 1-7) (Karsten and Holzinger, 2014; López and Soto, 2019; Zhuang, 2018). Using global genomic approaches such as DNA arrays, proteomics and cDNA subtractive hybridization, researchers confirmed the existence of specific biofilm-related genes or proteins in sessile bacterial cells (Chua et al., 2014; O'Toole et al., 2000; Zhao et al., 2017; Zou et al., 2012, 2012). Some of them even tracked the physiological changes and biochemical pathways of bacteria shifted from one lifestyle to another (Chua et al., 2013; O'Toole et al., 2000; Qayyum et al., 2016). Current studies, even with limitations, have demonstrated that the physiological properties of immobilized algal cells vary from their planktonic counterparts (Zhuang et al., 2018). Sessile cells seem therefore to acclimate to

the local conditions within the biofilm. Other research works also demonstrated that proteome profiles of planktonic and sessile cyanobacteria were different (Baqué et al., 2013; Romeu et al., 2020), but none of them focused on the physiological transition of algal lifestyle. It should be pointed out that increasing knowledge on sessile cell acclimation will provide important information regarding microalgae biofilm formation. Particularly, it may help identifying detrimental conditions and stressful factors that impact productivity. Therefore, studies on sessile cells acclimation and in particular, microalgae physiological transition from planktonic to immobilized state (or the opposite transition) should be carried out.

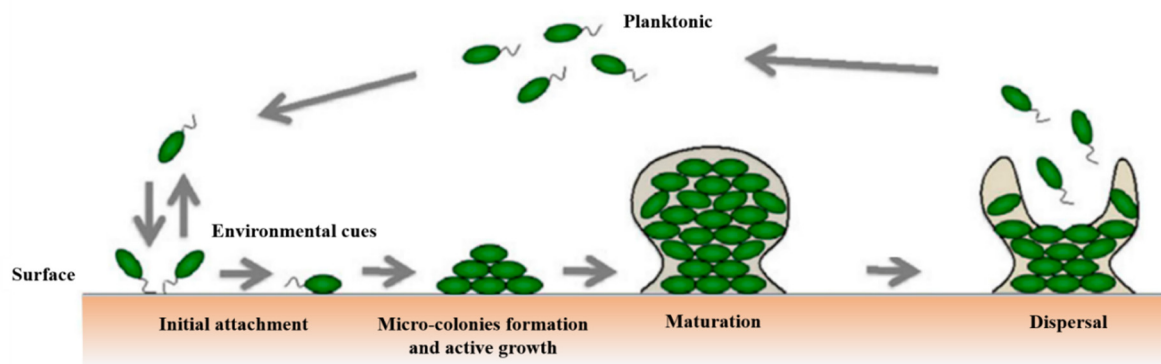


Figure 1-7. Schematic representation of microbial biofilm development, adapted from bacterial biofilm (López and Soto, 2019).

1.4. Interest of microalgae

Microalgae have been widely recognized as a potential source for biodiesel, livestock feed/food and high-valuable compounds. Examples are given hereafter:

Human nutrients Humans have been consuming algae as a supplementation and food source for thousands of years. Because of in-rich bioactive composition (see Fig. 1-8), such as carbohydrates, fatty acids, amino acids, pigments, vitamins, etc., microalgae have become one of the forward-looking solutions for sustainable food sources with nutritional qualities and functional values (Barkia et al., 2019; Kent et al., 2015; Kusmayadi et al., 2021).

For instance, microalgae produce the long-chain polyunsaturated fatty acids (LC-PUFAs) like docosahexaenoic acid (DHA) and eicosapentaenoic acid (EPA), which are well-known omega-3 fatty acids in human nutrients and play important roles in our neural system and immune system (Boelen et al., 2013; Uauy et al., 2000).

Chlorella and *Spirulina* are the first commercial microalgae (commercialized in 1950s and 1970s, respectively) since they contain a high level of polysaccharides, amino acids and other health-enhancing nutrients (Hoseini et al., 2013; Hudek et al., 2014; Liu and Hu, 2013). *Haematococcus* and *Dunaliella* also have huge potentials to accumulate antioxidants, e.g., ketocarotenoid and astaxanthin, under certain conditions (Lemoine and Schoefs, 2010; Seabra and Pedrosa, 2010; Xu and Harvey, 2019). Therefore, microalgae, as a food supplementation for human, has a great development prospect in market.

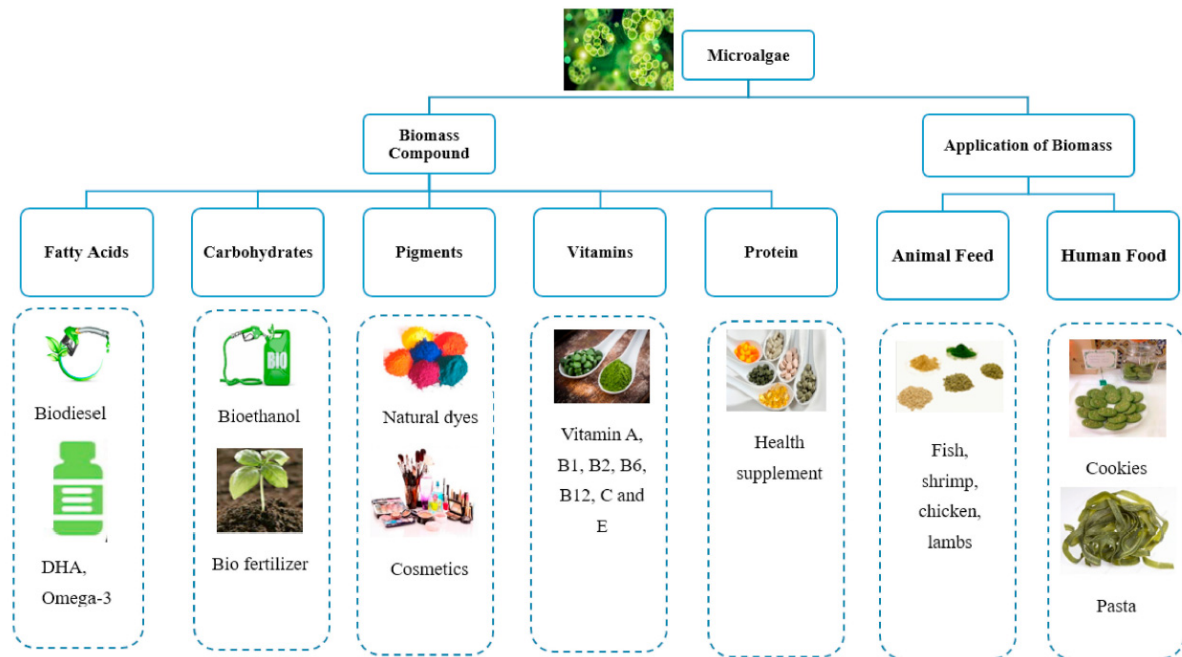


Figure 1-8. Bio-products acquired from algal biomass and their applications (Kusmayadi et al., 2021).

Animal/aquaculture feed Microalgae show high nutritional values for animals due to their bioactive compounds. In poultry diets, microalgae (*Arthrospira platensis*) biomass dried powder is used as the dietary substitution of soy protein, which distinctly improved meat quality (more tender and softer), increases the meat color and reduces metallic flavor and hardness (Altmann et al., 2018). Live microalgae can be used as aquaculture feeds for all growth stages of bivalve mollusks (like mussels, scallops and oysters), and for the juvenile stages of crustaceans and some fish (Sirakov et al., 2015). Additionally, as an additive in aquaculture, microalgae can increase fish weight (triglyceride and protein contents in muscle) and improve their resistance to diseases (Fleurence et al., 2012; Sirakov et al., 2015).

Pharmaceuticals The health-promoting effects of bioactive molecules, such as long-chain polyunsaturated fatty acids, chlorophyll, carotenoids, phycobiliproteins and enzymes

make microalgae important sources of those pharmaceuticals (Yan et al., 2016). Some microalgae extracts show antiviral, antimicrobial, and antifungal properties. Extracts from *Chlorella* and *Spirulina* are also added as ingredients into the skincare and haircare products (Jha et al., 2017). In a review (Skjånes et al., 2021), where the data was mainly collected from *Chlorella* strains, the authors illustrated the potential application of microalgae in anti-cancerous drugs. Due to the GRAS (generally recognized as safe) status of microalgae, a broad field of microalgae application in human nutrients, feeds, and pharmaceuticals are thus developed (Jha et al., 2017; Molino et al., 2018).

Wastewater treatment Water pollution has become an environmental issue of global concern. Numerous chemical compounds in municipal, industrial, and agricultural waters, showing high loads of nutrients (N and P), heavy metals and micro-plastics, threaten our nutrition and health (Wollmann et al., 2019). Microalgae cultivation provides the possibility to efficiently remove the pollutants along with biomass/energy production. To date, the main species participating in algae-based wastewater treatment (WWT) are *Chlorophyta* microalgae, such as *Chlorella* and *Scenedesmus*, and cyanobacteria like *Oscillatoria*., and *Anabaena ssp.* (Abinandan and Shanthakumar, 2015; Cuellar-Bermudez et al., 2017; Martins et al., 2011). The algae-based WWT presents considerable advantages: 1) cleans up the water bodies and reduces hazardous contaminations (e.g., heavy metals and micro-plastics); 2) produces useful biomass or energy-rich compounds (like carbohydrates and lipids); 3) provides oxygen for bacteria used in WWT plants, reducing energy input for aeration; 4) reduces greenhouse gases (GHG) emissions; and 5) reduces costs for water clean-up (Gouveia et al., 2016).

CO₂ fixation Microalgae are light-driven cellular factories that convert atmospheric CO₂ into raw materials for human food and renewable biofuels. Microalgae cultivation represents therefore an attractive approach to sequester CO₂ coming from fossil fuels combustion, natural decomposition and respiration, etc., consequently reducing the GHG effects. For instance, Tang et al. (2011) showed high rates CO₂ fixation by several microalgae species (0.260-0.288 g L⁻¹ day⁻¹; 0.887 - 0.993 d⁻¹) under a CO₂ feeding concentration ranging from 5% to 20%.

Compared to the other CO₂ capture and storage (CCS) technologies (e.g., chemical absorption, physical separation, oxy-fuel separation and supercritical CO₂ power cycles), CO₂ sequestration via microalgae presents several advantages: 1) it reduces the utilization of solvents while producing renewable materials and 2) it presents lower operational costs than the convention technologies (Klinthong et al., 2015; Li et al., 2013; Razzak et al., 2017).

Biofuel production Over the past decades, the interest by biofuel production from microalgae has remarkably increased due to the fossil fuels depletion, their drastically increasing prices, and the rising recognition of their impact on global climate changes.

Microalgae generally contain 20–50% lipids on dry biomass basis, and some strains can even accumulate up to 70-90% lipids under some particular conditions (e.g., nutrients limitation, high light, high salinity, etc.) (Morales et al., 2021; Ng et al., 2017). Compared to oil producer crops, such as soybean, canola and sunflower, microalgae are expected to produce lipids 10 - 100 folds higher on each hectare of land (Greenwell et al., 2010; Schenk et al., 2008). After biomass harvesting, microalgae can be converted into biofuels, such as biomethanol by fermentation, biodiesel by the transesterification of lipids, and fuel gases (e.g., H₂) through biomass gasification (Razzak et al., 2017).

Despite these benefits, microalgae cultures also pose many challenges, including slow growth in conditions triggering high lipid content and high energy demand in downstream processing (Pienkos and Darzins, 2009). Understanding the genetic and metabolic regulations of lipid metabolism using genomic approaches may be helpful for strain improvement, maybe increasing the cost-effectiveness of biofuels production by microalgae (Sharma et al., 2018). Furthermore, technological innovation on downstream processes is also required.

1.5. Why *Chlorella vulgaris*?

In this thesis, we will focus on biofilms of *C. vulgaris* which is a green microalga with a spherical structure and 2-10 µm in diameter. The schematic ultrastructure of *C. vulgaris* is shown in Fig. 1-9 (Safi et al., 2014).

Due to the high photosynthetic efficiency, high reproductive rate, structural robustness, and adaption plasticity to complex conditions, it is often used as a model organism to investigate the effect of environmental parameters on growth and metabolism, in general (Lou et al., 2021; Safi et al., 2014; Slaveykova and Wilkinson, 2002).

Besides, *C. vulgaris* is also an attractive strain to produce compounds, such as carbohydrates, lipids, proteins, vitamins and minerals, etc. (Ru et al., 2020). The following composition has been reported: carbohydrate (20 – 40%), lipid (14 – 55%) and protein (51–58%) (Markou et al., 2015; Nordin et al., 2019). Under some particular conditions (high

light, high temperature, high salinity, nutrients limitation, etc.), the accumulation of carbohydrates and/or lipids may be further enhanced (Chia et al., 2015; Yun et al., 2019).

C. vulgaris biomass is largely used as human food/nutritional supplements, in aquaculture and for bioenergy production (e.g., biodiesel, bioethanol and biomethane) (Ahmad et al., 2020; Sakarika and Kornaros, 2019; Shalaby and Yasin, 2013). Other applications are also well-known in WWT, for instance, for inorganic ions, heavy metals and CO₂ mitigation. Taken together, *C. vulgaris* is a promising algal species for laboratory research and large-scale cultivation.

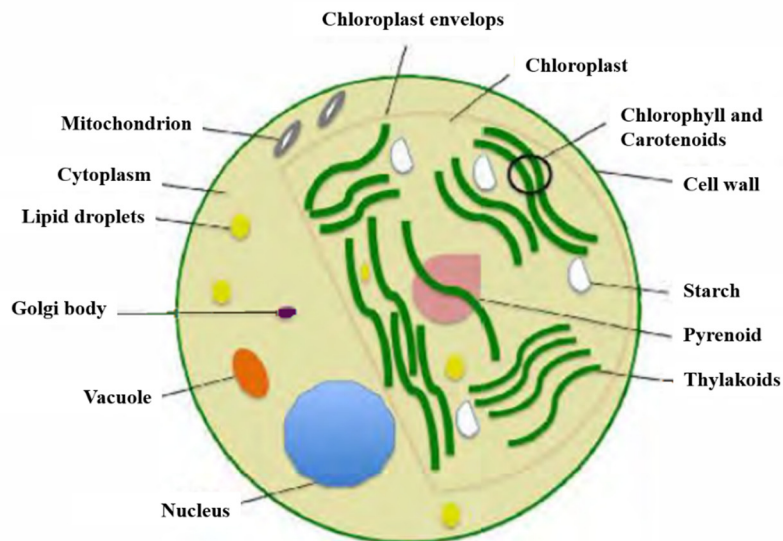


Figure 1-9. Schematic ultrastructure of *C. vulgaris* representing different organelles (Safi et al., 2014).

B- Microalgae cultivation systems

To date, numerous microalgae cultivation systems have been designed with the goal of achieving cost-efficiently high biomass productivity. According to microalgae lifestyle, cultivation systems can be divided into two main groups: **suspended cultivation systems** and **immobilized cultivation systems**. In this section, different types of cultivation systems are illustrated with several examples. On the basis of the production target, economic and operational feasibility, the most appropriated system for microalgae cultivation is chosen after weighing advantages and disadvantages of each design.

2. Suspended cultivation systems

1.1. Open systems

Outdoor open ponds (or raceways) are the simplest and most common systems for microalgae cultivation (Fig. 1-10 a). They have been widely used for large-scale microalgae cultivation for biomass and biofuel production, wastewater treatment and CO₂ mitigation (Ashokkumar and Rengasamy, 2012; Jo et al., 2020; Nielsen et al., 2011; Rayen et al., 2019). One of the major advantages of open ponds is that they are easier to construct and operate compared to most closed systems. However, those systems also show some drawbacks, such as poor light use efficiency, low biomass concentration (generally around 0.5 - 1 g L⁻¹) (Pienkos and Darzins, 2009), huge evaporation losses and large requirement of land space. In addition, contamination by predators, pathogens, and other algae restricts the growth of the targeted strains. Another noteworthy point is that efficient mixing through several devices (like paddle wheels) in order to avoid poor mass transfer are extremely energy demanding (Borowitzka, 1999; Kumar et al., 2015).

1.2. Closed systems

In order to overcome drawbacks of raceways, various closed systems have been designed (Fig. 1-10 b-f). In these systems, microalgae are cultivated in column, tubes, bags or other transparent materials without being directly exposed to the atmosphere, which can therefore

B - Microalgae cultivation systems

reduce the probability of contamination and evaporation. Mono-algal species can therefore be cultivated in closed photo-bioreactors (PBRs). In addition, due to the better light utilization and gas transfer, the cultures grown in closed PBRs usually present higher biomass density (around 20 g L^{-1}) and productivity than those in open systems (Ugwu et al., 2008; Wang et al., 2012). At present, the commonly used closed systems are tubular, vertical-column, plat-plate, thin-film and hemispherical PBRs. However, these reactors also exhibit limitations for large-scale microalgae cultivation, such as the high costs for system installation and maintenance, and surface biofouling, etc.

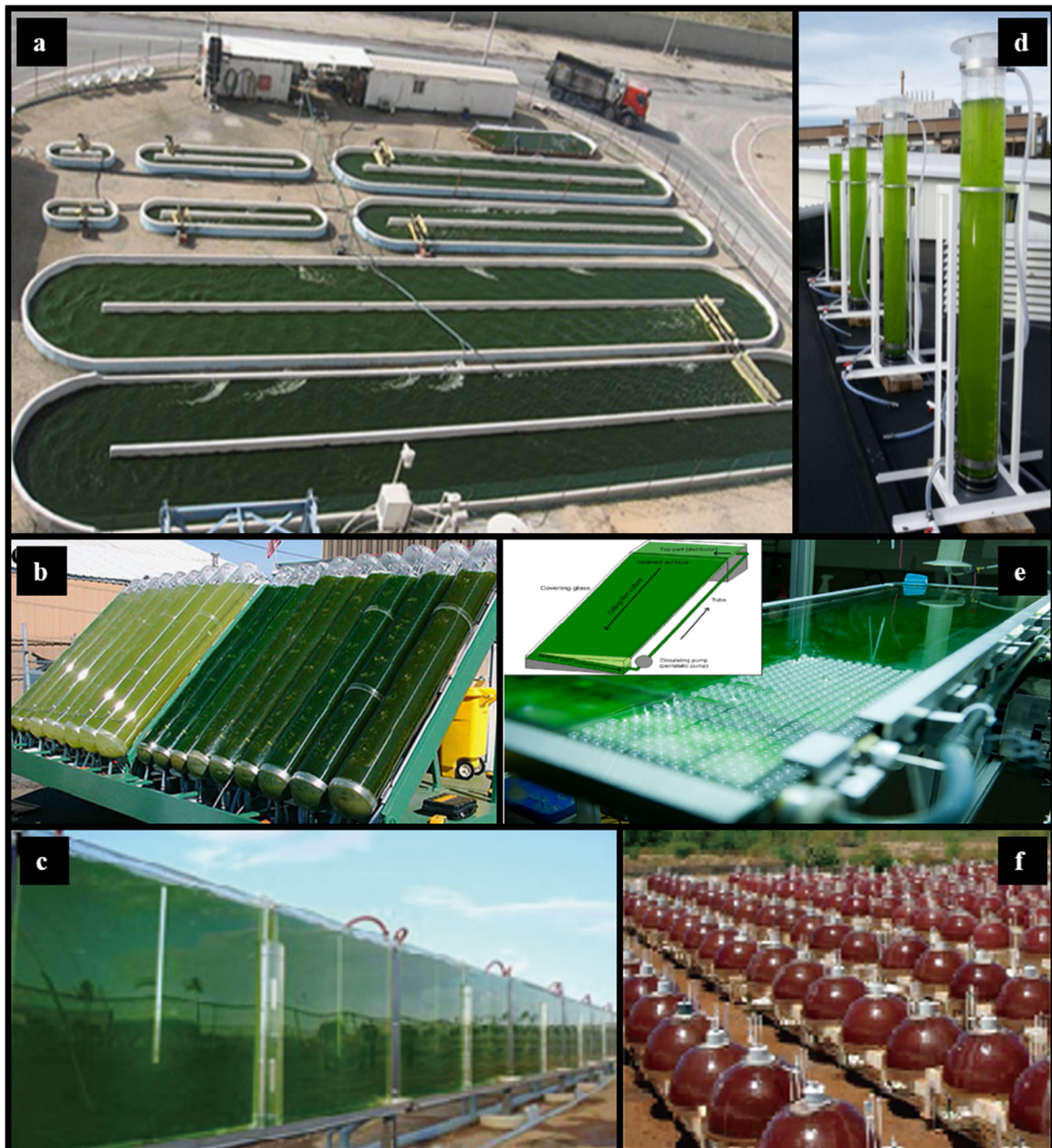


Figure 1-10. Suspended systems for microalgae cultivation. a) Open raceway ponds, b) Tubular PBRs and c) Flat-plate PBRs (Bitog et al., 2011); d) Vertical-column PBRs, <https://www.abire.org/consortium/sst/>; e) Thin-film PBRs (Pruvost et al., 2017); f) Hemispherical PBRs, <http://pt.slideshare.net/supplementalscience/astaxanthin-slides>.

However, no matter open ponds or closed PBRs, they all show: low biomass concentration, high water demand, high harvesting and dewatering energy costs, which all impact negatively the economics of microalgae cultivation. Therefore, more cost-efficient cultivation technologies must be developed.

3. Immobilized cultivation systems

Cells can be either entrapped in an optically transparent polymeric matrix (e.g., carrageenan, alginate, chitosan; enclosure method), or immobilized on the surface of supports/carriers forming biofilms (non-enclosure method) (Katarzyna et al., 2015; Mallick, 2002). Enclosed cultivation systems are capable of protecting cells against shear stress and contaminations, and have been successfully used to grow a series of robust algal species, such as *C. vulgaris* (Nguyen-Ngoc and Tran-Minh, 2007), *Haematococcus pluvialis*, *Botryococcus braunii* (Rooke et al., 2011) and *Cyanidium caldarium* (Homburg et al., 2019). However, due to the high prices of polymeric matrix, the scaling-up of this configuration is very difficult. Therefore, with respect to the immobilized systems, here we only focus on the non-enclosure methods: biofilm-based approaches, and in this thesis the words “immobilized” and “sessile” cells/cultures will specifically refer to the surface attached cells/cultures.

Depending on the applications, various microalgae biofilm systems have been designed and constructed in past years. Researchers grouped them based on the geometry configurations, design, operation strategies and support materials (Choudhary et al., 2017; Hoh et al., 2016). For instance, they can be classified into constantly submerged, intermittently submerged and perfused biofilm systems according to the relative position of medium and immobilized microalgae, or be sorted into vertical, angled and horizontal systems based on the orientation of the support configuration (Berner et al., 2015; Zhuang, 2018). Some systems are presented in Fig. 1-11. Algal footprint or surface productivities in those systems under different conditions are also displayed in Table 1-1, Table 1-2 and Table 1-3.

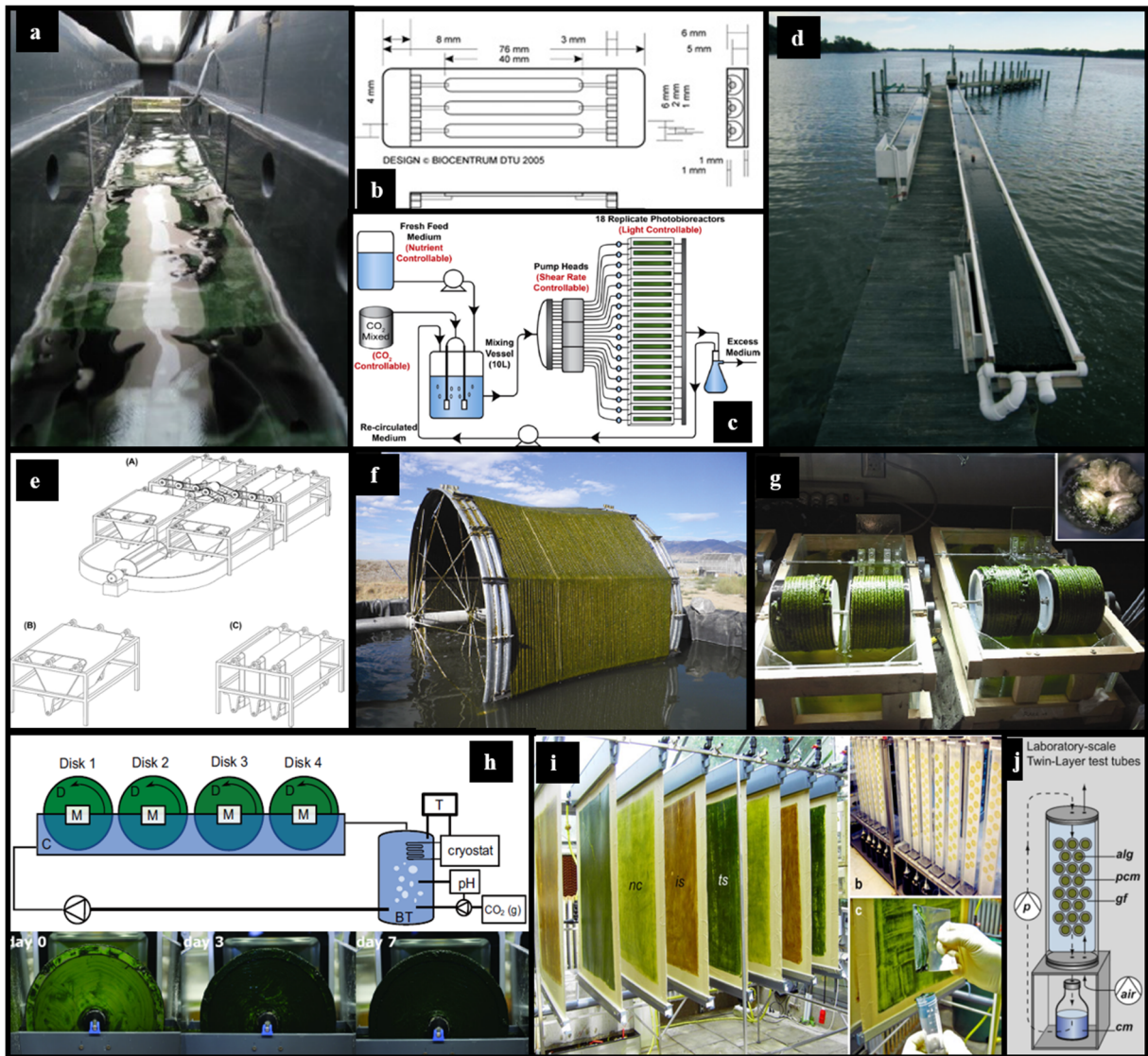


Figure 1-11. Biofilm-based systems for microalgae cultivation. a) Flow-lane system (Guzzon et al., 2019), b) Microfluidic flow cell system (Nielsen et al., 2011), c) Flat plate parallel horizontal photobioreactor system (Schnurr et al., 2013), d) Algal turf scrubber system (Adey et al., 2013), e) Revolving algal biofilm system (Gross and Wen, 2014), f) and g) Rotating algal biofilm reactor (Bernstein et al., 2014), h) Algadisk lab scale reactor (Blanken et al., 2014), i) and j) Twin-layer system (Schultze et al., 2015).

2.1. Constantly submerged biofilm systems

Constantly submerged biofilm systems (Fig. 1-11 a-c, Table 1-1) are generally designed as channels, where microalgae biofilms and the substrates they attach to are covered by a thin layer of liquid, which could be moved by a pump or the gravity generated by a small angle. The typical submerged-based systems are flow-lane incubators (Bruno et al., 2012; Guzzon et al., 2021, 2019, 2008; Zippel et al., 2007) and microfluidic flow cells (Boelee et al., 2011; Fanesi et al., 2021; Irving and Allen, 2011; Le Norcy et al., 2019).

The flow-lane system has been reported as a standardized laboratory incubator for investigating the effect of the environmental factors (Guzzon et al., 2021, 2019, 2008; Zippel et al., 2007). Guzzon et al. (2019) also used this system to investigate the photosynthetic performance of algal-bacterial biofilms and the feasibility of these communities to treat wastewater under different light intensities, flow velocity and temperature. Biomass productivity of $0.01 - \sim 2.10 \text{ g m}^{-2} \text{ d}^{-1}$ was reported in this study. Using this type of system, Bruno et al. (2012) acquired a slightly higher productivity at $3.3 \text{ g m}^{-2} \text{ d}^{-1}$ for cyanobacteria biofilms.

Microfluidic flow cells are optically transparent systems, often combined with confocal laser scanning microscopy (CLSM) to characterize the kinetics of growth and architectures of microalgae biofilms (Fanesi et al., 2021, 2019; Le Norcy et al., 2019). A flow cell with the PVC (polyvinyl chloride) plastic sheet has been also used as a bioreactor to test the potential of microalgae biofilms for removing both N and P from municipal wastewater. A biomass productivity in a range of $2.1-7.7 \text{ g m}^{-2} \text{ d}^{-1}$ was reported here (Boelee et al., 2011). Both systems seem to be ideal tools in tracking dynamics of algal biofilm development under various conditions at lab-scale.

Besides, other constantly submerged systems, like horizontal flat panel (HFP) photo-bioreactor can be used to test nutrients removal efficiency by microalgae biofilms. As shown by Sukačová et al. (2015), $97 \pm 1\%$ of total P from wastewater was removed within only 24 h in a HFP reactor and algal biofilm achieved a biomass production rate up to $12.21 \pm 10 \text{ g m}^{-2} \text{ d}^{-1}$.

2.2. Intermittently submerged biofilm systems

According to the moving parts, intermittently submerged systems (Fig. 1-11 d-h, Table 1-3) can be sorted into two groups: 1) stationary systems, like algal turf scrubber (ATS), in which the medium periodically flow through immobilized cells, and 2) rotation systems, e.g., rotating algal biofilm photo-bioreactor (RABR), where the supports (like algal disk and conveyor belt) periodically move through liquid medium. In both systems, algal biofilms are exposed either to fresh medium/liquid phase or in contact with light and atmospheric CO_2 intermittently. This might be one reason why intermittently submerged systems sometimes show an excellent performance in terms of biomass productivity (Blanken et al., 2017;

Huang et al., 2016; Li et al., 2017). For instance, an ATS system was yearly employed by Adey et al. (2013) to examine the effect of support material on algal productivity. Results of this work reported productivity as high as 60 -70 g m⁻² d⁻¹ in August and September, and a yearly average productivity of 36.9 g m⁻² d⁻¹. In addition to algal biomass production, ATS system has been proved as a relative mature configuration for wastewater bio-remediation (Craggs et al., 1996; Kebede-westhead et al., 2003; Mulbry et al., 2010).

RABRs have been extensively used for microalgae biofilm cultivation and wastewater treatment (Bernstein et al., 2014; Gross et al., 2013a; Hillman and Sims, 2020; Iman Shayan et al., 2016). Christenson and Sims (2012) showed that their designed RABR can achieve an effective nutrients removal rate (2.1 g m⁻² day⁻¹ for dissolved P and 14.1 g m⁻² day⁻¹ for dissolved N) and a high biomass productivity up to 31 g m⁻² d⁻¹. In this case, an efficient spool harvesting approach was also proposed to obtain the concentrated biomass (12-16% solids). This brings new evidence that biofilm-based cultivation methods outcompete their suspended analogs, particularly in terms of reducing the capital costs in downstream (harvesting and dewatering) processes.

However, challenges have been recognized regarding these intermittently submerged systems: at low speed, immobilized cells may be dehydrated and/or photo-inhibited when exposed to the air phase due to a long irradiance-exposure interval, especially under high light; in contrast, the large shear force caused by high velocity may lead to biomass detachment. Therefore, flow/rotation rate optimization is needed for the design/operation of those systems.

2.3. Perfused biofilm system

Perfused biofilm system (Fig. 1-11 i and j, Table 1-3), also called as “Twin-Layer system”, is characterized by the separation of immobilized cells from bulk water through a support. While cells are in direct contact with air and light, nutrients and moisture are provided through diffusion/evaporation force (Podola et al., 2017). In perfused systems, supports are generally porous materials, e.g., filter membranes (Dora Allegra Carbone et al., 2017; Nowack, 2005), printing paper (Naumann et al., 2013), or artificial textile materials (Zhang et al., 2015), which guarantee the nutrients mass transfer and water supplement.

Due to the absence of a liquid phase over the biofilm, these systems present some benefits: 1) reducing light attenuation resulting from the absorption and/or reflection by suspended

particles (Podola et al., 2017); 2) allowing immobilized cells to contact the gas phase directly, thus potentially improving algal photosynthesis and consequently biofilm growth (Huang et al., 2016); 3) minimizing the shear stress forces and thus avoiding biomass losses, and 4) reducing water consumption. Nevertheless, some challenges must be overcome when using such perfused systems. For instance, there is a rising risk for biofilms suffering dehydration. Maintaining a high humid environment is therefore crucial for successful biofilm cultivation in perfused systems (Naumann et al., 2013). In closed reactors or greenhouse, the humid air circulating around with air pumps might be a solution, as described by Shiratake et al. (2013), but it will undoubtedly increase the operational costs. On the other hand, algal biofilms, in particular the thick or compact ones, are vulnerable to the nutrients diffusive limitation. Based on this, harvest frequency optimization is of utmost importance to maintain the high productivity of those systems.

Do et al. (2019) adapted an angled Twin-Layer Porous Substrate Photo-bioreactor (TL-PSBR) to assess the effect of inoculum density and storage duration (inoculum storage period at 4 °C before immobilization) on biomass and astaxanthin productivities of *H. pluvialis*. After 24-h storage together with a starting density of 5 g m⁻², biomass and astaxanthin productivities of 8.7 g m⁻² d⁻¹ and 170 mg m⁻² d⁻¹ were achieved, respectively. Another perfused system was described by Liu et al. (2013) for outdoor *Scenedesmus obliquus* biofilms for biofuel production. High biomass productivity in a range of 50–80 g m⁻² d⁻¹ was here reported. In addition to biomass and compounds production, perfused systems have been also used for wastewater nutrients recovery (González et al., 2020; Shi et al., 2007).

2.4. Other sorted biofilm systems

According to the geometry of the configuration, current algal biofilm-based systems can also be grouped into horizontal and vertical systems. Compared to horizontally-oriented systems, vertical reactors present the additional advantage of reducing the footprint area. However, care must be taken regarding the distance between the cultivation modules to avoid the self-shading. Zhang et al. (2018) optimized the distance between modules in a vertical-algal-biofilm enhanced raceway pond for nutrient removal and biodiesel production. They showed that the light availability for microalgae increased with the interval distance between modules (from 2 to 8 cm), and the maximal nutrient removal efficiency was

achieved at an operation distance of 6 cm. It is worth noting that the operation distance is generally dependent on the size of modules (Sukačová et al., 2020; Zhang et al., 2018).

Table 1-1. Constantly submerged systems.

System	Inoculum	Light ($\mu\text{mol photons m}^{-2} \text{s}^{-1}$)	Substrate	Flow rate	Productivity ($\text{g m}^{-2} \text{d}^{-1}$)
Reference	Conditions [$^{\circ}\text{C}$,% CO_2]	Light/dark (h:h)	Cultivation area (m^2)	Medium	Duration
Flow-lane incubator	Biofilm community from sedimentation tank of WW plant	15-120	Polycarbonate slides	25 and 100 L h^{-1}	$\sim 0.5 - \sim 2.0$
(Zippel et al., 2007)	20-21.5 $^{\circ}\text{C}$	16 h L:8 h D	0.0019	BG 11	35d (most assays)
Flow-lane incubator	Biofilm community from sedimentation tank of WW plant	15-120	Polycarbonate slides	25 and 100 L h^{-1}	0.01-2.10
(Guzzon et al., 2019)	20 or 30 $^{\circ}\text{C}$	N.R.	0.0019	BG 11	30d
Flow-lane incubator	Cyanobacterial biofilm	90	Polycarbonate slides	25 L h^{-1}	0.02-3.33
(Bruno et al., 2012)	25 $^{\circ}\text{C}$	16 h L:8 h D	N.R.	BG 11	25-30d
Flow cells	Biofilm community from settling tank of WW plant	230	Plastic sheet	0.3-5 L min^{-1}	2.1-7.7
(Boelee et al., 2011)	22 $^{\circ}\text{C}$	Continuous	0.018	Synthetic wastewater effluent	15d
Aquarium	<i>Chlorella vulgaris</i> <i>Scenedesmus dimorphus</i>	100	stainless steel polypropylene acrylic polycarbonate	30 mL s^{-1}	12.2 (mixotrophic growth) 5.1 (autotrophic growth) 5.3 (mixotrophic growth) 2.8 (autotrophic growth)
(Roostaei et al., 2018)	25 $^{\circ}\text{C}$	12 h L:12 h D	0.0015	MB3N, WW (/glucose)	9d
Horizontal flat panel photobioreactor	Biofilm community from the pools of a rendering plant	Sunlight	Concrete slab	Concrete slab	5.6 \pm 1
(Sukačová et al., 2015)	19-24 $^{\circ}\text{C}$	14 h L:10 h D	2	2	5d
Horizontal flat panel photobioreactor	Biofilm community from the pools of a rendering plant	90	Concrete slab	8.8 L min^{-1}	12.21 \pm 10
(Sukačová et al., 2015)	19-24 $^{\circ}\text{C}$	Continuous	0.06	Artificial wastewater	4d

N.R. Not reported; WW plant, wastewater treatment plant.

Table 1-2. Intermittently submerged systems.

System	Inoculum	Light ($\mu\text{mol photons m}^{-2} \text{s}^{-1}$)	Substrate	Cultivation mode	Productivity ($\text{g m}^{-2} \text{d}^{-1}$)
Reference	Conditions [$^{\circ}\text{C}$, % CO_2]	Light/dark (h:h)	Cultivation area (m^2)	Medium	Duration
Algal turf scrubber	Biofilm community from a bay	Sunlight	Fiberglass troughs	Semi-continuous	36.9 (yearly average productivity)
(Adey et al., 2013)	Outdoor	N.R.	9.3 or 14.9	Brackish water from a bay	Every 7d or 14d harvest/regrowth (22 months)
Pilot-scale rotating algal biofilm system	<i>C. vulgaris</i>	Average: 642	Cotton duct	Semi-continuous	1.99 ± 0.15 (January–February) [#] 4.29 ± 0.23 (May–June) [#]
(Gross et al., 2013b)	Average: 25.5 $^{\circ}\text{C}$, Greenhouse	Algal production greenhouse	3.5	Modified BBM	Every 3, 5, 7 or 10d harvest/regrowth
Lab-scale Rotating algal biofilm system	<i>C. vulgaris</i>	110-120	Cotton duct	Semi-continuous	3.51 ± 0.048 [#]
(Gross et al., 2013b)	25 $^{\circ}\text{C}$, 0.03 % CO_2	Continuous	0.045	Modified BBM	7d
Pilot-scale revolving algal biofilm system	<i>C. vulgaris</i>	Natural light	Cotton duct	Regrowth	5.8 [#]
(Gross and Wen, 2014)	11-35 $^{\circ}\text{C}$, Greenhouse	N.R.	2.94 or 1.85	Modified BBM	Every 7d harvest/regrowth (yearlong)
Rocking cultivation chamber	<i>C. vulgaris</i>	100	Stainless steel	Batch	0.04 ± 0.01 [#]
(Shen et al., 2014)	26 ± 2 $^{\circ}\text{C}$	Continuous	0.019	Modified BBM	15d
Rotating flat plate photobioreactor	<i>C. vulgaris</i>	139	Polyvinyl chloride, polypropylene	Regrowth	0.13, 0.26, 0.46
(Melo et al., 2018)	22 ± 2 $^{\circ}\text{C}$	12 h L:12 h D	0.0004	BBM/2	Harvest cycles of 8 days

N.R. Not reported. [#] donates the productivity based on the surface area of the attaching material.

Table 1-3. Perfused systems.

System	Inoculum	Light ($\mu\text{mol photons m}^{-2} \text{s}^{-1}$)	Substrate	Medium supply mode	Productivity ($\text{g m}^{-2} \text{d}^{-1}$)
Reference	Conditions [$^{\circ}\text{C}$, % CO_2]	Light/dark (h:h)	Cultivation area (m^2)	Medium	Duration
Algal disk/vertical plate photobioreactor	<i>Scenedesmus obliquus</i>	Natural solar radiation (outdoor) Indoor irradiance	Cellulose acetate/nitrate membrane	Dripped in	50-80 (outdoor), 108.1-119.3 (indoor)
(Liu et al., 2013)	$30 \pm 2^{\circ}\text{C}$, 2% CO_2	N.R.	0.001	BG 11	7d (outdoor), 3d (indoor)
Twin-Layer biofilm Photobioreactor	<i>Haematococcus pluvialis</i>	400-600	Kraft paper	Pumped in	8.75*
(Do et al., 2019)	$23-26^{\circ}\text{C}$, 1% CO_2	Continuous	0.05	BG-11	10d
Vertical phototrophic biofilm reactor	Biofilm community from settling tank of WW plant	180	Polyethylene-based woven geotextile	Dripped in	7 (average value)
(Boelee et al., 2014)	21°C , CO_2 in medium	Continuous	0.125	Synthetic wastewater	Every 2,4 and 7d harvest/regrowth
Porous substratum biofilm reactor	<i>C. vulgaris</i>	Sunlight	Canvas	Diffusion (capillary forces)	52*
(Shen et al., 2017)	$26-42^{\circ}\text{C}$, 5% CO_2	Light/ dark	N.R.	Wastewater	5d
Twin-Layer biofilm photobioreactor	<i>Halochlorella rubescens</i>	1023	Polycarbonate membranes	Pumped in	31.2*
(Schultze et al., 2015)	$28.0-31.5^{\circ}\text{C}$, 3% CO_2	14 h L:10 h D	2.54×10^{-4}	1:2 ASP12:BBM	3d

N.R. Not reported; WW, wastewater treatment plant; * represents the largest productivity with the best combination of cultivation factors.

4. Advantages of biofilm-based culture systems compared to suspension systems

In the past years, microalgae biofilm-based cultivation technologies gain more and more attention, and various innovative systems have been designed and operated. Along with the unceasing research, several remarkable characteristics of the biofilm-based systems can be underlined. Advantages compared to the conventional suspended designs are reported hereafter:

- Better light penetration and shortened mass transfer pathway (nutrients, gases and metabolites) (Huang et al., 2016; Podola et al., 2017);
- Higher biomass density (~10 - 20% biomass content) (Christenson and Sims, 2012; Gross et al., 2013a; Sebestyén et al., 2016) and productivity (Table 1-4) (Christenson and Sims, 2012; Lee et al., 2014);
- Lower operation (mixing, harvesting and dewatering) costs (Christenson and Sims, 2012; Morales et al., 2020); and
- Considerably lower water requirement (Ozkan et al., 2012).

Though biofilm-based systems exhibit such advantages, this cultivation technology is still at its infancy stage. Further efforts focusing on the design of cost-efficient systems should be made. In addition, studies on biofilm-based microalgae cultivations on long-term and at large-scale should be also carried out to fully confirm their potential for several applications (bio-actives, biofuel production, etc.).

Table 1-4. Comparison of suspended and biofilm-based cultivations.

Reference	Biofilm			suspension		
	System	Duration	Productivity	System	Duration	Productivity
(Gross et al., 2013a)	Rotating algal bio-film reactor	7 days	3.51 g m ⁻² d ⁻¹	Flat panel photobioreactor	7 days	0.26 g L ⁻¹ d ⁻¹
(Gross and Wen, 2014) [#]	Triangular, vertical evolving algal bio-film system	7 days	8.51 g m ⁻² d ⁻¹ 18.92 g m ⁻² d ⁻¹	Raceway pond	7 days	5.5 g m ⁻² d ⁻¹
(Lee et al., 2014) [#]	Attached algal system in pond	18 days	13.5 g m ⁻² d ⁻¹	Raceway pond	18 days	6.1 g m ⁻² d ⁻¹
(Huang et al., 2016) [*]	Twin-layer system	7 days	7-12.5 g m ⁻² d ⁻¹	Closed glass serum bottle	7 days	1-9 g m ⁻² d ⁻¹
(Christenson and Sims, 2012) [*]	Rotating algal bio-film reactor	18 days	0.11 g m ⁻² d ⁻¹	Water tank	26 days	0.015 g L ⁻¹ d ⁻¹

^{*}represents the rough productivity calculated from figures in the cited study. [#] donates the maximal productivity reported in this study.

C- Process operational factors impacting bio-film development and productivity

From initial cell attachment to the dispersal phase, biofilm-based processes are affected by many factors. For artificially cultured biofilms, these factors are generally the nature of the support, the inoculum process, hydrodynamics of the system, environmental parameters (light availability in terms of quality and intensity, nutrients concentration, temperature, pH, etc.), and other factors such as harvesting frequency. In this thesis, the parameters that affect algal biofilm cultivation were all termed as operational factors.

1. Operational factors - Support

Numerous research works have studied the growth performance of microalgae biofilms on different materials. However, only few of them further quantified the effect of material properties, including the surface micro-texture and physical-chemical properties, like surface hydrophobicity, roughness and surface chemical groups, on microalgae adhesion and biofilm development (Gross et al., 2016; Ozkan and Berberoglu, 2011; Palmer et al., 2007; Roostaei et al., 2018; Sekar et al., 2004). Moreover, most of these studies only considered one or several properties at one time, which might not be able to fully reflect the influence of materials, hence, more comprehensive researches are need in the future. Fig. 1-12 shows the most important support properties that can mediate microbial adhesion and biofilm formation.

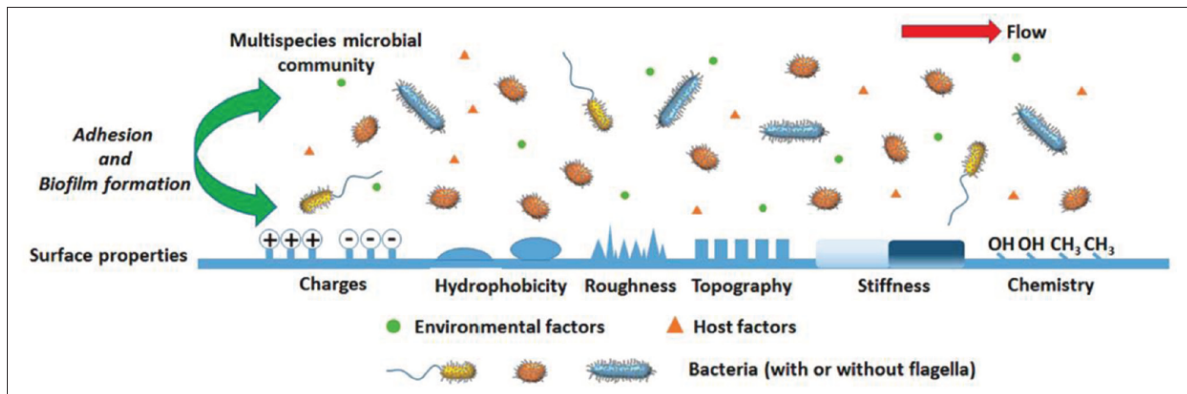


Figure 1-12. Schematic illustration of bacterial adhesion and the effects of material properties on cells adhesion and biofilm formation (Song et al., 2015).

1.1. Surface micro-texture

It has been shown that microalgae attachment and growth are strongly affected by the surface micro-texture.

The interaction between a cell and a support has been described by the contact point theory proposed by Scardino et al.(2006) and Cui et al.(2013). It should be pointed out that the size and the settlement behavior of the target cell (Callow et al., 2002) are taken into account in this thermodynamic approach. Accordingly, the energy required for adhesion to occur (W) is expressed as follows (Cui et al. 2013):

$$W = \gamma \times \Delta A \quad (1)$$

where γ stands for the support surface free energy and ΔA is the change of support surface area due to the cell attachment (see below, Fig. 1-13).

For a material with a certain surface free energy (γ), the less change in the support surface area (ΔA), the less energy is needed for adhesion to occur, thus the easier for a cell to settle down.

Fig. 1-13 (Cui et al. 2013) shows the three possible patterns of a cell in close contact with a support: aligning, conforming and bridging.

If the cell settles in an aligning mode (on a flat region of the support), the support surface area will be increased. The increased part corresponds to the surface area of the cell minus the contact area between cell and the support. Therefore, with the expansion of the total surface area, more energy for cell settlement and attachment is required. In the bridging mechanism (cell diameter larger than pore size) the whole surface area is increased, more energy is thus required for adhesion to occur. Compared to the other two modes, cells settling into the pore of the support (conforming) apparently decreases the increase of total area of support due to the more contact points (Fig. 1-13). Therefore, less energy is required for cell attachment in this pattern.

Therefore, taking into account the contact point theory, a general trend can be predicted: the cell size close to the pore size of support benefits attachment and possibly further biofilm development, while either larger or smaller cell will reduce the contact points thus reducing the adhesion strength (Cao et al., 2009; Cui et al., 2013; Scardino et al., 2006).

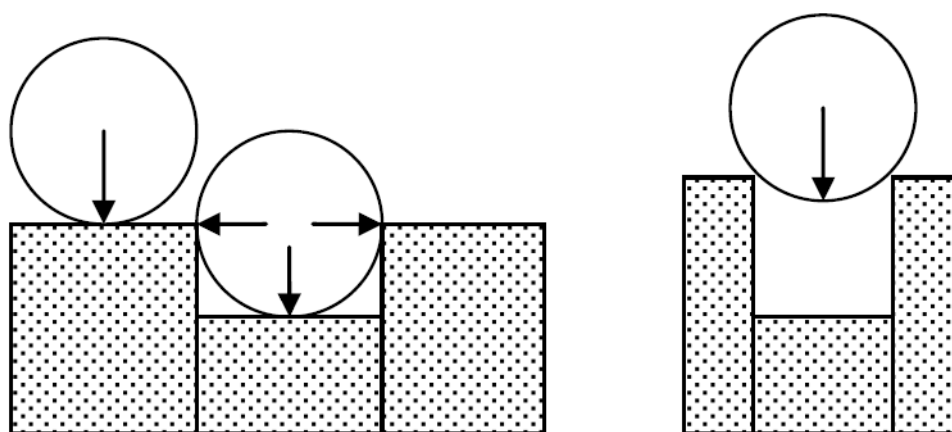


Figure 1-13. Schematic representation of cell attachment to different surface features. From left to right are aligning, conforming and bridging, respectively (Cui et al., 2013).

Sathananthan et al. (2013) monitored algal biofilm growth on different fabricated supports. A higher biomass productivity was obtained for the deep-groove support (20 μm) compared to that on shallow-groove (1.5 μm) or smooth supports. As explained by the authors, the deeper grooves are on the same size scale of the immobilized algal cells ($\sim 10\text{-}15\ \mu\text{m}$), allowing cells to embed into them.

Gross et al. (2016) also reported the highest attachment density of *C. vulgaris* for mesh

materials with an opening size of 0.5 mm compared to that of materials of 0.05 or 6.40 mm mesh size. From observations with scanning electron microscopy (SEM), the authors detected algal cell aggregates which exceeded the 0.05 mesh pore size. A decrease in the cell attachment to the 0.05 mm mesh opening supports was thus explained by the inability of algal aggregates to embed into the mesh pores. The authors also deduced that the low cell aggregates retention on larger mesh materials (6.40 mm) may be due to cell aggregates losses.

1.2. Surface roughness

Generally, cell adhesion increases with high surface roughness. This is likely due to the fact that a rougher support provides a higher contact area for cell adhesion compared to smooth ones. In addition, cells retained in surface grooves are protected from bulk hydrodynamic conditions. Asperities and hydrodynamic stagnant zones on rough supports can increase the ability for intercepting and retaining cells and thus increase cell adhesion, which will in turn improve the biomass yield (Sekar et al., 2004; Zhang et al., 2020).

According to the work of De Assis et al. (2019), the highest cell retention (defined as the firmly cell attachment to the substratum) capability on cotton compared with other tested materials (nylon and polyester) is certainly due to the higher roughness of this support. In another study, a linear correlation between *C. vulgaris* attachment capability and the support roughness has been reported as well (Tang et al. (2021).

However, some other researchers noticed that though the high surface roughness improves algal cells attachment, it shows no significant effect on the overall growth of microalgae biofilm afterwards (Irving and Allen, 2011; Schnurr and Allen, 2015; Zhang et al., 2020). This is mostly due to the fact that as a biofilm develops, newly generated cells growing far from the support surface are no longer affected by the surface properties.

1.3. Surface hydrophobicity

Some research works have demonstrated an increase of cell attachment with surface and cell hydrophobicity (Finlay et al., 2002; Ozkan and Berberoglu, 2013a). The theory behind is the

following: “hydrophobic molecules, particles, and cells, prefer a hydrophobic environment, and will therefore adhere to each other to minimize their contact with water” (Schnurr and Allen, 2015). However, contradictory results can be found in the literature. Indeed, some other studies reported weak or no correlation between the hydrophobicity of supports and cells immobilization (Genin et al., 2014; Irving and Allen, 2011). Ji et al. (2014) even observed that *Pseudochlorococcum sp.* cells preferred the hydrophilic membranes (including polyethersulfone, nylon, cellulose acetate, cellulose nitrate membranes). More biomass was accumulated on those supports compared to that on hydrophobic membranes. The discrepancy among data might be due to different algal strains employed, other support properties such as micro-texture, roughness, etc.

1.4. Chemical composition

At molecular level, the interaction between a cell and the support is affected by their surface functional composition. However, up to now, most information on this topic comes from bacteria biofilms (Consumi et al., 2020; Li and Cheng, 2019; Renner and Weibel, 2011; Shahzadi et al., 2018). Owing to the limited number of studies (Rajendran and Hu, 2016; Yuan et al., 2019; Zhang et al., 2020), the effect of functional groups involved in microalgae cell adhesion to a support remains unclear. Those functional groups mainly include hydroxyl, carboxylic, phosphoric, and amine groups, etc. (Renner and Weibel, 2011).

In summary, support selection is a critical step for the design of biofilm-based technologies as it affects strongly microalgae cells adhesion. Therefore, when researchers or producers select materials for microalgae biofilm cultivation, some criteria must be taken into account as following:

- High support roughness – the supports with high roughness may increase cells adhesion strength, for example, the “valleys” or “ridges” act as anchors sheltering cells from shear stresses. Artificially patterning the surface to increase support roughness can be also implemented.
- High hydrophobicity – a general trend is that hydrophobic surface benefits algal adhesion.

- Long durability – Supports structure must be kept during algal growth and harvesting cycles (Shen et al., 2015).

2. Operational factors – Microalgae/inoculum

The choice of microalgae depends on its properties (ability to form a biofilm, sensibility to culture conditions such as light, temperature, specific growth rate, ability to accumulate certain compounds, ...) and the target product.

In addition, the inoculation step is of prime importance for microalgae biofilms cultivation. In this thesis, the operational factors related to the inoculation stage were divided into four categories: inoculum density, inoculum time, algae species and their properties.

2.1. Inoculum density

Inoculum density is a crucial operational factor affecting microalgae biofilm growth and productivity. The increasing growth rate with inoculum size has been observed in the immobilized cultures of *Pseudochlorococcum sp.* (from 0.05 to 3–5 g m⁻²) (Ji et al., 2014), *B. braunii* (from 1.9 to 7.9-10.1 g m⁻²) (Cheng et al., 2018) and *C. vulgaris* (from 2.5 to 12.5 g m⁻²) (Huang et al. 2016). However, a significant reduction in growth rate and productivity were obtained for densities higher than the optimal which may be attributed to limitations in light and/or nutrients and quorum-sensing as the authors suggested.

Other studies confirmed that light penetration and nutrients transport are negatively impacted by increased biofilm thickness (Huang et al., 2016; Piciooreanu, 2000; Schnurr et al., 2014). On the other hand, quorum sensing, a well-known cell density-dependent mechanism, may inhibit biofilm further evolution (Fuqua et al., 2001; Sharif et al., 2008). Biofilm development inhibition associated to the declined expression of biofilm-related genes with increasing inoculum density have been observed in cyanobacteria and bacteria biofilms (Karatan and Watnick, 2009; Nagar and Schwarz, 2015; Sharif et al., 2008; Yildiz and Visick, 2009). And we believe that these mechanisms may also occur in eukaryotic microalgae biofilms.

However, up to now, knowledge about the effect of inoculum density on microalgae biofilm

cultivation is seldom available. More work should be thus carried out to better understand the underlying mechanisms.

2.2. Inoculum/colonization time

Microbial adhesion is divided into two main processes - reversible and irreversible attachment. Initially, cells get close to a surface in a state of reversible or temporary adhesion (cells, which continue to move along the surface, can be removed by gentle washing from the substratum). When cells reside for some critical time, they become irreversibly bound through the mediation of a cementing substance (such cells are no longer motile) (Characklis and Cooksey, 1983;Vigeant et al., 2002). Afterwards, growth occurs and biofilm evolves.

As reported by Genin et al. (2014), the colonization time (a period during which at least one cell layer covers the entire material) seems to be of utmost importance to biofilm formation and biomass productivity. It has also been reported that the attachment strength of diatoms increased with the length of inoculation time (Leadbeater and Callow, 1992; Woods and Fletcher, 1991). Therefore, the inoculum/colonization time as an operational factor should be also taken into account in microalgae biofilm-based cultivation process.

2.3. Microalgae species

It is known that productivity (biomass/products) is species-dependent. The selection of the microalgae genus/species is therefore one important optimization task to be considered when developing a biofilm-based process. Accordingly, Shen et al. (2014) tested six freshwater algae species for biofilm-based production of biomass. Their data showed that *Chlorococcum sp.* was the best candidate because of its highest adhesion rate and biomass productivity. Two screened lipid-rich microalgae, *Scenedesmus* SDEC-8 and *Chlorella* SDEC-18, were also cultivated by (Yu et al., 2020) using biofilm-based system.

According to (Irving and Allen, 2011), under sterile conditions, *S. obliquus* attained thicker biofilms ($54 \pm 31 \mu\text{m}$) than those of *C. vulgaris* ($7 \pm 6 \mu\text{m}$). This may be related to differences in extracellular properties of these two strains. Indeed, as the authors suggested, *S. obliquus* has

ability to produce large amount of EPS which together with bristles or spines on the cell wall may facilitate the cell-cell and cell-substrate attachments. In another study, differences in the attachment strength of four marine diatom strains to glass RFC (Radial Flow Chamber) discs were also observed, the strongest adhesion was recorded for *Amphora coffeaeformis*. This was explained by the fact that as a small algae, *A. coffeaeformis* produces a greater amount of adhesive mucilage relative to its cell size than larger species (Woods and Fletcher 1991).

2.4. Microalgae properties

Cell properties such as surface free energy, hydrophobicity, charge, EPS content/composition, and the inherent physiological properties like cell activity and cellular composition affect biofilm formation. Information on inoculum properties may help understanding the microalgae biofilm formation mechanisms.

Surface hydrophobicity/hydrophilicity is an important surface characteristic which impacts the interactions cells-to-cells and cells-to-supports. Although not universal, a general trend that hydrophobic surface benefits algal adhesion has been observed, as already mentioned before (Holland et al., 2004; Ozkan and Berberoglu, 2013a; Schilp et al., 2007).

Ozkan and Berberoglu (2013b) quantified the adhesion rates of the hydrophobic algae *Botryococcus sudeticus* and the hydrophilic algae *C.vulgaris* through the thermodynamic DLVO (Derjaguin-Landau-Verwey-Overbeek) and XDLVO (Extended Derjaguin-Landau-Verwey-Overbeek) models. Results show that *B. sudeticus* presented a higher adhesion rate and strength due to the strong attractive cell-cell and cell-substrata interactions. Additionally, the hydrophobicity of cells varies greatly among algal strains, which may be attributed to the differences in their cell wall structures and surface functional groups (Shen et al., 2014).

Surface charge of algae (electrostatic interactions) - Surface charge is another parameter associated with the initial adhesion (Shen et al., 2014; Xia et al., 2016). Due to the existence and abundance of surface functional groups such as carboxyl, phosphoryl and hydroxyl groups, microalgae generally present a negatively charged surface (Xia et al., 2016). However, these groups can be deprotonated or protonated based on the pH of system. Specifically, when microalgae are considered at low pH, these groups on cell wall are protonated, creating a net

positive surface charge. In contrast, these groups get deprotonated at high pH, resulting in a net negative surface charge. While at the intermediate pH, protonation is equal to deprotonation, resulting in surface charge neutralization known as the point of zero charge (PZC). These variations in surface charge can induce electrostatic repulsion or attraction of cells-to-supports and cells-to-cells, thus impacting biofilm formation (Bitton et al., 1980; Ozkan and Berberoglu, 2013a).

EPS - Studies showed that EPS matrix consist of polysaccharides, proteins, and DNA, etc. These compounds rich in functional groups such as carboxylate, phosphate, amine, which can accelerate the microbial adhesion to solid surfaces and enhance the interaction between cells and substrates (He et al., 2016; Lubarsky et al., 2010; Parikh and Chorover, 2006; Sheng et al., 2010).

EPS determine the micro-environmental conditions for biofilm cells by affecting matrix properties, e.g., hydrophobicity, charge, porosity, water content, density and mechanical stability (Flemming et al., 2007). EPS can also provide sites for nutrients absorption from solution, allowing microalgae accessible for the biofilm growth mode (Zhuang et al., 2016). Therefore, factors that increase EPS accumulation can improve microalgae biofilm formation and productivity, such as the presence of bacteria or some divalent cations.

It has been previously reported that pre-coated cotton with bacteria and their EPS improved *Scenedusmus* biofilms growth. After a period of 10 days, a 230% increase in terms of biomass density was achieved compared to those grown on uncoated supports (Zhuang et al., 2016). Similarly, Irving and Allen (2011) also found that under non-sterile conditions, *C. vulgaris* biofilms were thicker ($52 \pm 19 \mu\text{m}$) than those in sterile conditions ($7 \pm 6\mu\text{m}$) after 7-day cultivation, suggesting that the presence of bacteria and EPS can improve microalgae biofilms growth.

In culture medium, the existence of divalent cations, Mg^{2+} and Ca^{2+} , can promote *Chlorella* adhesion and the following biofilm formation through enhancing the biosynthesis of EPS polysaccharides and proteins, respectively, on the cell wall (He et al., 2016). Besides, nutrient deficiency was also reported to induce EPS accumulation, and improve the marine microalgae aggregations (Lee et al., 2009; Lupi et al., 1994).

Physiological state The physiological state of microalgae (involving photosynthetic activity, composition, cell viability, etc.) affects cell attachment to the substrate. However, due to the wide variety of organisms growing under different conditions, it is difficult to find generalities in the literature on this subject.

Researchers have proved that algae physiological state was driven by environmental conditions and that physiology significantly influences the quantity and quality of algal EPS, thus affecting the initial colonization and subsequent biofilm growth (Gerbersdorf and Wieprecht, 2015). For instance, some reports indicated that microalgae increased their EPS production as the culture aged and that cells with EPS peak content at stationary growth phase attached strongly (Becker, 1996; Gerbersdorf and Wieprecht, 2015; Shen et al., 2015).

Konno (1993) also demonstrated that the settling velocity of *Nitzschia linearis* varies greatly with the physiological activity (cell viability which is associated with variations in surface properties - composition and surface charge) and that the velocity of cells in stationary phase was faster than those in the logarithmic growth phase. However, Sekar et al. (2004) later observed an opposite result for *Nitzschia amphibia* when they studied the initial events of biofilms development, which was in agreement with the findings that log-phase *Chlorella* attached vigorously when compared to cells in the other growth phases (Zaidi and Tosteson, 1972). These differences may be related to the different growth environments or species specificity. Previous studies reported that live cells attached more when compared to dead cells which may due to more EPS secretion with normal physiological and metabolic functions (Sekar et al., 2004; Golberg et al., 2016).

To sum up, optimizing the inoculum density, colonization time, as well as selecting the most appropriated algae species for a certain production purpose are essential steps in the development of efficient microalgae biofilm cultivation systems.

3. Operational factors - culture conditions control

3.1. Light availability

Similar to suspended cultures, growth rate and biomass productivity of microalgae biofilms increase with the raising light intensity within an appreciated range. If increasing continuously

light over photo-saturation region, photo-inhibition and photo-oxidation will occur, which may lead to the decline of growth, or even cells death (Bartosh and Banks, 2007; Carvalho and Malcata, 2003; Severes et al., 2017).

Liu et al. (2013) have demonstrated that in a range of 0 - 150 $\mu\text{mol m}^{-2} \text{s}^{-1}$, the biomass productivity of *S. obliquus* biofilms on membranes increased from 0.7 to 10 $\text{g m}^{-2} \text{d}^{-1}$, but significantly declined when the light exceeded to 150 $\mu\text{mol m}^{-2} \text{s}^{-1}$. Also, the effect of light stress on fluvial biofilms exposed to 500 $\mu\text{mol m}^{-2} \text{s}^{-1}$ (Corcoll et al., 2012) or under 1000 $\mu\text{mol m}^{-2} \text{s}^{-1}$ (Barral-Fraga et al., 2018) in the downstream of rivers was already reported. In order to reduce photo-damage caused by the excess light absorption, some algae acclimated to the high light via tuning the content of pigments, the number of photosynthesis reaction centers or the size of LHCs antennae (Carvalho et al., 2011; Melis et al., 1998). Indeed, the reduced chlorophyll content, and the smaller and fewer antennae can respectively reduce the photons absorption and slow down the electron transfer, which can subsequently protect the photosynthesis systems from photo-damage (Corcoll et al., 2012; Tikkanen et al., 2012). However, the photo-acclimation processes have been seldom documented in algal biofilms.

Noteworthy, in phototrophic biofilms, light attenuation always occurs with the increase of biofilm depth. As illustrated by Huang et al. (2016), *C. vulgaris* biofilms with inoculum densities lower than 40 g m^{-2} (corresponding with a biofilm thickness of $41.31 \pm 3.73 \mu\text{m}$) were effectively illuminated at a light intensity of 120 $\mu\text{mol m}^{-2} \text{s}^{-1}$, while the effectively illuminated portion was declined to 40% when cell density was up to 100 g m^{-2} . This was also observed in growing algal biofilms, in which light availability decreased exponentially with the increase of sessile cells concentration (Barranguet et al., 2004; Jacobi et al., 2012; Schnurr et al., 2014).

Increasing light intensity seems to be a solution to address the problem of photo-limitation in deep layers, however, photo-inhibition or photo-oxidation may occur at the biofilm surface if the over-high light is supplied. Schnurr et al. (2014) have proposed that the modifications in light direction into algal biofilms, in particular the light from both sides of flat-plate PBRs, allows more photons to penetrate into the deep layers. This method indeed increased the biofilm growth rates and overall productivity, nevertheless, it is not suitable for the systems which are placed horizontally and that only have one side optically transparent. Therefore, the trade-off between light and cell density in algal biofilms should be studied in depth.

3.2. Nutrients concentration

Nutrients including macro-element (e.g., N and P) and trace elements (e.g., Fe, Ca, Mg) are prerequisites for microalgae maintenance, division/growth, macromolecules accumulation and other activities, so it is not surprising to observe that nutrients concentration is highly correlated to the development of microalgae biofilm (Gerbersdorf and Wieprecht, 2015).

Within a reasonable range, the increase in nutrients concentration, particularly in N and P, can enhance biomass accumulation and growth rate. Ji et al. (2014) have described that the growth rate of *Pseudochlorococcum sp.* biofilms was steeply improved when the N and P concentrations were respectively increased in the range of 0 - 8.8 mmol L⁻¹ and 0 - 0.22 mmol L⁻¹, and then decreased as both nutrients exceeded those ranges. Experimental and modeling results in another research also showed that the biomass productivity of *Chlorococcum sp.* biofilms was enhanced as the increase of initial total nitrogen concentration from 30 to 70 mg L⁻¹ (Shen et al., 2014).

Although nutrients starvation (like nitrogen), or the combined reduction in Fe, trace elements (Te) and Ca may induce more EPS secretion and enhance consequently cells adhesion (Lupi et al., 1994; Walach and Pirt, 1986), those caused by cells consumption along with diffusion limitations in mature/thick biofilms prone to trigger cells dispersal or biofilm dissolution (McDougald et al., 2012). In addition, the excessive nutrients loading rates should be avoided since the high inorganic ions may cause the increase of salinity or osmotic pressure (Ahmad and Hellebust, 1984), which may bring toxicity to cells, like the high loads of NO₃⁻ (Kızılkaya and Unal, 2019), NH₄⁺ (Markou and Muylaert, 2016) and heavy metal ions (Pandey, 2020). Therefore, optimization of nutrients supply is considerably required for maintaining biofilm integrity and further growth, which finally determine the biomass productivity.

3.3. Hydrodynamic regime

In constantly submerged or intermittently submerged systems, the velocity of the supplied medium relative to the immobilized cultures (due to the medium flow or the supports rotating)

affects microalgae biofilm development. The flow or rotation rate influence mass transfer (e.g., nitrate, phosphate, CO₂, O₂, etc.) and metabolites removal within biofilms, thus enhancing algal growth. High velocity could reduce the boundary layers and increase the transfer rate, but sometimes it may also impose shear stresses resulting in biomass losses at the surface of biofilms (Zhuang, 2018). Therefore, an appropriate hydrodynamic regime should be implemented when considering the maximization of biomass yield. For instance, in a rotating algal biofilm cultivation system where cells are alternatively in liquid and gaseous phases, an appropriate rotation rate is strongly desired for the absorption balance of nutrient and CO₂, and simultaneously maintaining the moisture. In a study carried out by Gross et al. (2013b), the rotation rate lower than 4 rpm tend to dry out *C. vulgaris* biofilms owing to the long atmosphere-exposure, while at a higher rate of 6 rpm, algal biofilm was observed to shear off. Besides, the hydrodynamic regime was also found to impact the architecture and cohesion strength of microalgae biofilms. Fanesi et al. (2019) described that at low flow rate (50 μL min⁻¹), *C. vulgaris* biofilms showed low stability and cohesion, generating loose layers. In contrast, a ten-times higher flow rate distinctly improved the biofilms cohesion, and therefore increased biomass accumulation.

3.4. CO₂ supplement

CO₂ is an essential substrate for microalgae photosynthesis, hence its supply must be considered in an optimization bioprocess procedure. According to the reactor design, CO₂ can be firstly dissolved in a thin-liquid film then applied by the submerged cultures or be directly absorbed by sessile cells through a gas-solid (biofilm phase) contact in intermittently submerged and perfused systems (Huang et al., 2016; Zhuang, 2018). Thus compared to suspended systems where cells live in the bulk liquid, an efficient CO₂ transfer may occur in the latter biofilm-systems due to the shorter pathway thus improving the biomass productivity (Gross et al., 2013b; Huang et al., 2016).

Due to the diversity in configurations and other cultivation parameters, the effect of CO₂ supply on algal biofilm growth is still inconclusive. It was demonstrated that with the increase of CO₂ concentration in a range of 0.625% - 4.0 % w/w, the biomass productivity of *Chlorella sorokiniana* biofilms in the algal disk reactor was significantly improved, but at the

concentration of 4.0% - 10% w/w no further increase was found (Blanken et al., 2017). On the other hand, Gross et al. (2013b) observed that in a rotating algal biofilm system in which CO₂ concentration was controlled in the gaseous phase to 3% w/w, *C. vulgaris* biofilm yield and productivity were not significantly improved compared to atmospheric conditions. The results discrepancy between those works might be related to differences in the biofilm systems, algal species and other cultivation parameters.

3.5. pH

The pH affects the initial formation and development of microalgae biofilm. Medium pH can influence the cell-cell and cell-support interaction by modulating their physical-chemical characteristics and surface properties, e.g., zeta potential, composition of functional groups, hydrophobicity, polarity, electron-donor and electron-acceptor features of cells and/or support as already mentioned (Djeribi et al., 2013; McDaniel et al., 2015; Park and Abu-Lail, 2011). For instance, Yuan et al. (2019) demonstrated that the attached cell density of freshwater *Chlorella sp.* on PVC and glass, and marine algae *Chlorella sp.* and *Nannochloris oculata* on glass decreased with the raising pH (from 5.5 - 8.1), those results were attributed to the changes in the electrostatic interaction (associated with surface zeta potential of cells and substrates).

Sekar et al. (2004) also found that the highest *N. amphibia* sessile cell density on titanium occurred when the pH was 7, 8 and 9. This is in accordance with the acceptable pH range for the biofilm formation and growth of most algal species (Katarzyna et al., 2015).

4. Other operational factors

Some other operational factors like temperature and harvest frequency can also affect the microalgae biofilm growth and productivity. However, in the majority of the microalgae biofilm studies, temperature is mostly controlled between 23 - 28 °C in indoor cultivation (Table 1-1, 1-2, 1-3).

Gross et al. (2013) showed that 7 days was the optimum time interval for algal biofilm harvesting (harvesting frequencies tested: every 3, 5, 7 or 10 days), within which biofilm

remained stable and showed the highest daily productivity. However, the optimal harvesting frequency must be identified for each biofilm-based process.

In conclusion, when attempting to maximize the growth rate and biomass productivity of algal biofilms, optimization of all the operational factors is required. Thus studying the effect of those factors on biofilm formation and development may help to predict stressful factors and help thus the operator to modify the culture conditions/reactor design to maintain a maximal productivity. Besides, this kind of works will bring new knowledge on photosynthetic biofilms that are still far less studied than bacterial biofilms.

5. Conclusion

Microalgae biofilm-based cultivation technology has become a promising alternative to the traditional suspended cultures. It gives a new direction for the cost-effective production and harvesting of microalgae. This review provides comprehensive information from microalgae (definition), metabolism (including cell cycle, photosynthesis, photo-acclimation), lifestyles (planktonic versus sessile modes), and applications, to the current biofilm systems used for microalgae cultivation, and ultimately to the crucial operational factors that impact algal biofilm formation and development.

Due to the complexity of the target algal species, cultivation systems and cultivation conditions, microalgae biofilms showed remarkable different production efficiencies and economic benefits. Therefore, optimization of parameters in the overall process become necessary to attain high biofilm productivities. In addition, biofilm-based cultivation technology is still in its early stage of development and most of researches are at laboratory- or pilot-scales. Studies at large-scale in outdoor conditions are needed to clearly confirm the feasibility of microalgae biofilm-based systems not only for biomass production but also for other applications, e.g., high-value compounds production, wastewater treatment in WWT plants, feedstock and biofuels productions.

Knowledge gap

In summary, this overall review indicates insufficient knowledge on the following aspects:

- Overall, though extensive studies have illustrated the effect of light intensity on the physiological activity and growth of microalgae cultures, there is still little information about the synergistic effect between light intensity and inoculum density, especially in biofilm-based cultures. Indeed, the light penetration capability through early-stage biofilms is strongly related to the initial inoculum density, which can eventually impact the overall biofilm productivity. Therefore, the knowledge on the trade-off between inoculum density and light in immobilized cultures for optimizing biomass or valuable compounds productions is required.
- Literature has reported that micro-environmental conditions for microalgae that grown in planktonic or biofilm environments are quite different. Therefore, there might be a physiological transition in microalgae when they are shifted from planktonic to biofilm lifestyle, which has been reported in bacteria. However, to our best knowledge, the physiological regulation or acclimation of planktonic microalgae to the biofilm-based lifestyle has never been studied, although this knowledge may provide warning signals to judge whether the biofilm conditions are conducive to the growth of microalgae. Therefore, studies on this topic should be conducted.
- Support material is an essential factor affecting cells attachment and biofilm formation, however, how support impact the growth performance and physiology of sessile cells has been seldom investigated. A comprehensive analysis involving the physical-chemical properties and micro-texture of support, and the cells-support interaction may provide an insight to better understand the effect of support on cells adhesion and biofilm growth. Finally, further research is needed to select the potential materials that are suitable for supporting algal biofilm growth.

**CHAPTER II *Chlorella vulgaris* biofilm
dynamics in a continuous photo-bioreactor**

Preamble

As stated in the literature review (section C), operational factors such as light and inoculum density are crucial factors affecting microalgae biofilm development and productivity. Light influences phytoplankton growth and physiological activities (e.g., photosynthetic activity and composition) and has been extensively investigated. Nevertheless, there is still a lack of information regarding the effect of the combined interactions of light and inoculum density on microalgae biofilms. Indeed, biofilms are vulnerable to photo-limitation due to the light attenuation over depth (as shown in the schematic diagram below, Fig. 2-1). Appropriately increasing light or reducing inoculum density may thus moderate this problem. But if light is increased too much, the up layers have the probability to be photo-inhibited. While if using very low inoculum dose, biofilm growth duration might be delayed. Therefore, the trade-off between light and inoculum density should be studied in-depth. With this aim, we characterized the dynamics of *C. vulgaris* biofilms under different combined conditions in terms of light and inoculum density, and estimated the maximal productivities. Changes in sessile cells behaviors (physiology) were also monitored in order to better understand the impact of operational parameters on biofilm development. This study may provide some guidance for experimental design, optimization of operational factors, and improvement of systems in large-scale biofilm cultivation.

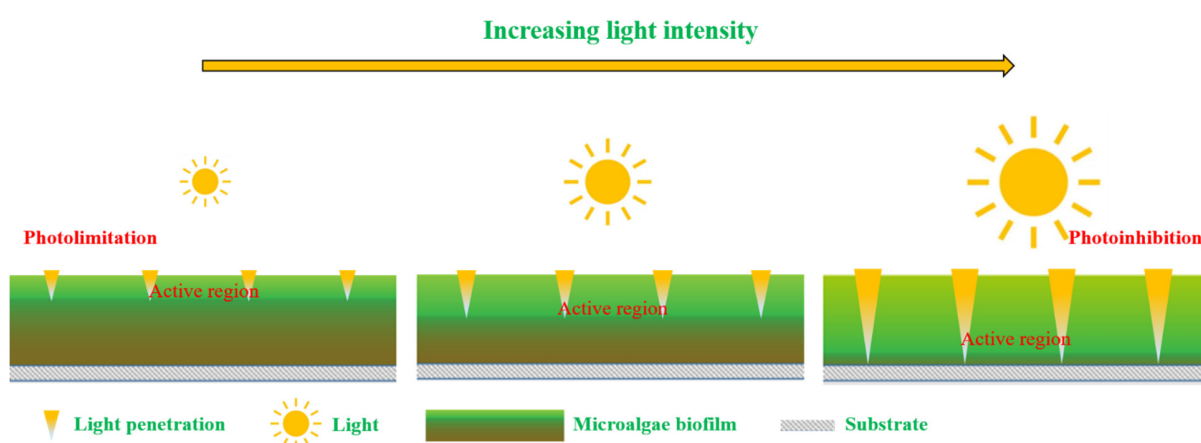


Figure 2-1. Schematic representation of light profiles through an algae biofilm at various light intensities, adapted from (Schnurr and Allen, 2015).

Chlorella vulgaris biofilm dynamics in a continuous photo-bioreactor

Abstract

Due to their potential for industry, microalgae biofilms have been largely studied in past decade. Studies investigating the effect of several factors such as light intensity, nutrients or inoculum concentrations on biofilm dynamics have been undertaken. However, very few studies discuss sessile cell behavior or focus on the underlying mechanisms such as cell acclimation. This information is though important and may help optimizing biofilm-based reactors. This work investigates the dynamics of *Chlorella vulgaris* biofilms in a flow-lane system. Combined conditions in light and inoculum density (0.14×10^6 cells cm^{-2} , LC, and 4.54×10^6 cells cm^{-2} , HC; $100 \mu\text{mol m}^{-2} \text{s}^{-1}$, LL, and $300 \mu\text{mol m}^{-2} \text{s}^{-1}$, HL) were applied. The impact of the operational factors light intensity and inoculum cell density on biofilm development and composition was therefore assessed. Parameters such as cellular composition, in particular cellular chlorophyll (Chl) *a* content and relative macromolecular pools (e.g., carbohydrates and lipids), bulk nutrients concentrations were monitored daily. Results showed that biofilms followed a common growth pattern under all conditions tested: after a 1-day lag phase and a growth phase, a plateau is reached. Biofilms at high inoculum density exposed at $100 \mu\text{mol m}^{-2} \text{s}^{-1}$ (HC-LL biofilms) presented the highest division rate and maximal biomass productivity ($0.65 \text{ g m}^{-2} \text{ d}^{-1}$). Low productivities ($0.15\text{-}0.65 \text{ g m}^{-2} \text{ d}^{-1}$) were though measured maybe due to the high detachment or cotton support/strain properties. Interestingly, cellular Chl *a* content rapidly decreased within only 1-3 days for all the biofilms, suggesting a rapid acclimation mechanism. Additionally, in HC-biofilms, the relative carbohydrates content exhibited an overall increasing trend and lipids to proteins ratio maintained constant. Overall, inoculum cell density together with Chl *a* content (cell physiology) and light intensity strongly impacted biofilm kinetics and composition. This study provides insights into biofilm dynamics and behavior in response to the environmental changes and may give us some guidance for the optimization of operational parameters of microalgae biofilms in a lab-scale system.

Keywords: Acclimation, *Chlorella vulgaris*, kinetics, macromolecular composition, microalgae biofilms

1. Introduction

Microalgae are photosynthetic microorganisms showing a huge potential for biomass and valuable bio-compounds production due to their high photosynthetic efficiency and growth rate (Darvehei et al., 2018; Wang et al., 2017). Compared to terrestrial crops, microalgae present several advantages: the ability to use waste gas streams and wastewater as low-cost nutrients sources for growth and to grow on non-arable land with a smaller footprint (Correa et al., 2020; Molazadeh et al., 2019). Microalgae are usually cultivated in conventional suspended systems such as open ponds and closed photo-bioreactors (Chiaramonti et al., 2013; Wang et al., 2012). However, some researchers argue that no significant improvements or breakthroughs in productive efficiency have been made in the past half century with suspended approaches (Huang et al., 2021; Wang et al., 2017). This can be traced back to the inherent property of suspended cultures, i.e., low biomass concentration, therefore, large energy for harvesting processes is usually required (Berner et al., 2015; Gudín and Therpenier, 1986; Wang et al., 2017).

Biofilm-based microalgae cultivation, in which high-cell-density community grow on a substratum, has been proved to be a promising alternative to the suspended methods (Boelee et al., 2014; Huang et al., 2016). Biomass can be easily harvested from the substrate by simply scraping. The harvested biomass may contain 75 – 85 % water which can be originally comparable to the centrifuged biomass from suspension (Gross et al., 2013b; Katarzyna et al., 2015; Podola et al., 2017). Biofilm cultivation technologies can therefore reduce the huge water consumption suspended cultures need, and improve the biomass harvesting efficiency (Berner et al., 2015; Rosli et al., 2020). In addition, biofilm-based cultivation method also exhibits higher biomass productivity probably due to a higher light availability compared to their suspended counterparts, as demonstrated in previous studies (Huang et al., 2016; Lee et al., 2014; Wang et al., 2015). Consequently, increasing interest in the biofilm-based technology has been inspired since last decade.

Various lab- or pilot-scale biofilm systems have been designed, e.g., twin-layer biofilm system (Dora Allegra Carbone et al., 2017), rotating biofilm reactor (Christenson and Sims, 2012), algadisk reactor (Blanken et al., 2014), algal turf scrubber (Salvi et al., 2021), etc. Among them, a flow-lane system has been reported to provide a standardized laboratory incubator for investigating the development of microalgae biofilms (Berner et al., 2015; Bruno et al., 2012; Zippel et al., 2007). By using this system, the biofilm growth properties such as the lag time, growth rate and maximal biomass production, or the identification of taxonomic composition in field biofilms can be characterized (Guzzon et al., 2021; Zippel et al., 2007). The researchers also used this incubator to assess the effect of the environmental factors such as light intensity, flow velocity and temperature on biofilm development or physiological behaviors (Guzzon et al., 2021, 2019, 2008; Zippel et al., 2007).

To date, experimental data and/or kinetic models describing the suspended microalgae growth in function of cultivation factors (e.g., light, nutrients availability, CO₂ concentration, pH, etc.) have been numerously reported and summarized in (Lee et al., 2015) and the references therein. However, the knowledge of immobilized algal kinetics is still scarce (Fanesi et al., 2021; Mohd-Sahib et al., 2018; Rosli et al., 2020, 2019). Further research is still needed to better understand the growth performance and physiological properties of microalgae in biofilm-based cultivation systems. Indeed, this information is essential for the optimization of the culture conditions/operational parameters, or the design and improvement of biofilm-based systems (Huang et al., 2021; Mohd-Sahib et al., 2018; Moreno Osorio et al., 2020; Schnurr et al., 2013). Previous works have demonstrated that operational factors such as light intensity, inoculum density, substrate properties, cultivation system design, and hydrodynamics affect the biofilm development and productivity (Fanesi et al., 2021; Gross et al., 2016; Kim et al., 2018; Shen et al., 2017). For instance, a maximal productivity ($\sim 27.5 \text{ g m}^{-2} \text{ d}^{-1}$) of *C. vulgaris* biofilm was obtained when the initial inoculum density reached to 12.5 g m^{-2} , but further increase in inoculum size reduced the productivity due to the poor light penetration and respiration (Huang et al., 2016). Light limitation in thick biofilms may be mitigated by increasing the incident light intensity (Schnurr and Allen, 2015), however, it should be controlled within a reasonable range to avoid photo-inhibition (Grenier et al., 2019). Therefore, the trade-off between inoculum density and light for optimizing biofilm development should be studied in-depth. Also, support selection has been recognized as another crucial operational factor when growing algal biofilms

(Genin et al., 2014; Gross et al., 2016; Irving and Allen, 2011). This is because support properties (e.g., micro-texture and physical-chemical properties) impact cells adhesion and short-term biofilm growth, which will in turn affect the final biomass yield and productivity (Irving and Allen, 2011; Schnurr and Allen, 2015; Zhang et al., 2020). Cotton, a potential support for microalgae growth, has been widely used as cotton duct, rag, denim, corduroy, sheet, rope and ball, etc. in biofilms cultivation (Christenson and Sims, 2012; Gross et al., 2013b; Hodges et al., 2017; Kesaano et al., 2015; Zhuang et al., 2016).

A considerable number of studies demonstrated that planktonic algae have physiological mechanisms to cope with changing growth conditions (Rai and Gaur, 2001; Young and Schmidt, 2020). Acclimation to light and/or nutrients have been largely discussed for suspended cultures (Jungandreas et al., 2014; Katayama et al., 2018; Sciandra et al., 2000), but only few works focused on biofilms (Corcoll et al., 2012; Wang et al., 2015). It should be stressed that acclimation describes changes of the macromolecular composition of an organism that occurs in response to variation of environmental conditions. In particular, photo-acclimation often occurs via synthesis or breakdown of specific components of the photosynthetic apparatus (Anning et al., 2000; Post et al., 1984; Raven and Geider, 2003). This process occurs over time scale of hours to days but it is species- and conditions-specific. To the best of our knowledge, the information on photosynthetic biofilm acclimation mechanisms is still limited. This is in particular due to the complexity of those communities (3D structure where light and nutrient gradients may form, diverse microbial spatial distribution, dynamically renewed biomass, ...) and of their interaction with the environment (hydrodynamics, incoming light, nutrients, gases...) (Berner et al., 2015; Bishop et al., 1995; Ji et al., 2014; Miranda et al., 2017; Sutherland, 2001). Nevertheless, Wang et al. (2015) proposed a mechanism describing light transfer in microalgae biofilms and its relationship with biomass evolution (Fig. 2-2). On the contrary to suspended cultures, where an increase in chlorophyll per cell generally occurs over cultivation time due to self-shading (Lehmuskero et al., 2018; Masojídek et al., 2021; Schnurr et al., 2014), the authors observed a decreasing trend in the cellular Chl content with the increase of biomass. As depicted in Fig. 2-2, in the earlier phase (with low biomass density) of immobilized growth, the pigment content in each cell is high so that the light decreases sharply over each biofilm layer. In a later stage, cellular Chl content decreases, which may reduce the light attenuation through the algal layers and consequently increase the actively photosynthetic regions. This may represent an

acclimation strategy for algal biofilms to increase the light use efficiency by increasing the light penetration within the biofilm.

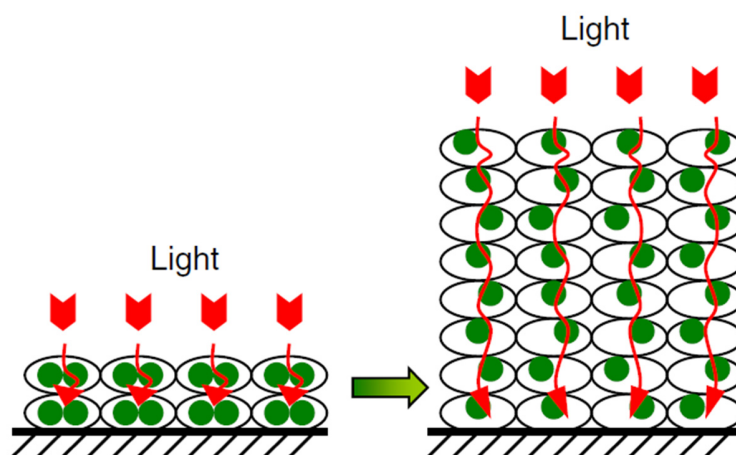


Figure 2-2. Schematic model for the chlorophyll and light distribution inside the microalgae biofilm (green dots indicate the chlorophyll, and red arrows suggest light penetration path inside the biofilm, Wang et al., 2015).

In this study, *C. vulgaris* biofilms dynamics was studied in a flow-lane system at laboratory scale. The effect of operational parameters including light intensity and inoculum cell density/physiology was assessed. When referring to “Physiology” effect, we meant the impact of the chlorophyll content of the inoculum cells on biofilm formation. In order to better understand sessile cells behavior (physiology) under different conditions, the cellular composition (i.e., cellular Chl *a* and macromolecules contents) and nutrients availability in the bulk medium (i.e., nitrate, phosphate and inorganic carbon) were monitored daily. First, with this work, we aim at better understanding biofilm development dynamics and acclimation under different operation conditions (light intensity and inoculum cell density/physiology). Our study also provides some preliminary data for the optimization of operational parameters of *C. vulgaris* biofilms in a lab-scale-based system.

2. Materials and Methods

2.1. Planktonic culture maintenance

The microalgae used in this thesis, *Chlorella vulgaris* (Chlorophyta - Trebouxiophyceae) SAG 211–11b, was purchased from Algal Culture Collection of University of Göttingen (SAG, Germany). The 3N-Bristol medium (Bischo and Bold, 1963) contains (per liter): 748 mg NaNO₃, 28 mg CaCl₂·2H₂O, 75 mg MgSO₄·7H₂O, 21 mg FeEDTA, 75 mg K₂HPO₄, 174 mg KH₂PO₄, 20 mg NaCl, 3 mg H₃BO₃, 6 mg MnCl₂·4H₂O, 303 µg ZnSO₄·7H₂O, 121 µg CuSO₄·7H₂O, 22 µg MoO₃ 85%, and 137 µg CoSO₄·7H₂O.

Planktonic cultures of *C. vulgaris* were inoculated with a cell concentration of 3.0×10^5 cells mL⁻¹ in 100 mL borosilicate tubes with 70 mL medium and cultured under continuous irradiance of 50 µmol m⁻² s⁻¹ at 25°C in a Multi-Cultivator (MC1000-OD, Photon Systems Instruments, Drasov, Czech Republic, see experimental protocols in Fig. 2-3). The cultures were bubbled with filtered air and grown for 7 days. A planktonic cell suspension at approximately 3.0×10^7 cell mL⁻¹ (Chl *a* content of 0.63 ± 0.10 pg cell⁻¹) was used as inoculum for the biofilm assays.

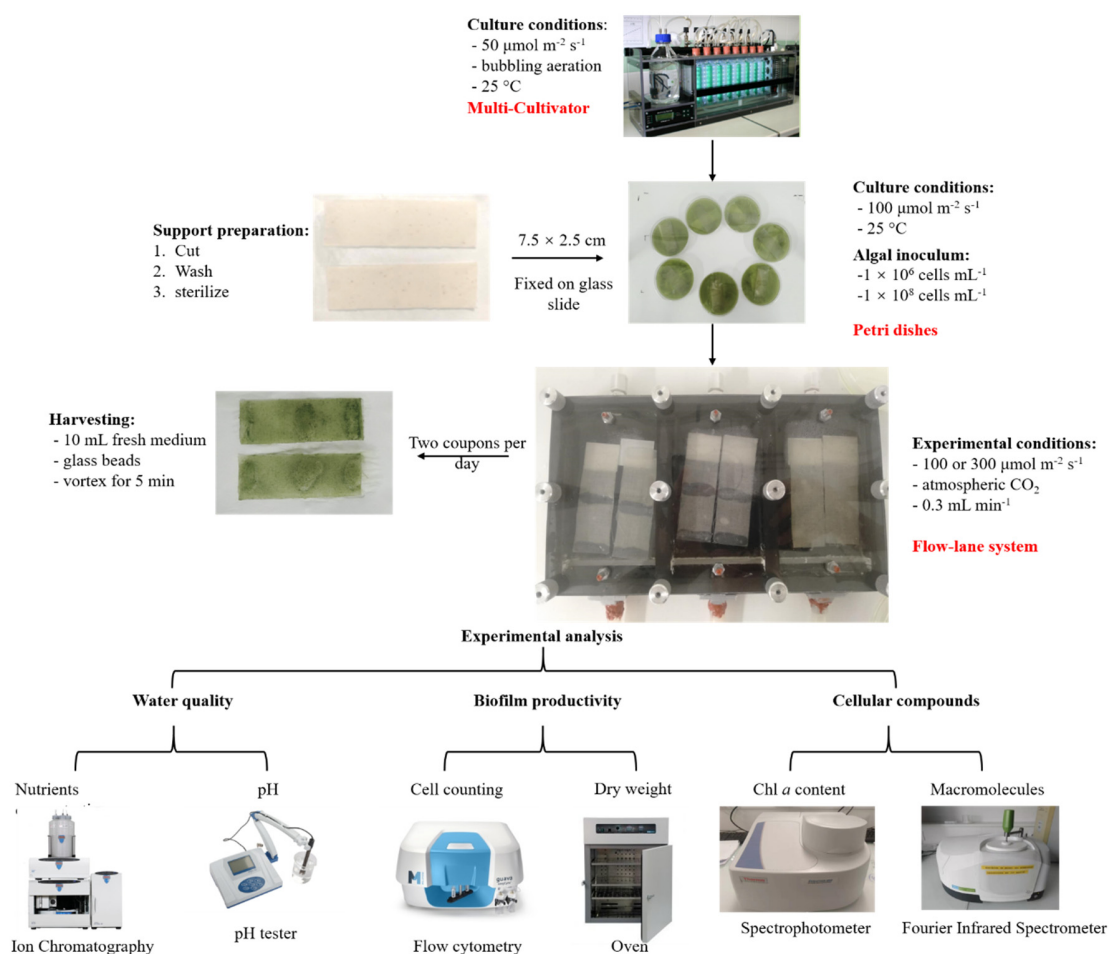


Figure 2-3. Experimental protocols for biofilm cultivation and experimental analysis.

2.2. Biofilm inoculation and dynamics

Cotton was used as the substrate for *C. vulgaris* biofilm development in this work. Indeed, several works described cotton as an excellent support for microalgae growth (Christenson and Sims, 2012; Gross et al., 2013). This fabric material was cut into square pieces ($7.5 \text{ cm} \times 2.5 \text{ cm}$) and glued on glass slides ($7.5 \text{ cm} \times 2.5 \text{ cm} \times 0.1 \text{ cm}$). The coupons (composed of cotton sheet and glass slide) were first sterilized (with a small amount of Milli-Q water) in Petri dishes at 121°C for 15 min. Afterwards, 20 mL of two planktonic cell suspensions obtained from the inoculum (section 2.1), 1.0×10^6 and $1.0 \times 10^8 \text{ cell mL}^{-1}$, were poured into the sterilized Petri dishes (90-mm diameter) and placed under continuous $100 \pm 5 \mu\text{mol m}^{-2} \text{s}^{-1}$ illumination (Viugreum 50W LED outdoor floodlights, the irradiance was measured by a LI-190R Quantum Sensor, LI-COR Biosciences GmbH, Bad Homburg, Germany) and at 25°C . After 24-h

incubation, the coupons were washed slightly to remove non tightly attached cells and then transferred into the flow-lane system. Two initial cell concentrations were tested in this study: 0.14×10^6 cells cm^{-2} (low inoculum density, LC, corresponding to 1.0×10^6 cell mL^{-1}) and 4.54×10^6 cells cm^{-2} (high inoculum density, HC, corresponding to 1.0×10^8 cell mL^{-1}).

The flow-lane system consists of three chambers (Fig. 2-3 and Fig. S2-1), each chamber had a dimension of 11.0 cm \times 6.5 cm \times 1.0 cm. Two coupons were placed in each chamber, thus the bioreactor at one time could handle 6 coupons. The chambers were then closed with a transparent plastic cover. Fresh medium was pumped into the chambers with a flow rate of 0.3 mL min^{-1} . Light was placed above the reactor and illuminated the coupons continuously at 100 ± 5 (low light, LL) or 300 ± 15 $\mu\text{mol m}^{-2} \text{s}^{-1}$ (high light, HL). Before placing coupons, the flow lane was disinfected with sodium hypochlorite (0.5% v/v) and then rinsed with 2L sterilized distilled water.

In order to assess the effect of cell density/physiology and light intensity, several experiences were carried out (Table 2-1). Two coupons were sampled daily until the stationary phase was reached. Areal concentrations in cell and dry biomass, and biofilm composition were measured daily. The effluent was also collected from the outlet to monitor nutrients (NO_3^- and PO_4^{3-}) concentration over time. The pH was also measured daily.

Table 2-1. Experimental design with different conditions in terms of inoculum density, light intensity, and cellular Chl *a* content and relative carbohydrates/lipids contents in immobilized cultures at day 0. LC and HC represent the low ($\sim 0.14 \times 10^6$ cells cm^{-2}) and high inoculum cell density ($\sim 4.54 \times 10^6$ cells cm^{-2}), respectively; LL and HL are low ($100 \mu\text{mol m}^{-2} \text{s}^{-1}$) and high light intensity ($300 \mu\text{mol m}^{-2} \text{s}^{-1}$), respectively (same implication in the following table).

Treatment	Light ($\mu\text{mol m}^{-2} \text{s}^{-1}$)	Inoculum density ($\times 10^6$ cells cm^{-2})	Chl <i>a</i> content (pg cell $^{-1}$)	Carbohydrates to proteins ratio	Lipids to proteins ratio
LL \times LC	100	0.14 ± 0.00	0.18 ± 0.01	1.01 ± 0.02	0.25 ± 0.02
LL \times HC	100	4.54 ± 1.35	0.30 ± 0.04	0.67 ± 0.07	0.18 ± 0.01
HL \times HC	300	4.54 ± 1.35	0.30 ± 0.04	0.67 ± 0.07	0.18 ± 0.01

2.3. Biomass recovery from the support

Biofilm on cotton textile was harvested with 10 mL Bristol medium using a 50 mL centrifugation tube (containing glass beads), by vigorously oscillating with a vortex mixer (ZX4 IR, Fisherbrand, Fisher Scientific, USA). The optimal vortexing time of 5 min (Fig. S2-2) was applied in order to maximize cell harvesting. Cell and dry biomass concentrations were then measured.

2.4. Specific growth rate

Cells were counted using the Flow cytometer (Guava EasyCyte HT; Millipore, USA). The cells areal density (cells cm⁻²) was calculated based on the area of cotton support. The specific growth rate (μ_{cells} , d⁻¹) of biofilms at exponential growth phase was therefore calculated using Eq. (1):

$$\mu_{\text{cells}}(\text{d}^{-1}) = (\ln C_2 - \ln C_1) / (t_2 - t_1) \quad (1)$$

Where C_2 and C_1 stand for the cells areal density (cell m⁻²) at day t_2 and day t_1 (t_1 and t_2 respectively stand for the beginning and the end of exponential growth phase).

2.5. Biomass productivity

After a washing step with fresh Bristol medium, the pellet was dried at 100 °C until a constant weight. The biomass areal density (X , g m⁻²) was calculated afterwards. The maximal biomass productivity (P_x , g m⁻² d⁻¹) at exponential growth phase was therefore calculated using Eq. (2):

$$P_x(\text{g m}^{-2} \text{d}^{-1}) = (X_2 - X_1) / (t_2 - t_1) \quad (2)$$

Where X_2 and X_1 are the biomass areal density (g m⁻²) at day t_2 and day t_1 .

2.6. Cellular compounds

Chl *a* was extracted from cells using dimethyl sulfoxide (DMSO) (Wellburn, 1994), and quantified by measuring the absorption at 649 nm and 665 nm with an Evolution 60S UV-

visible spectrophotometer (Thermo Scientific, Madison, WI, USA). The concentration of Chl *a* was calculated by Eq. (3) (Wellburn, 1994):

$$\text{Chl } a \text{ (}\mu\text{g mL}^{-1}\text{)} = 12.19 \times \text{OD}_{665} - 3.45 \times \text{OD}_{649} \quad (3)$$

Chl *a* content (pg cell⁻¹) was estimated considering the amount of cells harvested from the support. The specific growth rate according to the changes in Chl *a* concentration ($\mu_{\text{Chl } a}$, d⁻¹) was calculated using Eq. (1), where C_2 and C_1 stand for the Chl *a* concentration (mg cm⁻²) at day t_2 and day t_1 .

ATR-FTIR PerkinElmer Spectrum-two spectrometer (PerkinElmer, Waltham, MA, USA) was employed to determine the variations in cellular macromolecular composition. The harvested cells were re-suspended in Milli-Q water and washed twice. 1-2 μL concentrated sample was transferred to the 45° ZeSe flat crystal of FTIR spectrometer to record the infrared spectra in a range of 4000 to 400 cm⁻¹ using an accumulation of 32 scans at a spectral resolution of 4 cm⁻¹. The samples were dried naturally by evaporation at a room temperature for 20 min. Before loading microalgae samples, the device with an empty crystal ran as a background operation. The spectra were baselined and specific macromolecular pools were characterized with maximum absorption values at the corresponding spectral ranges: carbohydrates (C–O–C; 1200–950 cm⁻¹), lipids (C=O; 1750–1700 cm⁻¹), proteins (Amide I; 1700–1630 cm⁻¹) (Fanesi et al., 2019). The maximum absorption value of amide I at the range of 1700–1630 cm⁻¹ was recognized as an internal reference peak, and the relative carbohydrates or lipids contents were therefore respectively represented by the ratio of carbohydrates or lipids band to the amide I band (Meng et al., 2014).

2.7. Nutrients concentration in the bulk water

Effluents from the bioreactor were filtered with 0.2 μm filters (Whatman GF/F). The concentration of inorganic nutrients (NO_3^- and PO_4^{3-}) was quantified with an Ion Chromatography (ICS-5000, ThermoFisher Scientific Inc, USA) after a proper (50 \times) dilution with Milli-Q water.

2.8. Statistical analysis

All the results were presented as mean values \pm standard deviations. Analysis of variations in dynamics was performed with (One-way ANOVA), specific growth rates in cell and Chl *a* concentration for biofilms was carried out by Students' *t*-tests using IBM SPSS Statistics 25.0 (SPSS Inc., Chicago, IL).

3. Results and discussion

3.1. Biofilm dynamics

Fig. 2-4 presents biofilm dynamics for the combined conditions of light intensity and cell density. The biomass dynamics is depicted in Fig. S2-3. Images of confocal laser scanning microscopy of HC-LL and LC-LL biofilms at day 3 are also shown in Fig. 3-6B. From those images, it appears that cell distribution is far from being uniform. Cells do attach and form clusters on the loosely connected fibers of cotton. This will be further discussed in Chapter III.

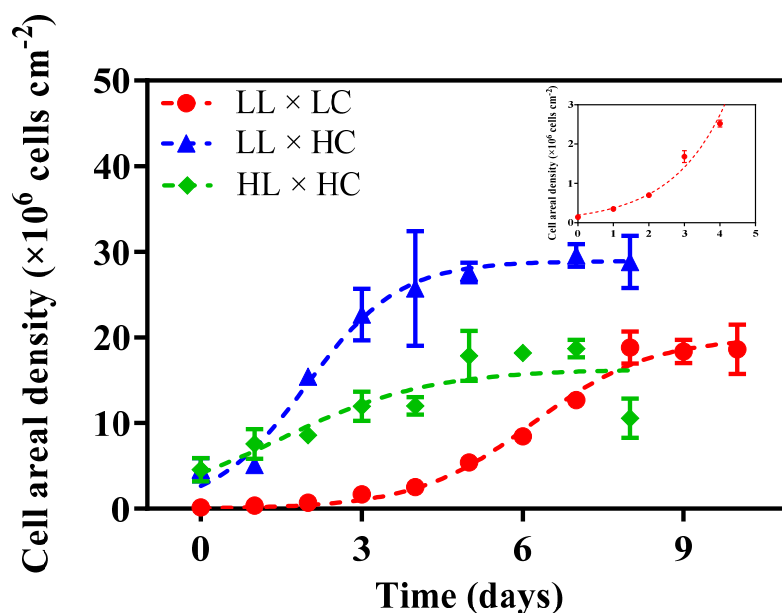


Figure 2-4. Dynamics of *C. vulgaris* biofilms under different conditions. LC and HC represent the low ($\sim 0.14 \times 10^6$)

cells cm^{-2}) and high inoculum cell density ($\sim 4.54 \times 10^6$ cells cm^{-2}), respectively; LL and HL are low ($100 \mu\text{mol m}^{-2} \text{s}^{-1}$) and high light intensity ($300 \mu\text{mol m}^{-2} \text{s}^{-1}$), respectively (same implication in the following figures). All the results are shown as mean value \pm SD ($n \geq 2$).

First, a common development pattern is observed for all conditions tested (Fig. 2-4): after an active growth phase, a plateau stage is reached. This is in agreement with the broadly described biofilm developmental cycle which consists in several stages: (1) initial attachment to a surface, (2) formation of microcolonies, (3) maturation of the biofilm and (4) dispersal (Achinas et al., 2019; Guzmán-Soto et al., 2021; Tolker-Nielsen, 2015). This is also in line with data described by Roostaei et al. (2018) and Fanesi et al. (2021) for *C. vulgaris* biofilms developed on several supports and profiles determined by Zippel et al. (2007) on river biofilms developed in a flow-lane reactor. In another study, Buhmann et al. (2012) described the impact of static versus continuous-flow conditions on biofilm formation. Without liquid flow, the microalgae biofilm growth curve reached a plateau after 5 days, whereas growth under continuous flow proceeded until the end of the assay (15 days). This behavior was explained by nutrient depletion in static conditions. However, in our study, no limitation in terms of carbon, nitrogen or phosphorus seem to occur as shown in Fig. 2-5. Indeed, all the parameters were maintained almost constant and close to those of the original supplied medium during the whole cultivation period. Therefore, we believe that most likely the curves reached a plateau because growth was counterbalanced by equal losses generated by detachment, as reported by Boelee et al. (2014).

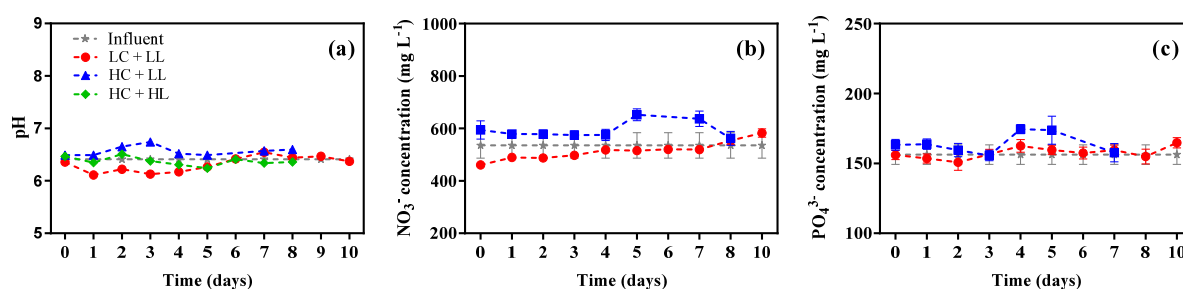


Figure 2-5. pH (a), nitrate (b) and phosphate (c) ions concentration in aqua-medium over time (the gray dashed lines represent the average values of inlet medium). All the results are shown as mean value \pm SD ($n = 3$).

Second, it clearly appears that biofilm dynamics is impacted by the operational conditions

applied. Biofilms developed at high inoculum density and under $100 \mu\text{mol m}^{-2} \text{s}^{-1}$ (HC-LL biofilms) grew faster with a shorter exponential growth phase (day 1-3, Fig. S2-4) than those at low cell density (LC-LL biofilms). This is in agreement with other studies that showed an increase in the growth rate with inoculum size in immobilized cultures of *Pseudochlorococcum sp.* (from 0.05 to 3–5 g m^{-2}) (Ji et al., 2014), *Botryococcus braunii* (from 1.9 to 7.9-10.1 g m^{-2}) (Cheng et al., 2018) and in *C. vulgaris* biofilms grown on filter membranes at an inoculum range of 2.5 - 12.5 g m^{-2} (Huang et al. 2016). This suggests that there is an optimal inoculum density to promote biofilm grow and productivity. If the inoculum concentration exceeds a certain threshold, limitations in light and nutrients will impact negatively the biofilm growth rate (Blanken et al., 2014; Cheng et al., 2018; Huang et al., 2016; Ji et al., 2014). Nevertheless, it should be stressed that the cellular chlorophyll content of the HC and LC biofilms are significantly different (Table 2-1). The interplay between inoculum density and Chl *a* content may impact the obtained results. Assays described in the next chapter were thus carried out to assess separately the effect of the inoculum cell density and cell physiology (here, Chl *a* content) on biofilm development.

In addition, a linear growth phase and a plateau followed the short exponential growth phase in HC biofilms. This suggests light limitation maybe due to a high biofilm concentration (~1.6 and 2.2 times higher in cell concentration and in dry weight, respectively, than LC-biofilms). In order to test the hypothesis of light limitation, HC-biofilms were exposed to higher light intensity ($300 \mu\text{mol m}^{-2} \text{s}^{-1}$, Fig. 2-4). A decrease of the specific cell division rate (0.23d^{-1}) was measured compared to that of the biofilm exposed to $100 \mu\text{mol photons m}^{-2} \text{s}^{-1}$, suggesting that this light intensity impact negatively biofilm growth. A shorter exponential phase was also detected (day 1-3, Fig. S2-4). This may be attributed to the photo-inhibition of cells under the high light. This result is in agreement with data from (Liao et al., 2018) which demonstrated that a light intensity in the range of 180 to 240 $\mu\text{mol photons m}^{-2} \text{s}^{-1}$ inhibited the growth of *C. vulgaris* suspended cultures. Other studies also reported a decrease in the growth rate of algal biofilms from a wastewater treatment plant exposed at irradiance of 210 - 350 $\mu\text{mol m}^{-2} \text{s}^{-1}$ due to the photo-inhibition (Guzzon et al., 2019). But this is strongly species-dependent and may be related to the light history cells experienced (Mouget et al., 2008). In our study, the sessile cells exposed to $300 \mu\text{mol photons m}^{-2} \text{s}^{-1}$ may behave similarly.

3.2. Biomass productivity

Biomass productivity was also determined in all conditions (Table 2-2). Though an improvement of productivity was measured for HC-LL biofilms (more than 3 times higher than for LC-biofilms and HL- biofilms), values are quite low ($0.15 - 0.65 \text{ g m}^{-2} \text{ d}^{-1}$) compared to most studies on *C. vulgaris* biofilms (Table S2-1). As expected, algal biofilm productivity depends on the cultivation conditions. Indeed, a wide range (from 0.04 to $80.00 \text{ g m}^{-2} \text{ d}^{-1}$) was reported in previous reviews which compile a high number of studies at lab and pilot scales (Berner et al., 2015; Rosli et al., 2020; Schnurr and Allen, 2015).

Table 2-2. Maximum biomass production and productivity of *C. vulgaris* biofilms inoculated with different cell density under different light intensity. All the results are shown as mean value \pm SD ($n \geq 2$). Values with different letters represent the statistical differences among biofilms under different conditions at level of $P < 0.05$.

Treatment	Light ($\mu\text{mol m}^{-2} \text{ s}^{-1}$)	Inoculum cell density ($\times 10^6 \text{ cells cm}^{-2}$)	Maximum biomass (g m^{-2})	Maximal productivity ($\text{g m}^{-2} \text{ d}^{-1}$)
LL \times LC	100	0.14 ± 0.00	1.86 ± 0.66^a	0.20 ± 0.07^a
LL \times HC	100	4.54 ± 1.35	4.13 ± 0.06^b	0.65 ± 0.01^b
HL \times HC	300	4.54 ± 1.35	1.54 ± 0.12^a	0.15 ± 0.00^a

Low biomass productivity may be explained by several mechanisms. First, it may be due to the low cell retention capability of the cotton support. Indeed, previous studies have demonstrated that the opening/pore/mesh size of supports close to or smaller than algal cell or cell consortia benefit adhesion (Cui et al., 2013; Gross et al., 2016). In addition to the pore size, other support characteristics like physical-chemical properties (e.g., hydrophobicity, roughness, functional groups) have also been proved to impact algal adhesion/retention (Barros et al., 2019; Genin et al., 2014; Gross et al., 2016; Ozkan and Berberoglu, 2011). The effect of those properties on *C. vulgaris* attachment and biofilm development will be studied in the next chapter.

A high detachment rate may also explain the low productivity values observed in our conditions. Indeed, almost 23% of the sessile cells were detached from the support in the first 24h (Fig. S2-5). However, complementary work must be carried out to determine the

detachment rate over time. Moreover, it has been shown that that *C. vulgaris* biofilms formed under low shear stress are less cohesive and more prone to detachment than those developed at higher shear stress (Fanesi et al., 2021). In our conditions, biofilms were formed at much lower shear stress (0.013 mPa, supplementary data for Chapter II- estimation of shear stress) than those reported by Fanesi et al. (2021), which may lead to loose biofilms and consequently high biomass loss.

Furthermore, we cannot rule out that quorum sensing mechanisms occur in our biofilms leading to detachment. Quorum sensing is a well-known cell density-dependent mechanism which affects the expression of biofilm-related genes through cell communication employing autoinducers (secreted by cells) (Fuqua et al., 2001; Sharif et al., 2008). Quorum-sensing has been shown to inhibit biofilm formation in cyanobacteria and bacteria biofilms (Karatan and Watnick, 2009; Nagar and Schwarz, 2015; Sharif et al., 2008; Yildiz and Visick, 2009).

In addition, the low biomass productivity may be also linked to the algal strain we used. Hultberg et al. (2014) reported a very low biomass productivity ($0.05 \text{ g m}^{-2} \text{ d}^{-1}$) for biofilms of *C. vulgaris* CCAP 211-11B after 7 days of cultivation at $100 \mu\text{mol m}^{-2} \text{ s}^{-1}$. This result may be explained by the low amount of EPS produced by *C. vulgaris* as reported by several studies (Chiou et al., 2010; Fanesi et al., 2019; Irving and Allen, 2011). It should be reminded that the EPS play a major role on cell adhesion and biofilm development (Babiak and Krzemińska, 2021; Fanesi et al., 2019; Xiao and Zheng, 2016).

On the whole, an increased knowledge of the biofilm properties such as cohesiveness, EPS content and composition, cell-support interactions and gene-expression is required to better understand the development of phototrophic biofilms, in particular, on fabrics. This will be one of the subjects tackled in the next chapter.

3.3. Biofilm chemical composition dynamics

Although the effect of the combined conditions (inoculum density and light intensity) on algal biofilm productivity has been described in several works (Huang et al., 2016; Ji et al., 2014; Shen et al., 2017), only few discussed the underlying mechanisms. One of the goals of the present study is therefore to better understand the physiological mechanisms triggered during

biofilm development. Indeed this will bring new knowledge on photosynthetic biofilms and certainly help developing more productive biofilm-based systems.

Fig. 2-6 illustrates the evolution of Chl *a* content in *C. vulgaris* biofilms over time. Unexpectedly, a fast decrease in the Chl *a* content was detected within only one day of cultivation for the three conditions tested. Changes in environmental conditions may have triggered this behavior. Indeed, it should be reminded that cell attachment to the support occurred in a Petri dish containing high-cell-density cultures (see section 2.2). In those conditions, cells were certainly exposed to very low light intensity due to self-shading. It is likely that light availability per cell may have increased after the support being transferred to the flow-lane system, subsequently leading to a reduction of the cellular Chl *a* content. In addition, a decrease of the initial cell density due to detachment of loosely attached or unattached cells to the cotton may have also increased light availability after the transfer (see section 3.3). Our results suggest therefore a fast mechanism of acclimation in the sessile cells in order to cope with the new local conditions at the fabrics surface. This is also in agreement with Ritz et al. (2000) who demonstrated a fast change in the cellular chlorophyll content in approximately 5h when *Rhodella violacea* low-light acclimated suspended cells ($40 \mu\text{mol m}^{-2} \text{s}^{-1}$) were transferred to higher irradiance ($1000 \mu\text{mol m}^{-2} \text{s}^{-1}$). In another work with suspended cultures, Neidhardt et al. (1998) showed an accumulation of chlorophyll in only 4h when high-light photo-acclimated cells of *Dunaliella salina* ($2000\text{-}2500 \mu\text{mol m}^{-2} \text{s}^{-1}$) were exposed to low-light conditions ($50\text{-}70 \mu\text{mol m}^{-2} \text{s}^{-1}$).

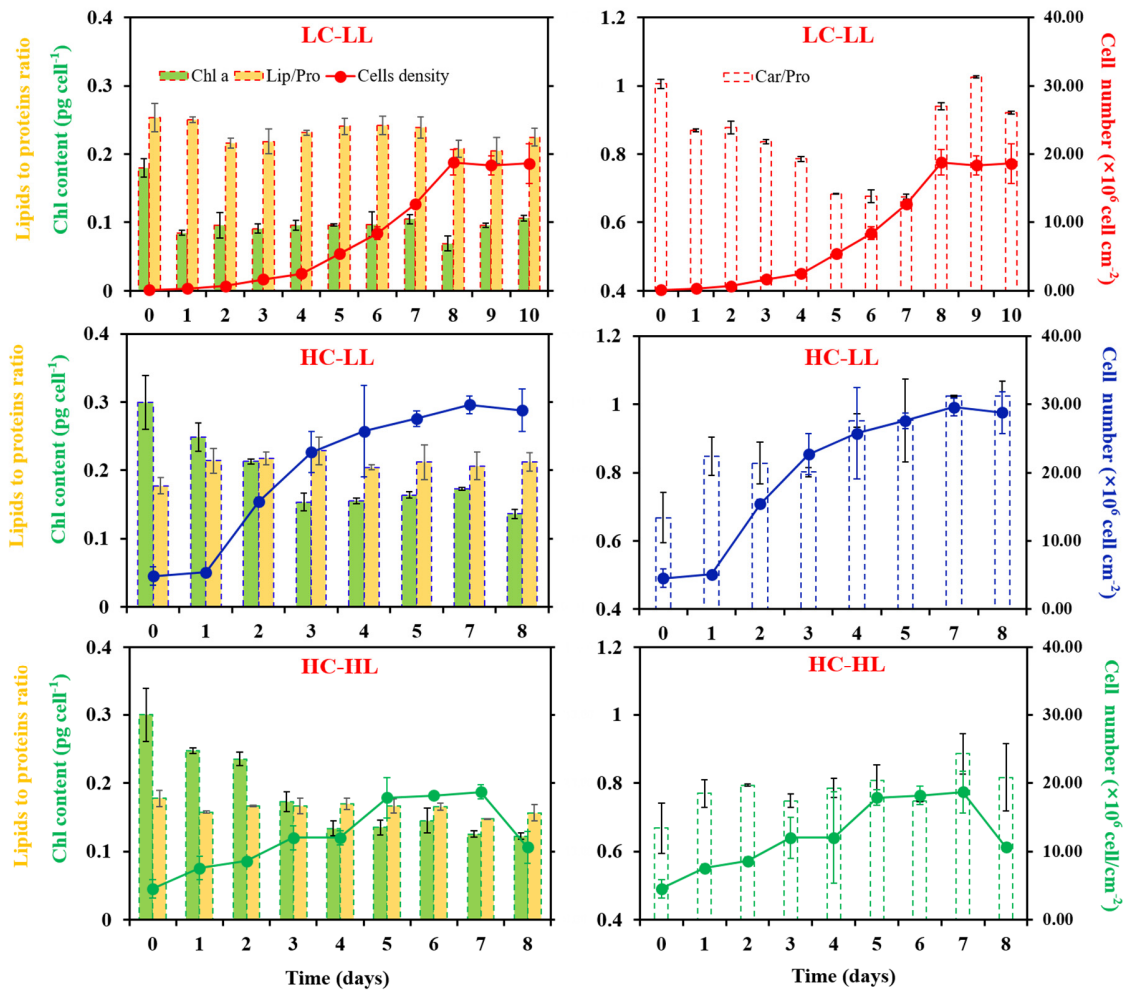


Figure 2-6. Dynamics of cellular Chl *a* content (green bars), carbohydrates (Car/Pro, white bars) and lipids to proteins ratio (Lip/Pro, yellow bars) with regard to the changes in immobilized cell concentration (aligned dots) under combined conditions of light intensity (LL, low light; HL, high light) and inoculum density (LC, low inoculum density; HC, high inoculum density). All the results are shown as mean value \pm SD ($n \geq 2$).

Interestingly, full acclimation in LC-biofilm seems to occur after only 1 day while 3 days are required for HC-biofilms. The time for attaining full acclimation and the new cellular steady-state Chl *a* content is therefore dependent on the initial operating conditions.

Fig. 2-7 shows the rates of cell division and chlorophyll production for each condition. From our data, it is likely that the decrease of the cellular Chl *a* content in HC-biofilms is due to dilution caused by cell division (Fig. 2-7, $\mu_{\text{cells}} > \mu_{\text{Chl } a}$, $P < 0.05$). On the contrary, similar rates of division and chlorophyll production were determined for the LC-biofilm. This is in agreement

with both works of (Post et al., 1984) and (Anning et al., 2000) that demonstrated that Chl *a* pools in low light photo-acclimated cells were not actively degraded but simply diluted by cell division when transferred to high light. Post et al. (1984) also emphasized that the dilution in cellular Chl *a* during the transition from low to high light does not imply that Chl *a* synthesis stops but rather that the division rate influences the rate of change of this pigment more significantly than the rate of synthesis.

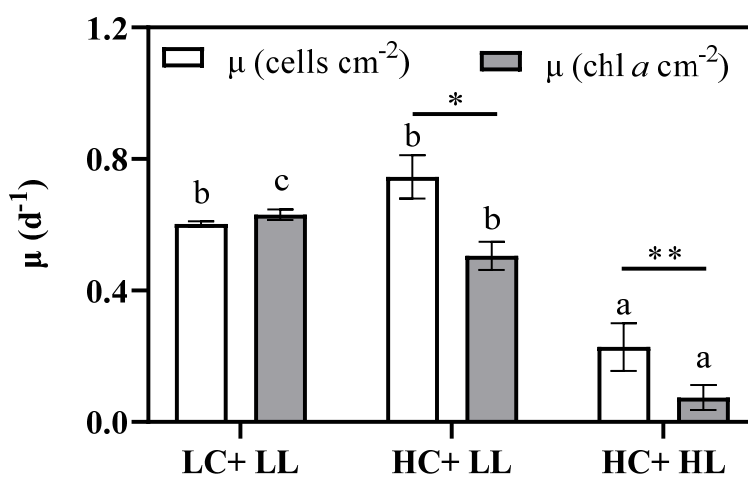


Figure 2-7. Growth rate of sessile cell concentration and Chl *a* concentration for biofilms under different conditions. All the results are shown as mean value \pm SD ($n \geq 2$). Bars with different letters represent the statistical differences among biofilms under different conditions at level of $P < 0.05$, while ** and * respectively depict the differences between cell division rate and Chl *a*-concentration changing rate at $P < 0.01$ and $P < 0.05$, and ns represents no difference.

To better understand sessile cells behavior, the relationship between cell areal density and cellular Chl *a* content of immobilized *C. vulgaris* is plotted in Fig. 2-8. Data suggests that the cellular Chl *a* content decreases with cell division for HC-biofilms, as already mentioned. However, it seems that this behavior is dependent on the initial Chl *a* content of the sessile cells (Table 2-1, and Fig. 2-8). Unlike LC-biofilms, a decrease in the chlorophyll content is observed for HC-biofilms, even for similar cell areal concentrations. Experiments described in chapter III were therefore carried out to better understand this behavior.

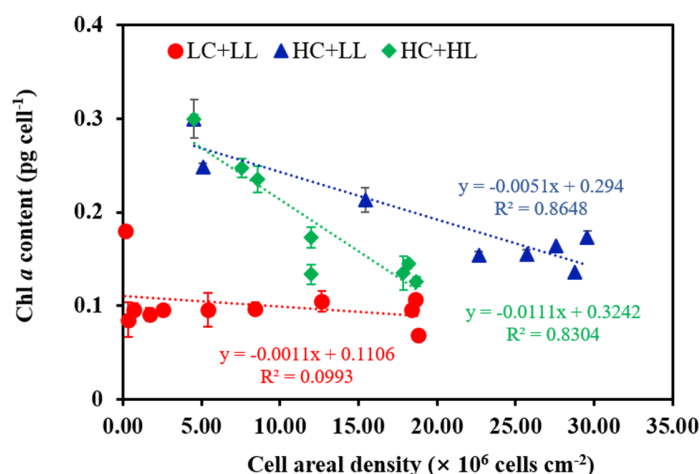


Figure 2-8. The relationship between cellular Chl *a* content and cell concentration on cotton support under combined conditions of light intensity and inoculum density. All the results are shown as mean value \pm SD ($n \geq 4$).

In order to better characterize photosynthetic biofilms in terms of chemical composition, the ratios of carbohydrates and lipids to proteins were measured over time (Fig. 2-6). It has been largely demonstrated that cellular carbohydrates and lipids content in suspended cultures are affected by environmental factors (Fanesi et al., 2017; Li et al., 2011; Wagner et al., 2017). However, little is known about their dynamics on biofilms formed under different culture conditions (Fanesi et al., 2019; Yuan et al., 2020b). In our study, while the lipids pool is stable over time (Fig. 2-6), a completely different pattern is obtained for carbohydrates. An increasing trend (a slight increase for the biofilm exposed to $300 \mu\text{mol m}^{-2} \text{s}^{-1}$) is observed for HC-biofilms, while it declined first during the exponential growth and rose afterwards when attaining the plateau for LC-biofilms. It is likely that during exponential growth, energy from photosynthesis is mainly used for cell division instead of being used for carbohydrates storage in LC-biofilms (Brányiková et al., 2011).

Taken all results together, the following hypothesis on biofilm dynamics under different conditions (initial cell concentration/physiology) is suggested: HC-biofilms presented a higher initial cell concentration and chlorophyll content compared to LC-biofilms (~ 30 and 1.7 times, respectively) so that the light penetration is expected to be lower in HC-biofilms. During cultivation, the cell concentration and dry matter increased while the cellular chlorophyll content decreased mainly due to dilution by cell division. Cells become therefore more transparent in HC-biofilms allowing light to penetrate at larger depth. In those conditions of higher light

intensity, HC-biofilms increase their carbohydrate pool compared to LC-biofilms. On the contrary, in LC-biofilms, an initial low cell concentration and/or chlorophyll content allow light to fully penetrate the biofilm leading to exponential growth. Cells maintained therefore their chlorophyll content (rate of division is similar to that of chlorophyll production). A decreasing trend in the ratio of carbohydrates to proteins may be linked to an increase in the cell protein content for cell division. To the best of our knowledge, these results have been barely reported. Indeed, Wang et al. (2015) described a decrease in the cell chlorophyll content of *S. dimorphus* microalgae biofilms developed on cellulose acetate/nitrate membranes with time. On the other hand, Huang et al. (2016) showed a decrease in chlorophyll content (per dry matter) for *C. vulgaris* biofilms on membranes between day 1 and 3. However, much higher biomass densities were studied in both works and no chemical composition in terms of macromolecular pools was described. Our study provide evidence that a similar acclimation mechanism may occur in immature biofilms formed on fabrics. Our findings also highlighted changes in chemical composition over time in photosynthetic biofilms (Fanesi et al., 2019; Yuan et al., 2020b).

More work is however required to better understand mechanisms of acclimation on phototrophic biofilms and fully characterize them in terms of structure and chemical composition. The effect of initial cell concentration and physiological properties (i.e., cellular chlorophyll content) on biofilm development and productivity should be better understood. Experiments aiming at investigating the effect of each parameter separately are described in the following chapter.

4. Conclusion

In this study, the dynamics of *C. vulgaris* biofilms was studied in a continuous laboratory scale reactor. The effect of the operational light intensity and inoculum cell density on biofilm development and composition was assessed. First, our results clearly showed a common development pattern already described for bacterial and other photosynthetic biofilms. Mechanisms of photo-limitation and photo-inhibition seem to occur elucidating the observed development profile. Biomass productivity was though quite low and probably explained by high detachment, support or strain properties. Interestingly, a fast acclimation mechanism (in 24h) has been identified probably associated to the sessile cell response to environmental

changes in terms of light availability. In addition, a decrease in the chlorophyll content of sessile cells during growth in HC-biofilms occurred. This may be a community response to increase light availability to cells within the biofilms. Overall, inoculum cell density together with chlorophyll *a* content (cell physiology) and light intensity strongly impacted biofilm kinetics and composition. Our study provides thus some preliminary data for the optimization of operational parameters of *C. vulgaris* biofilms in a lab-scale-based system. It also generates several scientific questions, some of those that will be discussed in the further chapters.

Supplementary data

Estimation of shear stress

As the velocity profile is unknown, the wall shear stress is defined as a function of friction factor:

$$\tau_w = \frac{f * \rho * v_s^2}{2}$$

where:

τ_w is the wall shear stress (N m⁻²),

f is the friction factor (dimensionless),

ρ is the density of the fluid (kg m⁻³),

v_s is the flow velocity (m s⁻¹).

If the flow is laminar (i.e. the Reynold's number is less than ~2300), the friction factor itself can be defined as a function of Reynold's number. For a rectangular conduit in which the width greatly exceeds the height:

$$f = \frac{96}{Re}$$

The Reynold's number gives a measure of the ratio of inertial forces to viscous forces, and is calculated as:

$$Re = \frac{\rho * v_s * D_h}{\mu_v}$$

where:

D_h is the hydraulic diameter of the chamber (m),

μ_v is the viscosity of the fluid (kg m⁻¹ s⁻¹).

For a flow chamber, the hydraulic diameter is modelled as:

$$D_h = \frac{4A}{P}$$

where:

A is the cross-sectional area of the flow chamber (m²),

P is the wetter perimeter (m).

The parameters for this particular chamber are given below:

Chamber height h: 0.009m,

Chamber width w: 0.065m,

Density (ρ) of water at 25° C: 997.044 kg m⁻³,

Viscosity (μ) of water at 25° C: 0.89×10^{-3} kg m⁻¹ s⁻¹,

Flow rate of water through the chamber: 0.3 ml/min = 0.5×10^{-8} m³ s⁻¹.

The rest of the required values can be calculated from the formulae provided above:

Hydraulic diameter (D_h): 0.028 m,

Reynold's number (Re): 0.27,

Friction factor (f): 355.63,

Shear stress (τ_w): 1.3×10^{-5} N m⁻² = 1.3×10^{-5} Pa = 1.3×10^{-2} mPa.

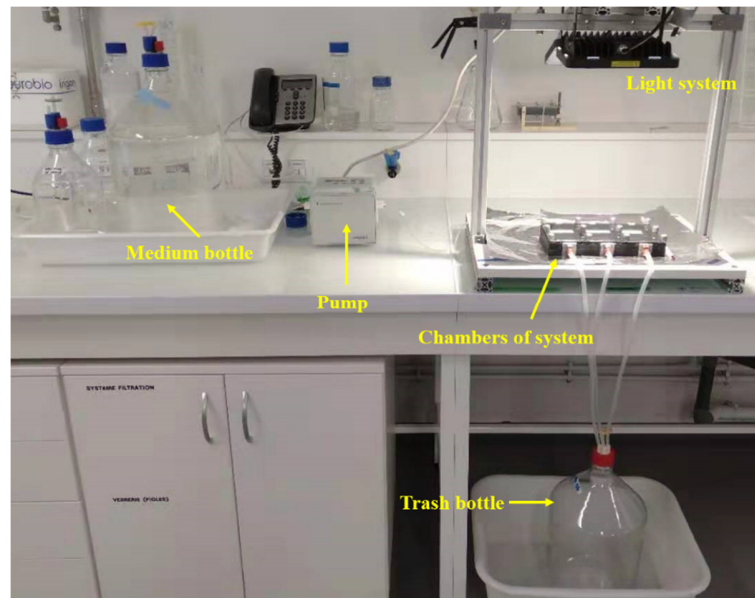


Figure S2-1. Configuration of flow-lane system for microalgae biofilm cultivation.

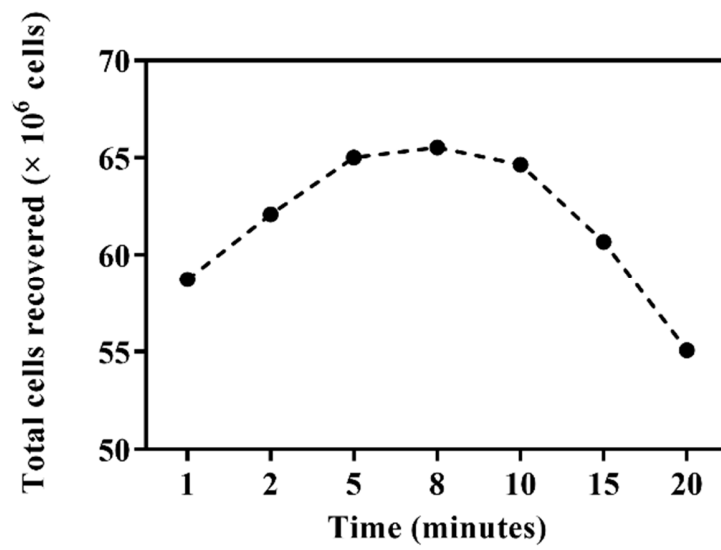


Figure S2-2. Oscillation recovery capability as a function of vortexing time during harvesting process.

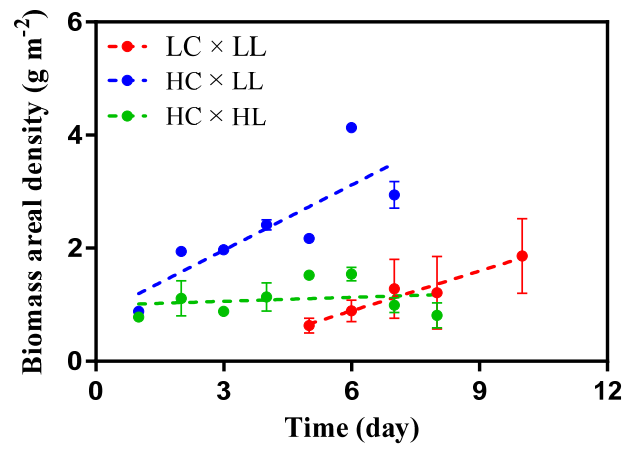


Figure S2-3. Dynamics of biomass areal density of *C. vulgaris* biofilms under different conditions.

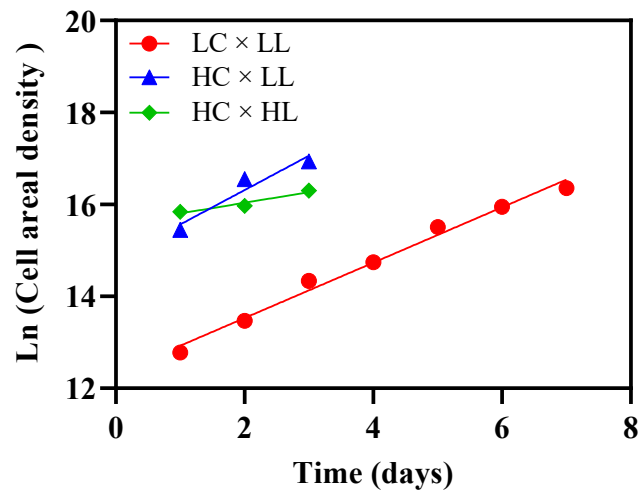


Figure S2-4. Logarithm of cell concentration of *C. vulgaris* biofilms under different conditions at exponential phase.

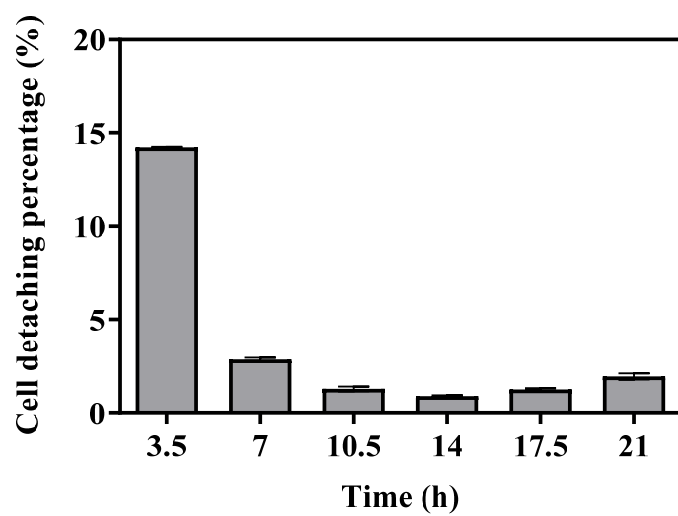


Figure S2-5. Cell detachment percentage of immobilized *C. vulgaris* on cotton support in the first 24 h.

Table S2-1. Productivity of *C. vulgaris* biofilms under different conditions.

System	Species of <i>C. vulgaris</i>	Light ($\mu\text{mol m}^{-2} \text{s}^{-1}$)	Substrate	Cultivation mode	Productivity ($\text{g m}^{-2} \text{d}^{-1}$)
Reference	Conditions [$^{\circ}\text{C}$, % CO_2]	Light/dark (h:h)	Cultivation area (m^2)	Medium	Duration
Pilot-scale rotating algal biofilm system	UTEX #265	Average: 642	Cotton duct	Semi-con.	4.29
(Gross et al., 2013b)	Average: 25.5 $^{\circ}\text{C}$, Greenhouse	Algal production greenhouse	3.5	Modified BBM	May-June
Lab-scale Rotating algal biofilm system	UTEX #265	110-120	Cotton duct	Semi-con.	3.51
(Gross et al., 2013b)	25 $^{\circ}\text{C}$, 0.03 % CO_2	Continuous	0.045	Modified BBM	7d
Pilot-scale revolving algal biofilm system	UTEX #265	Natural light	Cotton duct	Regrowth	5.8
(Gross and Wen, 2014)	11-35 $^{\circ}\text{C}$, Greenhouse	N.R.	2.94 or 1.85	Modified BBM	Harvest cycles of 7 d
Membrane biofilm reactor	UTEX 29-ATCC®30,581™	50	Mixed cellulose esters membrane	Batch	12.64 \pm 0.94
(Rincon et al., 2017)	26 \pm 2 $^{\circ}\text{C}$, 0.03 % CO_2	14 h L:10 h D	0.00152	With lycerol /urea	8d
Rocking cultivation chamber	ACUF_809	100	Stainless steel	Batch	0.04
(Shen et al., 2014)	26 \pm 2 $^{\circ}\text{C}$	Continuous	0.019	Modified BBM	15d
Rotating flat plate photobioreactor	SAG 211-12	139	Polyvinyl chloride, polypropylene	Regrowth	0.13, 0.26, 0.46
(Melo et al., 2018)	22 \pm 2 $^{\circ}\text{C}$	12 h L:12 h D	0.0004	BBM/2	Harvest cycles of 8 d

**CHAPTER III. Effect of textile supports,
inoculum cell density and inoculum
physiological properties on the
immobilized growth of *Chlorella vulgaris***

Preamble

As illustrated in chapter II, *C. vulgaris* biofilms, which grew on cotton in a continuous system, rapidly acclimated to the defined conditions within only 3 days but showed very low biomass productivities (only 0.15-0.65 g m⁻² d⁻¹) compared to other reports, though no stressful external factor (nutrients, pH, ...) during the whole cultivation was identified. We hypothesized that the low productivity may be linked to the losses generated by detachment and/or low inoculum cell concentration that may be related to support properties. Therefore, in order to verify our hypothesis, in this chapter the material properties of 5 different textile materials and their effects on cells retention capability was firstly investigated (step 1, Fig. 3-1). A new inoculation procedure was also implemented (cell filtration on the supports). Accordingly, Cotton and Terrazzo with different properties were selected to study the effect of support, inoculum density and inoculum properties (Chl *a* content related to the light history of the cells, here, cells pre-acclimated to 50 and 300 μmol m⁻² s⁻¹ before inoculation) on biofilm development, activity and composition. The impact of the two factors studied conjointly in chapter II, inoculum cell density (step 2) and properties (step 3), were here evaluated separately. Biofilm properties were characterized after 3 days, a time point the immobilized cells completed the acclimation process to the sessile growth mode, as described in Chapter II. In addition, the optimal condition regarding the support, inoculum density and light history for improving the biomass productivity was also identified.

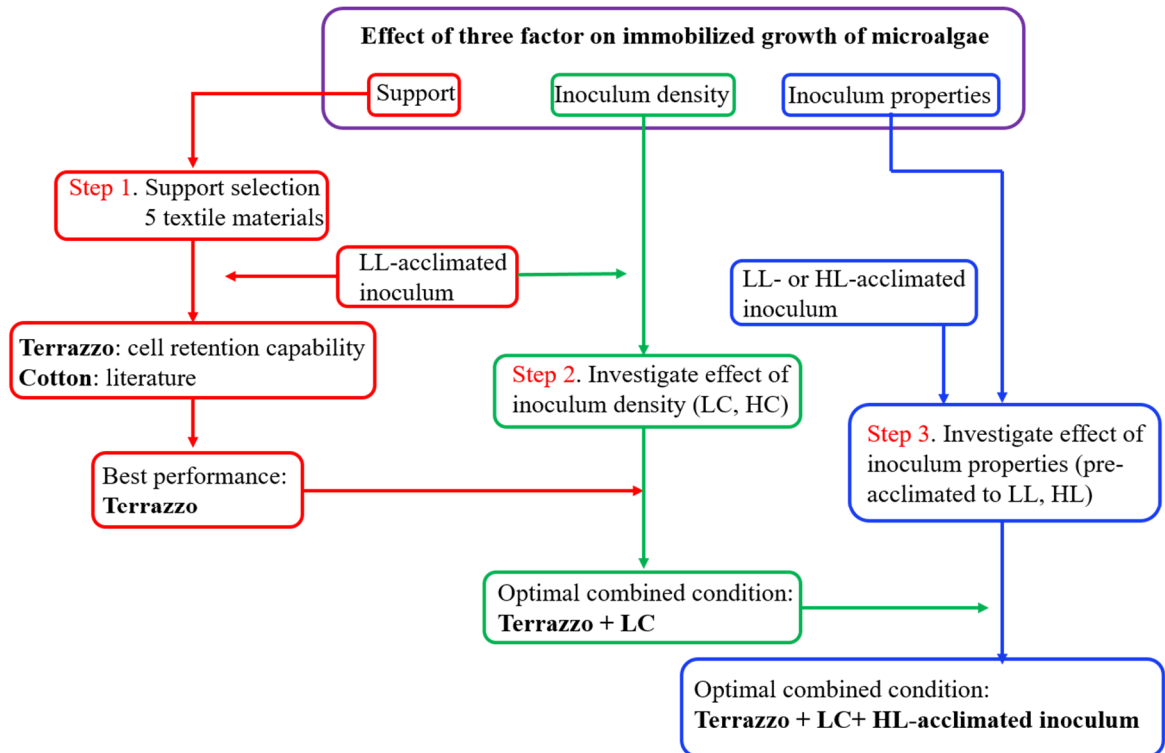


Figure 3-1. Flowchart of the main contents of Chapter III. LC and HC represent the low ($\sim 1.5 \times 10^6$ cells cm^{-2}) and high inoculum cell density ($\sim 7.0 \times 10^6$ cells cm^{-2}), respectively; LL- and HL-acclimated inoculum stands for cells pre-acclimated to low ($50 \mu\text{mol m}^{-2} \text{s}^{-1}$) and high light intensity ($300 \mu\text{mol m}^{-2} \text{s}^{-1}$) before inoculation, respectively.

Effect of textile supports, inoculum cell density and inoculum physiological properties on the immobilized growth of *Chlorella vulgaris*

Abstract

Microalgae biofilm-based cultivation has been considered lately as a promising alternative for microalgae production. It has been shown that process operational factors, such as the support and inoculum properties, may play an important role on cell colonization and biofilm development but more work is required to assess their impact on productivity and in particular on sessile cells physiology and activity. The final goal of this work is therefore to identify promising supports for biofilm based-systems and to assess the impact of the cited operational factors on productivity. Cell retention/detachment ability of 5 textile materials (Terrazzo, Nordkap, Mariella, Sun silk and Cotton) were first estimated and Terrazzo was shown to be the most performant support. Moreover, in order to get a better insight into cell-support interaction, supports (micro-texture, hydrophobicity, roughness and chemical functional groups) were characterized. Terrazzo and Cotton, already investigated in Chapter II, were then chosen as support for the biofilm studies. Cell/biofilm distribution patterns on the supports were assessed using complementary imaging tools (CLSM - Confocal Laser Scanning Microscopy, ESEM -Environmental Scanning Electron Microscopy, OCT - Optical Coherence Tomography). Our data clearly show a reduction in biofilm growth with inoculum density, which may be linked to the light/nutrients availability. In addition, biofilms starting with cells photo-acclimated to high light (BP-HL) presented a higher biomass productivity compared to that pre-acclimated to low light. Three times higher biomass productivity was obtained for Terrazzo compared to that on Cotton described in chapter II. Therefore, Terrazzo was confirmed as a promising support for microalgae biofilm-based systems and the operational factors to obtain the maximal biomass productivity were identified.

Keywords: *Chlorella vulgaris*, Microalgae biofilms, Physiological properties, Surface physical-chemical properties, Textile materials

1. Introduction

Biofilm-based microalgae cultivation presents several advantages over conventional suspended approaches such as reduced costs of harvesting operations (i.e., with a simple method of scraping concentrated cultures from the solid surfaces), energy demand and water use (Christenson and Sims, 2012; Gross et al., 2015; Johnson and Wen, 2010). Interest in these kinds of technologies has been thus increasing lately. Studies proposing innovative designs and culture conditions optimization have also emerged lately in order to fully confirm the interest of the biofilm approach for large-scale cultivation (Genin et al., 2014; Li et al., 2017).

The inoculation step is of prime importance for microalgae biofilms formation, affecting the final biomass yield and productivity (Genin et al., 2014; Moreno Osorio et al., 2020; Zheng et al., 2019). Recent studies have reported that factors such as inoculum density and the nature of substrates (on which cells grow) affect the initial colonization (Gross et al., 2016; Irving and Allen, 2011; Shen et al., 2017). Indeed, biofilm productivity can be improved by increasing the inoculum size (Ji et al., 2014; Zhang et al., 2014). A maximal productivity of $57.87 \text{ g m}^{-2} \text{ d}^{-1}$ under optimal inoculum density of 18 g m^{-2} was recorded by Shen et al. (2017). However, care must be taken because over a certain density threshold, the productivity does not increase further and even decreases due to light attenuation and/or nutrients limitation (Huang et al., 2016; Schnurr et al., 2014; Schnurr and Allen, 2015). On the other hand, the properties of substrates (e.g., surface free energy, hydrophobicity, micro-pattern, etc.) play an important role in cells colonization (Chen et al., 2014; Gross et al., 2016; Tsavatopoulou and Manariotis, 2020). Studies demonstrated that *C. vulgaris* adhesion was significantly influenced by the surface free energy of supports (Mohd-Sahib et al., 2018; Sirmirova et al., 2013). Some studies also reported that biofilm formation and growth positively correlated with the surface hydrophobicity (Ozkan and Berberoglu, 2011; Tsavatopoulou and Manariotis, 2020). Also, the micro-texture of supports such as microgrooves act as anchor points that can protect cells from shear stress (Huang et al., 2018). Therefore, appropriate support selection must be considered when designing and optimizing biofilm-based systems (Sukačová et al., 2020).

Supports must be cost-effective, nontoxic, resistant and accessible (Zhang et al., 2017). However, many supports currently used are unproductive (glass, stainless steel, polyvinyl chloride) (Gross et al., 2016; Hultberg et al., 2014), disposable and not long-term resistant

(filter/printing paper, cardboard) (Johnson and Wen, 2010; Tran et al., 2019) or even show toxicity to cells (copper and admiralty brass) (Sekar et al., 2004). Pioneering studies have demonstrated that fabric materials are promising and could be reused to support the microalgae growth (Gross et al., 2013b; Gross and Wen, 2014; Hart et al., 2021; Johnson and Wen, 2010; Moreno Osorio et al., 2019). However, these studies mainly focus on the initial cells attachment and/or overall biofilm productivity (Brockhagen, 2021; De Assis et al., 2019; Gross and Wen, 2014; Moreno Osorio et al., 2019), very few considered the influence of the nature (i.e. micro-texture and physical-chemical properties) of textile supports on biofilm formation, cell distribution patterns, physiological state of immobilized cells which will in turn affect biomass productivity.

Therefore, the goal of this work is to assess the impact of fabrics properties (micro-texture and physical-chemical properties), inoculum density and physiology on the initial colonization by *C. vulgaris* in a short term (3 days, a period during which cells fully acclimate to the new environmental conditions imposed by the sessile state, as observed in chapter II) to identify the most appropriate support for biofilm development. Assays were also carried out to identify the underlying mechanisms of microalgae-support interaction. In order to do so, the cells adherence/detachment performances of *C. vulgaris* on 5 textile materials were firstly investigated. Cotton, considered as an excellent material for biofilm development (Christenson and Sims, 2012; Gross et al., 2013b) already studied in chapter II, and Terrazzo with the highest cells-loading capacity were then selected to assess the impact of support characteristics on biofilm production, activity and composition. The surface micro-patterns (i.e., mesh size, mesh areal density, etc.) of the two supports and the distribution of cells on their surface were observed at micro-scale with imaging tools (e.g., Confocal Laser Scanning Microscopy, CLSM, and Environmental Scanning Electronic Microscopy, ESEM). In addition, the physical-chemical properties (i.e., roughness, hydrophobicity, functional groups) of supports were determined, and the physiological status of the pre-acclimated cells and sessile cells was also carried out by PAM. The selection of a promising support for further biofilm cultivation system is also expected.

2. Materials and Methods

2.1. Planktonic culture maintenance

Chlorella vulgaris SAG 211–11b (Göttingen, Germany) was cultured semi-continuously in 1-L transparent bottles with 800 mL 3N-Bristol medium (Bischo and Bold, 1963) at 25°C. The cultures were bubbled with filtered air under continuous illuminations of 50 (low light, LL) and 350 $\mu\text{mol m}^{-2} \text{s}^{-1}$ (high light, HL) (Viugreum 50W LED outdoor floodlights, the irradiance was measured by QSL-2100 quantum scalar irradiance sensor, Biospherical Instruments, San Diego, CA, USA). The cultures were kept in exponential phase with a max cell concentration of 5.8×10^6 cells mL^{-1} by daily dilution in order to maintain a chlorophyll (Chl) *a* concentration of 0.5 - 1.5 mg Chl *a* L^{-1} to ensure optimal light penetration. The planktonic cultures were pre-acclimated to 50 or 350 $\mu\text{mol m}^{-2} \text{s}^{-1}$ for at least 8 days before starting any experiment (for *C. vulgaris*, typically 5 days were enough to have a stabilization of Chl *a* content and growth rate, see Fig. 3-2). Several characteristics of the suspended culture cells (growth rate, cell volume, photosynthetic activity and cellular composition) were determined.

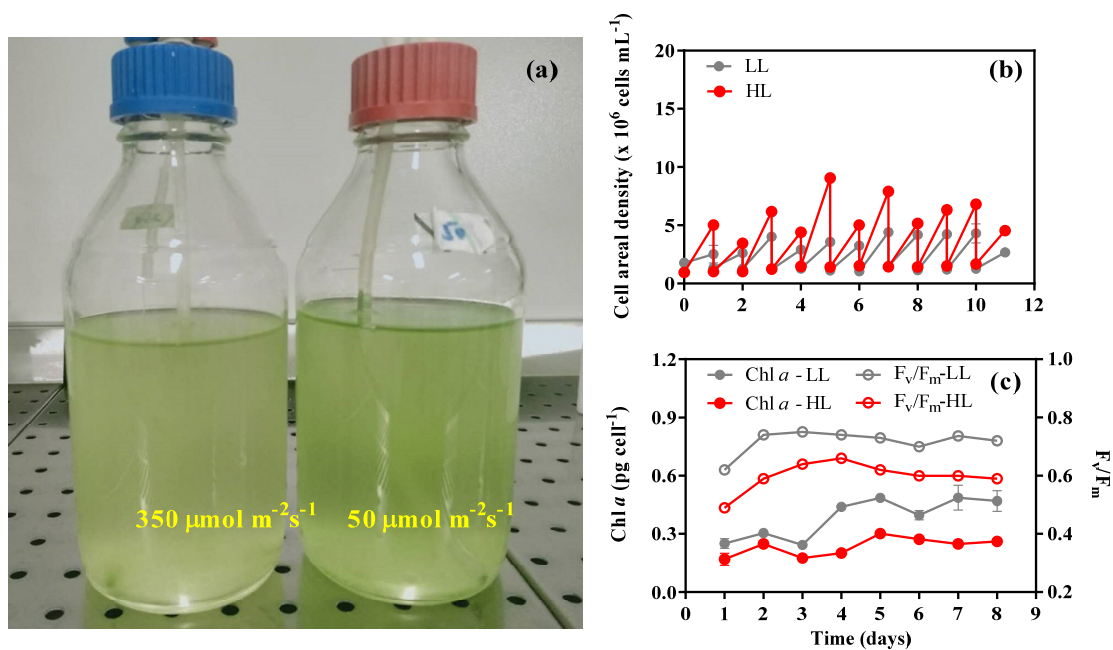


Figure 3-2. Suspended cultures (before dilution) (a), cell concentration (b), cellular chl *a* content and maximum quantum yield (F_v/F_m) (c) over time under 50 (low light, LL) and 350 $\mu\text{mol m}^{-2} \text{s}^{-1}$ (high light, HL) in the pre-acclimated process.

2.2. Microalgae inoculation

Cells immobilization on supports can be achieved either by cells active motion towards

the support surface, or by cells being transported by gravity or convection, or even by artificially filtering cells (Cui et al., 2013; Kreis et al., 2018; Murphy and Berberoglu, 2014; Ozkan and Berberoglu, 2011; Shi et al., 2014). According to (Hart et al., 2021), artificial immobilization allows greater flexibility in systems design and helps operational optimization. Compared to the inoculation process described in chapter II where the coupons were inoculated by placing cotton in static suspended cultures (conventional approach) for 24h, we used here a filtration method (see below) which is time-saving (the process needs only several minutes) and shows the approximately same biomass accumulation rate after 3 days as that in chapter II (Fig. S3-1).

The microalgae immobilization was carried out by filtrating a defined volume of suspended culture on the materials which were previously cut into pieces ($2.4\text{ cm} \times 2.4\text{ cm}$, with an effective colonization area of 2.01 cm^2). Before the immobilization of cells, the materials were sterilized in Milli-Q water at 121°C for 15min. After 10-time filtration of the same algal solution, the materials were washed slightly in Petri dishes to remove the loosely attached cells. They were then placed in Multi-well culture plates (6 wells) filled with 8 mL of 3N-Bristol medium and exposed to $100\ \mu\text{mol m}^{-2}\text{ s}^{-1}$ (measured with a LI-190R Quantum Sensor, LI-COR Biosciences GmbH, Bad Homburg, Germany).

2.3. Selection of textile supports

The selection of the supports was based on the criteria of cells-loading capacity (i.e., how many cells were retained on the support), durability and cost-effectiveness. Here, 4 textile materials including Terrazzo, Nordkap, Mariella, Sun silk (purchased online, <https://www.tissusactifs.fr/>) and cotton (purchased from a hardware store, Fig. 3-3) were tested.

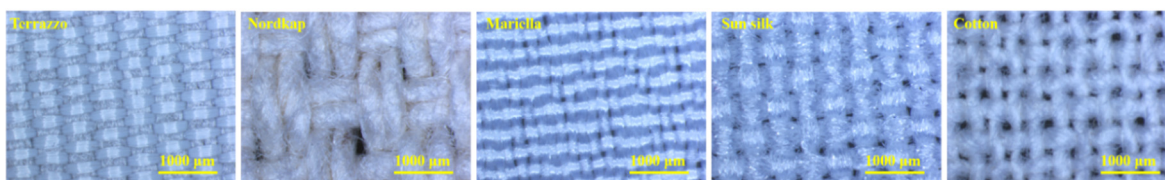


Figure 3-3. Micro-texture of textile materials observed with $30\times$ magnification.

For cells-loading test assay, suspended cultures ($1.0 \times 10^7\text{ cells mL}^{-1}$, 2 mL, pre-acclimated to $50\ \mu\text{mol m}^{-2}\text{ s}^{-1}$) were filtered on those 5 textile materials. In order to stabilize the attached cells, the coupons were incubated for several hours. After 6-h incubation under

100 $\mu\text{mol m}^{-2} \text{s}^{-1}$, cells in solution and on the bottom of plates (detached proportion), and those on textile materials (successfully immobilized fraction) were quantified using the Flow cytometer (Guava EasyCyte HT; Millipore, USA) to characterize cell attachment and detachment (see 2.5 section). The cells on textile materials were harvested with 10 mL medium in 50 mL centrifugation tubes (containing glass beads) by vigorously vortexing for 5 min.

2.4. Immobilization and growth of *C. vulgaris* on two textile supports (Cotton and Terrazzo)

Cotton and Terrazzo were selected to assess the influence of the support and inoculum density/physiological properties on biofilm growth. Multi-well culture plates were used as bioreactors for *C. vulgaris* immobilized growth. Two initial cell densities corresponding to $(1.5 \pm 0.2) \times 10^6$ cells cm^{-2} (low inoculum cell density, LC, 0.2 ± 0.02 g m^{-2}) and $(7.0 \pm 1.4) \times 10^6$ cells cm^{-2} (high inoculum cell density, HC, 0.8 ± 0.16 g m^{-2}) were obtained by filtrating specific volumes of planktonic culture (pre-acclimated to 50 and 350 $\mu\text{mol m}^{-2} \text{s}^{-1}$) on Cotton and Terrazzo. After filtration, the textile was sewed up with a silicon pad (2.4 cm \times 2.4 cm, preventing the supporting system floating and thus cells dehydration) and then placed in the multi-well culture plate under 100 $\mu\text{mol m}^{-2} \text{s}^{-1}$. Considering the fast acclimation of *C. vulgaris* observed in chapter II, the coupons were incubated for three days. The medium was completely renewed every day to avoid nutrient limitation.

In order to test the impact of inoculum physiological properties (Chl *a* content) on biofilm formation, composition and activity, cells pre-acclimated to 50 (LL-acclimated cells) and 350 $\mu\text{mol m}^{-2} \text{s}^{-1}$ (HL-acclimated cells) were filtrated on Terrazzo with low initial cell density and then exposed to 100 $\mu\text{mol m}^{-2} \text{s}^{-1}$. After 3-days growth, the sessile cells were harvested from the supports and further measurements were conducted to assess the impact of inoculum physiology or light history on biofilm growth/development, activity and composition. Here, biofilms formed from cells photo-acclimated to 50 $\mu\text{mol m}^{-2} \text{s}^{-1}$ were designated as BP-LL biofilms (Biofilms Produced with Low Light acclimated cells) and those formed from cells photo-acclimated to 350 $\mu\text{mol m}^{-2} \text{s}^{-1}$ as BP-HL biofilms (Biofilms Produced with High Light acclimated cells).

2.5. Relative biomass increase and cell areal density on textile supports and percentage of unattached biomass

After three days, cells were mechanically harvested in 10 mL Bristol medium supplied with glass beads. Although several harvesting steps were performed, we could not fully recover the cells from the supports. A green color was still observed after this procedure. Therefore, in order to fully estimate the immobilized biomass, Chl *a* left on the coupons was extracted according to the method described in section 2.7.3. The number of residual cells was afterwards estimated based on the average cellular Chl *a* content which was measured from the easily recovered cells. The relative biomass increase to the initial population on the coupon (R_c) and the cell areal density (D_c) were therefore calculated according to Eq. (1) and Eq. (2), respectively:

$$R_c = (C_v + C_{chl} - C_0)/C_0 \quad (1)$$

$$D_c = (C_v + C_{chl})/E_{area} \quad (2)$$

Where C_v and C_{chl} represent cell numbers obtained by mechanically harvesting and by Chl *a*-content measurements after 3 days, respectively. C_0 stands for the cells on supports at the beginning of the experience; whereas E_{area} (cm²) represents the apparent area of the support (Fig. S3-2, E_{area} of Cotton and Terrazzo are 5.76 and 2.78 cm², respectively).

In order to assess cell detachment, cells in the liquid and on the bottom of wells (unattached proportion, $C_{unattached}$) were measured prior to renewing the medium. Cell detaching percentage (D_p) was calculated by Eq. (3):

$$D_p = C_{unattached}/(C_v + C_{chl} + C_{unattached}) \quad (3)$$

2.6. Micro-texture and physical-chemical properties of textile supports

2.6.1. Mesh size and mesh areal density

The micro-texture of the textile materials was observed using a stereomicroscope (Zeiss, Discovery V12, Germany). The images were taken in a size of 2.30 mm × 1.72 mm with 63 × magnification. The length and width of the mesh size was measured for all tested materials, and the mesh areal density (i.e., the opening area in 1 m² of material) was

quantified using Fiji software.

2.6.2. Roughness of surface

Surface roughness of the textile materials was quantified using a microtopographe (TIL CHR 150). At least five positions on each type of material were randomly selected and determined. The surface roughness (Ra) was analyzed by Mountains Map Universal software (Digital Surf Sarl 3.0; Besancon, France) and roughness profiles for the tested materials are shown in Fig. S3-3.

2.6.3. Hydrophobicity

The hydrophobicity of textile materials was determined using the sessile drop test with an automatic drop tensiometer (Tracker Teclis/IT Concept, France). 5 μL of distilled water (as reference liquid) was pipetted onto the surface of horizontally placed materials, and the images of water drops were analyzed using WDROP 2010 software to characterize the static water contact angle (θ) which reflects the hydrophobicity ($0^\circ < \theta \leq 90^\circ$, hydrophilic surface; $90^\circ < \theta < 180^\circ$, hydrophobic surface; $\theta = 180^\circ$, ultra-hydrophobic surface). The larger the contact angle, the higher the hydrophobicity of materials.

2.6.3. Chemical properties (FTIR spectroscopy)

ATR-FTIR PerkinElmer Spectrum-two spectrometer (PerkinElmer, Waltham, MA, USA) was used to analysis the chemical properties of the textile materials. Infrared spectra were recorded in the range of 4000 to 400 cm^{-1} using an accumulation of 32 scans at a spectral resolution of 4 cm^{-1} . Before loading materials, the empty crystal was measured as background.

2.7. Physiological characterization of pre-acclimated cells and sessile cells

2.7.1. Cell morphology

Average cell size was determined considering a minimum of 300 individual cells using an AxioSkop 2 plus microscope (Carl Zeiss, Oberkochen, Germany) under 63 \times magnification (Hillebrand et al., 1999).

2.7.2. Variable chlorophyll *a* fluorescence measurements and relative electron transport rate (rETR) estimation

Photosynthetic activity of immobilized *C. vulgaris* after 3 days was assessed with Pulse Amplitude Modulation (PAM) fluorometer (AquaPen, AP 110-C, Photon Systems Instruments, Drasov, Czech Republic). After 10 min of dark-adaptation, the samples were exposed to a stepwise increase of seven actinic lights (from 0 to 1000 $\mu\text{mol m}^{-2} \text{s}^{-1}$, blue led at 455 nm) with 60s intervals to construct the electron transport rate versus photon flux density (ETR/PFD) curves. Photosynthetic parameters such as the maximum quantum yield (F_v/F_m) and the effective quantum yield ($\Delta F/F'_m$), and the relative electron transport rate (rETR) were calculated as described in (Guzzon et al., 2019). Additionally, the rETR vs. PFD curves were fitted with the function $\text{rETR} = \text{rETR}_{\text{max}} (1 - e^{-\alpha I/\text{rETR}_{\text{max}}})$ (Webb et al., 1974), to estimate the maximum rate of relative ETR (rETR_{max}), where α and E_k represent the initial slope of curves and photo-saturation ($E_k = \text{rETR}_{\text{max}}/\alpha$), respectively.

2.7.3. Cellular composition: Chlorophyll *a* and macromolecules

Chl *a* was extracted from harvested cells and residual cells on supports using dimethyl sulfoxide (DMSO) (Wellburn, 1994), and quantified by measuring the absorption at 649 nm and 665 nm with an Evolution 60S UV–visible spectrophotometer (Thermo Scientific, Madison, WI, USA). The Chl *a* concentration was calculated by Eq. (4) (Wellburn, 1994):

$$\text{Chl } a \text{ } (\mu\text{g mL}^{-1}) = 12.19 \times \text{OD}_{665} - 3.45 \times \text{OD}_{649} \quad (4)$$

The average cellular Chl *a* content (pg cell^{-1}) was calculated considering the extracted cell number.

Macromolecular composition was analyzed with the FTIR spectrometer. The spectra were baselined and maximum absorption values in the spectral ranges corresponding to specific macromolecular pool: carbohydrates (C–O–C; 1200–950 cm^{-1}), proteins (Amide I; 1700–1630 cm^{-1}) were used to calculate the relative carbohydrates contents to proteins (Duygu et al., 2012; Fanesi et al., 2019).

2.8. Biofilm imaging

Textiles materials and immobilized cells at day 3 were observed at micro-scale. In order

to observe the overall distribution of cells on Cotton and Terrazzo, the stereomicroscope was used to acquire images. The images were taken in a size of 2.30 mm × 1.72 mm with 63 × magnification. In addition, due to the emission of chlorophyll *a* autofluorescence at 639 nm, cells on supports could be detected using an inverted Zeiss LSM700 confocal microscope (Carl Zeiss microscopy GmbH, Jena, Germany) equipped with a LD Plan-Neofluar 20×/0.4 Korr M27 objective with a 0.4 N.A. (numerical aperture) (Fanesi et al., 2019). The obtained images were 640 × 640 μm in size with a z-step of 3.94 μm and a lateral resolution of 1.25 μm.

In order to further investigate the interaction of algal cells with the fibers of supports, an environmental scanning electron microscope (ESEM, FEI Quanta 200) was used to obtain SEM images with 500× and 2000× magnification. A small piece of supports (5 mm × 5 mm) was examined at 20 kV accelerating voltage with a working distance of 14 mm in a high vacuum mode. The chamber was precooled to 7~8 °C which can be used for the determination of samples in a solid-liquid phase and minimize drying. Each support observation was performed in at least three random positions.

In addition, biofilm formation on Terrazzo inoculated with a LC-inoculum (Low cell density, $\sim 1.5 \times 10^6$ cells cm⁻²) was observed by Optical Coherence Tomograph (OCT; Ganymede 621, Thorlabs GmbH, luebeck, Germany) equipped with a telecentric scan lens (OCT-LK3-BB). The images were acquired at a speed of 25kHz per A-scan and an averaging of 6 A-scans. The field of view was 4 × 4 mm (XY) and the axial depth 1 mm (Z). The lateral and axial resolution were 8 μm and 1.45 μm, respectively. A refractive index of 1.33 was used for all the image acquisitions, as the biofilm was imaged *in situ* in liquid medium (Wagner and Horn, 2017). Images were then analysed using the software ThorImageOCT 5.4.4 (Thorlabs, luebeck, Germany).

3. Results and discussion

In this chapter, the main goal is to select an appropriate textile for *C. vulgaris* development. We also aim at better understanding of the underlying mechanisms responsible for cell retention on the different supports tested. To do so, fabrics hydrophobicity, roughness and mesh areal density were first determined.

Physical-chemical characterization of both *C. vulgaris* and the two selected fabrics (Terrazzo and Cotton) was performed afterwards by FTIR. Accordingly, molecular

mechanisms were briefly suggested. Imaging tools (SEM, CLSM) were then applied to assess cell/biofilm distribution on Terrazzo and Cotton, and OCT was also used to observe the culture dynamics on Terrazzo. Finally, the impact of the two factors studied conjointly in chapter II, inoculum cell density and cell physiology (related here to Chl *a* content), on biofilm development, productivity, activity and composition were evaluated separately.

3.1. Support selection for microalgae immobilized growth

Fig. 3-4 shows cells retention and detachment for the different textiles. A highest cell areal density (17.0×10^6 cells cm^{-2}) and a low detachment (36.3%) were obtained for Terrazzo compared with the other materials. On the other hand, though Nordkap showed high cell retention capability/low detachment, it could not be further used due to its deformation after sterilization and mechanical harvesting. Low cell areal densities ($1.5\text{--}2.2 \times 10^6$ cells cm^{-2}) and high releasing percentages (43.60%, 50.56% and 78.25%, respectively) were obtained when using Cotton, Mariella and Sun silk. These preliminary data may suggest that Terrazzo is a promising material for biofilm-based microalgae cultivation.

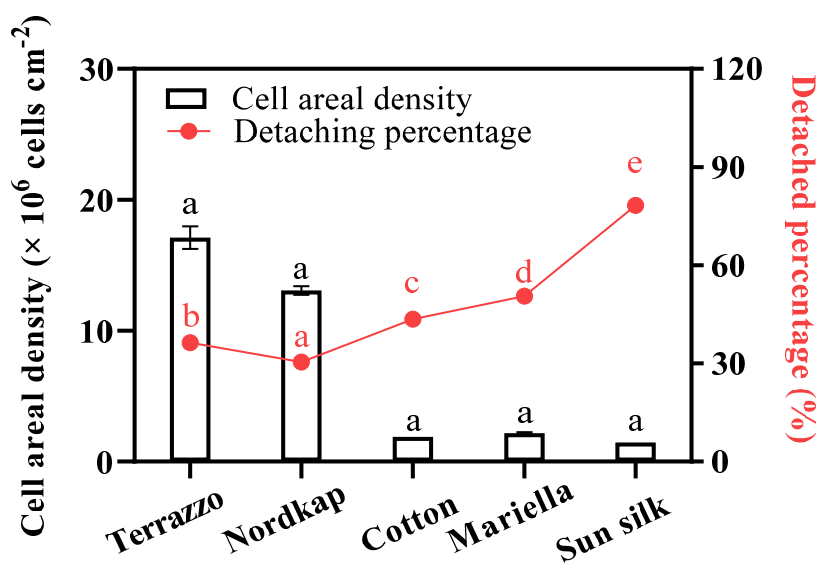


Figure 3-4. Cell areal density and cell detachment percentage on different textile materials after 6-h incubation. All the results were shown as mean value \pm SD ($n = 3$). Bars and dots with different letters represent the statistical differences among different textile materials at a level of $P < 0.05$.

It has been reported that properties of supports, such as mesh (or opening and pore) size, roughness, hydrophobicity and surface functional groups, can impact cell immobilization.

For instance, Gross et al. (2016) illustrated that the mesh size strongly impacted the cells immobilization/detachment of *C. vulgaris* on 6 different materials (stainless steel, aluminum, polyester, high-density polyethylene, nylon, polypropylene). Cui et al. (2013) also demonstrated that cell attachment increases with the decrease of the support's pore size until the size is close or smaller to that of the algal cell. In our work, it appears that cells retention on textile materials is negatively correlated with the mesh areal density ($R^2 = 0.8994$, based on second-order polynomial fitting, Fig. S3-4), rather than the surface pore size (Table 3-1). An increasing mesh areal density is observed from Terrazzo to Cotton (Terrazzo < Nordkap < Mariella < Sun silk and Cotton; Table 3-1 and Fig. 3-3), and their cell loading capacity therefore showed an opposite trend. It should be also reminded that *C. vulgaris* cells are much smaller (2-10 μm) than the mesh size of the most textile materials used here (table 3-1).

Table 3-1. Physical-chemical properties of textile materials.

Textile material	Composition	Mesh Length (μm) \times width (μm)	Mesh density ($\text{cm}^2 \text{m}^{-2}$)	Contact angle ($^\circ$)	Roughness (μm)	Weight (g m^{-2})
Terrazzo	polyamide	N.D.	~ 0	131.5	16.48 ± 6.55	180
Nordkap	100% cotton	$(0\sim 274) \times (0\sim 105)$	14.52	110.9	55.52 ± 4.91	370
Mariella	100% polyester	$(38\sim 143) \times (35\sim 87)$	29.20	ND	27.55 ± 3.97	100
Sun silk	100% polyester	$(144\sim 372) \times (18\sim 160)$	74.58	35.4	49.00 ± 8.02	180
Cotton	100% cotton	$(277\sim 376) \times (133\sim 344)$	101.90	128.0	37.02 ± 10.86	N.D.

N.D. represents not detected.

On the other hand, support hydrophobicity is another important parameter when considering microalgae biofilm formation, but its effect is still somewhat inconclusive. Many researchers have stated that hydrophobic surface promotes cells adhesion. The hypothesis behind is that hydrophobic cells attach easier to each other or to the hydrophobic surfaces in order to decrease their contact with water (Ozkan and Berberoglu, 2011; Palmer et al., 2007; Roostaei et al., 2018; Sekar et al., 2004). Some other studies, however, observed no or weak correlations between the hydrophobicity of supports and cells adhesion (Genin et al., 2014; Irving and Allen, 2011; Schnurr and Allen, 2015). In our study, although Cotton presents high hydrophobicity ($\theta = 128^\circ$) as Terrazzo, the cells retention was 11 fold less than that on the latter support (Table 3-1, Fig. 3-4), suggesting that the surface hydrophobicity of the material has minor effect on *C. vulgaris* adhesion. This finding is in agreement with another study that demonstrated no clear correlation between attached cell density of *C. vulgaris* and *Senedescumus obliquus* and the hydrophobicity of materials such as borosilicate glass, polyethylene, polyurethane, and poly(methyl methacrylate) (Irving and Allen, 2011).

In addition to hydrophobicity, surface roughness did not seem to affect algal retention (Table 3-1, Fig. 3-4), although an enhancement of microalgae attachment to supports with roughness has been extensively reported (Huang et al., 2018; Sekar et al., 2004; Zhang et al., 2020; Zhang et al., 2017).

In conclusion, cell retention in fabrics is correlated to the mesh areal density and seems less influenced by support hydrophobicity and roughness. Considering the best performance of Terrazzo in terms of cell retention/detachment, this support together with cotton which was already investigated in chapter II and in many other works (Christenson and Sims, 2012; de Assis et al., 2019; Gross et al., 2013b; Moreno Osorio et al., 2020, 2019), were chosen for further studies presented hereafter.

3.2. Understanding the interaction between Terrazzo/Cotton and *C. vulgaris* at different scales

FTIR spectra (Fig. 3-5) allow to identify functional groups on the surface of the support that may established molecular interactions with those at the cell surface. The spectra of supports (Cotton and Terrazzo) show broad and intense peaks from 3000 to 3500 cm^{-1} , suggesting the existence of the O-H and N-H stretching vibrations (Shahzadi et al., 2018),

which may suggest that the supports interact with *Chlorella* cells (cell-support) through hydrogen bonding. As already demonstrated by Bajpai et al. (2011), both bacteria and fabrics (like cotton) have abundant free hydroxyl groups that may participate in the cell-support interaction. In addition, peaks at 1633.97 and 1537.32 cm^{-1} corresponding to C=O of amide-I and N-H stretch of amide-II, respectively, were observed on Terrazzo (Duygu et al., 2012). This is linked to the polyamide fibers which may promote the immobilization of cells on Terrazzo through hydrogen bonding (Bajpai et al., 2011; He et al., 2016; Nomura and Terwilliger, 2019). Additionally, proteins on the microalgal cell wall may supply free electrons to unsaturated bonds on Terrazzo fibers through functional groups, e.g., the alkylation of amino group, enhancing the cell-support interaction (Chen et al., 2014). In contrast, C-O bonds probably associated to polysaccharides were reported on Cotton through the characteristic peaks at 1054.50 and 1038.88 cm^{-1} (Duygu et al., 2012). The interaction between polysaccharides on the surface and the cells may play a role on the cell initial adherence to Cotton fibers (Bajpai et al., 2011). On the whole, our data suggests that the interaction between Terrazzo or Cotton and *C. vulgaris* cells is dependent on the surface chemical composition, as expected.

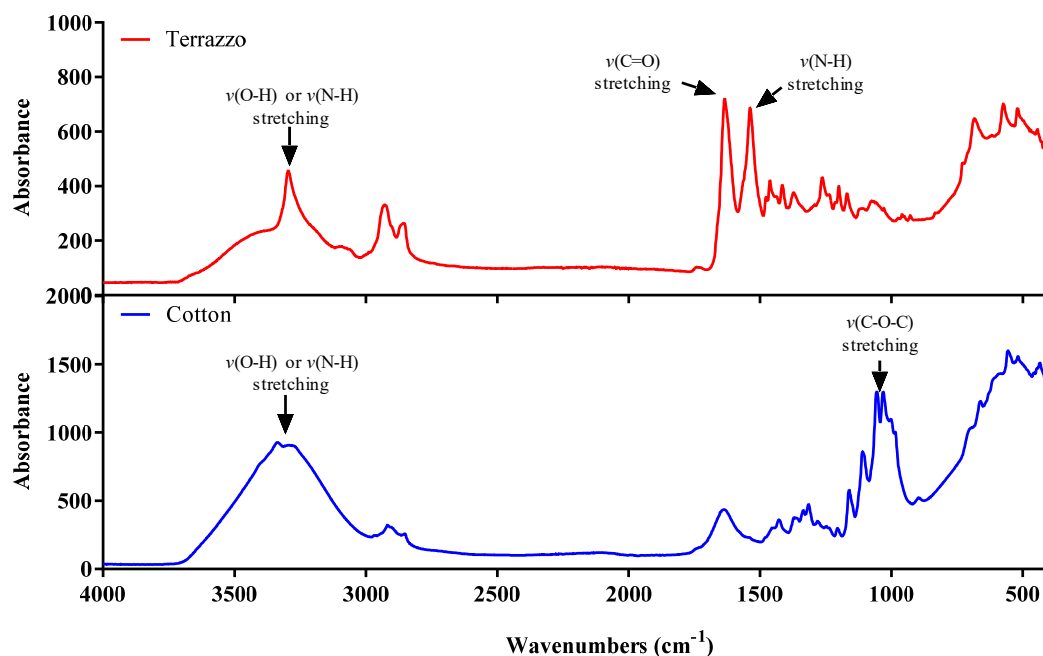


Figure 3-5. FTIR spectra of Cotton and Terrazzo supports.

In order to go further in the understanding of the interactions between cells and the

supports, different imaging tools were used (CLSM, SEM and OCT). From Fig 3-6, it appears that microalgal cells do not cover uniformly the entire fabric (CLSM and SEM images) at day 3. Cell distribution pattern also seem different for the two supports. Indeed, cells seem to be attached on and in between the tightly woven fibers on Terrazzo while they do attach and grow mainly on the superficial and loosely connected fibers of Cotton (Videos in supplementary data). Similar cell distribution pattern on loosely knitted cotton and nylon fibers has been reported by de Assis et al. (2019), but currently no information on the tightly woven materials like Terrazzo is available.

Clusters of cell layers can be also observed on Terrazzo. Interestingly, images at macroscopic scale (Fig. S3-2) clearly show differences in cells distribution on the two tested supports. After 3-day cultivation, cells spread across the surface of Cotton (5.76 cm²) but kept concentrated on Terrazzo (2.78 cm²). This is likely due to low strength of cell-cell and cell-fibers interactions when algal cells grew on Cotton. Such a spreading mechanism on Cotton was also reported in another work which used two *Chlorella* strains at their early colonization stage (mono layer) (Moreno Osorio et al., 2020).

Fig. 3-7 shows biofilm structural dynamics on Terrazzo obtained by OCT imaging. A support structure composed of tightly fibers is detected (Fig. 3-7, day 0) which is consistent with the low mesh areal density determined previously (Table 3-1). In agreement with CLSM data (Fig. 3-6), OCT images also confirm the spatial biofilm heterogeneity on the support. In addition, biofilm growth is visible from day 2 onwards.

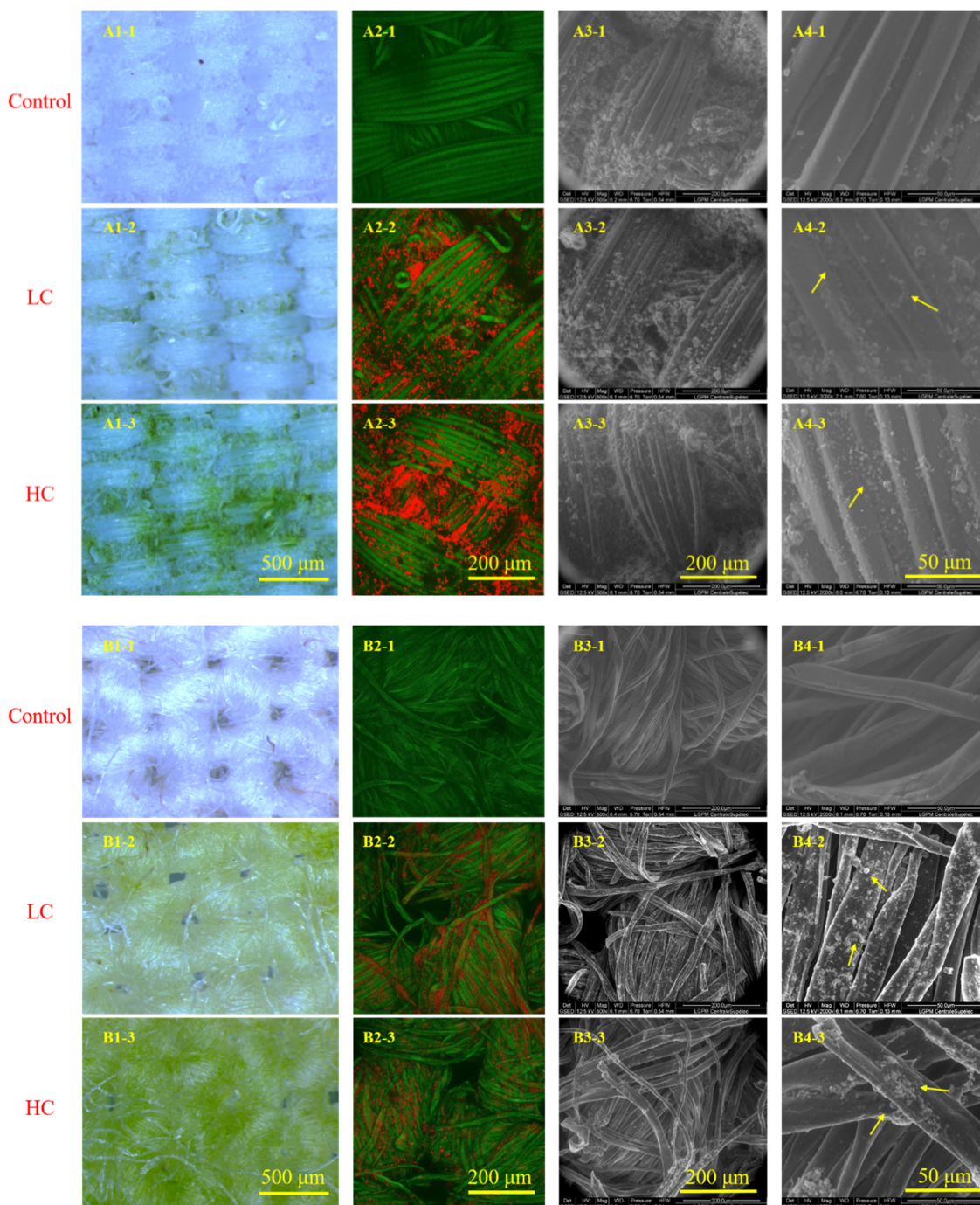


Figure 3-6. Microscopic structural observation of supports (Control) and cells attached on their fibers at day 3 (LC, supports inoculated with low cell density; HC, supports inoculated with high cell density. A, Terrazzo; B, Cotton). A1 and B1 represent stereomicroscope images, A2 and B2 represent CLSM images, and A3, A4, B3 and B4 are SEM images (yellow arrows indicate cell or cells clusters on the support fibers).

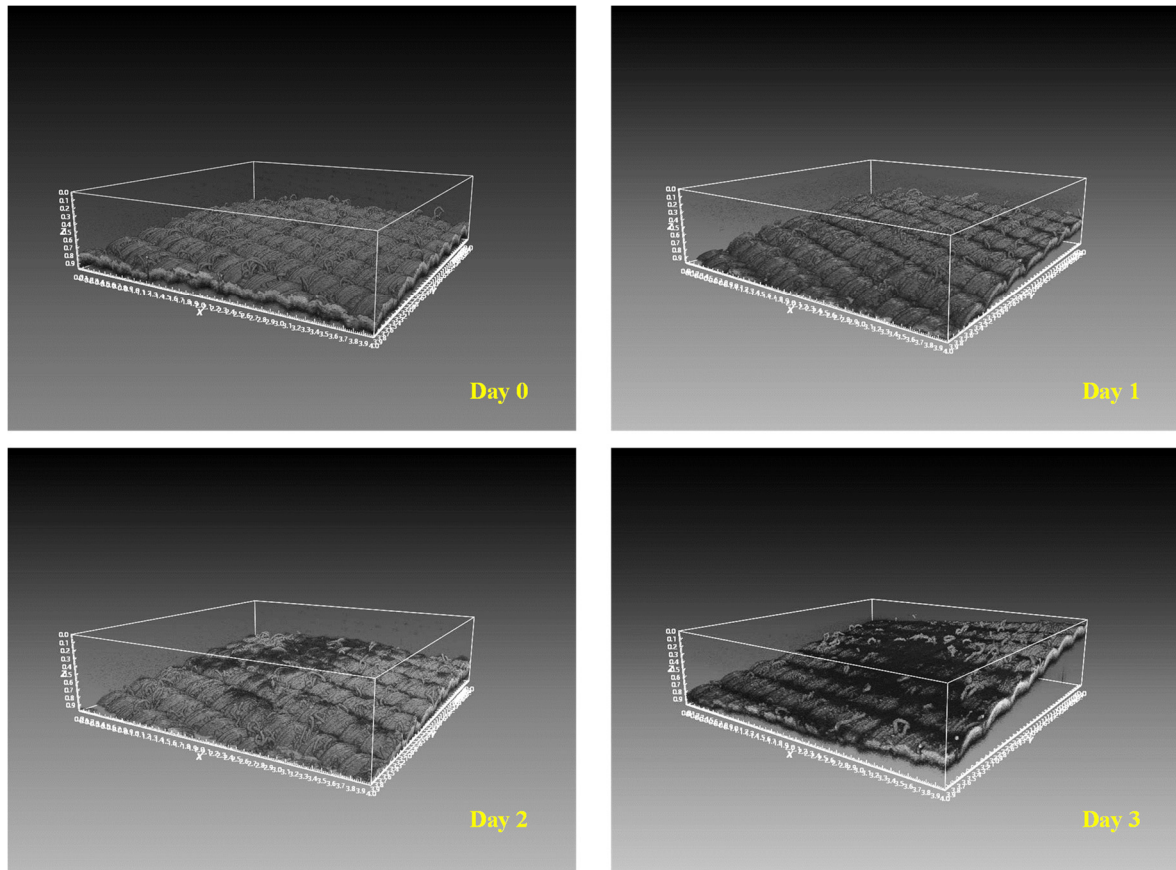


Figure 3-7. OCT images of LC-inoculated biofilm on Terrazzo support during 3-days cultivation.

Fig. 3-8 presents cell areal density on Cotton and Terrazzo for the two conditions tested in terms of inoculum density. A higher cell density on Terrazzo was measured compared to that on Cotton (Fig. 3-8, $P < 0.05$), suggesting the impact of the textile support on biofilm development. The effect of inoculum density on biomass production and productivity will be discussed later on in section 3.3.

Results of cell density are in agreement with those obtained by micro-scale imaging. Indeed, the tightly knitted fibers and crevices among fibers on Terrazzo (see CLSM and SEM images, Fig. 3-6A) certainly benefited cells immobilization probably due to their anchoring action as it has been reported by Cui et al. (2013). Molecular interactions established between the cell and the fibers may also play role in cell attachment. On the other hand, loosely connected fibers on Cotton (Fig. 3-6B) affect negatively biofilm production (Fig. 3-8). This is also in agreement with our results on cell-loading capability (Fig. 3-4) described in section 3.1, and data reported by (Cui et al., 2013; Gross et al., 2016).

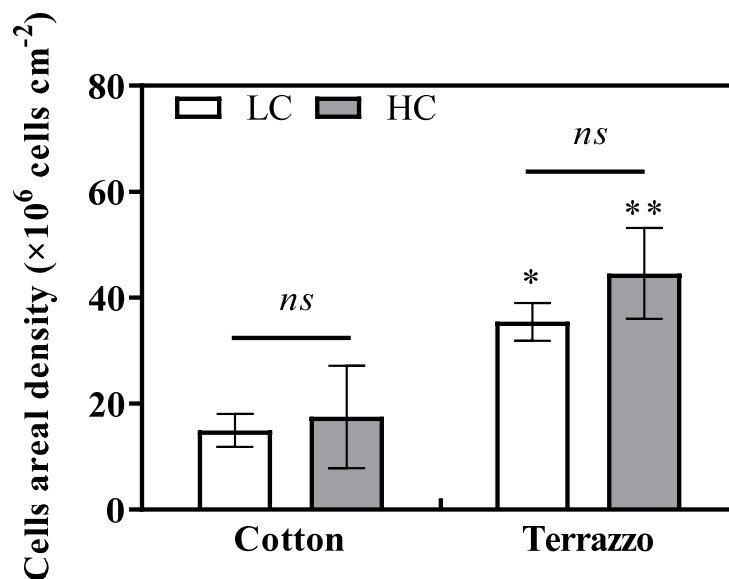


Figure 3-8. Cell areal density of biofilms (with the pre-acclimated inoculum at $50 \mu\text{mol m}^{-2} \text{s}^{-1}$) on Cotton and Terrazzo after 3-days cultivation. All the results were shown as mean value \pm SD ($n = 3$). Bars with** and * respectively depict the differences between biofilms on two types of supports at a level of at $P < 0.01$ and $P < 0.05$, while *ns* represents no difference between two inoculum densities.

To sum up, the spatial organization of fibers on Terrazzo and Cotton may have an impact on cell-support interaction and cell retention capability, which in turn will affect biofilm development. The highest cell loading capability (section 3.1) and cell density on Terrazzo may be correlated to its tightly knitted fibers. Heterogeneous distribution of cells (CLSM imaging) and biofilm (OCT imaging) on supports is observed, as expected.

3.3. Does the support and inoculum density affect sessile cells growth, activity, composition and biofilm productivity?

Relative biomass increase (R_c) and detachment for Cotton and Terrazzo inoculated with $50 \mu\text{mol m}^{-2} \text{s}^{-1}$ pre-acclimated cells are illustrated in Fig. 3-9a. Results show that, regardless of the support material, a higher relative biomass increase (~ 1.7 times) is obtained for the lower cell density (LC) (Fig. 3-9a, $P < 0.05$). Similar results were obtained for cells photo-acclimated to the higher light intensity ($350 \mu\text{mol m}^{-2} \text{s}^{-1}$; Fig. S3-5, $P < 0.05$). This result suggests that biomass production is negatively impacted by the inoculum cell density. This may be explained by a reduction in light and/or nutrients availability in biofilms due to an

increase of self-shading in denser populations as already reported on other work (Huang et al., 2016; Roberts et al., 2004; Roostaei et al., 2018). This subject will be further studied in the next chapter.

Data also show that productivity was ~ 3.2 times higher for Terrazzo compared to those of Cotton under LC-conditions (Fig. 3-9b, $P < 0.05$) regardless of the inoculum density, suggesting an impact of the material on biofilm development, as already stated. This data is also in agreement with the lower detachment percentage measured for biofilms developed on Terrazzo (Fig. 3-9a, $P < 0.05$).

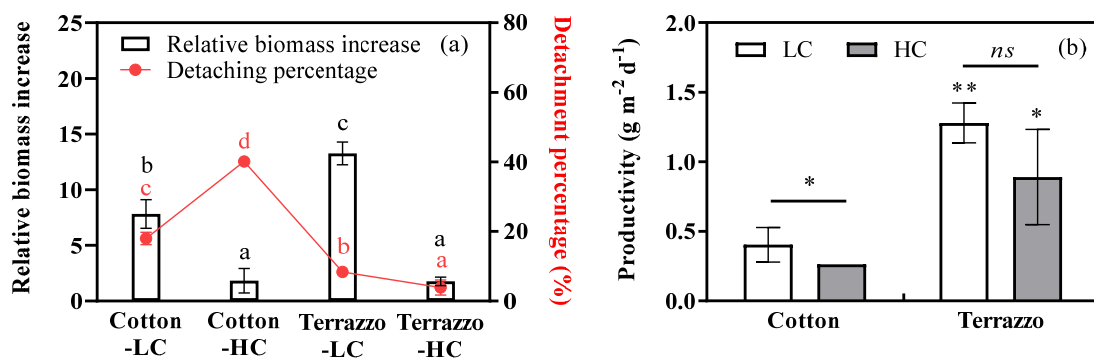


Figure 3-9. Effect of support and initial cell density (pre-acclimated to $50 \mu\text{mol m}^{-2} \text{s}^{-1}$) on relative biomass increase and detachment percentage (a) and biomass productivity (b) after 3-days cultivation of *C. vulgaris* biofilms. All the results were shown as mean value \pm SD ($n = 3$). Bars and dots with different letters represent the statistical differences at a level of $P < 0.05$, while bars with ** and * respectively depict the differences between immobilized cultures at $P < 0.01$ and $P < 0.05$, and *ns* represents no difference between two inoculum densities.

Due to the better growth performance at low inoculum density, we decided to study the physiological properties of the cells grown on Terrazzo and Cotton in LC-condition. Interestingly, differences in photosynthetic activity and composition of cells developed on Terrazzo and Cotton were found (Fig. 3-10).

Though similar maximum quantum yield (F_v/F_m around 0.7, Table S3-1) and cellular Chl *a* ($P > 0.05$, Fig. 3-10a) were measured for cells on both supports, cells on Terrazzo presented a higher electron transport capacity (1.32 times higher) compared to those on Cotton (Fig. 3-10b, $P < 0.05$). This behavior may be associated to the differences in light availability to the sessile cells on these two supports due to the different spatial organization of cells and material micro-texture. Similarly, Vivier et al. (2021) found that microphytobenthonic

biofilms presented different photosynthetic performance due to their unparalleled light availabilities conferred by the different micro-topographies of supports (PVC or concretes). The improvement of the photosynthetic capacity of algal biofilms with increasing light availability have been demonstrated in previous studies (Lavaud et al., 2007; Perkins et al., 2010; Guzzon et al., 2021). In the current study, the shading effect of loosely connected fibers of Cotton due to interlaced fibers and the cellular self-shading may reduce the incoming photon flux for photosynthesis in this support. In contrast, cells or cell clusters grown on Terrazzo are mainly distributed on the top of the surface (SEM images in Fig. 3-6 A4, and videos scanned by CLSM in supplementary data) due to the very tight woven pattern of this textile. In those conditions, an increase in light availability for each cell may be expected, allowing a greater $rETR_{max}$ yield of the sessile cells (Fig. 3-10b). This may also explain the higher relative biomass increase and productivity observed for Terrazzo.

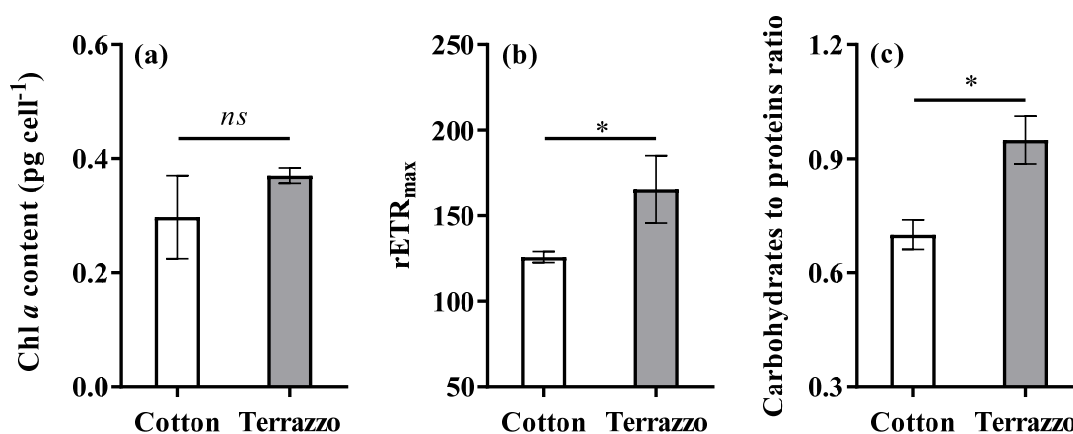


Figure 3-10. Chl *a* content (a), relative maximum electron transport rate ($rETR_{max}$, b) and carbohydrates to proteins ratio (c) of *C. vulgaris* biofilms (with the pre-acclimated inoculum at $50 \mu\text{mol m}^{-2} \text{s}^{-1}$) grown on Cotton and Terrazzo after 3-days cultivation at LC condition. All the results were shown as mean value \pm SD ($n = 3$). Bars with * represent the statistical differences between the immobilized cultures on two supports at a level of $P < 0.05$, and *ns* represents no difference.

In addition, no significant differences in cell volume and photosynthetic activity parameters other than $rETR_{max}$ (alpha, E_k ; Table S3-1 and Fig. 3-10b) were measured while a higher relative pool of carbohydrates was measured for sessile cells on Terrazzo (Fig. 3-10c, $P < 0.05$). This is in agreement with our hypothesis of higher light availability in the Terrazzo support. An increase in carbohydrates accumulation was also reported when *C. vulgaris* was cultivated in a revolving algal biofilm system under greater light intensities

(Gross and Wen, 2014). This is also in agreement with data described in Chapter IV. To the best of our knowledge, this is the first study addressing the characterization of cell morphology, photosynthetic activity and macromolecular composition that confirms that support impacts the physiological properties of sessile cells.

3.4. Does the light history of inoculum cells affect biofilm growth and productivity?

In this section, we will focus on the impact of inoculum cell's physiological properties on biofilm formation on Terrazzo, its composition, activity and productivity at LC conditions. Indeed, as far as we know, no information on the subject is available for biofilms. On the other hand, a broad number of studies have been undertaken with suspended cultures to investigate the role of cells physiology, such as chlorophyll content or cell size, on phytoplankton growth (MacIntyre et al., 2002; Post et al., 1984; Sukenik et al., 1990; Urabe and Kagami, 2001). Some of them predicted that, the lower the chlorophyll quota (expressed as Chl *a*/C, Chl *a*/cell or Chl *a*/cell volume), the more transparent the microalgae and the higher the growth rate or productivity achieved in suspended cultures before photo-inhibition occur (MacIntyre et al., 2002; Martínez et al., 2018; Sukenik et al., 1990). It has been also reported a decrease in the algal growth rate with the increasing cell size (Key et al., 2010; López-Sandoval et al., 2014; Urabe and Kagami, 2001). Regarding biofilms, Corcoll et al. (2012) showed rapid changes in photosynthetic processes of fluvial biofilms after a sudden increase or decrease in the incoming light which were dependent on the initial photo-acclimation conditions (light at which biofilm grew before implementing the stress).

From the latter considerations, we hypothesized that the cell's inoculum properties affect biofilm development. It may therefore represent one of the factors to be taken into account to optimize biofilm-based systems. Accordingly, in order to assess the impact of inoculum cell properties, which depend on the light to which they were exposed (cell light history), on biofilm development, suspended cells photo-acclimated to 50 and 350 $\mu\text{mol m}^{-2} \text{s}^{-1}$ were immobilized on terrazzo at LC-condition. Sessile cells were all then illuminated with 100 $\mu\text{mol m}^{-2} \text{s}^{-1}$ and their growth, composition and photosynthetic activity were measured after 3-day incubation.

Results show an increase in R_c (1.8 times, $P < 0.001$, Fig. 3-11a) and an improvement in productivity (1.5 times, $P < 0.01$, Fig. 3-11b) in the BP-HL biofilm (Biofilm formed from

cells photo-acclimated to $350 \mu\text{mol m}^{-2} \text{s}^{-1}$) compared to those exposed to low light intensity (BP-LL, Biofilm formed from cells photo-acclimated to $50 \mu\text{mol m}^{-2} \text{s}^{-1}$). This may be related to the smaller volume (0.69 times, $P < 0.001$, Fig. 3-12a) and lower cellular Chl *a* quota (0.54 times, $P < 0.01$, Fig. 3-12b) of HL-acclimated cells than those of the LL-acclimated inoculum. This is in agreement with studies showing that smaller cells with an higher metabolic rate lead to a greater biomass accumulation (Key et al., 2010; Urabe and Kagami, 2001). Our data is also in line with findings described by Martinez et al. (2018) who predicted that, the lower the chlorophyll quota (Chl *a/C*), the higher the maximal productivity achieved in a suspended culture. Moreover, a slightly higher electrons/energy transport capacity (rETR_{max} , 1.2 times, $P < 0.01$, Fig. 3-13) may also explain the higher growth rate of BP-HL biofilms as more photosynthetic energy could have been used for growth (Malapascua et al., 2014; Ng et al., 2020). On the other hand, the lower relative carbohydrates pool size (0.70 times, $P < 0.001$, Fig. 3-11c) in BP-HL biofilms was probably a consequence of the larger photosynthetic energy direction to produce proteins for cell division. More work is though required to elucidate these observations and fully understand the effect of inoculum's physiology on biofilm development.

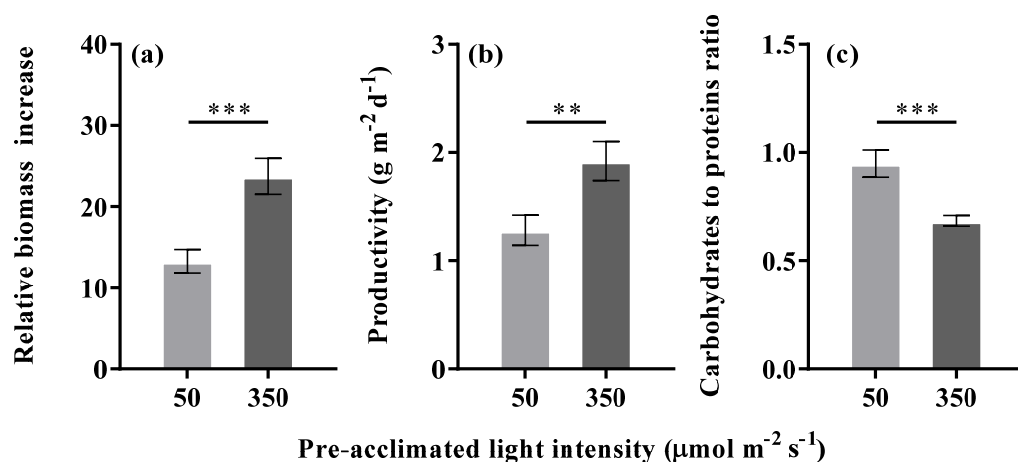


Figure 3-11. Relative biomass increase (a), biomass productivity (b) and relative carbohydrates pool size (c) of 3-day *C. vulgaris* biofilms (inoculated with the pre-acclimated cells to 50 and $350 \mu\text{mol m}^{-2} \text{s}^{-1}$) grown on Terrazzo at LC-conditions. All the results were shown as mean value \pm SD ($n = 3$). Bars with *** and ** respectively depict the differences between immobilized cultures at $P < 0.001$ and $P < 0.01$.

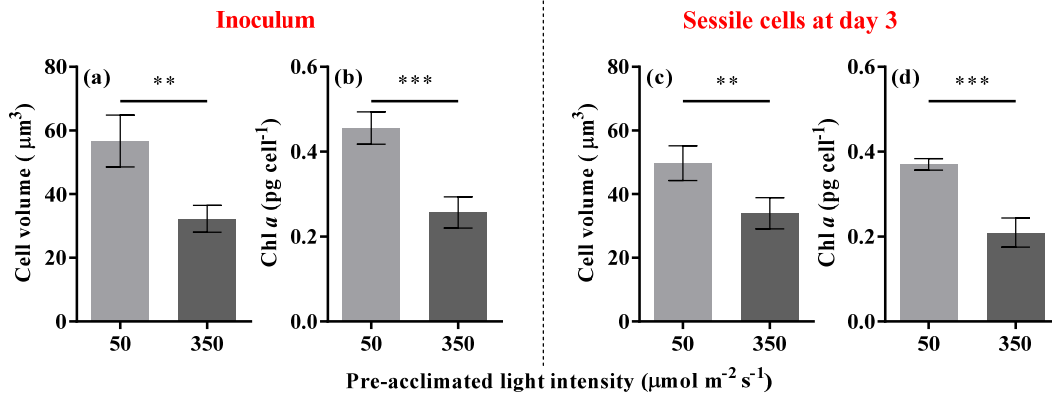


Figure 3-12. Average cell volume (a, c) and cellular Chl *a* content (b, d) of pre-acclimated cells at 50 and 350 $\mu\text{mol m}^{-2} \text{s}^{-1}$ light intensities and sessile cells on Terrazzo at day 3 at LC-condition. All the results were shown as mean value \pm SD ($n = 3$). Bars with *** and ** respectively depict the differences between cultures at $P < 0.001$ and $P < 0.01$.

In addition, photosynthetic parameters such as F_v/F_m , α , $rETR_{\text{max}}$ and E_k are often used to describe the photo-acclimation state of microalgae when environmental conditions change, especially with respect to light conditions (Cointet et al., 2019; McMinn and Hegseth, 2004; Ralph and Gademann, 2005). Similar photosynthetic parameters ($P > 0.05$, Fig. 3-13) for biofilms developed at both conditions suggest photo-acclimation to 100 $\mu\text{mol m}^{-2} \text{s}^{-1}$ after 3 days. Such a short-term photo-acclimation process (within 3-5 days) was also observed in previous research work (Anning et al., 2000; Fisher et al., 1996; Ritz et al., 2000) and is also in agreement with data described in Chapter II and Chapter IV.

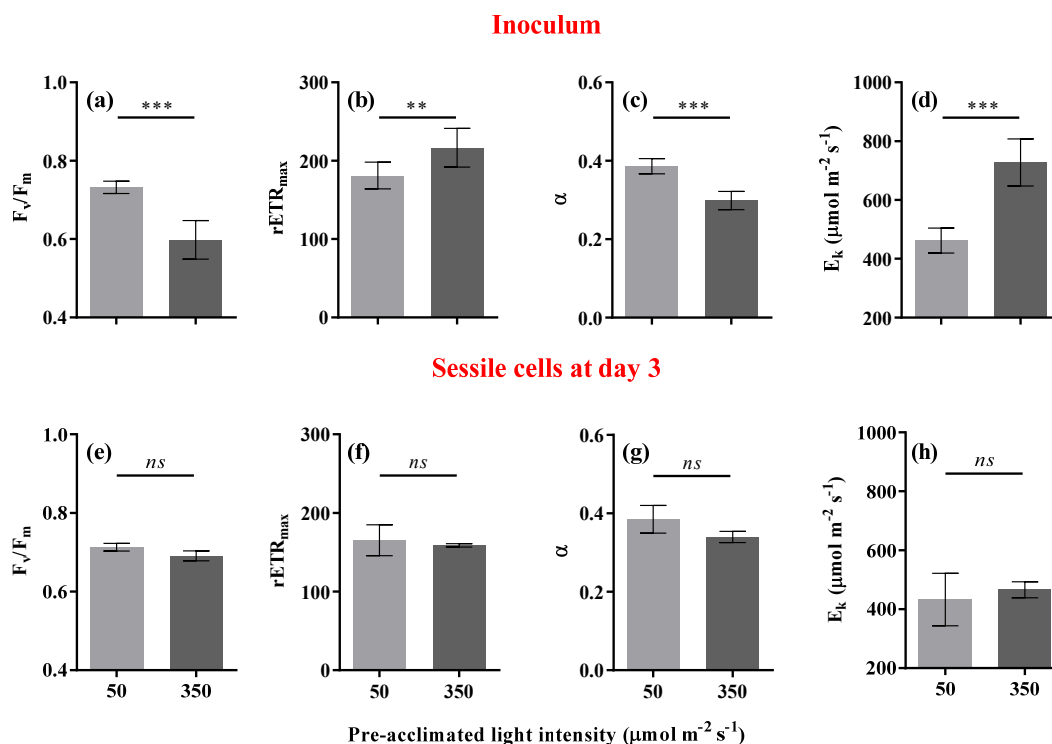


Figure 3-13. Photosynthetic parameters (F_v/F_m , α , $rETR_{max}$ and E_k) of pre-acclimated cells at 50 and 350 $\mu\text{mol m}^{-2} \text{s}^{-1}$ light intensities (above) and sessile cells on Terrazzo at day 3 (below) at LC-condition. All the results were shown as mean value \pm SD ($n = 3$). Bars with *** and ** respectively depict the differences between cultures at $P < 0.001$ and $P < 0.01$, and *ns* represents no difference.

4. Conclusions

The aim of this work was to identify promising supports for biofilm-based technologies (high biomass concentration and productivity, low detachment), to better understand the mechanisms of interaction between microalgae cells and the support, to evaluate the effect of operating factors (inoculum density/physiology, support) on biofilm development, activity and composition. Here, four conclusions could be drawn:

- Support properties, such as micro-texture and physical-chemical nature affect sessile cells distribution, biofilm growth, photosynthetic activity and composition. Higher $rETR_{max}$ and carbohydrate to protein ratio were determined for Terrazzo compared to Cotton.
- The results clearly show a reduction in biofilm growth with inoculum density, probably associated to a reduction in light and/or nutrients availability. This subject will be thoroughly developed in the next chapter.

- Inoculum physiology/cell light history affects biofilm growth and properties. A higher biomass productivity was reported for biofilm starting with cells photo-acclimated to high light (BP-HL).

- Conditions to get the highest biomass productivity were identified: *C. vulgaris* biofilms should be grown on Terrazzo, inoculated with a low cell density ($\sim 1.5 \times 10^6$ cells cm^{-2}) whose cells were pre-acclimated to high light intensity ($350 \mu\text{mol m}^{-2} \text{s}^{-1}$). Accordingly, a productivity of $1.92 \text{ g m}^{-2} \text{ d}^{-1}$, 3 times higher than that on Cotton ($0.65 \text{ g m}^{-2} \text{ d}^{-1}$) described in chapter II, was obtained.

Taken together, our data confirms that the operating factors, such as the support, inoculum density and the physiological state of the cells used for biofilm formation must be closely considered when optimizing biofilm-based systems.

Supplementary data

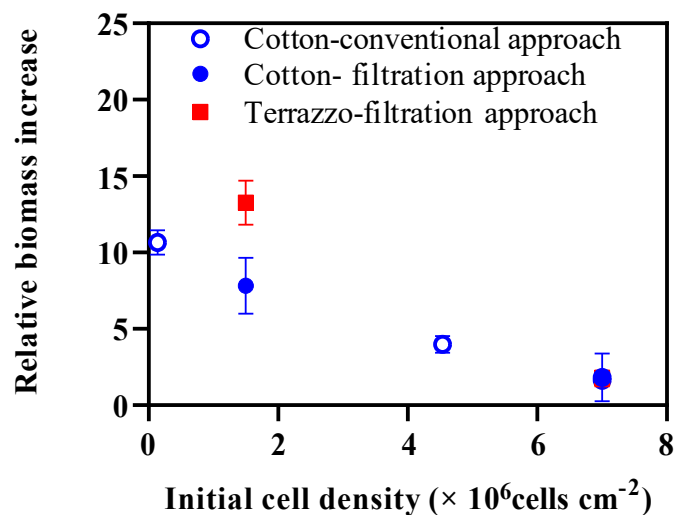


Figure S3-1. Relative biomass increase of *C. vulgaris* biofilms grown on Cotton and Terrazzo after 3-days cultivation as a function of inoculation approaches. Conventional approach refers to the procedure used in Chapter II.

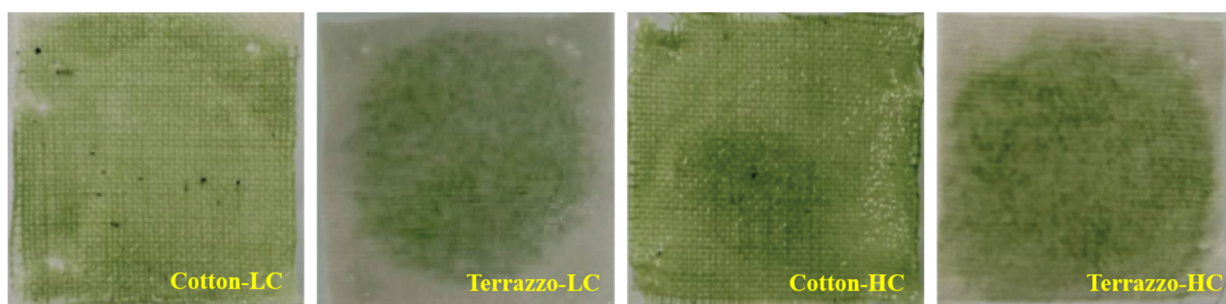


Figure S3-2. Images of *C. vulgaris* growing on Cotton and Terrazzo supports at day 3.

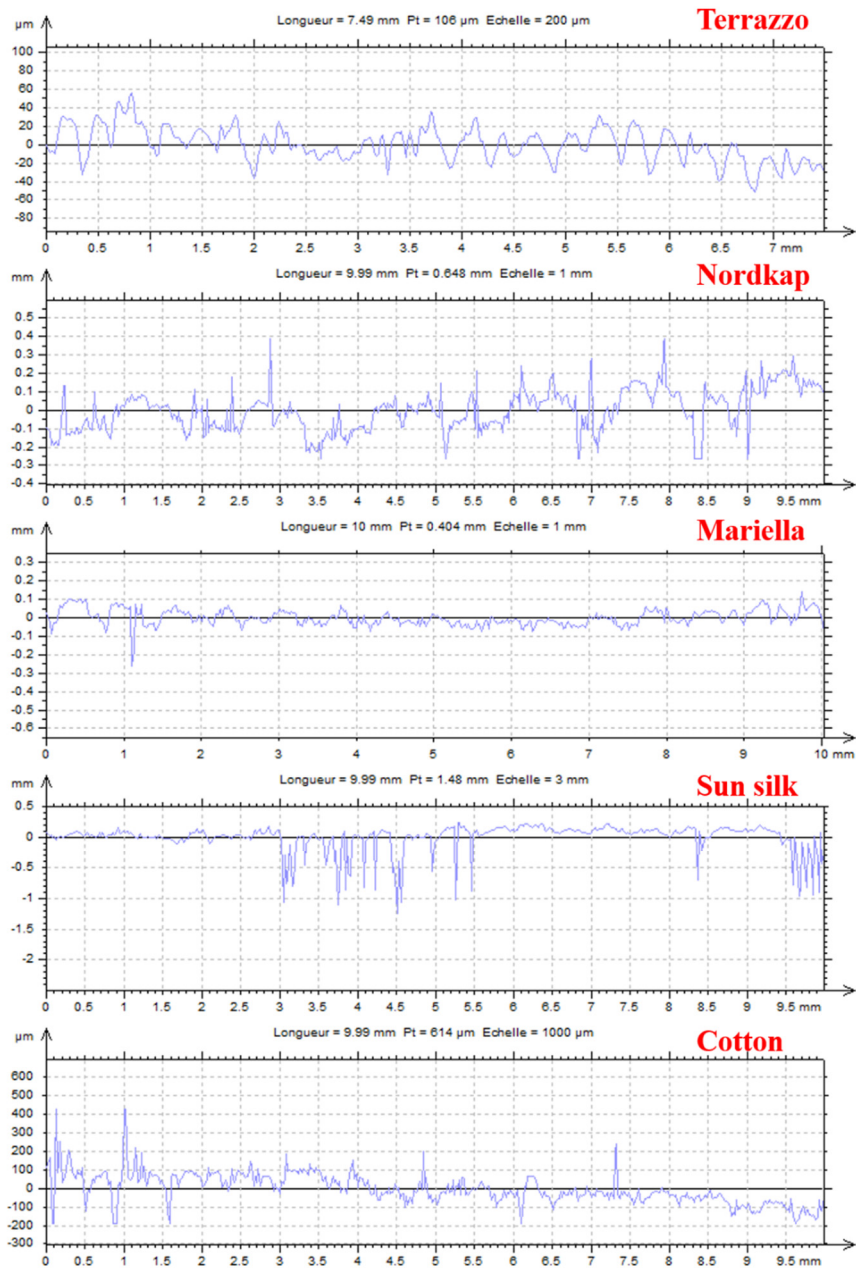


Figure S3-3. Roughness profile of the textured textile materials.

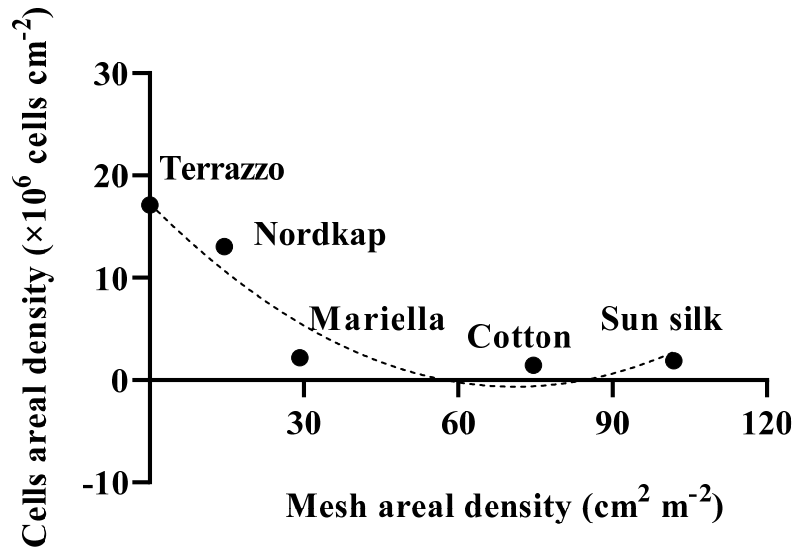


Figure S3-4. Cells retention capability of textile materials as a function of the surface mesh areal density.

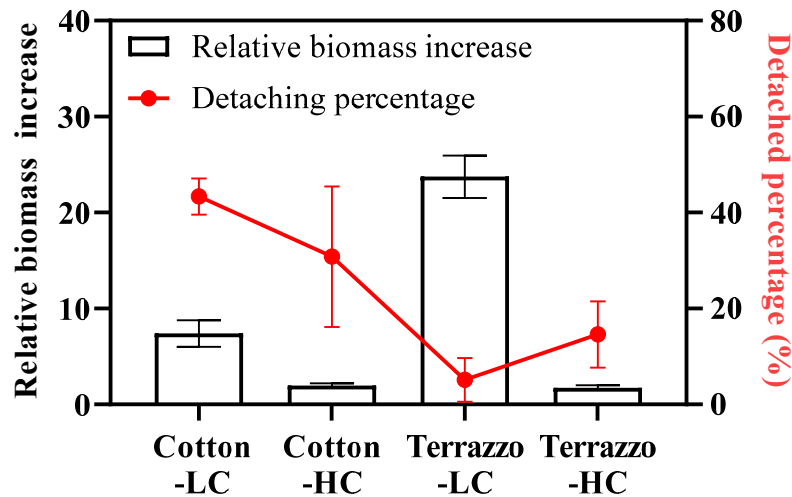


Figure S3-5. Effect of support and initial cell density on relative biomass increase and detachment percentage after 3-days cultivation of *C. vulgaris* biofilms that pre-acclimated to 350 $\mu\text{mol m}^{-2} \text{s}^{-1}$.

Table S3-1. Morphology, photosynthetic activity and cellular composition of immobilized *C. vulgaris* (pre-acclimated to 50 $\mu\text{mol m}^{-2} \text{s}^{-1}$) after 3-days cultivation.

Group	Cell volume (μm^3)	F_v/F_m	α	E_k ($\mu\text{mol m}^{-2} \text{s}^{-1}$)	Lipids to proteins ratio
Cotton -LC	47.3±2.7	0.68±0.02	0.36±0.03	349±15	0.16±0.00
Cotton -HC	44.9±1.9	0.66±0.02	0.35±0.02	381±90	0.16±0.01
Terrazzo -LC	49.7±5.4	0.71±0.00	0.39±0.03	433±89	0.17±0.00
Terrazzo -HC	45.2±5.2	0.66±0.02	0.35±0.01	378±27	0.15±0.01

Supplementary data in videos

The growth pattern of *C. vulgaris* on Cotton support: <https://youtu.be/z8HdjORaYo8>

The growth pattern of *C. vulgaris* on Terrazzo support: <https://youtu.be/wwSvrw7spvw>

CHAPTER IV. Biomass production and physiology of *Chlorella vulgaris* during the early stages of immobilized state are affected by light intensity and inoculum cell density

Preamble

Though Terrazzo yielded a higher biomass productivity compared to cotton support, there are still challenges in using fabric supports for microalgae biofilm cultivation. Firstly, it is difficult to completely harvest the biomass from fabric materials using mechanical method solely. The residual cells could be served as the colonies for the regrowth, however, they will bring barriers to precisely estimate the productive efficiency of biofilm systems. Secondly, using the system in which cells were grown on fabric materials and submerged in liquid makes it uneasy to control the biofilm process due to detachment, even though they were immobilized on Terrazzo (~ 36% of detachment rate). Hence, in this chapter, we used a simple Twin-layer system with perfused processes, in which biofilms grown on filter membranes can be easily harvested, to carry on investigating the effect of light intensity (50, 250 and 500 $\mu\text{mol m}^{-2} \text{s}^{-1}$) and inoculum density (4.8 and 28.8×10^6 cells cm^{-2}) under more controlled conditions. The immobilized cultures were still maintained for 3 days in order to simplify the experimental design. The growth performance (relative biomass increase to initial) and physiological properties (including the photosynthetic activity and cellular compositions) of microalgae biofilms under different combined conditions were characterized. These results may provide information to predict the adverse parameters, and to optimize the operational factors for microalgae biofilm-based cultivation.

Biomass production and physiology of *Chlorella vulgaris* during the early stages of immobilized state are affected by light intensity and inoculum cell density

Abstract

The interest for biofilm-based systems for microalgae and related compounds production has been increasing lately. Although extensive literature has been reported on productivity, the physiological characterization (photosynthetic activity and composition) of attached cells at early stages of biofilm development has seldom been investigated. In this work, the effect of light intensity and inoculum cell density on 3-days *Chlorella vulgaris* biofilms developed on membranes was studied. Biomass production was clearly impacted by mechanism of photo-limitation occurring in biofilms acclimated to low light intensity ($50 \mu\text{mol m}^{-2} \text{s}^{-1}$). A higher electron transport capacity and lower chlorophyll content in biofilms at high light intensity ($500 \mu\text{mol m}^{-2} \text{s}^{-1}$) were also measured which are in line with patterns observed for suspended microalgae cultures. In addition, optimal conditions in terms of light ($250 \mu\text{mol m}^{-2} \text{s}^{-1}$) combined with low ($4.8 \times 10^6 \text{ cells cm}^{-2}$) or high inoculum density ($28.8 \times 10^6 \text{ cells cm}^{-2}$) were identified to optimize biomass and lipids production, respectively. On the whole, measuring physiological profiles of immobilized cells at the initial stages of biofilm development provides information to efficiently operate and optimize biofilm-based systems.

Graphical abstract

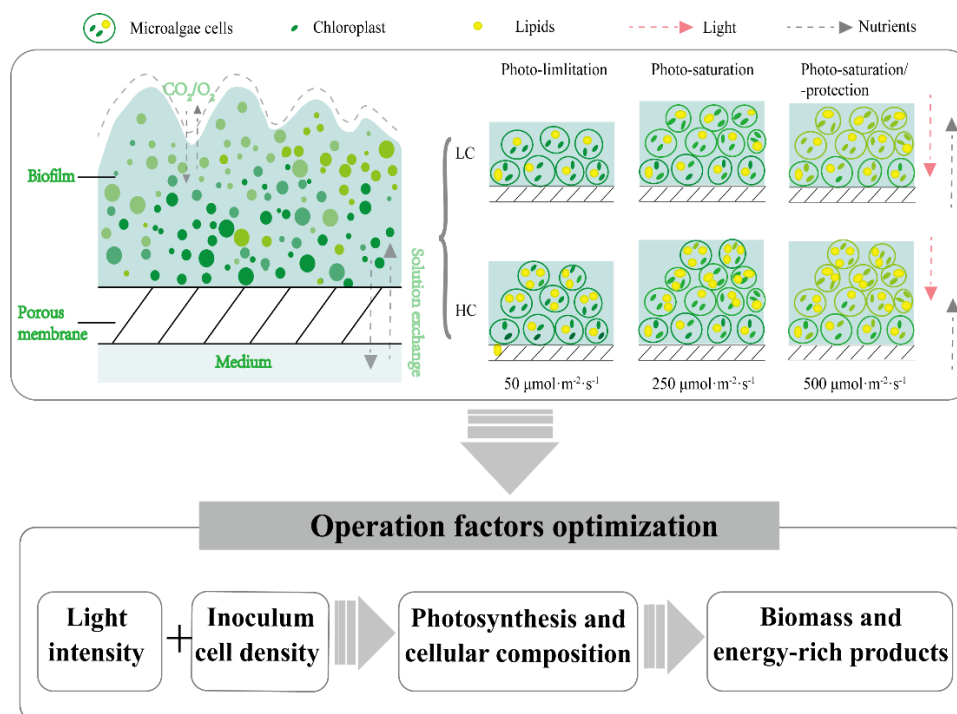


Figure 4-1. Graphical abstract of Chapter IV.

Keywords: *Chlorella vulgaris*, FTIR-spectroscopy, Macromolecular composition, Microalgae biofilms, Photosynthetic activity

1. Introduction

Microalgae are a promising source of valuable compounds (e.g., proteins, pigments, carbohydrates, lipids) produced by the conversion of photons into chemical energy via photosynthesis (Fernández-Reiriz et al., 1989; Kumar et al., 2010; Nguyen et al., 2019; Tan et al., 2020). Nowadays, biofilm-based systems for microalgae cultivation, where cells are growing attached to a substrate, have gained attention due to their higher productivity, lower water requirement and harvesting costs compared with conventional suspended culture technology (Ozkan et al., 2012; Roostaei et al., 2018). These systems have been widely used for biomass/biofuel production, CO_2 fixation, and wastewater treatment (Christenson and Sims, 2011; Mohd-Sahib et al., 2017; Roostaei et al., 2018; Yuan et al., 2020a). Among those, the twin-layer system (Dora Allegra Carbone et al., 2017; Murphy and Berberoglu, 2014), in which cells grow on porous supports such as membranes, printing paper or synthetic nonwoven/textile combinations, is often used at the lab and pilot scales (Podola et al., 2017; Venable and Podbielski, 2019). In particular, a direct exposure to gas and light are

supposed to enhance gas mass transfer and light utilization due to the absence of the liquid phase (Huang et al., 2016; Wang et al., 2015) improving therefore productivity. On the other hand, nutrients are transported by diffusion through the porous material into the biofilm. Limitation in nutrients can therefore occur in thick and/or compact biofilms, affecting in turn their behavior and productivity (Meng et al., 2021; Murphy and Berberoglu, 2014).

Recent studies investigated environmental and operational parameters that typically affect the formation and development of microalgae biofilms (Irving and Allen, 2011; Schnurr and Allen, 2015). Among those factors, the impact of light, nutrients availability, temperature, pH and shear stress on growth rate and productivity have been studied, but mostly over long-term period of development (i.e. from weeks to months) (Fanesi et al., 2021, 2019; Roostaei et al., 2018; Schnurr et al., 2014). On the other hand, other factors such as substrate properties (e.g., surface energy, hydrophobicity, micro-pattern, etc.) have been studied on the short-term formation of biofilms, especially during the initial adhesion phase (from several hours to 2-3 days) (Genin et al., 2014; Gerbersdorf and Wieprecht, 2015; Huang et al., 2018; Mohd-Sahib et al., 2018; Ozkan and Berberoglu, 2011; Schnurr and Allen, 2015). However, little information is available regarding the influence of process operational factors, such as light intensity and inoculum density, on biofilm growth, activity and composition at the early stages of biofilm development which in turn may affect biomass and compounds production. In our work, early stage of biofilm development refers to a period during which the cells attach firmly to the support, grow and fully acclimate to the new environmental conditions imposed by the sessile growth associated to the support.

Ji et al. (Ji et al., 2014) have reported that both biomass production and growth rate could be improved by increasing the inoculum density (from 0.05 to 3 g DW m⁻²). However, it must be kept in mind that over a certain density threshold, the cells would not grow further due to light attenuation and nutrients transfer limitation (Huang et al., 2016; Meng et al., 2021; Schnurr and Allen, 2015). In this context, light attenuation could be buffered by tuning the photon flux density (PFD) used for cultivation. However care must be taken since like for planktonic cultures, the growth rate and biomass productivity of microalgae biofilms increase with light intensity within a favorable range, but decrease if the PFD exceeds the light saturation point because of photo-inhibition (Grenier et al., 2019). In order to avoid such operational problems, monitoring the physiological properties of cells (activity and composition) in the early stages of immobilized growth might be of great help to rapidly identify possible limiting operational factors (e.g., light, nutrients, CO₂, humidity, etc.) and

thus adjust them to optimize the bioprocess performance (Huang et al., 2016; Murphy and Berberoglu, 2014; Shiratake et al., 2013; Wang et al., 2015). Nevertheless, although extensive literature has been reported on the productivity of biofilm-based systems as summarized in (Zhuang, 2018) and reference therein, the characterization of cell physiological parameters at early stages has seldom been mentioned.

The goal of our work was to assess the impact of light and initial cell density on biofilm/compounds production and on cells physiology at early stages (3 days) of biofilm formation in a twin layer system. In particular, we aimed at better understanding photosynthetic mechanisms on biofilms that certainly allow a reasoned choice of process operational parameters to optimize productivity. In order to do that, we immobilized *C. vulgaris* on membranes with two initial cell densities and illuminated the biofilms with three PFDs. A complete characterization of physiological parameters of the immobilized cells, from photosynthetic performance to macromolecular composition was conducted through which biofilm growth patterns and composition under different light and inoculum density combinations were explained.

2. Materials and Methods

2.1. Planktonic culture maintenance

Chlorella vulgaris SAG 211–11b (Göttingen, Germany) was cultured at 25°C semi-continuously in 1 L transparent bottles filled with 800 mL 3N-Bristol medium (Bischo and Bold, 1963). The cultures were bubbled with filtered air under a continuous illumination of either 50, 250 or 500 $\mu\text{mol m}^{-2} \text{s}^{-1}$ (Viugreum 50W LED outdoor floodlights, the PFDs were measured by QSL-2100 quantum scalar irradiance sensor, Biospherical Instruments, San Diego, CA, USA). The cultures were kept in exponential phase with a max cell concentration of 6.9×10^6 cells mL^{-1} (Flow cytometer, Guava EasyCyte HT; Millipore, USA) by daily dilution in order to maintain a chlorophyll (Chl) *a* concentration of 0.2-1.5 mg Chl *a* L^{-1} to ensure optimal light penetration. The planktonic cultures were pre-acclimated to each light condition for at least 8 days before starting any experiment (for *C. vulgaris*, typically 5 days were enough to have a stabilization of Chl *a* content and growth rate).

2.2. Immobilization and growth of *C. vulgaris* on membranes

Sterile Petri dishes (55-mm diameter) filled with 3 mL of 3N Bristol medium were used as bioreactors for *C. vulgaris* immobilized growth (Fig. 4-2). The support system consisted of two glass fiber filters (working as an absorbing material for the medium; 47-mm diameter, Whatman) and on top of that a nitrate cellulose filter (0.2- μm pore size; NC membrane, 25-mm diameter, Whatman) on which the cells of *C. vulgaris* were immobilized.

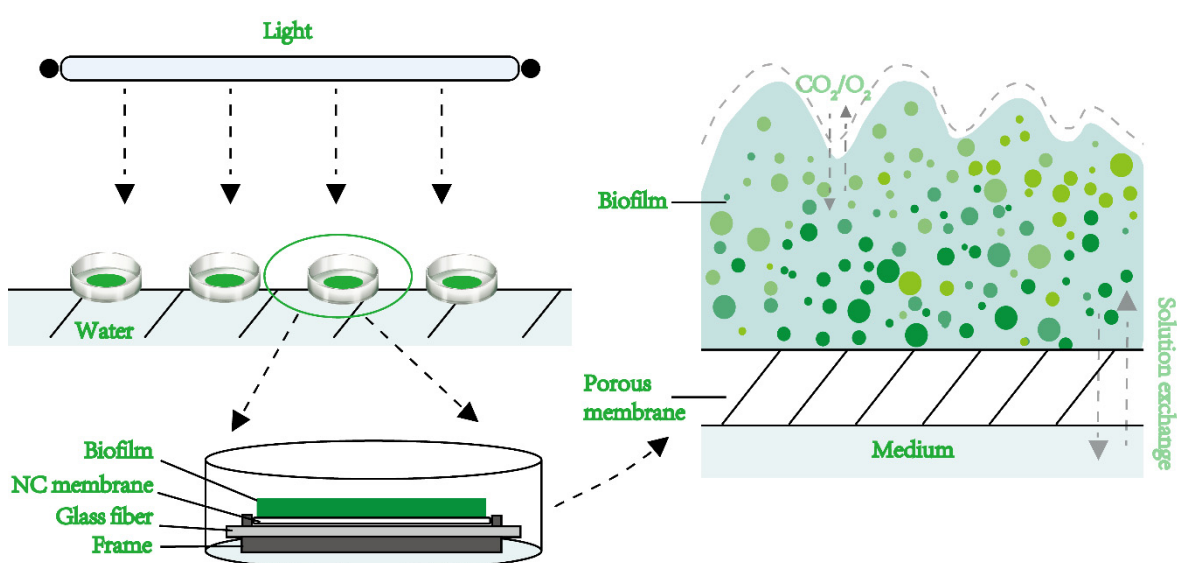


Figure 4-2. Schematic representation of the cultivation system used for the immobilized culture of *C. vulgaris* (NC membrane represents cellulose nitrate membrane filter).

In order to test the effect of PFD and the initial cell density on the immobilized growth of *C. vulgaris*, the pre-acclimated planktonic cells (grown at 50, 250 and 500 $\mu\text{mol m}^{-2} \text{s}^{-1}$) were vacuum-filtered on the NC membranes with an effective colonization area of 2.01 cm^2 . Two initial cell densities corresponding to $\sim 4.8 \times 10^6$ cells cm^{-2} (low initial cell density, LC, 0.4 ± 0.1 g m^{-2}) and $\sim 28.8 \times 10^6$ cells cm^{-2} (high initial cell density, HC, 2.6 ± 0.8 g m^{-2}) were obtained by filtrating specific volumes of planktonic cultures on the membranes. Once the cells were immobilized, the membranes were placed on the glass fiber filters and placed in Petri dishes illuminated at 50 (low light, LL), 250 (moderate light, ML) or 500 $\mu\text{mol m}^{-2} \text{s}^{-1}$ (high light, HL; Hansatech Instruments Quantitherm light meter/thermometer, Norfolk, England) depending on the experiments. The membranes were incubated for three

days and the medium was completely renewed every day. After three days of growth, the cells were harvested from the membranes using Bristol medium and further measurements were conducted to characterize a series of physiological parameters.

2.3. Microscopic observation of initially immobilized cultures

At day 0, the immobilized cultures at two cell density were scanned with a confocal laser scanning microscope (CLSM) to acquire z-stacks over the whole culture depth (Fig. S4-1). The confocal microscope set-up was as described in (Fanesi et al., 2021). An inverted Zeiss LSM700 confocal microscope (Carl Zeiss microscopy GmbH, Jena, Germany) equipped with a LD Plan-Neofluar 20×/0.4 Korr M27 was used to acquire images. Microalgae cells were detected on the base of chlorophyll *a* auto-fluorescence which was excited at 639 nm.

2.4. Relative biomass increase

Cells were harvested with 10 mL fresh Bristol medium. For the dry weight determination, the cell suspension was centrifuged and further washed in 10 mL of Bristol medium. After a second centrifugation step, the pellet was dried at 100 °C until a constant weight over time was reached. The relative biomass increase with respect to the initial level (R_b) was determined according to Eq. (1):

$$R_b = (X_t - X_0)/X_0 \quad (1)$$

Where X_t is biomass areal density (g m^{-2}) after three days ($t = 3$ days), and X_0 is biomass areal density (g m^{-2}) at the beginning of the immobilization.

2.5. Variable chlorophyll *a* fluorescence measurements and relative electron transport rate (rETR) estimation

Photosynthetic parameters were determined using a portable pulse amplitude modulation

(PAM) fluorometer (AquaPen, AP 110-C, Photon Systems Instruments, Drasov, Czech Republic). Measurements were performed in a 4 mL cuvette (light path of 10 mm). Illumination was provided by a blue LED (455 nm), the measuring light was $0.02 \mu\text{mol m}^{-2} \text{s}^{-1}$ and saturation pulses had an intensity of $3000 \mu\text{mol m}^{-2} \text{s}^{-1}$. Prior to measurements, all samples were diluted to an appropriate concentration (1×10^6 cells mL^{-1}). After 10 min of dark-adaptation, the samples were exposed to a stepwise increase of seven actinic lights (from 0 to $1000 \mu\text{mol m}^{-2} \text{s}^{-1}$) applied every 60s to construct the electron transport rate versus photon flux density (ETR/PFD) curves. The maximum quantum yield (F_v/F_m) and the effective quantum yield ($\Delta F/F'_m$) were calculated according to Eq. (2) and Eq. (3):

$$F_v/F_m = (F_m - F_0)/F_m \quad (2)$$

$$\Delta F_v/F'_m = (F'_m - F)/F'_m \quad (3)$$

where F_0 and F_m are the minimum and max fluorescence determined after 10 min dark-adaptation, whereas F and F'_m are the minimum and max fluorescence during illumination.

The relative electron transport rate (rETR) was calculated using the Eq. (4):

$$rETR = \Delta F_v/F'_m \times \text{PFD} \times 0.5 \quad (4)$$

Where PFD is the incident light and 0.5 is a factor assuming that two photons are required for linear electron transfer (Guzzon et al., 2019). Light curves were quantitatively compared using the parameters of maximum rate of relative ETR ($rETR_{\text{max}}$), α and E_k ($E_k = rETR_{\text{max}}/\alpha$) obtained by fitting the rETR/PFD curves with the function $rETR = ETR_{\text{max}} (1 - e^{-\alpha I / rETR_{\text{max}}})$ described by (Webb et al., 1974).

2.6. Determination of cellular compounds

Chl *a* was extracted from cells using dimethyl sulfoxide (DMSO) (Wellburn, 1994), and quantified by measuring the absorption at 649 nm and 665 nm with an Evolution 60S UV-visible spectrophotometer (Thermo Scientific, Madison, WI, USA). The Chl *a* concentration

was calculated by Eq. (5) (Wellburn, 1994):

$$\text{Chl } a \text{ (}\mu\text{g mL}^{-1}\text{)} = 12.19 \times OD_{665} - 3.45 \times OD_{649} \quad (5)$$

The Chl *a* content was normalized to the average cell volume, which was estimated with an AxioSkop 2 plus microscope (Carl Zeiss, Oberkochen, Germany).

The macromolecular composition of the cells was analyzed by means of an ATR-FTIR PerkinElmer Spectrum-two spectrometer (PerkinElmer, Waltham, MA, USA). Biofilm cells were re-suspended in 1 mL Milli-Q water and washed twice. 1-2 μL of the concentrated sample was deposited on the crystal of the spectrometer, and dried at room temperature for 20 min. Infrared spectra were recorded in the range of 4000 to 400 cm^{-1} using an accumulation of 32 scans at a spectral resolution of 4 cm^{-1} . Before loading algal samples, the empty crystal was measured as background. The spectra were baselined and maximum absorption values in the spectral ranges corresponding to specific macromolecular pool: carbohydrates (C–O–C; 1200–950 cm^{-1}), lipids (C=O; 1750–1700 cm^{-1}), proteins (Amide I; 1700–1630 cm^{-1}) were used to calculate the relative carbohydrates and lipids contents with respect to the proteins signal (Fig. S4-2) (Duygu et al., 2012; Fanesi et al., 2019).

Carbon and nitrogen contents of the biofilm samples were determined with an Elemental Analyzer (Organic Elemental Analyzer FLASH 2000 CHNS/O, Thermo Scientific) using 1~2 mg of dried biomass collected from biofilms that have been previously washed twice with miliQ water and dried at 100°C.

2.7. Statistics analysis

Statistical analysis was performed using IBM SPSS Statistics 25.0 (SPSS Inc., Chicago, IL). Two-way ANOVA was used to test the influence of PFD and initial cell density on the relative biomass increase, photosynthetic performance and cellular compounds of immobilized microalgae. Bonferroni significant difference test for pairwise comparisons testing was performed after the tests of normality and variance homogeneity. $P < 0.05$ indicates a statistically significant difference among tested values. Standard deviations were calculated from at least four independent biological replicates.

3. Results and discussion

3.1. Biomass production as a function of light intensity and initial inoculum density

In biofilms, microalgae cell behavior is strongly impacted by the local conditions (light, nutrients, biofilm properties such as density, thickness, gas exchange, ...) imposed by their new life style (sessile mode) (Fanesi et al., 2019; Huang et al., 2016; Schnurr et al., 2014; Yuan et al., 2021). This may impact biomass and compounds production and should be therefore studied in-depth.

Fig. 4-3 presents the relative biomass increase for the biofilms grown on membranes. Overall, our results show that when inoculated with lower cell density (LC), the immobilized cultures of *C. vulgaris* presented 3~5 times higher relative biomass increase than HC regardless of the light intensity ($P < 0.05$). On the other hand, light intensity stimulated biomass production, which is in agreement with other works (Huang et al., 2016; Kim et al., 2018).

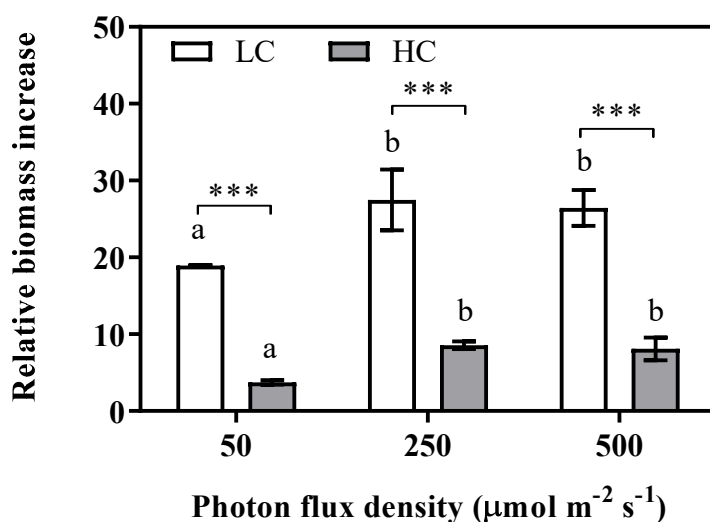


Figure 4-3. Effect of light intensity and initial cell density on the relative biomass increase of *C. vulgaris* biofilms after 3-days cultivation. All the results were shown as mean value \pm SD ($n \geq 4$). Bars with different letters represent the statistical differences among immobilized cultures under different light conditions at level of $P < 0.05$, while *** depicts the differences between biofilms with two inoculum cell densities at $P < 0.001$.

Indeed, regardless of the initial cell density the immobilized cells under LL showed lower relative biomass increase compared with biofilms exposed to ML and HL ($P < 0.05$). This suggests that the immobilized growth of *C. vulgaris* under $50 \mu\text{mol m}^{-2} \text{s}^{-1}$ may be photo-limited while that at higher light intensity were photo-saturated. This is not surprising as similar results have been reported by Grenier et al. (Grenier et al., 2019) for *Chlorella autotrophica* biofilms.

It also appears that biomass increase was negatively affected by the initial cell density (Fig. 4-3). These data can be explained by the fact that high cell density may affect light penetration and/or limit the diffusion of nutrients (Huang et al., 2016; Piciooreanu, 2000; Schnurr et al., 2014). Indeed, studies reported that in immobilized cultures the biomass productivity may depend on the biofilm thickness due to an exponential decrease of light (Barranguet et al., 2004; Schnurr et al., 2014). In our study, the two initial cell conditions did not produce biofilms with significantly different thickness (40 - 60 μm) but the HC culture presented a denser initial population as detected by CLSM (Fig. S4-1) which might have impacted biofilm growth. Finally, cell density dependent feedbacks (quorum-sensing) in cyanobacteria are also known to influence biofilm development as a function of the extracellular concentration of autoinducers (secreted by cells) which in turn affects the expression of biofilm-related gene (Nagar and Schwarz, 2015; Schatz et al., 2013). Therefore, we cannot rule out that similar mechanisms may have occurred in our immobilized cultures. Other studies should be further carried out to test such hypothesis and verify possible synergistic interactions of light and nutrients availability and, quorum sensing mechanisms.

On the whole, these results show that with the proper combination of light intensity and initial inoculum size the biofilm growth performance could be improved. For example, by illuminating the biofilms with $250 \mu\text{mol m}^{-2} \text{s}^{-1}$ at low initial cell density we obtained a 28-fold enhancement of biomass after 3 days of cultivation, whereas in (Shiratake et al., 2013), the authors only obtained a 3-fold increase of *Chlorella kessleri* after 4-day cultivation.

3.2. Monitoring the physiological state of cells in order to improve biomass and energy-rich compounds production

Although photosynthetic performance and macromolecular composition of microalgae

have been measured in suspended cultures (Cointet et al., 2019; Jiang et al., 2012), only few studies estimated these parameters for microalgae biofilm-based systems (Yuan et al., 2020b; Zhang et al., 2019). Indeed, estimating the health-state of early-stage biofilms by monitoring their physiological state would be of paramount importance to help the operator identifying stressful parameters in advance and to do reasoned operation choices. For instance, if limiting factors are identified, cultivating parameters or production strategies can be rapidly adjusted (light tuning, medium supply, etc.) to prevent adverse effects in the long-term biofilm cultivation and process productivity. Moreover, monitoring cell physiology also allows a better understanding of acclimation strategies in photosynthetic biofilms that still remains unclear (such as the interplay between photosynthetic activity and pools of macromolecules).

In biofilms, light availability and nutrient supply vary as a function of the inoculum size and/or with the biofilm thickness (Huang et al., 2016; Schnurr et al., 2014). From studies on the phytoplankton, we know that variations of these two factors induce a physiological reorganization spanning from light absorption to electron transport and to the final synthesis of macromolecules to acclimate themselves to the new conditions and maximize growth (Behrenfeld et al., 2008; Halsey and Jones, 2015; MacIntyre et al., 2000). Interestingly, similar responses occurred in our immobilized cultures. Like their planktonic counterparts, immobilized cells appear to acclimate to a range of light intensities and likely nutrients availability through a series of physiological adjustments in a short term (3 days). This is typically done to balance the incoming flux of energy and their energetic demand for growth in order to increase their fitness under each specific set of conditions (Behrenfeld et al., 2008; Halsey and Jones, 2015; McMinn and Hegseth, 2004).

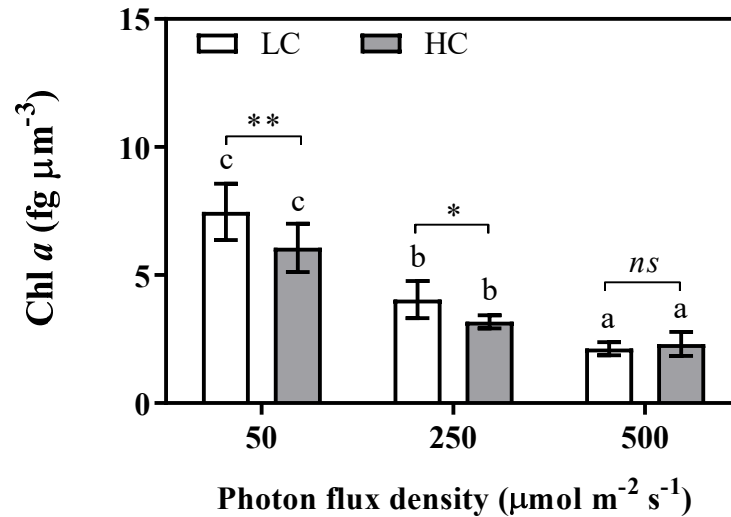


Figure 4-4. Effect of light intensity and initial cell density on Chl *a* content of *C. vulgaris* biofilms after 3-days cultivation. All the results were shown as mean value \pm SD ($n \geq 4$). Bars with different letters represent the statistical differences among immobilized cultures under different light conditions at level of $P < 0.05$ while ** and * respectively depict the differences between biofilms with two inoculum cell densities at $P < 0.01$ and $P < 0.05$, and *ns* represents no difference.

The first level at which microalgae can regulate excitation pressure is the absorption of light (Fanesi et al., 2016). This is typically reached by changing the amount of pigment content in the cells. Fig. 4-4 shows that Chl *a* content declined with increasing light intensity (from 7 to 2 $\text{fg } \mu\text{m}^{-3}$) ($P < 0.05$), suggesting a lower amount of photons absorbed by the cells as a protective strategy to diminish photons absorption and to avoid photo-damage (Chen et al., 2011; He et al., 2015). This is well described for planktonic microalgae cultures but no report of such a mechanism exists for microalgae biofilms. However, changes in accessory pigments content in natural biofilms have been reported as a photo-protective mechanism (Timoner et al., 2014).

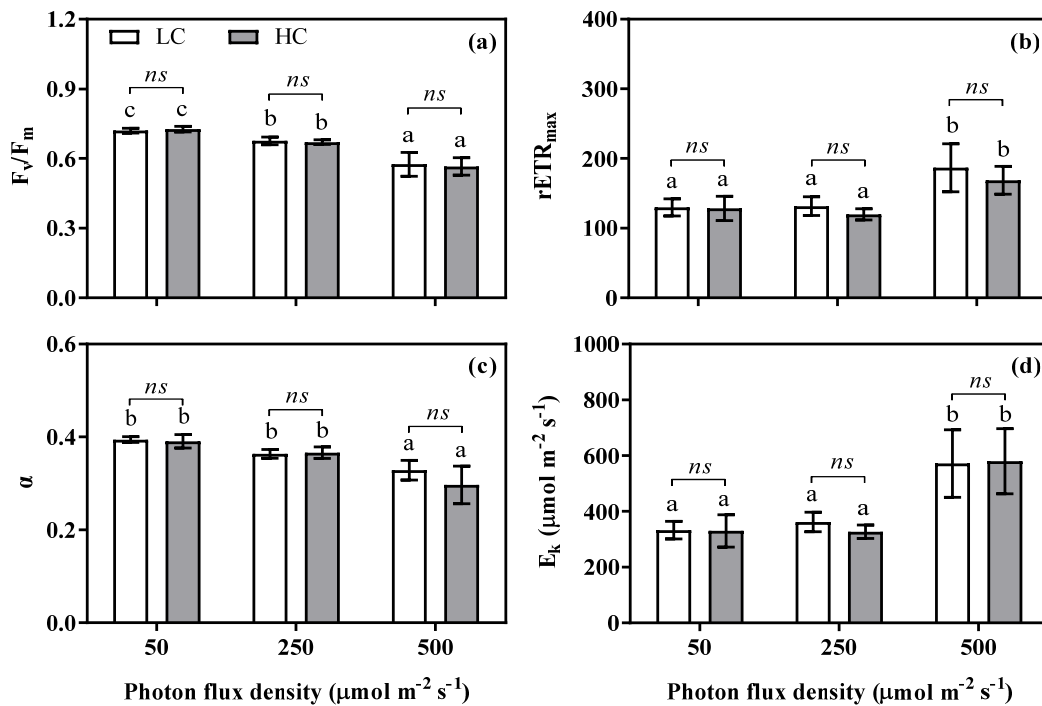


Figure 4-5. Effect of light intensity and initial cell density on photosynthetic parameters (a, F_v/F_m ; b, $rETR_{max}$; c, α ; d, E_k) of *C. vulgaris* biofilms after 3-days cultivation. All the results were shown as mean value \pm SD ($n \geq 4$). Bars with different letters represent statistical differences among immobilized cultures under different light conditions at $P < 0.05$ while *ns* depicts no difference between biofilms with two inoculum cell densities.

Another level at which microalgae can regulate excitation pressure is by modulating their photosynthetic capacity in order to meet the incoming flux of photons (MacIntyre et al., 2000). In this context, photosynthetic parameters such as F_v/F_m , α , $rETR_{max}$ and E_k are often used to describe the photo-acclimation state of microalgae when environmental conditions change, especially with respect to irradiance and nutrient levels (Cointet et al., 2019; McMinn and Hegseth, 2004; Ralph and Gademann, 2005). As depicted in Fig. 4-5, the cells exposed to the LL and ML presented a higher α (c.a 0.4), lower $rETR_{max}$ and E_k compared to those of HL acclimated cells, indicating that low-irradiance acclimated cells modified their photo-physiology to maximize light harvesting efficiency (Rincon et al., 2019). According to our expectations, algae photo-acclimated to LL and ML were more efficient in light utilization than those at HL, as shown by the initial slope (α) of the $rETR/PFD$ curves. Conversely, the higher $rETR_{max}$ (180 ± 10) and E_k ($575 \pm 5 \mu\text{mol m}^{-2} \text{s}^{-1}$) typically associating with HL demonstrated that the cells exposed to $500 \mu\text{mol m}^{-2} \text{s}^{-1}$ presented a higher electron transport capacity to face the high flux of incoming photons. A similar acclimation strategy with respect to light intensity has been described for fluvial biofilms (Corcoll et al., 2012),

suggesting that the cells at $500 \mu\text{mol m}^{-2} \text{s}^{-1}$ were in a high-light acclimation state. The maximum quantum yield (F_v/F_m) is typically used as a stress indicator to evaluate the health state of suspended cultures and in natural photosynthetic biofilms (Häubner et al., 2006; He et al., 2015; Malapascua et al., 2014). After 3 days, the immobilized cells grown at $500 \mu\text{mol m}^{-2} \text{s}^{-1}$ presented only a 0.14 lower F_v/F_m value with respect to the cultures grown at LL ($P < 0.05$, Fig 4-5a), indicating that the changes in Chl *a* content and in the photosynthetic parameters allowed the cells to optimize their energy harvesting ability and using efficiency to protect from over-excitation and photo-damage (Jerez et al., 2016; MacIntyre et al., 2000; Rincon et al., 2019).

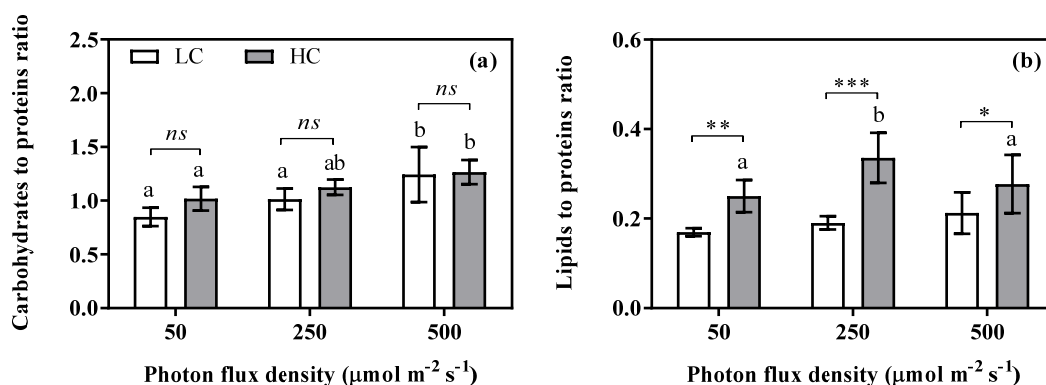


Figure 4-6. Effect of light intensity and initial cell density on carbohydrates (a) or lipids (b) to proteins ratio of *C. vulgaris* biofilms after 3-days cultivation. All the results were shown as mean value \pm SD ($n \geq 4$). Bars with different letters represent statistical differences among immobilized cultures under different light conditions at $P < 0.05$ while ***, ** and * respectively depict the differences between biofilms with two inoculum cell densities at $P < 0.001$, $P < 0.01$ and $P < 0.05$, and *ns* represents no difference.

In planktonic cultures of microalgae, the photo-acclimation state of the cells is not only reflected in different pigment contents and photosynthetic efficiency, but often also in changes of their macromolecular and elemental composition (Halsey and Jones, 2015). Storage pools such as carbohydrates and lipids serve typically as carbon and energy sinks during unbalanced growth as a results of high excitation pressure and/or nutrient limitation (Fanesi et al., 2017; Wagner et al., 2017). In this study, a significant increase of the carbohydrates to proteins ratio with light intensity was observed (46.4% and 24.4% increases at LC and HC biofilms exposed to $500 \mu\text{mol m}^{-2} \text{s}^{-1}$, respectively; Fig. 4-6a, $P < 0.05$). This is consistent with the high-light acclimation state of the cells and in accordance with other works (Ho et al., 2012; Jebsen et al., 2012).

On the other hand, the relative lipids content (Fig. 4-6b) and the C/N ratio (Fig. S4-3), two parameters that in microalgae are highly sensitive to N concentration in the environment seemed to be affected by the initial cell density. The lipid to protein ratio increased by 47.3%, 76.3% and 30.4% when biofilms at HC were exposed to LL, ML and HL, respectively, compared to those at LC (Fig. 4-6b). These results suggest an uncoupling of carbon assimilation from nitrogen uptake which could be associated with nitrogen limitation, in agreement with data reported in suspended cultures (Clément-Larosière et al., 2014; Griffiths et al., 2014; Wagner et al., 2019).

On the whole, the results show that the Chl *a* content, photosynthetic activity and the carbohydrates to proteins ratio were highly related to light intensity, while the initial cell density mostly affected the C/N and lipids to proteins ratio. In addition, optimal conditions for biofilm-based cultivation of *C. vulgaris* were identified. Combined conditions of 250 $\mu\text{mol m}^{-2} \text{s}^{-1}$ and low inoculum density (4.8×10^6 cells $\text{cm}^{-2}/0.4 \text{ g m}^{-2}$) promote biomass production by avoiding effects caused by photo-limitation at 50 $\mu\text{mol m}^{-2} \text{s}^{-1}$ (Fig. 4-3). On the other hand, if lipids are the target, combined conditions of 250 $\mu\text{mol m}^{-2} \text{s}^{-1}$ and high inoculum density (28.8×10^6 cells $\text{cm}^{-2}/2.6 \text{ g m}^{-2}$) should be applied. In conclusion, monitoring photosynthetic activity and cellular composition help better understanding photosynthetic mechanisms in biofilms but also allow to identify optimal strategies for biomass and compounds production.

4. Conclusion

In this work, biofilm production and the physiological properties (photosynthetic activity and composition) of sessile cells were assessed in response to two culture operational factors, PFD and inoculum cell density. Results showed that light intensity impacts biomass production. Mechanism of photo-limitation of biofilms exposed to LL was highlighted. Acclimation of sessile cells to light and probably to nutrients were confirmed by changes in the photosynthetic activity parameters and microalgae composition (Chl *a* content and relative lipid/carbohydrates pools). Optimal conditions to produce biomass or lipids were determined: 250 $\mu\text{mol m}^{-2} \text{s}^{-1}$ combined with LC or HC initial inoculum, respectively. On the whole, monitoring physiological profiles at the early stage of biofilms development

provides information to better understand photosynthetic mechanisms in biofilms and to operate efficiently biofilm-based systems in order to optimize biomass and macromolecules productions.

Supplementary data

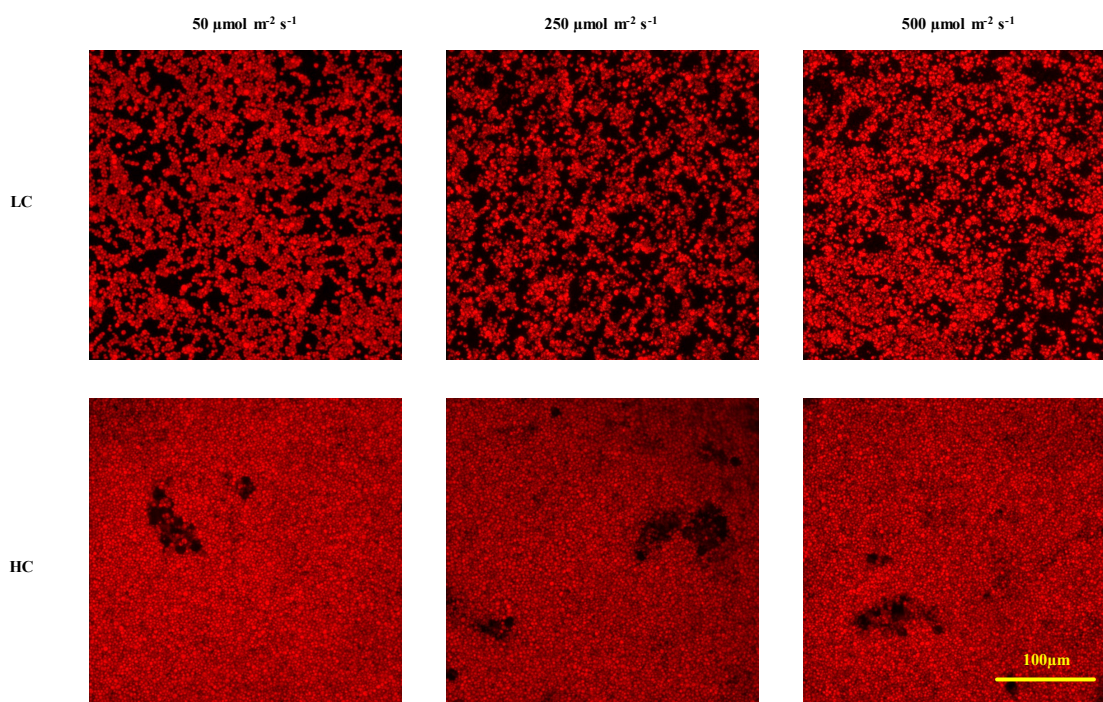


Figure S4-1. CLSM images of initially immobilized cultures with low and high cell densities originating from the pre-acclimated cultures which were exposed to 50, 250 and 500 $\mu\text{mol m}^{-2} \text{s}^{-1}$ light intensities (the average thicknesses of LC and HC cultures were 43.2 ± 4.0 and 51.2 ± 10.4 μm , respectively).

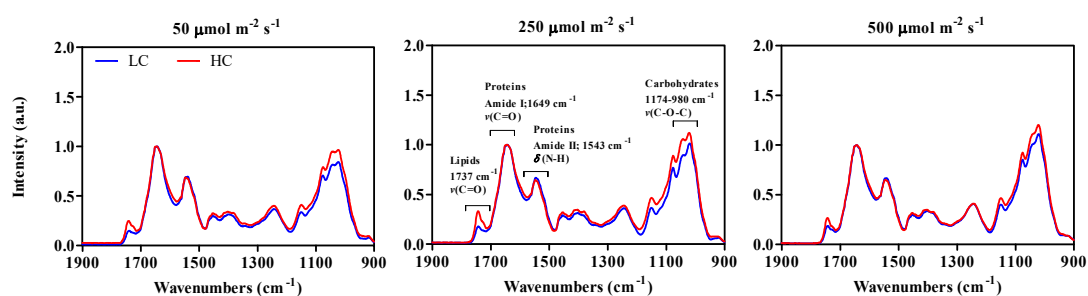


Figure S4-2. Normalized FTIR spectra of early-stage biofilms illuminated with three light intensities. The spectra were presented as the average of several measurements ($n \geq 8$) and normalized by Amide I band (1649 cm^{-1}) which was selected as an internal reference to assess the relative lipids and carbohydrates contents. The spectral peaks corresponding to main organic substances were marked in 250 $\mu\text{mol m}^{-2} \text{s}^{-1}$ as: carbohydrates (C–O–C; $1174\text{--}980 \text{ cm}^{-1}$), lipids (C=O; 1737 cm^{-1}), proteins (Amide I; 1649 cm^{-1}). ν = stretching, δ = bending vibrational modes in infrared spectroscopy.

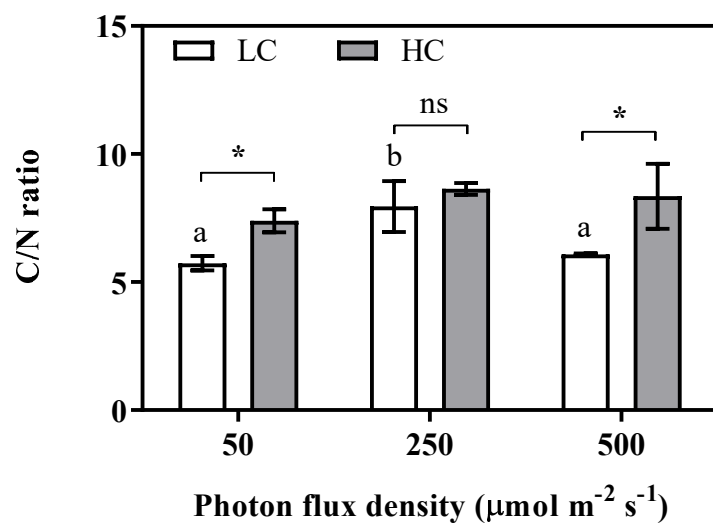


Figure S4-3. Effect of light intensity and initial cell density on cellular C/N ratio of *C. vulgaris* biofilms after 3-days cultivation.

**CHAPTER V. Physiological transition of
Chlorella vulgaris from planktonic to
immobilized conditions**

Preamble

Literature has shown that acclimation and regulation are cellular strategies allowing microalgae to adapt to changes in environmental conditions in order to optimize photosynthetic performance. These mechanisms have been investigated thoroughly in suspended cultures but only few studies focused on biofilms. Research works with bacteria demonstrated that different environmental cues are involved in the switch from planktonic to biofilm lifestyle. This induces physiological changes in bacteria (e.g., production of adhesions and polymers, surface appendages, expression of biofilm-related genes and proteins) that rapidly acclimate to the new local conditions and initiate biofilm formation. Accordingly, we do believe that during a transition from planktonic to immobilized state, physiological adjustments may also occur in microalgae, allowing them to acclimate to the new conditions. This mechanism was observed previously in Chapter II: interestingly, a very fast decrease in the cellular Chl *a* content was observed only after one day and full acclimation was achieved within the first 3 days. In this chapter, we aim at assessing physiological changes in even shorter time periods. To do so, the physiological transition of *C. vulgaris* from planktonic to immobilized conditions within the first 24h was characterized in the perfused system already described in Chapter III. The changes in cell concentration, morphology (cell size) and physiology (i.e., pigments, photosynthetic performance and macromolecular composition) were all quantified at 0h, 1h, 3h, 6h and 24h. We expect thus to get a better insight into mechanisms involved in microalgae biofilm formation and in particular, those related to the switch from planktonic to biofilm lifestyle.

Physiological transition of *Chlorella vulgaris* from planktonic to immobilized conditions

Abstract

The interest by the biofilm-based technologies is remarkably increasing due to their advantages compared to the conventional planktonic systems (e.g., higher productivity, lower water demand, low harvesting costs, ...) for microalgae cultivation. Though promising, a better understanding of biofilm formation mechanisms is still required to develop and run these systems at large-scale. Among them, the physiological transition from planktonic to immobilized state has never been studied before. Here we tracked the changes in growth and physiology (i.e. cell size, photosynthetic performance, carbon, nitrogen and Chl *a* quotas and macromolecular composition) of *Chlorella vulgaris* during the transition (over 24 hours) from planktonic to immobilized conditions. Results clearly confirmed that microalgae rapidly respond to the new conditions via physiological adjustment. Moreover, this behavior is specific to cells in the immobilized state. Very rapidly, cells use photosynthesis to grow (increase in size) and adjust the carbon allocation (increase in the relative carbohydrates pool). Triggering factors such as light, water availability, quorum sensing may induce this fast acclimation process.

Key words: Acclimation, *Chlorella vulgaris*, Immobilized state, Physiological transition, Planktonic state, microalgae biofilms

1. Introduction

Microalgae are capable of living in suspension in the water column (planktonic state) or in complex communities attached to substrates (biofilms) (Fanesi et al., 2021, 2019; Mantzorou and Ververidis, 2019; Morales et al., 2020; Pacheco et al., 2015). In response to changes in environmental conditions, microalgae are able to adjust the macromolecular composition through a process called acclimation (Raven and Geider, 2003). This mechanism operates on a time scale of hours to days. On the other hand, regulation which describes the adjustments of catalytic efficiency that occur without net synthesis or

breakdown of macromolecules operates on a time scale of seconds to minutes (Raven and Geider, 2003). At present, most of the knowledge we have about acclimation/regulation processes in microalgae comes from experiments performed on planktonic cells (Halsey and Jones, 2015; Raven and Geider, 2003). However, the recently developed biofilm-based systems (Mantzorou and Ververidis, 2019; Wang et al., 2017) require understanding of physiological mechanisms occurring in photosynthetic biofilms. Indeed, it is possible that the typical acclimation processes described for suspended cultures could not fit when microalgae live in sessile mode as cells in both lifestyles present various physiological properties (Wang et al., 2015; Zhuang et al., 2018).

In biofilms, microalgae cells are enclosed in an extracellular scaffold made of several polymers and water (Fanesi et al., 2019; Flemming et al., 2007), and this complex architecture creates a completely different micro-environment from their planktonic analogs that are typically surrounded by a less variable environment (Toninelli et al., 2016; Zhuang et al., 2018). Gradients of nutrients and light, bulk hydrodynamic conditions or humidity are already known to affect biofilm development (Huang et al., 2016; Murphy and Berberoglu, 2014; Podola et al., 2017; Shiratake et al., 2013). Initial adhesion, which may last several hours or days, is a key step affecting biofilm formation and development (D. A. Carbone et al., 2017; Sekar et al., 2004). This process is generally recognized as a lag phase of biofilm development and dramatic changes in physiological states may occur within this period in which planktonic cells need to rapidly acclimate to the new environmental conditions (Jungandreas et al., 2014; Meng et al., 2021). Up to date, information regarding the cellular adjustments occurring during a transition from the planktonic state to biofilm have been reported only for bacteria (Chua et al., 2013; Qayyum et al., 2016). Some works tried to decipher the driving force behind the lifestyle transition from the perspective of molecular pathway, like the expression of biofilm-associated genes or proteins (Qayyum et al., 2016; Waite et al., 2005). In (Jefferson, 2004), the authors listed a battery of genes implicated in cell motility, adhesion and quorum sensing that are essential players in biofilm formation. Also, phenotypic changes in e.g., cell morphology, cell surface structures and organelles (such as flagella, pili and appendages) participating in the biofilm formation were also observed from free-living to surface-attached cells (Kodjikian et al., 2003; O'Toole et al., 2000; Zhang et al., 2018). It should be stressed that planktonic microalgae can rapidly (i.e., from minutes to hours) acclimate to shifts in nutrients and light levels (Jungandreas et al., 2014; Sciandra et al., 2000). We therefore cannot rule out a physiological transition in

microalgae from planktonic to biofilm like that occurring in bacteria. To the best of our knowledge, only one study on microalgae has characterized the metabolic differences between planktonic cells and those in a mature biofilm (Romeu et al., 2020). However, information regarding how microalgae tune their physiological state in order to acclimate during a shift from planktonic to immobilized conditions has never been studied before.

The present work aims at characterizing the physiological behavior of microalgae when shifting from planktonic to immobilized state. In order to do so, we have immobilized *C. vulgaris* on filter membranes to track the physiological adjustments including growth, morphology (cell size), photosynthetic performance and macromolecular composition in the first 24h after immobilization. This study may give a basis and new insight for understanding the transition of microalgae from planktonic to benthic lifestyle.

2. Materials and Methods

2.1. Inoculum - Planktonic culture maintenance

Planktonic cultures of *Chlorella vulgaris* SAG 211–11b (Göttingen, Germany) were grown semi-continuously in a 1 L transparent bottle with 800 mL 3N-Bristol medium at an average irradiance of 250 $\mu\text{mol photons m}^{-2} \text{ s}^{-1}$ (Viugreum 50W LED outdoor floodlights, the irradiance was measured by QSL-2100 quantum scalar irradiance sensor, Biospherical Instruments, San Diego, CA, USA) at 25°C. The cultures were bubbled with filtered air and maintained within a range of chlorophyll *a* concentration from 0.25 to 1.0 mg L^{-1} by daily dilution. The planktonic cultures were pre-acclimated to the growth condition for at least 8 days before starting any experiment (after acclimation, the specific growth rate of the culture was $\mu = 1.4 \pm 0.24 \text{ d}^{-1}$).

2.2. Immobilized growth of *C. vulgaris* on filter membranes

Immobilized cells of *C. vulgaris* were cultured in the system reported in Fig. 5-1. The planktonic cells from the inoculum culture (section 2.1) were vacuum-filtered on nitrate cellulose filters (NC) (25-mm diameter, 0.2 μm pore size, Whatman, the effective colonization area was 2.01 cm^2) with an initial cell density of $(27.0 \pm 1.1) \times 10^6 \text{ cells cm}^{-2}$.

Membranes were then placed on the glass fiber filters (working as an absorbing material for the medium; 47-mm diameter, Whatman) and illuminated at $250 \mu\text{mol photons m}^{-2} \text{ s}^{-1}$. Filters were then placed in sterile petri dishes (55-mm diameter) filled with 3 mL of 3N-Bristol medium

After immobilization, the cells were harvested after 1h, 3h, 6h and 24h, respectively. Time 0 (0 h correspond to data of the planktonic culture (inoculum). Physiological measurements of the filtered cells just after immobilization were carried out in order to check if changes in variables occurred between the planktonic (inoculum) and the immobilized cultures. No differences were detected. Measurements were conducted immediately after sample collection at each time point to characterize a series of physiological parameters.

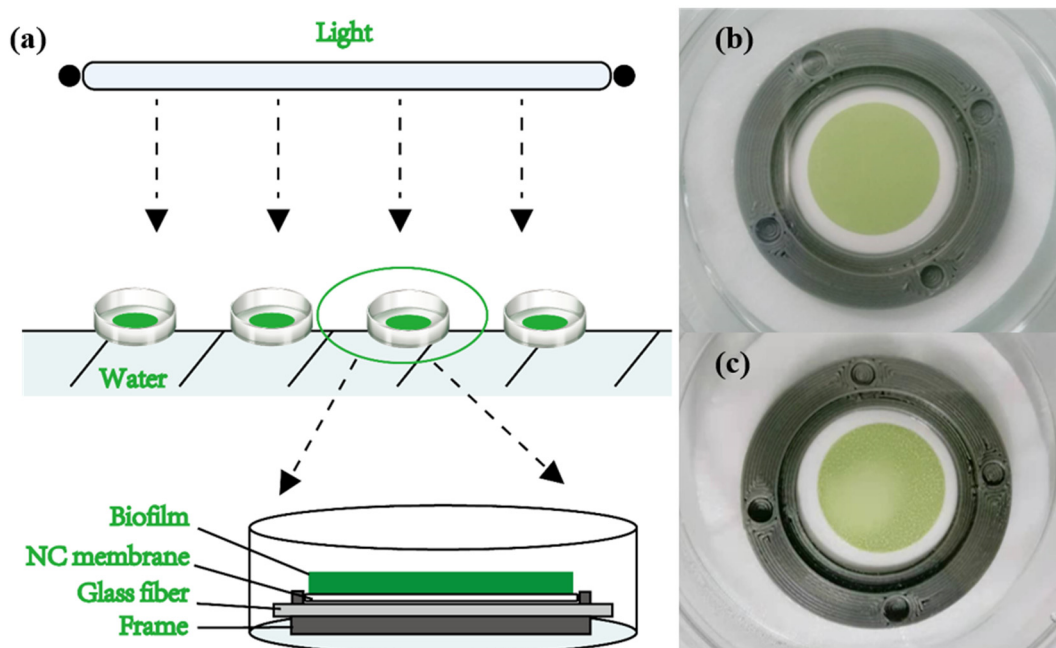


Figure 5-1. Schematic representation of the cultivation system used for the immobilized culture of *C. vulgaris* (NC membrane represents cellulose nitrate membrane filter) (a), photos of immobilized cells at the beginning (b) and end (c) of cultivation.

2.3. Suspended versus immobilized cultures

In order to compare the behavior of suspended and immobilized cells, suspended cultures with the same number of pre-acclimated cells as those filtrated on the membranes were grown in small glass containers with 3 mL Bristol medium (around 3.6 mm water depth). The cultures derived from the resuspension after filtrating the pre-acclimated cells were mixed with a magnetic stirrer and exposed to $250 \mu\text{mol photons m}^{-2} \text{ s}^{-1}$ at 25°C as the immobilized cells. At corresponding time points, suspended cells were collected

to determine the cell number and Chl *a* content.

2.4. Cell number

Total cells in planktonic and immobilized cultures were harvested with 3N-Bristol medium at each time point. Cell concentration (cells mL⁻¹) was determined by the Flow cytometry (Guava EasyCyte HT; Millipore, USA) as described in (Fanesi et al., 2021), and the cells areal density (cells cm⁻²) on the membrane was calculated based on the footprint area (2.01 cm⁻²).

2.5. Cell volume

Cell morphological changes were observed with an AxioSkop 2 plus microscope (Carl Zeiss, Oberkochen, Germany) under 63× magnification. Average volumetric cell size was determined considering a minimum of 300 individual cells by AxioVision SE64 Rel. 4.9.1 Software (Zeiss, White Plains, NY, USA) (Hillebrand et al., 1999).

2.6. Photosynthetic performance

Photosynthetic activity of immobilized *C. vulgaris* within the first 24h was assessed with Pulse amplitude modulation (PAM) fluorometer (AquaPen, AP 110-C, Photon Systems Instruments, Drasov, Czech Republic). After 10 min of dark-adaptation, the samples were exposed to a stepwise increase of seven actinic lights (from 0 to 1000 μmol photons m⁻² s⁻¹, blue led at 455 nm) with 60s intervals to construct the electron transport rate versus photon flux density (ETR/PFD) curves. Photosynthetic parameters such as the maximum quantum yield (F_v/F_m), the effective quantum yield (ΔF/F' _m), and the relative electron transport rate (rETR) were calculated as described in (Guzzon et al., 2019). Additionally, the rETR/PFD curves were fitted with the function $rETR = rETR_{max} (1 - e^{-\alpha I/rETR_{max}})$ (Webb et al., 1974), to estimate the maximum rate of relative ETR (rETR_{max}), the initial slope of curves α and photo-saturation E_k ($E_k = rETR_{max} / \alpha$).

2.7. Cell components: Chlorophyll *a*, macromolecular and elemental composition

Chl *a* was extracted with dimethyl sulfoxide (DMSO) and quantified as described by (Wellburn, 1994). The Chl *a* content was then normalized on a per-cell and on a per-volume basis. Chl *a* concentration ($\mu\text{g cm}^{-2}$) on the membrane was therefore calculated by the cellular Chl *a* content (pg cell^{-1}) and cell areal density (cells cm^{-2}).

ATR-FTIR PerkinElmer Spectrum-two spectrometer (PerkinElmer, Waltham, MA, USA) was employed to trace variations in cellular macromolecules composition as described in Fanesi et al. (2019). The spectra were baselined and specific macromolecular pools were characterized with maximum absorption values at the corresponding spectral ranges: carbohydrates (C–O–C; $1200\text{--}950\text{ cm}^{-1}$), lipids (C=O; $1750\text{--}1700\text{ cm}^{-1}$), proteins (Amide I; $1700\text{--}1630\text{ cm}^{-1}$).

Carbon (C) and nitrogen (N) content at 0h and 24h was measured with an elemental analyzer (Organic Elemental Analyzer FLASH 2000 CHNS/O, Thermo Scientific). Dried biomass (1~2 mg) harvested from planktonic or immobilized cultures was used for the analysis after being previously washed twice with MilliQ water and dried to constant at 100°C . Carbon and nitrogen quotas were reported over cell dry weight.

2.8. Light measurements in the biofilm and suspended cultures

Light intensity at the bottom of the biofilm was estimated according to the Lambert-Beer model (Grenier et al., 2019).

$$I_{bottom} = I_0 e^{-hb} \quad (1)$$

Where I_{bottom} ($\mu\text{mol photons m}^{-2}\text{ s}^{-1}$) corresponds to the light intensity in the deepest layer of the biofilm (in contact with the support), I_0 stands for the income light ($\mu\text{mol photons m}^{-2}\text{ s}^{-1}$), h is the biofilm thickness at time 0 ($51.2 \pm 10.4\ \mu\text{m}$, see supplementary data for Chapter IV) and b corresponds to the biofilm extinction coefficient ($5.5 \times 10^3\ \text{m}^{-1}$, Fanesi et al., unpublished data). The light attenuation ($A_{biofilm}$) in the biofilm was calculated using the following expression:

$$A_{biofilm} = 1 - I_{bottom}/I_0 \quad (2)$$

In order to calculate the average irradiance received by the microalgae in the suspended culture (see section 2.3), experiments were first carried out to measure the microalgae extinction coefficient. Beakers with cell concentrations between 5 and 30×10^6 cells mL⁻¹ were prepared and exposed to 250 $\mu\text{mol photons m}^{-2} \text{s}^{-1}$. An extinction coefficient of $3.84 \times 10^{-12} \text{ m}^2 \text{ cell}^{-1}$ was then calculated (Supplementary data, Fig. S5-1). Lee (1999) calculated a similar extinction coefficient for *Chlorella sp.*

The Lambert-Beer model was afterwards applied to determine the average light in the culture as described by Bernard et al. (2015) for the cell concentration of 1.67×10^7 cell mL⁻¹ and 3.6 mm depth. The average irradiance received by the microalgae was 223 $\mu\text{mol photons m}^{-2} \text{s}^{-1}$.

2.9. Relative air humidity for immobilized culture

In a perfused system, algal cells are separated from water column and directly contact the gas phase (Podola et al., 2017). As demonstrated by Häubner et al. (2006) and Shiratake et al. (2013), the relative air humidity inside the cultivation chambers affected the physiological properties (e.g., photosynthetic activity, chemical composition) and growth profiles of microalgae biofilms. In order to record the conditional changes in Petri dish (the chamber) after cells immobilization, a designed and calibrated sensor (Fig. S5-2) for determining the relative air humidity was employed.

2.10. Statistics

All experiments were performed with three independent biological replicates and the data were shown as mean values with standard deviations. In order to elucidate the physiological transition of microalgae after a shift from planktonic to immobilized growth over time, a principal component analysis (PCA) and a heatmap were computed using R software (R Core Team, 2014). The cell areal density, average cell bio-volume, and physiological transitions in photosynthetic parameters and biochemical composition over time were

statistically analyzed by one-way ANOVA using IBM SPSS Statistics 25.0 software (SPSS Inc., Chicago, IL). Scheffe's multiple comparisons procedure was carried out after the tests of normality and variance homogeneity. Student's *t*-test was employed to test for differences between C/N ratios of pre-acclimated planktonic and immobilized cells at end of cultivation. Significant differences at a level of $P < 0.05$ are shown with different letters.

3. Results and discussion

3.1. Short term physiological changes of immobilized cells

Environmental conditions (light, nutrients concentration, temperature, ...) may change rapidly on time scales that match those of cellular processes in aquatic ecosystems (MacIntyre et al., 2000). Indeed, besides regulation and adaptation, acclimation that occurs through synthesis or breakdown of specific components of the photosynthetic apparatus is the main mechanism affecting the photosynthetic processes of algae (Raven and Geider, 2003). As an example, changes in the pigment abundance of the marine phytoplankton have been described due to photo-acclimation that occurs on timescales typical of mixing in the open ocean while rapid changes in activity of different components of the photosynthetic apparatus were observed in estuaries (MacIntyre et al., 2000). Both mechanisms are thought to act according to the main rule of optimizing the photosynthetic performance. Indeed, a balance between light energy absorption and the overall utilization capacity of a cell must be maintained to optimize growth and protect the cell from excess energy. Extensive research on the subject has been performed on planktonic cultures (Anning et al., 2000; Jungandreas et al., 2014; Ritz et al., 2000) and on complex microphytobenthic communities (Mouget et al., 2008; Serôdio et al., 2012; van Leeuwe et al., 2008) or in general on mature natural biofilms (Karsten and Holzinger, 2014). However, no information concerning how microalgae acclimate/regulate during the first stages of substrate colonization exists, even though this knowledge could help understanding how microalgae biofilms form and develop.

For the first time, our results revealed that in *C. vulgaris* the transition from planktonic to immobilized state triggered very fast changes in the cells (Fig. 5-2, Fig. 5-3 and Fig. S5-3). The PCA (Fig. 5-2a) clearly shows a gradual separation of the samples along the PC1 (72% of variance explained) on the base of their physiological changes over time. In Fig. 5-

2b, the heatmap summarizes the changes in the physiological profile of the cells from the planktonic to the immobilized state. The heatmap suggests that the photosynthetic parameters and pigment presented a negative trend over time with respect to the compounds storage and cell volume.

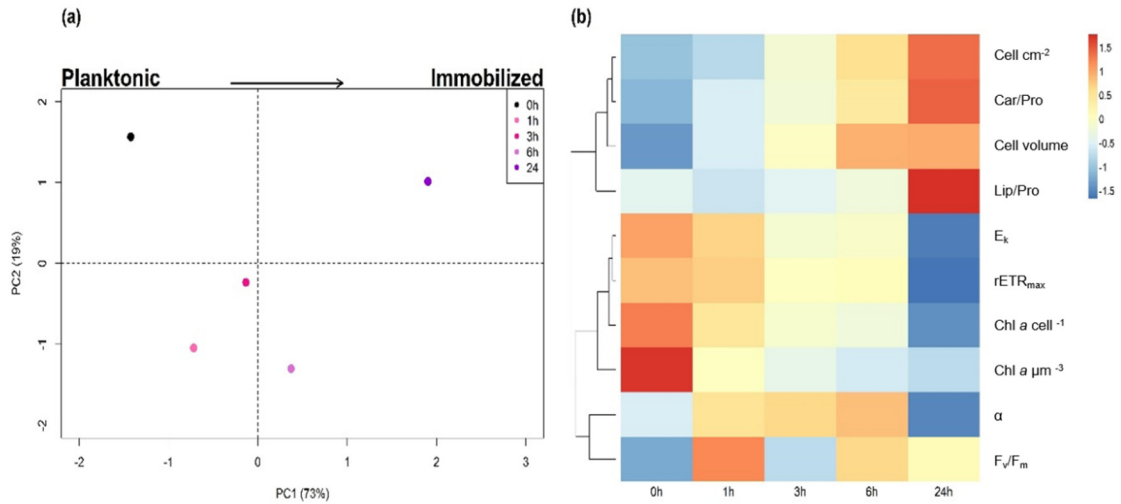


Figure 5-2. Scores plot of PCA (a) and heatmap (b) depicting the similarity between planktonic and immobilized cells and the patterns of the physiological parameters during the transition (24 hours), respectively. In the heatmap blue colors represent a low value for a specific parameter, whereas red color represents a high value for that parameter. Dendrograms cluster the parameters that presented similar patterns during the transition. Car/Pro and Lip/Pro represent carbohydrates and lipids to proteins ratios, respectively.

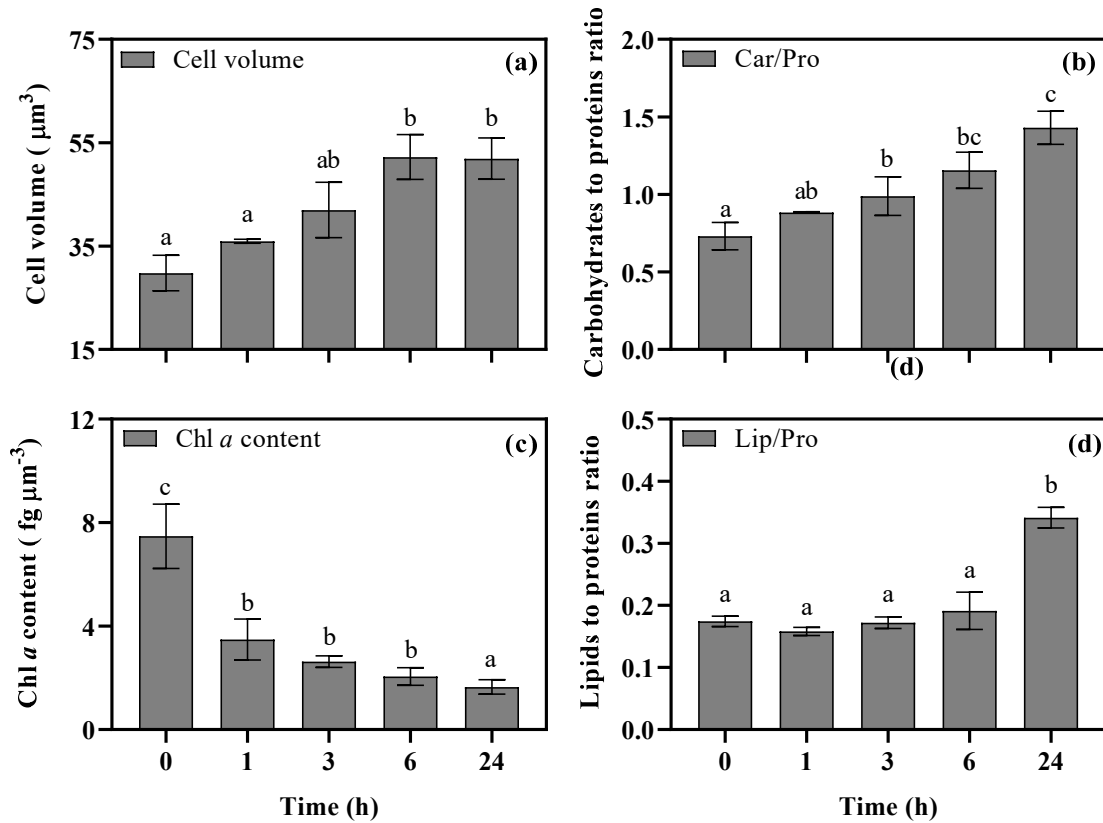


Figure 5-3. Changes in average cell volume (a), relative carbohydrates content (b), Chl *a* quota (c) and relative lipids content (d) over time. All the results were shown as mean value \pm SD ($n = 3$). Bars with different letters represent the statistical differences at level of $P < 0.05$.

Overall, regarding temporal changes, the cells reacted to the immobilization with an immediate (at 3 or 6 hours) increase in cell volume (Fig. 5-3a) and relative pool size of carbohydrates (Fig. 5-3b, Fig. S5-4), together with a decrease in Chl *a* content (Fig. 5-3c). Moreover, a decrease in the photosynthetic parameters ($rETR_{\max}$, E_k) were observed at 24 h (Fig. S5-3) together with an increase in the lipid content in the cells (Fig. 5-3d, and Fig. S5-4). Such temporal scales for physiological adjustments have never been described during a transition from planktonic to immobilized state for microalgae. However, microalgae (both planktonic and benthonic) are well known to rapidly tune physiological adjustments in order to cope with external changes (Karsten and Holzinger, 2014; Nymark et al., 2009; Sciandra et al., 2000).

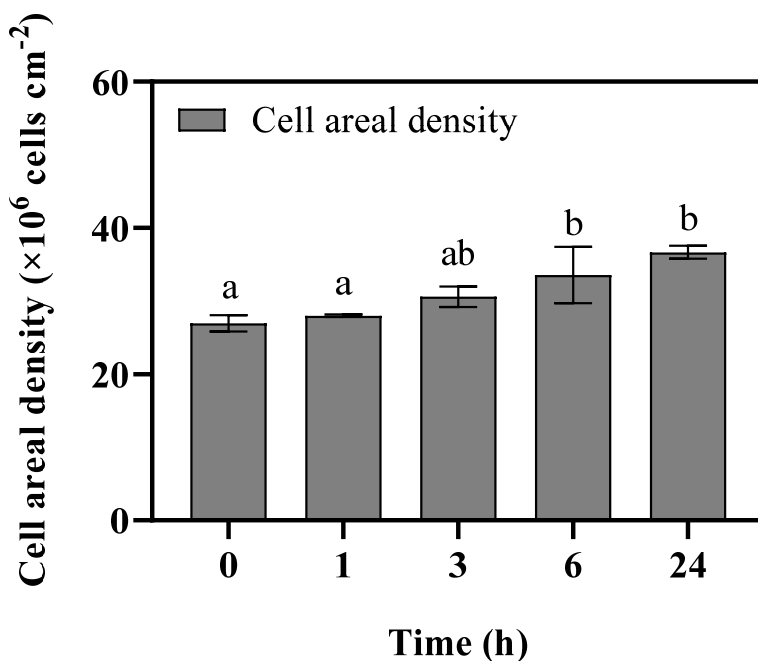


Figure 5-4. Evolution of cell areal density on membrane over time. All the results were shown as mean value \pm SD ($n = 3$). Bars with different letters represent the statistical differences at level of $P < 0.05$.

Interestingly, a low cell division rate (cell concentration increased only by a factor of 1.2 at 6h, Fig. 5-3a) and a significant change in cell growth (cell size doubled from 25 to 55 μm^3 , Fig. 5-3a) were observed in the first hours. A decrease in the Chl *a* concentration (3.75 times decrease, Fig. 5-3c) is therefore likely to be due to dilution by cell division/growth as suggested by the sharp decrease in the Chl *a* level (pg cell^{-1}) with the increase in cell volume (Fig. S5-5). The photosynthetic activity was though not affected in the first hours of immobilization (Fig. S5-3). Accordingly, we hypothesized that the rapid physiological changes occurred as a cell response to the shift in environmental conditions from suspension to the surface-associated growth. Therefore, during the first hours, sessile cells reacted to those changes by maintaining the photosynthetic activity, growing in size, accumulating carbohydrates while almost stopping division. In the literature, several works demonstrate cell physiological adjustments to cope to shifts in environmental conditions. For example, planktonic cells of *Phaeodactylum tricornerutum* subjected to a shift in light spectral quality (from blue to red light, or vice versa) exhibited changes in Chl *a* quota, effective quantum yield and cell macromolecules already after 2 hours from the shifts (Jungandreas et al., 2014). In line with our data, Sciandra et al. (2000) showed a rapid and transient change in cell size when *Cryptomonas* sp. suspended cells were light-shifted. Cell size dependence on light intensity was also reported by Fujiki and Taguchi (2002). Ritz et al. (2000) showed the arrest

of cell division when low-light acclimated *R. violacea* ($40 \mu\text{mol m}^{-2} \text{s}^{-1}$) suspended cells were transferred to higher irradiance (500 - ML, Middle Light and $1000 \mu\text{mol m}^{-2} \text{s}^{-1}$ - HL, High Light). Changes in pigments (phycobiliproteins, phycocyanin, phycoerythrin) contents and mRNA levels of specific genes were detected 8h after the transfer. On the other hand, studies that tracked the physiological changes and biochemical pathways of bacteria during planktonic-to-biofilm transition also confirmed the specific biofilm-related genes or proteins, which were only expressed in sessile but not planktonic bacterial cells (Chua et al., 2014; O'Toole et al., 2000; Zhao et al., 2017; Zou et al., 2012). Similarly, natural algal biofilms can rapidly adjust their metabolism (from minutes to hours) in response to emersion, stressful light conditions, humidity and temperature (Hubner et al., 2006; Perkins et al., 2001; Serdio et al., 2012; van Leeuwe et al., 2008). For instance, Corcoll et al. (2012) showed rapid changes (within 6h) in photosynthetic processes of fluvial biofilms after a sudden increase or decrease in the incoming light.

Accordingly, light to which cells are exposed is one of the factors that could have triggered such cellular physiological changes. Indeed, cells in the biofilm and in suspension are clearly submitted to different light patterns, in terms of intensity and quality as already reported by (Huang et al., 2016; Wang et al., 2021; Zhuang et al., 2018). While cells in concentrated suspended cultures are submitted to light and darkness cycles due to mixing which, in turn, will affect growth and photoacclimation mechanisms (Bernard et al., 2015; Combe et al., 2015), in a static system like that of our study, a light gradient may be established between the top and the bottom of the biofilm. In order to verify our hypothesis, light attenuation in the biofilm was calculated according to the Beer-Lambert law (see section 2.8). Light was attenuated of approximately 21% through the immobilized cells at the beginning of the experiment. Sessile cells were thus exposed to light intensity between 250 and $198 \mu\text{mol m}^{-2} \text{s}^{-1}$ (top and bottom of the biofilm, respectively) while cells in suspension (inoculum, see section 2.8) were submitted to an average light of $250 \mu\text{mol m}^{-2} \text{s}^{-1}$. This shift in light conditions may have affected cell behavior, triggering the observed physiological changes. Moreover, a shift in the relative water content in the gas space of the reactor was measured (Fig. S5-6). Water availability could have also act as a triggering factor as already observed elsewhere (Häubner et al., 2006; Shiratake et al., 2013). In a water-saturated atmosphere (liquid water or 100% air humidity), algae presented a high growth profile and photosynthetic efficiency, while at air humidities below 93%, both processes were strongly inhibited (Hubner et al., 2006). Moreover, quorum sensing

mechanisms cannot either be ruled out. Experiments aiming at better understanding the underlying mechanisms of acclimation/regulation should be therefore carried out in future works. A fully description of the different pigments content, rates of photosynthesis/respiration, enzyme activity would certainly allow to assess the underlying biological mechanisms. Furthermore, with the developments in genomics- and proteomics-based approaches, molecular mechanisms/pathways could be elucidated (Jefferson, 2004; Qayyum et al., 2016). Assays aiming at confirming the role of the hypothesized triggering factor(s) should be also carried out in a next step.

In order to further characterize carbon/nitrogen assimilation and assess cellular composition, carbon and nitrogen contents were determined at the beginning and at end of the experiment (Fig. 5-5). In contrast to nitrogen quota that kept stable, carbon quota significantly increased after 24h suggesting an assimilation of both nutrients. On the other hand, the C/N ratio significantly increased from 5 to ~ 10 (Fig. S5-7) suggesting an uncoupling between carbon assimilation and nitrogen uptake. This is also in agreement with the delayed decrease of $rETR_{max}$ and E_k after 24h and the rise in the relative lipid content (Fig. S5-3, Fig. 5-3d). On the other hand, a significant decrease of the Chl *a* content from 0 and 24h, by a factor of 4.6 (Fig. 5-3a). As previously stated, and explained in chapter II, this may be controlled by dilution due to cell growth/division.

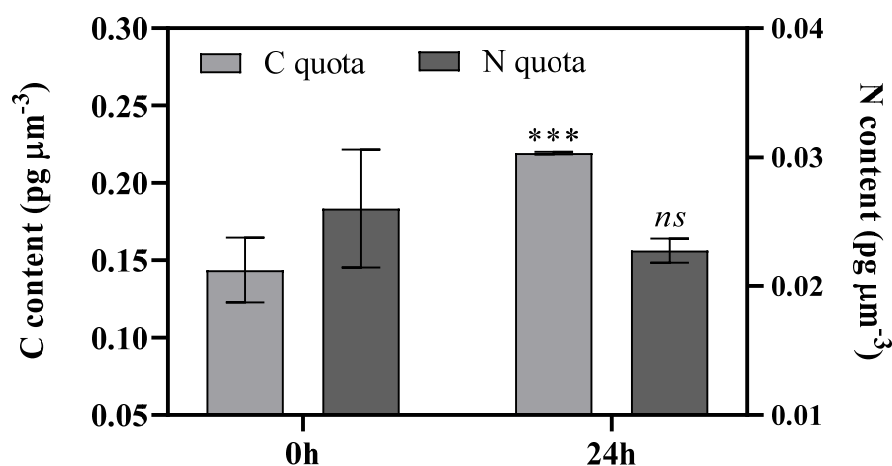


Figure 5-5. Carbon and nitrogen content at the beginning and end of cultivation. All the results were shown as mean value \pm SD ($n = 3$). Bars with *** depicts the statistical differences at a level of $P < 0.001$, while *ns* represents no difference.

Typically, nutrients may modulate photosynthetic activity in several ways depending on the limiting compound (Wykoff et al., 1998). The two main ways are the low repairing rate

of proteins in photosystems and the competition for ATP and reducing equivalents between C assimilation to nutrient uptake (Beardall et al., 2001; Turpin, 1991). On the other hand, a similar trend of rETR_{max} was found by Forster and Martin-Jézéquel (2005) investigating microphytobenthic diatoms. The authors proposed a link between nutrient availability and the Calvin cycle activity. Further experiments are required to deeply investigate the relationship between photosynthesis and nutrient uptake in photosynthetic biofilms.

3.2. Are the short-term physiological changes biofilm specific?

To further confirm that the physiological changes are driven by the transition from planktonic to immobilized state, suspended cells at 250 $\mu\text{mol m}^{-2} \text{s}^{-1}$ were transferred to a glass container and exposed to the same conditions as those of the immobilized counterparts (see section 2.3).

According to Fig. 5-6 and 5-7, no significant changes in size or Chl *a* content but a marked (72%) biomass increase were noticed in the first 6h for the planktonic cells. We therefore hypothesized that no significant shift in environmental conditions occurred when cells were transferred from the inoculum culture to the small container. Indeed, quite close average light intensity was determined in those two conditions (from 250 to 223 $\mu\text{mol m}^{-2} \text{s}^{-1}$ for the inoculum and suspended culture, respectively).

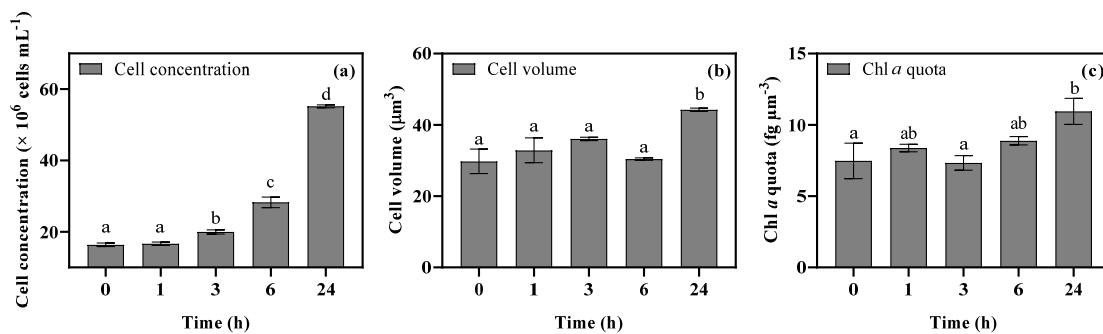


Figure 5-6. Changes of cell concentration (a), average cell volume (b) and Chl *a* quota ($\text{fg } \mu\text{m}^{-3}$) of planktonic culture over time. All the results were shown as mean value \pm SD ($n = 3$). Bars with different letters represent the statistical differences at level of $P < 0.05$.

From our data, it clearly appears that sessile cells and their planktonic counterparts do behave differently when exposed to the same incident light intensity. Our results are also in agreement with other studies that report differences among suspended and immobilized

cultures (Huang et al., 2016; Zhuang et al., 2018). For instance, it has been demonstrated that cells immobilized on surfaces may be less prone to self-shading (Huang et al., 2016) and more vulnerable to dehydration (Naumann et al., 2013; Shiratake et al., 2013). A higher availability to CO₂ compared to suspended counterparts may be also improved by the direct exposure to gas (Huang et al., 2016; Shiratake et al., 2013; Zhuang, 2018). Such a great physiological plasticity of cells growing in biofilms, as proposed by other authors, as a key feature to cope with the external variability as the biofilm develops (Forster and Martin-Jézéquel, 2005; Perkins et al., 2001). An increase of the chlorophyll content is observed for cells in suspension at the end of the assay (Fig. 5-7). This is probably associated to self-shading due to cell division.

On the whole, data show that the rapid morphological and physiological changes are specific of the cellular immobilized state. In addition, it is likely that changes in environmental conditions to which cells are exposed trigger those physiological changes.

Overall, the rapid acclimation/regulation process that the cells underwent immediately after being immobilized seemed to be aimed at optimizing fitness under the new growth conditions (Geider et al., 1997, 2009, 1998). Such a survival strategy has been often reported for the phytoplankton and it seems to suit also immobilized cells growing on surfaces. A similar strategy was recently described for biofilms of *C. vulgaris* growing at different hydrodynamic conditions but presenting identical growth rates (Fanesi et al., 2021). Further work should be carried out to identify the underlying acclimation/regulation mechanisms and the triggering factors.

4. Conclusion

This study for the first time tracked the physiological behavior of cultured microalgae from planktonic to immobilized condition. The results pointed out that cells rapidly acclimated to the new environmental conditions (surface-associated) by increasing the cell size and adjusting the carbon allocation (carbohydrates and lipids pool) (within 3h). Moreover, this behavior seems to be specific of the immobilized state of the cells. We also hypothesized that changes in the local environmental conditions to which cells are exposed might have been responsible for the described cellular behavior.

Although this work clearly presents the physiological adjustments of cells in planktonic-

to-immobilized transition, the environmental factors responsible for such changes are difficult to identify due to their complexity with the development of biofilms. According to our data, we hypothesized that light could act as a triggering factor. Indeed, cells in the biofilm and in suspension are clearly submitted to different light patterns (Huang et al., 2016; Zhuang et al., 2018). In addition to light, other factors such as water availability, CO₂, local pH, as well as signals related to quorum-sensing should not be excluded. Assays integrating genomics and proteomics approaches and methodologies to further characterize photosynthetic processes are required to fully comprehend the behavior of cells switching from planktonic to benthic modes. This will represent a step forward to better understand biofilm communities, for the selection of suitable strains and in optimizing the biofilm-based systems.

Supplementary data

Suspension absorption coefficient:

Figure S1 shows the linear regression of the light absorbance (A_ξ) at various cell concentration in suspended culture (slope is 5.94×10^9 cells m^{-2} , $P < 0.001$; see section 2.8). Suspension absorption coefficient (ξ) was determined according to the Lambert-Beer law (Lee, 1999):

$$A_\xi = \text{Log}(I_0/I_z) = \xi X z \quad (\text{S1})$$

where, I_0 and I_z are the light intensities at the surface and depth of z (distance from the illuminating surface), respectively, and X is the cell concentration.

The suspension absorption coefficient (ξ) could be obtained from Fig. S1.

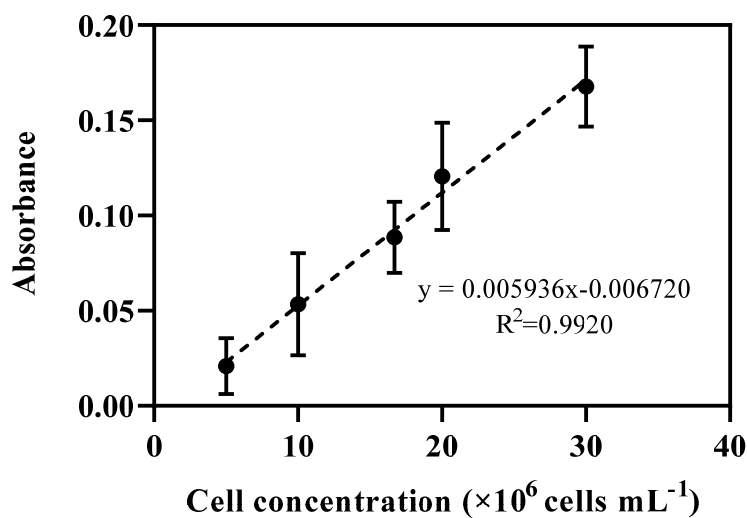


Figure S5-1. Linear correlation between the suspension absorbance and cell concentration. Points were from actual measurement of suspended cultures under $250 \mu\text{mol } m^{-2} s^{-1}$.

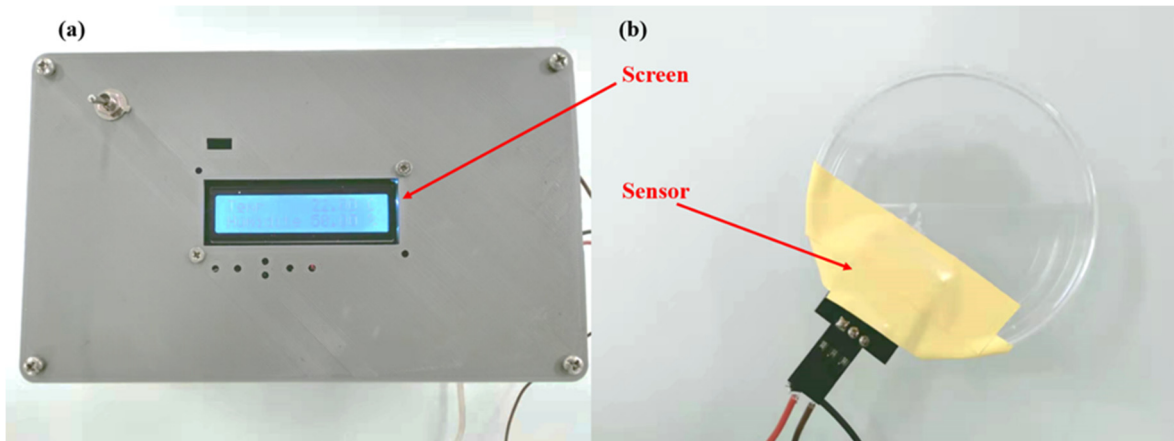


Figure S5-2. Image of the combined temperature/air humidity sensor (embedded in a Petri dish cover) used in this work.

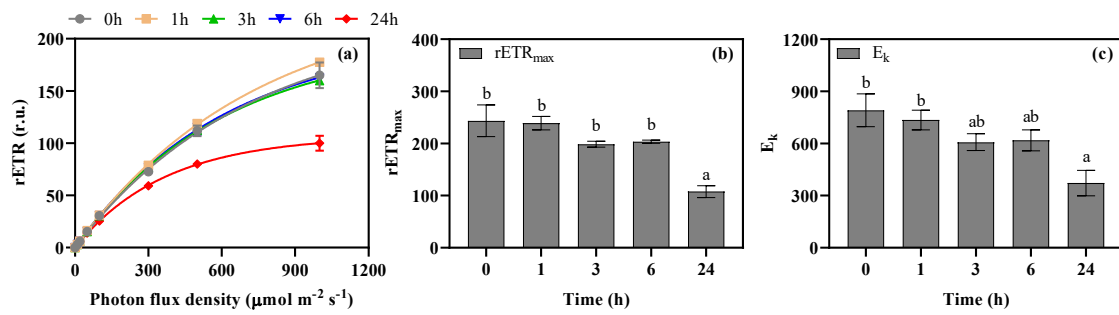


Figure S5-3. Changes in rETR/PFD curves (a), maximal relative electron transport rate (b), and photo-saturation irradiance (c) over time.

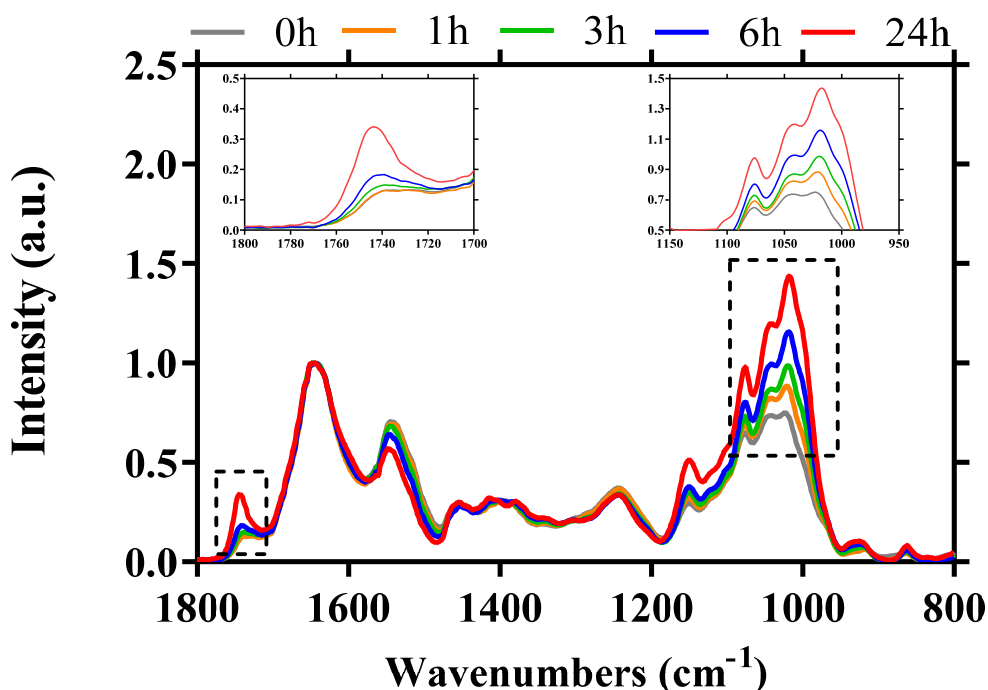


Figure S5-4. Changes of normalized FTIR spectra for *C. vulgaris* after a transition from planktonic to immobilized growth over time. The spectra were presented as the average of several measurements ($n = 3$) and normalized by Amide I band (1649 cm^{-1}) which was selected as an internal reference to assess the relative lipids and carbohydrates contents. The spectral peaks corresponding to main organic substances were marked in $250 \mu\text{mol m}^{-2} \text{ s}^{-1}$ as: carbohydrates (C–O–C; $1174\text{-}980 \text{ cm}^{-1}$), lipids (C=O; 1737 cm^{-1}), proteins (Amide I; 1649 cm^{-1}). ν = stretching, δ = bending vibrational modes in infrared spectroscopy.

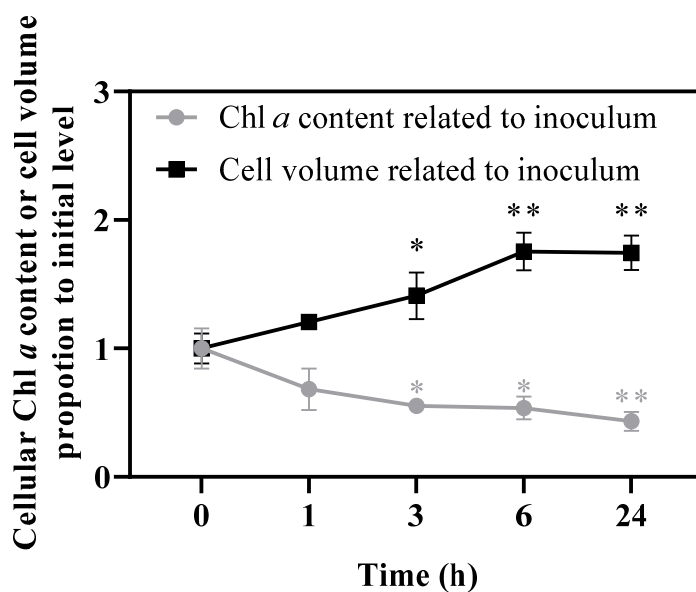


Figure S5-5. Cellular Chl *a* content (pg cell^{-1}) and cell volume in relation to the levels in inoculum.

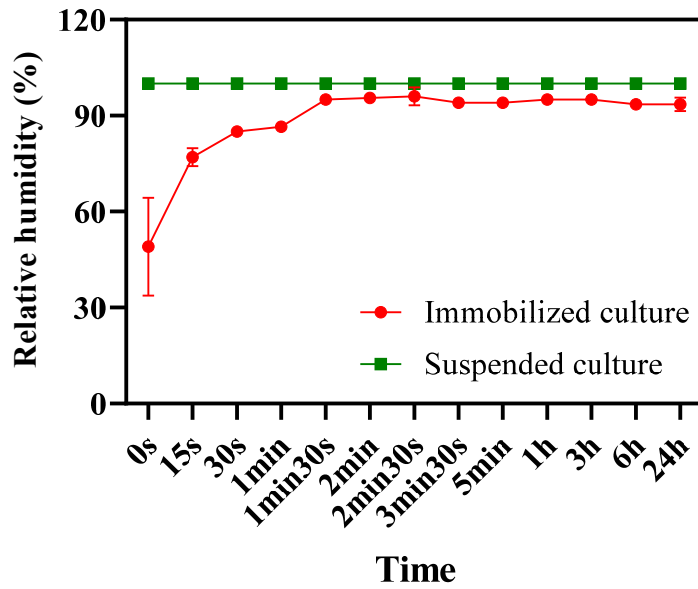


Figure S5-6. Changes in relative air humidity over time.

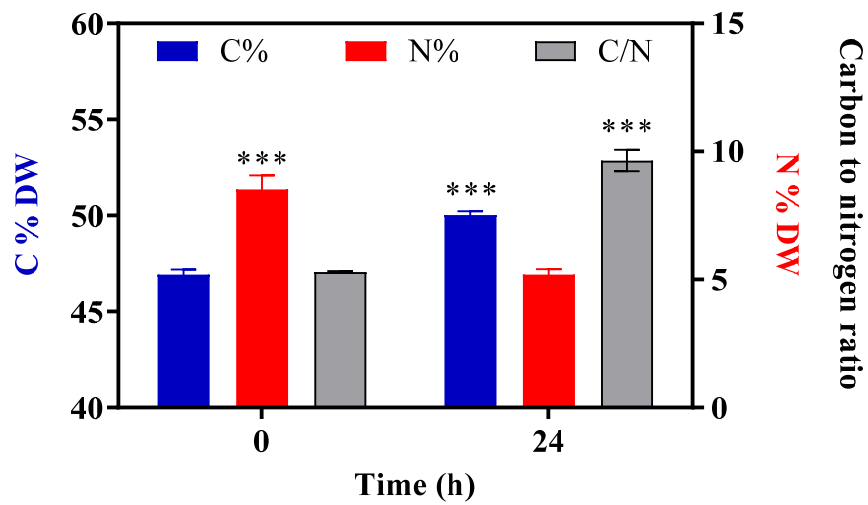


Figure S5-7. Carbon and nitrogen content by cell dry weight, and their ratio at the beginning and end of cultivation.

CHAPTER VI. General conclusions and perspectives

General conclusions and perspectives

1. General conclusion

This thesis aims at better understanding the effect of several operational factors (light, inoculum and support material) on biofilm development and sessile cells physiology in order to further help optimizing biofilm-based cultivation systems.

First, we explored microalgae biofilm dynamics in a continuous submerged photobioreactor through the evolution of sessile cell concentration and biofilm chemical composition over time (Chapter II). Results suggest that inoculum cell density together with Chl *a* content (cell physiology) and light intensity strongly impacted biofilm kinetics and composition. Biofilms at high inoculum density (4.54×10^6 cells cm^{-2}) exposed at $100 \mu\text{mol m}^{-2} \text{s}^{-1}$ presented the highest division rate and maximal biomass productivity. However, the biomass productivity ($0.15\text{-}0.65 \text{ g m}^{-2} \text{ d}^{-1}$) was significantly lower than that reported in the literature. This may be due to the high detachment and/or support/strain properties. In particular, the unexpected pattern of cellular Chl *a* content, which rapidly decreased within only 1-3 days, brought about valuable information on acclimation mechanisms on microalgae biofilm cultures. This provided a theoretical basis for the studies on early-stage biofilms in the following chapters. In addition, it appears that appropriately increasing the inoculum density can improve the carbohydrates accumulation.

In the next step (Chapter III), experimental assays were conducted to assess the effect of the operational factors (light intensity, inoculum density/properties and support) on early-stage (3-days) cultures. Results clearly confirm that support properties, particularly micro-texture (mesh size and density, fibers organization) affected the cell retention, growth, biomass productivity and composition. Terrazzo presenting the highest productivity was suggested as promising support for pilot and large-scale biofilm cultivation systems. The conditions leading to the highest biomass productivity were identified: Terrazzo support combined with low density ($\sim 1.5 \times 10^6$ cells cm^{-2}) of cells pre-acclimated to high light ($350 \mu\text{mol m}^{-2} \text{s}^{-1}$). Another cultivation system was afterwards used (Chapter IV) based on the concept of the Twin-layer reactor which is known as a highly productive system. Unlikely the submerged flow reactor previously studied in chapters II and III, while cells contact directly with atmospheric carbon dioxide, nutrients are provided through a membrane which

works as a support for biofilm growth. Among the light and inoculum density tested, optimal conditions to produce biomass or lipids were identified: $250 \mu\text{mol m}^{-2} \text{s}^{-1}$ combined with LC ($4.8 \times 10^6 \text{ cells cm}^{-2}$) or HC initial inoculum ($28.8 \times 10^6 \text{ cells cm}^{-2}$), respectively. Additionally, estimating the physiological state of early-stage biofilms would be of paramount importance to help the operator identifying stressful parameters in advance and to do reasoned operation choices.

Lastly, in order to get a better insight into the underlying mechanisms related to photosynthetic biofilms development, and in particular those of acclimation, the physiological transition of planktonic to immobilized states was tracked within a short term period (24h). Acclimation processes can be clearly observed through adjustments of light energy absorption (Chl *a* content), utilization (photosynthesis) and final re-direction among cell division, growth and macromolecular storages. Very fast changes in these parameters are expected to be induced by alternating environmental conditions when microalgae shifted from planktonic to the immobilized states. In addition, it has been demonstrated that this phenomenon is sessile cells specific. Light and/or water availability were suggested as the triggering factor(s) but clearly more work is required to shed light into acclimation mechanisms in biofilms.

Overall, the main conclusions are the following:

- Light intensity, inoculum density and properties and the support material do affect biofilm growth and productivity. Our findings clearly show that sessile cells physiology (composition and activity), which has been poorly studied, is impacted by those operational factors. In particular, our results suggest for the first time that cells should be pre-acclimated to high light intensity prior to support inoculation.
- High light and/or high inoculum density may lead to an imbalance between the energy supply and consumption, inducing changes in carbon allocation in the cell detected through carbohydrates and/or lipids accumulation. Therefore, combined conditions of light, inoculum density and duration should be precisely applied in the biofilm process according to the target product as in suspended culture systems.
- A general decreasing trend of relative biomass increase with the rise of the inoculum density after 3-day cultivation (Fig. 6-1) is observed in all conditions tested (support, light intensity, ...), which may be explained by the reduction in light and/or nutrients availability. Mechanisms of quorum sensing cannot though be ruled out and should be studied in future works.

- The support material should be carefully chosen for running biofilm-based systems. In particular, the micro-texture characteristics of textile substrates do influence cell/biofilm distribution, probably light availability and consequently biofilm productivity. Terrazzo textile has been identified as a promising support for biofilm development and will be tested in future work in the lab.
- The best biomass productivity ($6.54 \text{ g m}^{-2} \text{ d}^{-1}$) determined in our work was obtained using immobilized cultures grown on membranes, inoculated at low density ($4.8 \times 10^6 \text{ cells cm}^{-2}$) and exposed to $250 \mu\text{mol m}^{-2} \text{ s}^{-1}$ (Table. S6-1).
- For the first time, observations confirmed that algal cells change their morphology (cell size), growth (cell division) and physiological profiles (pigment content, photosynthetic activity and macromolecular composition) to acclimate to the new lifestyle when switching from planktonic to immobilized state.

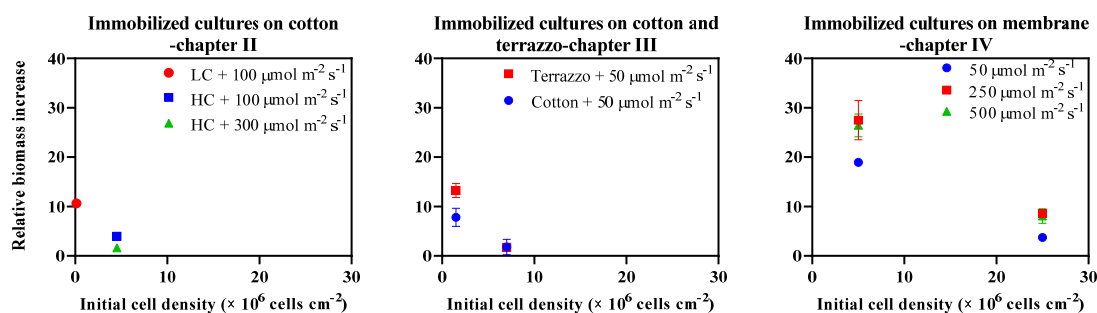


Figure 6-1. Relative growth rate of *C. vulgaris* under different defined conditions after 3-day cultivation. All the results were shown as mean value \pm SD.

Taken altogether, a framework for studying and identifying operational conditions which maximize microalgae biofilm cultivation was presented in this thesis. From a practical point of view, *C. vulgaris* growth, physiological profiles and the related environmental conditions were monitored at early-stage of culture. This may help operators to react by adjusting the production conditions to maintain high productivity. The impact of the inoculation step in the bioprocess is also highlighted. From a theoretical point of view, this work brought out new information regarding algal acclimation mechanisms in biofilms, which remain unclear.

2. Perspectives

From this work, we may find some enlightening perspectives and opportunities for further studies on microalgae biofilm cultivation. **Further researches may focus on:**

- Optimizing other operational factors like light quality, nutrients supply, temperature, hydrodynamic regime, colonization time, etc. (single and combined factors) in short- or long-term biofilm production;
- Identifying the appropriate materials and algal strains that are suitable for large-scale microalgae biofilm cultivation through the characterization of support and inoculum properties before large-scale operations, respectively. This process may not only improve microalgae biomass production but reduce the overall costs.
- Identifying the triggering factor(s) that induce the physiological transition of microalgae from planktonic to immobilized conditions. In particular, the light penetration, nutrients/gases concentration, as well as water availability over biofilm depth should be investigated. Unfortunately, little information is available on these spatial-dependent parameters on photosynthetic biofilms, which is partially due to the complexity of microalgae biofilms. Indeed, only few works apply microsensor-based tools to characterize photosynthetic activity of microalgae biofilm *in situ* (Gieseke and de Beer, 2004; Li et al., 2016). It may provide new insights in tracking the environmental changes from planktonic to biofilm lifestyles that trigger acclimation/regulation processes of immobilized cells.
- Using molecular tools (for instance, the genomics- and proteomics-based approaches) to assess if quorum sensing is one of the driving forces behind the lifestyle transition. These tools combined with other chemical and imaging approaches will certainly help elucidating the underlying biological mechanisms responsible for biofilm development and activity.

Supplementary data

Table S6-1. Biomass productivities of immobilized cultures in each chapter.

Chapter	system	Materials	Productivity ($\text{g m}^{-2} \text{d}^{-1}$)
II	Flow-lane	Cotton	$0.15 \pm 0.00 - 0.65 \pm 0.01$
III	Multi-wells plate	Cotton	$0.20 \pm 0.07 - 0.65 \pm 0.01$
III	Multi-wells plate	Terrazzo	$0.89 \pm 0.34 - 1.28 \pm 0.14$
IV	Petri dish	Membrane	$2.61 \pm 0.23 - 6.54 \pm 0.38$

Reference:

- Abinandan, S., Shanthakumar, S., 2015. Challenges and opportunities in application of microalgae (Chlorophyta) for wastewater treatment: A review. *Renew. Sustain. Energy Rev.* 52, 123–132. <https://doi.org/10.1016/j.rser.2015.07.086>
- Achinas, S., Charalampogiannis, N., Euverink, G.J.W., 2019. A brief recap of microbial adhesion and biofilms. *Appl. Sci.* 9, 2801. <https://doi.org/10.3390/app9142801>
- Adey, W.H., Laughinghouse, H.D., Miller, J.B., Hayek, L.A.C., Thompson, J.G., Bertman, S., Hampel, K., Puvanendran, S., 2013. Algal turf scrubber (ATS) flowways on the Great Wicomico River, Chesapeake Bay: productivity, algal community structure, substrate and chemistry. *J. Phycol.* 49, 489–501. <https://doi.org/10.1111/jpy.12056>
- Ahmad, I., Abdullah, N., Koji, I., Yuzir, A., Mohamad, S.E., 2021. Potential of microalgae in bioremediation of wastewater. *Bull. Chem. React. Eng. Catal.* 16, 413–429. <https://doi.org/10.9767/bcrec.16.2.10616.413-429>
- Ahmad, I., Hellebust, J.A., 1984. Osmoregulation in the extremely euryhaline marine microalga *Chlorella autotrophica*. *Plant Physiol.* 74, 1010–1015. <https://doi.org/10.1104/pp.74.4.1010>
- Ahmad, M.T., Shariff, M., Md. Yusoff, F., Goh, Y.M., Banerjee, S., 2020. Applications of microalga *Chlorella vulgaris* in aquaculture. *Rev. Aquac.* 12, 328–346. <https://doi.org/10.1111/raq.12320>
- Aigner, S., Glaser, K., Arc, E., Holzinger, A., Schletter, M., Karsten, U., Kranner, I., 2020. Adaptation to aquatic and terrestrial environments in *Chlorella vulgaris* (Chlorophyta). *Front. Microbiol.* 11, 585836. <https://doi.org/10.3389/fmicb.2020.585836>
- Altmann, B., Neumann, C., Velten, S., Liebert, F., Mörlein, D., 2018. Meat quality derived from high inclusion of a microalga or insect meal as an alternative protein source in poultry diets: a pilot study. *Foods* 7, 34. <https://doi.org/10.3390/foods7030034>
- Anning, T., MacIntyre, H.L., Pratt, S.M., Sammes, P.J., Gibb, S., Geider, R.J., 2000. Photoacclimation in the marine diatom *Skeletonema costatum*. *Limnol. Oceanogr.* 45, 1807–1817. <https://doi.org/10.4319/lo.2000.45.8.1807>
- Ashokkumar, V., Rengasamy, R., 2012. Mass culture of *Botryococcus braunii* Kutz. under open raceway pond for biofuel production. *Bioresour. Technol.* 104, 394–399. <https://doi.org/10.1016/j.biortech.2011.10.093>
- Babiak, W., Krzemińska, I., 2021. Extracellular polymeric substances (EPS) as microalgal bioproducts: A review of factors affecting eps synthesis and application in flocculation processes. *Energies* 14, 4007. <https://doi.org/10.3390/en14134007>
- Bajpai, V., Dey, A., Ghosh, S., Bajpai, S., Jha, M.K., 2011. Quantification of bacterial adherence on different textile fabrics. *Int. Biodeterior. Biodegrad.* 65, 1169–1174. <https://doi.org/10.1016/j.ibiod.2011.04.012>
- Baqué, M., Scalzi, G., Rabbow, E., Rettberg, P., Billi, D., 2013. Biofilm and planktonic lifestyles differently support the resistance of the desert cyanobacterium *Chroococcidiopsis* under space and martian simulations. *Orig. Life Evol. Biospheres* 43, 377–389. <https://doi.org/10.1007/s11084-013-9341-6>
- Barkia, I., Saari, N., Manning, S.R., 2019. Microalgae for high-value products towards human health and nutrition. *Mar. Drugs* 17, 304. <https://doi.org/10.3390/md17050304>
- Barral-Fraga, L., Martiñá-Prieto, D., Barral, M.T., Morin, S., Guasch, H., 2018. Mutual interaction between arsenic and biofilm in a mining impacted river. *Sci. Total Environ.* 636, 985–998. <https://doi.org/10.1016/j.scitotenv.2018.04.287>
- Barranguet, C., Van Beusekom, S., Veuger, B., Neu, T., Manders, E., Sinke, J., Admiraal,

- W., 2004. Studying undisturbed autotrophic biofilms: still a technical challenge. *Aquat. Microb. Ecol.* 34, 1–9. <https://doi.org/10.3354/ame034001>
- Barros, A.C., Gonçalves, A.L., Simões, M., 2019. Microalgal/cyanobacterial biofilm formation on selected surfaces: the effects of surface physicochemical properties and culture media composition. *J. Appl. Phycol.* 31, 375–387. <https://doi.org/10.1007/s10811-018-1582-3>
- Bartosh, Y., Banks, C.J., 2007. Algal growth response and survival in a range of light and temperature conditions: implications for non-steady-state conditions in waste stabilisation ponds. *Water Sci. Technol.* 55, 211–218. <https://doi.org/10.2166/wst.2007.365>
- Beardall, J., Young, E., Roberts, S., 2001. Approaches for determining phytoplankton nutrient limitation. *Aquat. Sci.* 63, 44–69. <https://doi.org/10.1007/PL00001344>
- Becker, K., 1996. Exopolysaccharide production and attachment strength of bacteria and diatoms on substrates with different surface tensions. *Microb. Ecol.* 32, 23–33. <https://doi.org/10.1007/BF00170104>
- Behrenfeld, M.J., Halsey, K.H., Milligan, A.J., 2008. Evolved physiological responses of phytoplankton to their integrated growth environment. *Philos. Trans. R. Soc. B Biol. Sci.* 363, 2687–2703. <https://doi.org/10.1098/rstb.2008.0019>
- Bernard, O., Mairet, F., Chachuat, B., 2015. Modelling of microalgae culture systems with applications to control and optimization, in: *Microalgae Biotechnology, Advances in Biochemical Engineering/Biotechnology*. Springer, Cham, pp. 59–87. https://doi.org/10.1007/10_2014_287
- Berner, F., Heimann, K., Sheehan, M., 2015. Microalgal biofilms for biomass production. *J. Appl. Phycol.* 27, 1793–1804. <https://doi.org/10.1007/s10811-014-0489-x>
- Berner, T., Dubinsky, Z., Wyman, K., 1989. Photoadaptation and the “package” effect in *Dunaliella tertiolecta* (Chlorophyceae). *J. Phycol.* 25, 70–78. <https://doi.org/10.1111/j.0022-3646.1989.00070.x>
- Bernstein, H.C., Kesaano, M., Moll, K., Smith, T., Gerlach, R., Carlson, R.P., Miller, C.D., Peyton, B.M., Cooksey, K.E., Gardner, R.D., Sims, R.C., 2014. Direct measurement and characterization of active photosynthesis zones inside wastewater remediating and biofuel producing microalgal biofilms. *Bioresour. Technol.* 156, 206–215. <https://doi.org/10.1016/j.biortech.2014.01.001>
- Bischo, H.W., Bold, H.C., 1963. *Phycological studies IV. Some soil algae from enchanted rock and related algal species*. University of Texas Publication: Austin, TX, USA.
- Bishop, P.L., Zhang, T.C., Fu, Y.C., 1995. Effects of biofilm structure, microbial distributions and mass transport on biodegradation processes. *Water Sci. Technol.* 31, 143–152. [https://doi.org/10.1016/0273-1223\(95\)00162-G](https://doi.org/10.1016/0273-1223(95)00162-G)
- Bišová, K., Zachleder, V., 2014. Cell-cycle regulation in green algae dividing by multiple fission. *J. Exp. Bot.* 65, 2585–2602. <https://doi.org/10.1093/jxb/ert466>
- Bitog, J.P., Lee, I.B., Lee, C.G., Kim, K.S., Hwang, H.S., Hong, S.W., Seo, I.H., Kwon, K.S., Mostafa, E., 2011. Application of computational fluid dynamics for modeling and designing photobioreactors for microalgae production: A review. *Comput. Electron. Agric.* 76, 131–147. <https://doi.org/10.1016/j.compag.2011.01.015>
- Blanken, W., Janssen, M., Cuaresma, M., Libor, Z., Bhaiji, T., Wijffels, R.H., 2014. Biofilm growth of *Chlorella sorokiniana* in a rotating biological contactor based photobioreactor. *Biotechnol. Bioeng.* 111, 2436–2445. <https://doi.org/10.1002/bit.25301>
- Blanken, W., Schaap, S., Theobald, S., Rinzema, A., Wijffels, R.H., Janssen, M., 2017. Optimizing carbon dioxide utilization for microalgae biofilm cultivation. *Biotechnol. Bioeng.* 114, 769–776. <https://doi.org/10.1002/bit.26199>

- Boelee, N.C., Janssen, M., Temmink, H., Taparavičiūtė, L., Khiewwijit, R., Jánoska, Á., Buisman, C.J.N., Wijffels, R.H., 2014. The effect of harvesting on biomass production and nutrient removal in phototrophic biofilm reactors for effluent polishing. *J. Appl. Phycol.* 26, 1439–1452. <https://doi.org/10.1007/s10811-013-0178-1>
- Boelee, N.C., Temmink, H., Janssen, M., Buisman, C.J.N., Wijffels, R.H., 2011. Nitrogen and phosphorus removal from municipal wastewater effluent using microalgal biofilms. *Water Res.* 45, 5925–5933. <https://doi.org/10.1016/j.watres.2011.08.044>
- Boelen, P., van Dijk, R., Sinninghe Damsté, J.S., Rijpstra, W.I.C., Buma, A.G., 2013. On the potential application of polar and temperate marine microalgae for EPA and DHA production. *AMB Express* 3, 1–9. <https://doi.org/10.1186/2191-0855-3-26>
- Borowitzka, M.A., 1999. Commercial production of microalgae: ponds, tanks, tubes and fermenters. *J. Biotechnol.* 70, 313–321. [https://doi.org/10.1016/S0168-1656\(99\)00083-8](https://doi.org/10.1016/S0168-1656(99)00083-8)
- Boudarel, H., Mathias, J.D., Blaysat, B., Grédiac, M., 2018. Towards standardized mechanical characterization of microbial biofilms: analysis and critical review. *Npj Biofilms Microbiomes* 4, 17. <https://doi.org/10.1038/s41522-018-0062-5>
- Brányiková, I., Maršáľková, B., Doucha, J., Brányik, T., Bišová, K., Zachleder, V., Vítová, M., 2011. Microalgae-novel highly efficient starch producers. *Biotechnol. Bioeng.* 108, 766–776. <https://doi.org/10.1002/bit.23016>
- Brockhagen, B., 2021. Improved growth and harvesting of microalgae *Chlorella vulgaris* on textile fabrics as 2.5D substrates. *AIMS Bioeng.* 8, 16–24. <https://doi.org/10.3934/bioeng.2021003>
- Bruno, L., Di Pippo, F., Antonaroli, S., Gismondi, A., Valentini, C., Albertano, P., 2012. Characterization of biofilm-forming cyanobacteria for biomass and lipid production. *J. Appl. Microbiol.* 113, 1052–1064. <https://doi.org/10.1111/j.1365-2672.2012.05416.x>
- Buhmann, M., Kroth, P.G., Schleheck, D., 2012. Photoautotrophic-heterotrophic biofilm communities: a laboratory incubator designed for growing axenic diatoms and bacteria in defined mixed-species biofilms. *Environ. Microbiol. Rep.* 4, 133–140. <https://doi.org/10.1111/j.1758-2229.2011.00315.x>
- Callow, M.E., Jennings, A.R., Brennan, A.B., Seegert, C.E., Gibson, A., Wilson, L., Feinberg, A., Baney, R., Callow, J.A., 2002. Microtopographic cues for settlement of zoospores of the green fouling alga *Enteromorpha*. *Biofouling* 18, 229–236. <https://doi.org/10.1080/08927010290014908>
- Cao, J., Yuan, W., Pei, Z.J., Davis, T., Cui, Y., Beltran, M., 2009. A preliminary study of the effect of surface texture on algae cell attachment for a mechanical-biological energy manufacturing system. *J. Manuf. Sci. Eng.* 131. <https://doi.org/10.1115/1.4000562>
- Carbone, D. A, Gargano, I., Pinto, G., Natale, A., Pollio, A., 2017. Evaluating microalgal attachment to surfaces: a first approach towards a laboratory integrated assessment. *Chem. Eng. Trans.* 57, 73–78. <https://doi.org/10.3303/CET1757013>
- Carbone, Dora Allegra, Olivieri, G., Pollio, A., Gabriele, Melkonian, M., 2017. Growth and biomass productivity of *Scenedesmus vacuolatus* on a twin layer system and a comparison with other types of cultivations. *Appl. Microbiol. Biotechnol.* 101, 8321–8329. <https://doi.org/10.1007/s00253-017-8515-y>
- Carvalho, A.P., Malcata, F.X., 2003. Kinetic modeling of the autotrophic growth of *Pavlova lutheri*: study of the combined influence of light and temperature. *Biotechnol Prog* 19, 1128–1135.
- Carvalho, A.P., Silva, S.O., Baptista, J.M., Malcata, F.X., 2011. Light requirements in

- microalgal photobioreactors: an overview of biophotonic aspects. *Appl. Microbiol. Biotechnol.* 89, 1275–1288. <https://doi.org/10.1007/s00253-010-3047-8>
- Chen, X., Goh, Q.Y., Tan, W., Hossain, I., Chen, W.N., Lau, R., 2011. Lumostatic strategy for microalgae cultivation utilizing image analysis and chlorophyll *a* content as design parameters. *Bioresour. Technol.* 102, 6005–6012. <https://doi.org/10.1016/j.biortech.2011.02.061>
- Chen, X., Liu, T., Wang, Q., 2014. The growth of *Scenedesmus sp.* attachment on different materials surface. *Microb. Cell Factories* 13, 1–6. <https://doi.org/10.1186/s12934-014-0142-z>
- Cheng, P., Wang, Y., Osei-Wusu, D., Liu, T., Liu, D., 2018. Effects of seed age, inoculum density, and culture conditions on growth and hydrocarbon accumulation of *Botryococcus braunii* SAG807-1 with attached culture. *Bioresour. Bioprocess.* 5, 15. <https://doi.org/10.1186/s40643-018-0198-4>
- Chia, M.A., Lombardi, A.T., da Graça Gama Melão, M., Parrish, C.C., 2015. Combined nitrogen limitation and cadmium stress stimulate total carbohydrates, lipids, protein and amino acid accumulation in *Chlorella vulgaris* (Trebouxiophyceae). *Aquat. Toxicol.* 160, 87–95. <https://doi.org/10.1016/j.aquatox.2015.01.002>
- Chiaramonti, D., Prussi, M., Casini, D., Tredici, M.R., Rodolfi, L., Bassi, N., Zittelli, G.C., Bondioli, P., 2013. Review of energy balance in raceway ponds for microalgae cultivation: Re-thinking a traditional system is possible. *Appl. Energy* 102, 101–111. <https://doi.org/10.1016/j.apenergy.2012.07.040>
- Chiou, Y.T., Hsieh, M.L., Yeh, H.H., 2010. Effect of algal extracellular polymer substances on UF membrane fouling. *Desalination* 250, 648–652. <https://doi.org/10.1016/j.desal.2008.02.043>
- Choudhary, P., Malik, A., Pant, K.K., 2017. Algal biofilm systems: an answer to algal biofuel dilemma, in: *Algal Biofuels*. Springer, Cham, pp. 77–96.
- Christenson, L., Sims, R., 2011. Production and harvesting of microalgae for wastewater treatment, biofuels, and bioproducts. *Biotechnol. Adv.* 29, 686–702. <https://doi.org/10.1016/j.biotechadv.2011.05.015>
- Christenson, L.B., Sims, R.C., 2012. Rotating algal biofilm reactor and spool harvester for wastewater treatment with biofuels by-products. *Biotechnol. Bioeng.* 109, 1674–1684. <https://doi.org/10.1002/bit.24451>
- Chua, S.L., Liu, Y., Yam, J.K.H., Chen, Y., Vejborg, R.M., Tan, B.G.C., Kjelleberg, S., Tolker-Nielsen, T., Givskov, M., Yang, L., 2014. Dispersed cells represent a distinct stage in the transition from bacterial biofilm to planktonic lifestyles. *Nat. Commun.* 5, 1–12. <https://doi.org/10.1038/ncomms5462>
- Chua, S.L., Tan, S.Y.Y., Rybtke, M.T., Chen, Y., Rice, S.A., Kjelleberg, S., Tolker-Nielsen, T., Yang, L., Givskov, M., 2013. Bis-(3'-5')-cyclic dimeric GPM regulates antimicrobial peptide resistance in *Pseudomonas aeruginosa*. *Antimicrob. Agents Chemother.* 57, 2066–2075. <https://doi.org/10.1128/AAC.02499-12>
- Clément-Larosière, B., Lopes, F., Gonçalves, A., Taidi, B., Benedetti, M., Minier, M., Pareau, D., 2014. Carbon dioxide biofixation by *Chlorella vulgaris* at different CO₂ concentrations and light intensities. *Eng. Life Sci.* 14, 509–519. <https://doi.org/10.1002/elsc.201200212>
- Cointet, E., Wielgosz-Collin, G., Bougaran, G., Rabesaotra, V., Gonçalves, O., Méléder, V., 2019. Effects of light and nitrogen availability on photosynthetic efficiency and fatty acid content of three original benthic diatom strains. *PLOS ONE* 14, e0224701. <https://doi.org/10.1371/journal.pone.0224701>
- Combe, C., Hartmann, P., Rabouille, S., Talec, A., Bernard, O., Sciandra, A., 2015. Long-term adaptive response to high-frequency light signals in the unicellular

- photosynthetic eukaryote *Dunaliella salina*. *Biotechnol. Bioeng.* 112, 1111–1121. <https://doi.org/10.1002/bit.25526>
- Consumi, M., Jankowska, K., Leone, G., Rossi, C., Pardini, A., Robles, E., Wright, K., Brooker, A., Magnani, A., 2020. Non-destructive monitoring of *P. fluorescens* and *S. epidermidis* biofilm under different media by fourier transform infrared spectroscopy and other corroborative techniques. *Coatings* 10, 930. <https://doi.org/10.3390/coatings10100930>
- Corcoll, N., Bonet, B., Leira, M., Montuelle, B., Tlili, A., Guasch, H., 2012. Light history influences the response of fluvial biofilms to Zn exposure. *J. Phycol.* 48, 1411–1423. <https://doi.org/10.1111/j.1529-8817.2012.01223.x>
- Correa, D.F., Beyer, H.L., Possingham, H.P., García-Ulloa, J., Ghazoul, J., Schenk, P.M., 2020. Freeing land from biofuel production through microalgal cultivation in the Neotropical region. *Environ. Res. Lett.* 15, 094094. <https://doi.org/10.1088/1748-9326/ab8d7f>
- Craggs, R.J., Adey, W.H., Jessup, B.K., Oswald, W.J., 1996. A controlled stream mesocosm for tertiary treatment of sewage. *Ecol. Eng.* 6, 149–169. [https://doi.org/10.1016/0925-8574\(95\)00056-9](https://doi.org/10.1016/0925-8574(95)00056-9)
- Cuellar-Bermudez, S.P., Aleman-Nava, G.S., Chandra, R., Garcia-Perez, J.S., Contreras-Angulo, J.R., Markou, G., Muylaert, K., Rittmann, B.E., Parra-Saldivar, R., 2017. Nutrients utilization and contaminants removal. A review of two approaches of algae and cyanobacteria in wastewater. *Algal Res.* 24, 438–449. <https://doi.org/10.1016/j.algal.2016.08.018>
- Cui, Y., Yuan, W., Cao, J., 2013. Effects of surface texturing on microalgal cell attachment to solid carriers. *Int. J. Agric. Biol. Eng.* 6, 44–54.
- Darvehei, P., Bahri, P.A., Moheimani, N.R., 2018. Model development for the growth of microalgae: A review. *Renew. Sustain. Energy Rev.* 97, 233–258. <https://doi.org/10.1016/j.rser.2018.08.027>
- De Assis, L.R., Calijuri, M.L., Assemany, P.P., Berg, E.C., Febroni, L.V., Bartolomeu, T.A., 2019. Evaluation of the performance of different materials to support the attached growth of algal biomass. *Algal Res.* 39, 101440. <https://doi.org/10.1016/j.algal.2019.101440>
- Djeribi, R., Boucherit, Z., Bouchloukh, W., Zouaoui, W., Latrache, H., Hamadi, F., Mena, B., 2013. A study of pH effects on the bacterial surface physicochemical properties of *Acinetobacter baumannii*. *Colloids Surf. B Biointerfaces* 102, 540–545. <https://doi.org/10.1016/j.colsurfb.2012.08.047>
- Do, T.T., Ong, B.N., Nguyen Tran, M.L., Nguyen, D., Melkonian, M., Tran, H.D., 2019. Biomass and astaxanthin productivities of *Haematococcus pluvialis* in an angled twin-layer porous substrate photobioreactor: effect of inoculum density and storage time. *Biology* 8, 68. <https://doi.org/10.3390/biology8030068>
- Duygu, D.Y., Udoh, A.U., Ozer, T.B., Akbulut, A., Erkaya, I.A., Yildiz, K., Guler, D., 2012. Fourier transform infrared (FTIR) spectroscopy for identification of *Chlorella vulgaris* Beijerinck 1890 and *Scenedesmus obliquus* (Turpin) Kützing 1833. *Afr. J. Biotechnol.* 11, 3817–3824.
- Escoubas, J.M., Lomas, M., LaRoche, J., Falkowski, P.G., 1995. Light intensity regulation of cab gene transcription is signaled by the redox state of the plastoquinone pool. *Proc. Natl. Acad. Sci.* 92, 10237–10241. <https://doi.org/10.1073/pnas.92.22.10237>
- Fanesi, A., Lavayssière, M., Breton, C., Bernard, O., Briandet, R., Lopes, F., 2021. Shear stress affects the architecture and cohesion of *Chlorella vulgaris* biofilms. *Sci. Rep.* 11, 1–11. <https://doi.org/10.1038/s41598-021-83523-3>
- Fanesi, A., Paule, A., Bernard, O., Briandet, R., Lopes, F., 2019. The architecture of

- monospecific microalgae biofilms. *Microorganisms* 7, 352. <https://doi.org/10.3390/microorganisms7090352>
- Fanesi, A., Wagner, H., Becker, A., Wilhelm, C., 2016. Temperature affects the partitioning of absorbed light energy in freshwater phytoplankton. *Freshw. Biol.* 61, 1365–1378. <https://doi.org/10.1111/fwb.12777>
- Fanesi, A., Wagner, H., Wilhelm, C., 2017. Phytoplankton growth rate modelling: can spectroscopic cell chemotyping be superior to physiological predictors? *Proc. R. Soc. B Biol. Sci.* 284, 20161956. <https://doi.org/10.1098/rspb.2016.1956>
- Fernández-Reiriz, M.J., Perez-Camacho, A., Ferreiro, M.J., Blanco, J., Planas, M., Campos, M.J., Labarta, U., 1989. Biomass production and variation in the biochemical profile (total protein, carbohydrates, RNA, lipids and fatty acids) of seven species of marine microalgae. *Aquaculture* 83, 17–37. [https://doi.org/10.1016/0044-8486\(89\)90057-4](https://doi.org/10.1016/0044-8486(89)90057-4)
- Finlay, J.A., Callow, M.E., Ista, L.K., Lopez, G.P., Callow, J.A., 2002. The influence of surface wettability on the adhesion strength of settled spores of the green alga *Enteromorpha* and the diatom *Amphora*. *Integr. Comp. Biol.* 42, 1116–1122. <https://doi.org/10.1093/icb/42.6.1116>
- Fisher, T., Minnaard, J., Dubinsky, Z., 1996. Photoacclimation in the marine alga *Nannochloropsis* sp. (Eustigmatophyte): a kinetic study. *J. Plankton Res.* 18, 1797–1818. <https://doi.org/10.1093/plankt/18.10.1797>
- Flemming, H.C., Neu, T.R., Wozniak, D.J., 2007. The eps matrix: the “house of biofilm cells.” *J. Bacteriol.* 189, 7945–7947. <https://doi.org/10.1128/JB.00858-07>
- Flemming, H.C., Wingender, J., 2010. The biofilm matrix. *Nat. Rev. Microbiol.* 8, 623–633. <https://doi.org/10.1038/nrmicro2415>
- Fleurence, J., Morançais, M., Dumay, J., Decottignies, P., Turpin, V., Munier, M., Garcia-Bueno, N., Jaouen, P., 2012. What are the prospects for using seaweed in human nutrition and for marine animals raised through aquaculture? *Trends Food Sci. Technol.* 27, 57–61. <https://doi.org/10.1016/j.tifs.2012.03.004>
- Forster, R.M., Martin-Jézéquel, V., 2005. Photophysiological variability of microphytobenthic diatoms after growth in different types of culture conditions. *Phycologia* 44, 393–402. [https://doi.org/10.2216/0031-8884\(2005\)44\[393:PVOMDA\]2.0.CO;2](https://doi.org/10.2216/0031-8884(2005)44[393:PVOMDA]2.0.CO;2)
- Fuqua, C., Parsek, M.R., Greenberg, E.P., 2001. Regulation of gene expression by cell-to-cell communication: acyl-homoserine lactone quorum sensing. *Annu. Rev. Genet.* 35, 439–468. <https://doi.org/10.1146/annurev.genet.35.102401.090913>
- Geider, R., MacIntyre, H., Kana, T., 1997. Dynamic model of phytoplankton growth and acclimation: responses of the balanced growth rate and the chlorophyll *a*:carbon ratio to light, nutrient-limitation and temperature. *Mar. Ecol. Prog. Ser.* 148, 187–200. <https://doi.org/10.3354/meps148187>
- Geider, R.J., MacIntyre, H.L., Kana, T.M., 1998. A dynamic regulatory model of phytoplanktonic acclimation to light, nutrients, and temperature. *Limnol. Oceanogr.* 43, 679–694. <https://doi.org/10.4319/lo.1998.43.4.0679>
- Geider, R.J., Moore, C.M., Ross, O.N., 2009. The role of cost–benefit analysis in models of phytoplankton growth and acclimation. *Plant Ecol. Divers.* 2, 165–178. <https://doi.org/10.1080/17550870903300949>
- Genin, S.N., Stewart Aitchison, J., Grant Allen, D., 2014. Design of algal film photobioreactors: Material surface energy effects on algal film productivity, colonization and lipid content. *Bioresour. Technol.* 155, 136–143. <https://doi.org/10.1016/j.biortech.2013.12.060>
- Gerbersdorf, S.U., Wieprecht, S., 2015. Biostabilization of cohesive sediments: revisiting the role of abiotic conditions, physiology and diversity of microbes, polymeric

- secretion, and biofilm architecture. *Geobiology* 13, 68–97. <https://doi.org/10.1111/gbi.12115>
- Gieseke, A.R.M.I.N., de Beer, D.I.R.K., 2004. Use of microelectrodes to measure in situ microbial activities in biofilms, sediments, and microbial mats. *Mol. Microb. Ecol. Man.* 2, 1581–1612.
- González, I., Ekelhof, A., Herrero, N., Siles, J.Á., Podola, B., Chica, A.F., Martín, M.Á., Melkonian, M., Izquierdo, C.G., Gómez, J.M., 2020. Wastewater nutrient recovery using twin-layer microalgae technology for biofertilizer production. *Water Sci.* 82, 1044–1061. <https://doi.org/10.2166/wst.2020.372>
- Gouveia, L., Graça, S., Sousa, C., Ambrosano, L., Ribeiro, B., Botrel, E.P., Neto, P.C., Ferreira, A.F., Silva, C.M., 2016. Microalgae biomass production using wastewater: Treatment and costs. *Algal Res.* 16, 167–176. <https://doi.org/10.1016/j.algal.2016.03.010>
- Greenwell, H.C., Laurens, L.M.L., Shields, R.J., Lovitt, R.W., Flynn, K.J., 2010. Placing microalgae on the biofuels priority list: a review of the technological challenges. *J. R. Soc. Interface* 7, 703–726. <https://doi.org/10.1098/rsif.2009.0322>
- Grenier, J., Bonnefond, H., Lopes, F., Bernard, O., 2019. The impact of light supply to moving photosynthetic biofilms. *Algal Res.* 44, 101674. <https://doi.org/10.1016/j.algal.2019.101674>
- Griffiths, M.J., van Hille, R.P., Harrison, S.T.L., 2014. The effect of nitrogen limitation on lipid productivity and cell composition in *Chlorella vulgaris*. *Appl. Microbiol. Biotechnol.* 98, 2345–2356. <https://doi.org/10.1007/s00253-013-5442-4>
- Gross, M., Henry, W., Michael, C., Wen, Z., 2013a. Development of a rotating algal biofilm growth system for attached microalgae growth with in situ biomass harvest. *Bioresour. Technol.* 150, 195–201. <https://doi.org/10.1016/j.biortech.2013.10.016>
- Gross, M., Henry, W., Michael, C., Wen, Z., 2013b. Development of a rotating algal biofilm growth system for attached microalgae growth with in situ biomass harvest. *Bioresour. Technol.* 150, 195–201. <https://doi.org/10.1016/j.biortech.2013.10.016>
- Gross, M., Jarboe, D., Wen, Z., 2015. Biofilm-based algal cultivation systems. *Appl. Microbiol. Biotechnol.* 99, 5781–5789. <https://doi.org/10.1007/s00253-015-6736-5>
- Gross, M., Wen, Z., 2014. Yearlong evaluation of performance and durability of a pilot-scale Revolving Algal Biofilm (RAB) cultivation system. *Bioresour. Technol.* 171, 50–58. <https://doi.org/10.1016/j.biortech.2014.08.052>
- Gross, M., Zhao, X., Mascarenhas, V., Wen, Z., 2016. Effects of the surface physico-chemical properties and the surface textures on the initial colonization and the attached growth in algal biofilm. *Biotechnol. Biofuels* 9, 1–14. <https://doi.org/10.1186/s13068-016-0451-z>
- Gudin, C., Therpenier, C., 1986. Bioconversion of solar energy into organic chemicals by microalgae. *Adv. Biotechnol. Process* 6, 73–110.
- Guiry, M.D., 2012. How many species of algae are there? *J. Phycol.* 48, 1057–1063. <https://doi.org/10.1111/j.1529-8817.2012.01222.x>
- Guzmán-Soto, I., McTiernan, C., Gonzalez-Gomez, M., Ross, A., Gupta, K., Suuronen, E.J., Mah, T.F., Griffith, M., Alarcon, E.I., 2021. Mimicking biofilm formation and development: Recent progress in in vitro and in vivo biofilm models. *iScience* 24, 102443. <https://doi.org/10.1016/j.isci.2021.102443>
- Guzzon, A., Bohn, A., Diociaiuti, M., Albertano, P., 2008. Cultured phototrophic biofilms for phosphorus removal in wastewater treatment. *Water Res.* 42, 4357–4367. <https://doi.org/10.1016/j.watres.2008.07.029>
- Guzzon, A., Di Pippo, F., Bonavita, S., Congestri, R., 2021. Influence of light and flow on taxon composition and photosynthesis of marine phototrophic biofilm in

- photobioreactors. *Mar. Environ. Res.* 169, 105395. <https://doi.org/10.1016/j.marenvres.2021.105395>
- Guzzon, A., Di Pippo, F., Congestri, R., 2019. Wastewater biofilm photosynthesis in photobioreactors. *Microorganisms* 7, 252. <https://doi.org/10.3390/microorganisms7080252>
- Halsey, K.H., Jones, B.M., 2015. Phytoplankton strategies for photosynthetic energy allocation. *Annu. Rev. Mar. Sci.* 7, 265–297. <https://doi.org/10.1146/annurev-marine-010814-015813>
- Hart, R., In-na, P., Kapralov, M.V., Lee, J.G.M., Caldwell, G.S., 2021. Textile-based cyanobacteria biocomposites for potential environmental remediation applications. *J. Appl. Phycol.* 33, 1525–1540. <https://doi.org/10.1007/s10811-021-02410-6>
- Hase, E., Otsuka, H., Mihara, S., 1959. Role of sulfur in the cell division of *Chlorella*, studied by the technique of synchronous culture. *Biochim. Biophys. Acta* 35, 180–189.
- Häubner, N., Schumann, R., Karsten, U., 2006. Aeroterrestrial microalgae growing in biofilms on facades-response to temperature and water stress. *Microb. Ecol.* 51, 285–293. <https://doi.org/10.1007/s00248-006-9016-1>
- He, Q., Yang, H., Wu, L., Hu, C., 2015. Effect of light intensity on physiological changes, carbon allocation and neutral lipid accumulation in oleaginous microalgae. *Bioresour. Technol.* 191, 219–228. <https://doi.org/10.1016/j.biortech.2015.05.021>
- He, X., Wang, J., Abdoli, L., Li, H., 2016. Mg^{2+}/Ca^{2+} promotes the adhesion of marine bacteria and algae and enhances following biofilm formation in artificial seawater. *Colloids Surf. B Biointerfaces* 146, 289–295. <https://doi.org/10.1016/j.colsurfb.2016.06.029>
- Hillebrand, H., Durselen, C.D., Kirschtel, D., Pollinger, U., Zohary, T., 1999. Biovolume calculation for pelagic and benthic microalgae. *J. Phycol.* 35, 403–424. <https://doi.org/10.1046/j.1529-8817.1999.3520403.x>
- Hillman, K.M., Sims, R.C., 2020. Struvite formation associated with the microalgae biofilm matrix of a rotating algal biofilm reactor (RABR) during nutrient removal from municipal wastewater. *Water Sci. Technol.* 81, 644–655. <https://doi.org/10.2166/wst.2020.133>
- Ho, S.H., Chen, C.Y., Chang, J.S., 2012. Effect of light intensity and nitrogen starvation on CO_2 fixation and lipid/carbohydrate production of an indigenous microalga *Scenedesmus obliquus* CNW-N. *Bioresour. Technol.* 113, 244–252. <https://doi.org/10.1016/j.biortech.2011.11.133>
- Hodges, A., Fica, Z., Wanlass, J., VanDarlin, J., Sims, R., 2017. Nutrient and suspended solids removal from petrochemical wastewater via microalgal biofilm cultivation. *Chemosphere* 174, 46–48. <https://doi.org/10.1016/j.chemosphere.2017.01.107>
- Hoh, D., Watson, S., Kan, E., 2016. Algal biofilm reactors for integrated wastewater treatment and biofuel production: A review. *Chem. Eng. J.* 287, 466–473. <https://doi.org/10.1016/j.cej.2015.11.062>
- Holland, R., Dugdale, T.M., Wetherbee, R., Brennan, A.B., Finlay, J.A., Callow, J.A., Callow, M.E., 2004. Adhesion and motility of fouling diatoms on a silicone elastomer. *Biofouling* 20, 323–329. <https://doi.org/10.1080/08927010400029031>
- Homburg, S.V., Venkanna, D., Kraushaar, K., Kruse, O., Kroke, E., Patel, A.V., 2019. Entrapment and growth of *Chlamydomonas reinhardtii* in biocompatible silica hydrogels. *Colloids Surf. B Biointerfaces* 173, 233–241. <https://doi.org/10.1016/j.colsurfb.2018.09.075>
- Hoseini, S.M., Khosravi-Darani, K., Mozafari, M.R., 2013. Nutritional and medical applications of *spirulina* microalgae. *Mini-Rev. Med. Chem.* 13, 1231–1237.

- <https://doi.org/10.2174/1389557511313080009>
- Howard, A., Pelc, S.R., 1953. Synthesis of deoxyribonucleic acid in normal and irradiated cells and its relation to chromosome breakage. *Hered. Suppl* 6, 261–273.
- Huang, J., Chu, R., Chang, T., Cheng, P., Jiang, J., Yao, T., Zhou, C., Liu, T., Ruan, R., 2021. Modeling and improving arrayed microalgal biofilm attached culture system. *Bioresour. Technol.* 331, 124931. <https://doi.org/10.1016/j.biortech.2021.124931>
- Huang, Y., Xiong, W., Liao, Q., Fu, Q., Xia, A., Zhu, X., Sun, Y., 2016. Comparison of *Chlorella vulgaris* biomass productivity cultivated in biofilm and suspension from the aspect of light transmission and microalgae affinity to carbon dioxide. *Bioresour. Technol.* 222, 367–373. <https://doi.org/10.1016/j.biortech.2016.09.099>
- Huang, Y., Zheng, Y., Li, J., Liao, Q., Fu, Q., Xia, A., Fu, J., Sun, Y., 2018. Enhancing microalgae biofilm formation and growth by fabricating microgrooves onto the substrate surface. *Bioresour. Technol.* 261, 36–43. <https://doi.org/10.1016/j.biortech.2018.03.139>
- Hudek, K., Davis, L.C., Ibbini, J., Erickson, L., 2014. Commercial products from algae, in: *Algal Biorefineries*. Springer, Dordrecht, pp. 275–295. https://doi.org/10.1007/978-94-007-7494-0_11
- Hultberg, M., Asp, H., Marttila, S., Bergstrand, K.-J., Gustafsson, S., 2014. Biofilm formation by *Chlorella vulgaris* is affected by light quality. *Curr. Microbiol.* 69, 699–702. <https://doi.org/10.1007/s00284-014-0645-1>
- Iman Shayan, S., Agblevor, F.A., Bertin, L., Sims, R.C., 2016. Hydraulic retention time effects on wastewater nutrient removal and bioproduct production via rotating algal biofilm reactor. *Bioresour. Technol.* 211, 527–533. <https://doi.org/10.1016/j.biortech.2016.03.104>
- Irving, T.E., Allen, D.G., 2011. Species and material considerations in the formation and development of microalgal biofilms. *Appl. Microbiol. Biotechnol.* 92, 283–294. <https://doi.org/10.1007/s00253-011-3341-0>
- Jacobi, A., Steinweg, C., Sastre, R.R., Posten, C., 2012. Advanced photobioreactor LED illumination system: Scale-down approach to study microalgal growth kinetics: LED illumination of photobioreactors. *Eng. Life Sci.* 12, 621–630. <https://doi.org/10.1002/elsc.201200004>
- Jebsen, C., Norici, A., Wagner, H., Palmucci, M., Giordano, M., Wilhelm, C., 2012. FTIR spectra of algal species can be used as physiological fingerprints to assess their actual growth potential. *Physiol. Plant.* 146, 427–438. <https://doi.org/10.1111/j.1399-3054.2012.01636.x>
- Jefferson, K.K., 2004. What drives bacteria to produce a biofilm? *FEMS Microbiol. Lett.* 236, 163–173. <https://doi.org/10.1111/j.1574-6968.2004.tb09643.x>
- Jerez, C.G., Malapascua, J.R., Sergejevová, M., Masojídek, J., Figueroa, F.L., 2016. *Chlorella fusca* (Chlorophyta) grown in thin-layer cascades: Estimation of biomass productivity by in-vivo chlorophyll *a* fluorescence monitoring. *Algal Res.* 17, 21–30. <https://doi.org/10.1016/j.algal.2016.04.010>
- Jha, D., Jain, V., Sharma, B., Kant, A., Garlapati, V.K., 2017. Microalgae-based pharmaceuticals and nutraceuticals: an emerging field with immense market potential. *ChemBioEng Rev.* 4, 257–272. <https://doi.org/10.1002/cben.201600023>
- Ji, B., Zhang, W., Zhang, N., Wang, J., Lutz, G.A., Liu, T., 2014. Biofilm cultivation of the oleaginous microalgae *Pseudochlorococcum sp.* *Bioprocess Biosyst. Eng.* 37, 1369–1375. <https://doi.org/10.1007/s00449-013-1109-x>
- Jiang, Y., Yoshida, T., Quigg, A., 2012. Photosynthetic performance, lipid production and biomass composition in response to nitrogen limitation in marine microalgae. *Plant Physiol. Biochem.* 54, 70–77. <https://doi.org/10.1016/j.plaphy.2012.02.012>

- Jo, S.W., Do, J.M., Na, H., Hong, J.W., Kim, I.S., Yoon, H.S., 2020. Assessment of biomass potentials of microalgal communities in open pond raceways using mass cultivation. *PeerJ* 8, e9418. <https://doi.org/10.7717/peerj.9418>
- Johnson, M.B., Wen, Z., 2010. Development of an attached microalgal growth system for biofuel production. *Appl. Microbiol. Biotechnol.* 85, 525–534. <https://doi.org/10.1007/s00253-009-2133-2>
- Jungandreas, A., Schellenberger Costa, B., Jakob, T., von Bergen, M., Baumann, S., Wilhelm, C., 2014. The Acclimation of *Phaeodactylum tricornutum* to blue and red light does not Influence the photosynthetic light reaction but strongly disturbs the carbon allocation pattern. *PLoS ONE* 9, e99727. <https://doi.org/10.1371/journal.pone.0099727>
- Kana, T.M., Geider, R.J., Critchley, C., 1997. Regulation of photosynthetic pigments in microalgae by multiple environmental factors: a dynamic balance hypothesis. *New Phytol.* 137, 629–638. <https://doi.org/10.1046/j.1469-8137.1997.00857.x>
- Karatan, E., Watnick, P., 2009. Signals, regulatory networks, and materials that build and break bacterial biofilms. *Microbiol. Mol. Biol. Rev.* 73, 310–347. <https://doi.org/10.1128/MMBR.00041-08>
- Karsten, U., Holzinger, A., 2014. Green algae in alpine biological soil crust communities: acclimation strategies against ultraviolet radiation and dehydration. *Biodivers. Conserv.* 23, 1845–1858. <https://doi.org/10.1007/s10531-014-0653-2>
- Karygianni, L., Ren, Z., Koo, H., Thurnheer, T., 2020. Biofilm matrixome: extracellular components in structured microbial communities. *Trends Microbiol.* 28, 668–681. <https://doi.org/10.1016/j.tim.2020.03.016>
- Katarzyna, L., Sai, G., Singh, O.A., 2015. Non-enclosure methods for non-suspended microalgae cultivation: literature review and research needs. *Renew. Sustain. Energy Rev.* 42, 1418–1427. <https://doi.org/10.1016/j.rser.2014.11.029>
- Katayama, T., Nagao, N., Goto, M., Yusoff, F.M., Banerjee, S., Sato, M., Takahashi, K., Furuya, K., 2018. Growth characteristics of shade-acclimated marine *Chlorella vulgaris* under high-cell-density conditions. *J. Environ. Biol.* 39, 747–753. [https://doi.org/10.22438/jeb/39/5\(SI\)/3](https://doi.org/10.22438/jeb/39/5(SI)/3)
- Kebede-westhead, E., Pizarro, C., Mulbry, W.W., Wilkie, A.C., 2003. Production and nutrient removal by periphyton grown under different loading rates of anaerobically digested flushed dairy manure. *J. Phycol.* 39, 1275–1282. <https://doi.org/10.1111/j.0022-3646.2003.02-159.x>
- Kent, M., Welladsen, H.M., Mangott, A., Li, Y., 2015. Nutritional evaluation of australian microalgae as potential human health supplements. *PLOS ONE* 10, e0118985. <https://doi.org/10.1371/journal.pone.0118985>
- Kesaano, M., Gardner, R.D., Moll, K., Lauchnor, E., Gerlach, R., Peyton, B.M., Sims, R.C., 2015. Dissolved inorganic carbon enhanced growth, nutrient uptake, and lipid accumulation in wastewater grown microalgal biofilms. *Bioresour. Technol.* 180, 7–15. <https://doi.org/10.1016/j.biortech.2014.12.082>
- Key, T., McCarthy, A., Campbell, D.A., Six, C., Roy, S., Finkel, Z.V., 2010. Cell size trade-offs govern light exploitation strategies in marine phytoplankton. *Environ. Microbiol.* 12, 95–104. <https://doi.org/10.1111/j.1462-2920.2009.02046.x>
- Kim, S., Moon, M., Kwak, M., Lee, B., Chang, Y.K., 2018. Statistical optimization of light intensity and CO₂ concentration for lipid production derived from attached cultivation of green microalga *Ettlia sp.* *Sci. Rep.* 8, 15390. <https://doi.org/10.1038/s41598-018-33793-1>
- Kızılkaya, İ.T., Unal, D., 2019. Effects of Nitrate toxicity on free proline accumulation, chlorophyll degradation and photosynthetic efficiency in the green alga *Chlorella*

- vulgaris*. Int. J. Second. Metab. 6, 10–19.
- Klinthong, W., Yang, Y.H., Huang, C.H., Tan, C.S., 2015. A review: microalgae and their applications in CO₂ capture and renewable energy. Aerosol Air Qual. Res. 15, 712–742. <https://doi.org/10.4209/aaqr.2014.11.0299>
- Kodjikian, L., Burillon, C., Lina, G., Roques, C., Pellon, G., Freney, J., Renaud, F.N.R., 2003. Biofilm formation on intraocular lenses by a clinical strain encoding the ica locus: a scanning electron microscopy study. Investig. Ophthalmology Vis. Sci. 44, 4382–4387. <https://doi.org/10.1167/iovs.03-0185>
- Konno, H., 1993. Settling and coagulation of slender type diatoms. Water Sci. Technol. 27, 231–240. <https://doi.org/10.2166/wst.1993.0281>
- Kreis, C.T., Le Blay, M., Linne, C., Makowski, M.M., Bäumchen, O., 2018. Adhesion of *Chlamydomonas* microalgae to surfaces is switchable by light. Nat. Phys. 14, 45–49. <https://doi.org/10.1038/nphys4258>
- Kumar, A., Ergas, S., Yuan, X., Sahu, A., Zhang, Q., Dewulf, J., Malcata, F.X., van Langenhove, H., 2010. Enhanced CO₂ fixation and biofuel production via microalgae: recent developments and future directions. Trends Biotechnol. 28, 371–380. <https://doi.org/10.1016/j.tibtech.2010.04.004>
- Kumar, K., Mishra, S.K., Shrivastav, A., Park, M.S., Yang, J.W., 2015. Recent trends in the mass cultivation of algae in raceway ponds. Renew. Sustain. Energy Rev. 51, 875–885. <https://doi.org/10.1016/j.rser.2015.06.033>
- Kumar, N., Hans, S., Verma, R., Srivastava, A., 2020. Acclimatization of microalgae *Arthrospira platensis* for treatment of heavy metals in Yamuna River. Water Sci. Eng. 13, 214–222. <https://doi.org/10.1016/j.wse.2020.09.005>
- Kusmayadi, A., Leong, Y.K., Yen, H.W., Huang, C.Y., Chang, J.S., 2021. Microalgae as sustainable food and feed sources for animals and humans – Biotechnological and environmental aspects. Chemosphere 271, 129800. <https://doi.org/10.1016/j.chemosphere.2021.129800>
- Lacour, T., Babin, M., Lavaud, J., 2020. Diversity in xanthophyll cycle pigments content and related nonphotochemical quenching (NPQ) among microalgae: implications for growth strategy and ecology. J. Phycol. 56, 245–263. <https://doi.org/10.1111/jpy.12944>
- Laskin, A.I., 1982. Advances in applied microbiology. Academic Press, New York; Toronto.
- Lavaud, J., Strzepek, R.F., Kroth, P.G., 2007. Photoprotection capacity differs among diatoms: Possible consequences on the spatial distribution of diatoms related to fluctuations in the underwater light climate. Limnol. Oceanogr. 52, 1188–1194. <https://doi.org/10.4319/lo.2007.52.3.1188>
- Le Norcy, T., Faÿ, F., Obando, C.Z., Hellio, C., Réhel, K., Linossier, I., 2019. A new method for evaluation of antifouling activity of molecules against microalgal biofilms using confocal laser scanning microscopy-microfluidic flow-cells. Int. Biodeterior. Biodegrad. 139, 54–61. <https://doi.org/10.1016/j.ibiod.2019.03.001>
- Leadbeater, B.S.C., Callow, M.E., 1992. Formation, Composition and Physiology of Algal Biofilms, in: Melo, L.F., Bott, T.R., Fletcher, M., Capdeville, B. (Eds.), Biofilms - Science and Technology. Springer, Dordrecht, pp. 149–162. https://doi.org/10.1007/978-94-011-1824-8_15
- Lee, A.K., Lewis, D.M., Ashman, P.J., 2009. Microbial flocculation, a potentially low-cost harvesting technique for marine microalgae for the production of biodiesel. J. Appl. Phycol. 21, 559–567. <https://doi.org/10.1007/s10811-008-9391-8>
- Lee, C.G., 1999. Calculation of light penetration depth in photobioreactors. Biotechnol. Bioprocess Eng. 4, 78–81. <https://doi.org/10.1007/BF02931920>
- Lee, E., Jalalizadeh, M., Zhang, Q., 2015. Growth kinetic models for microalgae cultivation:

- A review. *Algal Res.* 12, 497–512. <https://doi.org/10.1016/j.algal.2015.10.004>
- Lee, Seung Hoon, Oh, H.M., Jo, B.H., Lee, S.A., Shin, S.-Y., Kim, H.S., Lee, Sang Hyup, Ahn, C.Y., 2014. Higher biomass productivity of microalgae in an attached growth system, using wastewater. *J. Microbiol. Biotechnol.* 24, 1566–1573. <https://doi.org/10.4014/jmb.1406.06057>
- Lehmuskero, A., Skogen Chauton, M., Boström, T., 2018. Light and photosynthetic microalgae: A review of cellular- and molecular-scale optical processes. *Prog. Oceanogr.* 168, 43–56. <https://doi.org/10.1016/j.pocean.2018.09.002>
- Lemoine, Y., Schoefs, B., 2010. Secondary ketocarotenoid astaxanthin biosynthesis in algae: a multifunctional response to stress. *Photosynth. Res.* 106, 155–177. <https://doi.org/10.1007/s11120-010-9583-3>
- Lepetit, B., Sturm, S., Rogato, A., Gruber, A., Sachse, M., Falciatore, A., Kroth, P.G., Lavaud, J., 2013. High light acclimation in the secondary plastids containing diatom *Phaeodactylum tricorutum* is triggered by the redox state of the plastoquinone pool. *Plant Physiol.* 161, 853–865. <https://doi.org/10.1104/pp.112.207811>
- Li, B., Duan, Y., Luebke, D., Morreale, B., 2013. Advances in CO₂ capture technology: A patent review. *Appl. Energy* 102, 1439–1447. <https://doi.org/10.1016/j.apenergy.2012.09.009>
- Li, C., Cheng, S., 2019. Functional group surface modifications for enhancing the formation and performance of exoelectrogenic biofilms on the anode of a bioelectrochemical system. *Crit. Rev. Biotechnol.* 39, 1015–1030. <https://doi.org/10.1080/07388551.2019.1662367>
- Li, T., Piltz, B., Podola, B., Dron, A., de Beer, D., Melkonian, M., 2016. Microscale profiling of photosynthesis-related variables in a highly productive biofilm photobioreactor: profiling biofilm in photobioreactor. *Biotechnol. Bioeng.* 113, 1046–1055. <https://doi.org/10.1002/bit.25867>
- Li, T., Strous, M., Melkonian, M., 2017. Biofilm-based photobioreactors: their design and improving productivity through efficient supply of dissolved inorganic carbon. *FEMS Microbiol. Lett.* 364. <https://doi.org/10.1093/femsle/fnx218>
- Li, Y., Han, D., Sommerfeld, M., Hu, Q., 2011. Photosynthetic carbon partitioning and lipid production in the oleaginous microalga *Pseudochlorococcum* sp. (Chlorophyceae) under nitrogen-limited conditions. *Bioresour. Technol.* 102, 123–129. <https://doi.org/10.1016/j.biortech.2010.06.036>
- Liao, Q., Chang, H.X., Fu, Q., Huang, Y., Xia, A., Zhu, X., Zhong, N., 2018. Physiological-phased kinetic characteristics of microalgae *Chlorella vulgaris* growth and lipid synthesis considering synergistic effects of light, carbon and nutrients. *Bioresour. Technol.* 250, 583–590. <https://doi.org/10.1016/j.biortech.2017.11.086>
- Liu, J., Hu, Q., 2013. *Chlorella*: industrial production of cell mass and chemicals, in: Richmond, A., Hu, Q. (Eds.), *Handbook of Microalgal Culture: Applied Phycology and Biotechnolog.* John Wiley & Sons, Ltd, Oxford, UK, pp. 327–338. <https://doi.org/10.1002/9781118567166.ch16>
- Liu, T., Wang, J., Hu, Q., Cheng, P., Ji, B., Liu, J., Chen, Y., Zhang, W., Chen, X., Chen, L., Gao, L., Ji, C., Wang, H., 2013. Attached cultivation technology of microalgae for efficient biomass feedstock production. *Bioresour. Technol.* 127, 216–222. <https://doi.org/10.1016/j.biortech.2012.09.100>
- López, Y., Soto, S.M., 2019. The usefulness of microalgae compounds for preventing biofilm infections. *Antibiotics* 9, 9. <https://doi.org/10.3390/antibiotics9010009>
- López-Sandoval, D.C., Rodríguez-Ramos, T., Cermeño, P., Sobrino, C., Marañón, E., 2014. Photosynthesis and respiration in marine phytoplankton: Relationship with cell size, taxonomic affiliation, and growth phase. *J. Exp. Mar. Biol. Ecol.* 457, 151–159.

- <https://doi.org/10.1016/j.jembe.2014.04.013>
- Lou, S., Lin, X., Liu, C., Anwar, M., Li, H., Hu, Z., 2021. Molecular cloning and functional characterization of CvLCYE, a key enzyme in lutein synthesis pathway in *Chlorella vulgaris*. *Algal Res.* 55, 102246. <https://doi.org/10.1016/j.algal.2021.102246>
- Lubarsky, H.V., Hubas, C., Chocholek, M., Larson, F., Manz, W., Paterson, D.M., Gerbersdorf, S.U., 2010. The stabilisation potential of individual and mixed assemblages of natural bacteria and microalgae. *PLoS ONE* 5, e13794. <https://doi.org/10.1371/journal.pone.0013794>
- Lupi, F.M., Fernandes, H.M.L., Tomé, M.M., Sá-Correia, I., Novais, J.M., 1994. Influence of nitrogen source and photoperiod on exopolysaccharide synthesis by the microalga *Botryococcus braunii* UC 58. *Enzyme Microb. Technol.* 16, 546–550. [https://doi.org/10.1016/0141-0229\(94\)90116-3](https://doi.org/10.1016/0141-0229(94)90116-3)
- MacIntyre, H.L., Kana, T.M., Anning, T., Geider, R.J., 2002. Photoacclimation of photosynthesis irradiance response curves and photosynthetic pigments in microalgae and cyanobacteria. *J. Phycol.* 38, 17–38. <https://doi.org/10.1046/j.1529-8817.2002.00094.x>
- MacIntyre, Hugh L., Kana, T.M., Geider, R.J., 2000. The effect of water motion on short-term rates of photosynthesis by marine phytoplankton. *Trends Plant Sci.* 5, 12–17. [https://doi.org/10.1016/S1360-1385\(99\)01504-6](https://doi.org/10.1016/S1360-1385(99)01504-6)
- Malapascua, J., Jerez, C., Sergejevová, M., Figueroa, F., Masojídek, J., 2014. Photosynthesis monitoring to optimize growth of microalgal mass cultures: application of chlorophyll fluorescence techniques. *Aquat. Biol.* 22, 123–140. <https://doi.org/10.3354/ab00597>
- Mallick, N., 2002. Biotechnological potential of immobilized algae for wastewater N, P and metal removal: A review. *Biometals* 15, 377–390.
- Mantzorou, A., Ververidis, F., 2019. Microalgal biofilms: A further step over current microalgal cultivation techniques. *Sci. Total Environ.* 651, 3187–3201. <https://doi.org/10.1016/j.scitotenv.2018.09.355>
- Markou, G., Depraetere, O., Vandamme, D., Muylaert, K., 2015. Cultivation of *Chlorella vulgaris* and *Arthrospira platensis* with recovered phosphorus from wastewater by means of zeolite sorption. *Int. J. Mol. Sci.* 16, 4250–4264. <https://doi.org/10.3390/ijms16024250>
- Markou, G., Muylaert, K., 2016. Effect of light intensity on the degree of ammonia toxicity on PSII activity of *Arthrospira platensis* and *Chlorella vulgaris*. *Bioresour. Technol.* 216, 453–461. <https://doi.org/10.1016/j.biortech.2016.05.094>
- Martínez, C., Bernard, O., Mairet, F., 2018. Maximizing microalgae productivity in a light-limited chemostat. *IFAC-Pap.* 51, 735–740. <https://doi.org/10.1016/j.ifacol.2018.04.001>
- Martins, J., Peixe, L., Vasconcelos, V.M., 2011. Unraveling cyanobacteria ecology in wastewater treatment plants (WWTP). *Microb. Ecol.* 62, 241–256. <https://doi.org/10.1007/s00248-011-9806-y>
- Masojídek, J., Ranglová, K., Lakatos, G.E., Silva Benavides, A.M., Torzillo, G., 2021. Variables governing photosynthesis and growth in microalgae mass cultures. *Processes* 9, 820. <https://doi.org/10.3390/pr9050820>
- Matthiessen, B., Mielke, E., Sommer, U., 2010. Dispersal decreases diversity in heterogeneous metacommunities by enhancing regional competition. *Ecology* 91, 2022–2033. <https://doi.org/10.1890/09-1395.1>
- McDaniel, K., Valcius, F., Andrews, J., Das, S., 2015. Electrostatic potential distribution of a soft spherical particle with a charged core and pH-dependent charge density. *Colloids Surf. B Biointerfaces* 127, 143–147.

- <https://doi.org/10.1016/j.colsurfb.2015.01.025>
- McDougald, D., Rice, S.A., Barraud, N., Steinberg, P.D., Kjelleberg, S., 2012. Should we stay or should we go: mechanisms and ecological consequences for biofilm dispersal. *Nat. Rev. Microbiol.* 10, 39–50. <https://doi.org/10.1038/nrmicro2695>
- McMinn, A., Hegseth, E.N., 2004. Quantum yield and photosynthetic parameters of marine microalgae from the southern Arctic Ocean, Svalbard. *J. Mar. Biol. Assoc. U. K.* 84, 865–871. <https://doi.org/10.1017/S0025315404010112h>
- Melis, A., Neidhardt, J., Benemann, J.R., 1998. *Dunaliella salina* (Chlorophyta) with small chlorophyll antenna sizes exhibit higher photosynthetic productivities and photon use efficiencies than normally pigmented cells. *J. Appl. Phycol.* 10, 515–525.
- Melo, M., Fernandes, S., Caetano, N., Borges, M.T., 2018. *Chlorella vulgaris* (SAG 211-12) biofilm formation capacity and proposal of a rotating flat plate photobioreactor for more sustainable biomass production. *J. Appl. Phycol.* 30, 887–899. <https://doi.org/10.1007/s10811-017-1290-4>
- Meng, Y., Li, A., Li, H., Shen, Z., Ma, T., Liu, J., Zhou, Z., Feng, Q., Sun, Y., 2021. Effect of membrane blocking on attached cultivation of microalgae. *J. Clean. Prod.* 284, 124695. <https://doi.org/10.1016/j.jclepro.2020.124695>
- Meng, Y., Yao, C., Xue, S., Yang, H., 2014. Application of fourier transform infrared (FT-IR) spectroscopy in determination of microalgal compositions. *Bioresour. Technol.* 151, 347–354. <https://doi.org/10.1016/j.biortech.2013.10.064>
- Miranda, A.F., Ramkumar, N., Andriotis, C., Höltkemeier, T., Yasmin, A., Rochfort, S., Wlodkowic, D., Morrison, P., Roddick, F., Spangenberg, G., Lal, B., Subudhi, S., Mouradov, A., 2017. Applications of microalgal biofilms for wastewater treatment and bioenergy production. *Biotechnol. Biofuels* 10, 1–23. <https://doi.org/10.1186/s13068-017-0798-9>
- Mitchell, P., 1966. Chemiosmotic coupling in oxidative and photosynthetic phosphorylation. *Biol. Rev.* 41, 445–501. <https://doi.org/10.1111/j.1469-185X.1966.tb01501.x>
- Mitchison, 1971. *The biology of the cell cycle*. Cambridge University Press, Cambridge.
- Mohd-Sahib, A.A., Lim, J.W., Lam, M.K., Uemura, Y., Ho, C.D., Oh, W.D., Tan, W.N., 2018. Mechanistic kinetic models describing impact of early attachment between *Chlorella vulgaris* and polyurethane foam material in fluidized bed bioreactor on lipid for biodiesel production. *Algal Res.* 33, 209–217. <https://doi.org/10.1016/j.algal.2018.05.017>
- Mohd-Sahib, A.A., Lim, J.W., Lam, M.K., Uemura, Y., Isa, M.H., Ho, C.D., Kutty, S.R.M., Wong, C.Y., Rosli, S.-S., 2017. Lipid for biodiesel production from attached growth *Chlorella vulgaris* biomass cultivating in fluidized bed bioreactor packed with polyurethane foam material. *Bioresour. Technol.* 239, 127–136. <https://doi.org/10.1016/j.biortech.2017.04.118>
- Molazadeh, M., Ahmadzadeh, H., Pourianfar, H.R., Lyon, S., Rampelotto, P.H., 2019. The use of microalgae for coupling wastewater treatment with CO₂ biofixation. *Front. Bioeng. Biotechnol.* 7, 42. <https://doi.org/10.3389/fbioe.2019.00042>
- Molino, A., Iovine, A., Casella, P., Mehariya, S., Chianese, S., Cerbone, A., Rimauro, J., Musmarra, D., 2018. Microalgae characterization for consolidated and new application in human food, animal feed and nutraceuticals. *Int. J. Environ. Res. Public Health* 15, 2436. <https://doi.org/10.3390/ijerph15112436>
- Morales, M., Aflalo, C., Bernard, O., 2021. Microalgal lipids: A review of lipids potential and quantification for 95 phytoplankton species. *Biomass Bioenergy* 150, 106108. <https://doi.org/10.1016/j.biombioe.2021.106108>
- Morales, M., Bonnefond, H., Bernard, O., 2020. Rotating algal biofilm versus planktonic cultivation: LCA perspective. *J. Clean. Prod.* 257, 120547.

- <https://doi.org/10.1016/j.jclepro.2020.120547>
- Moreno Osorio, J.H., De Natale, A., Del Mondo, A., Frunzo, L., Lens, P.N.L., Esposito, G., Pollio, A., 2020. Early colonization stages of fabric carriers by two *Chlorella* strains. *J. Appl. Phycol.* 32, 3631–3644. <https://doi.org/10.1007/s10811-020-02244-8>
- Moreno Osorio, J.H., Pinto, G., Pollio, A., Frunzo, L., Lens, P.N.L., Esposito, G., 2019. Start-up of a nutrient removal system using *Scenedesmus vacuolatus* and *Chlorella vulgaris* biofilms. *Bioresour. Bioprocess.* 6, 1–16. <https://doi.org/10.1186/s40643-019-0259-3>
- Morimura, Y., Yanagi, S., Tamiya, H., 1961. Synchronous mass culture of *Chlorella*. *Plant Cell Physiol.* 5, 85–93.
- Mouget, J., Perkins, R., Consalvey, M., Lefebvre, S., 2008. Migration or photoacclimation to prevent high irradiance and UV-B damage in marine microphytobenthic communities. *Aquat. Microb. Ecol.* 52, 223–232. <https://doi.org/10.3354/ame01218>
- Mulbry, W., Kangas, P., Kondrad, S., 2010. Toward scrubbing the bay: Nutrient removal using small algal turf scrubbers on Chesapeake Bay tributaries. *Ecol. Eng.* 36, 536–541. <https://doi.org/10.1016/j.ecoleng.2009.11.026>
- Murphy, T.E., Berberoglu, H., 2014. Flux balancing of light and nutrients in a biofilm photobioreactor for maximizing photosynthetic productivity. *Biotechnol. Prog.* 30, 348–359. <https://doi.org/10.1002/btpr.1881>
- Muylaert, K., Sanchez-Pérez, J.M., Teissier, S., Sauvage, S., Dauta, A., Vervier, P., 2009. Eutrophication and its effect on dissolved Si concentrations in the Garonne River (France). *J. Limnol.* 68, 368–374. <https://doi.org/10.4081/jlimnol.2009.368>
- Nagar, E., Schwarz, R., 2015. To be or not to be planktonic? Self-inhibition of biofilm development. *Environ. Microbiol.* 17, 1477–1486. <https://doi.org/10.1111/1462-2920.12583>
- Naumann, T., Çebi, Z., Podola, B., Melkonian, M., 2013. Growing microalgae as aquaculture feeds on twin-layers: a novel solid-state photobioreactor. *J. Appl. Phycol.* 25, 1413–1420. <https://doi.org/10.1007/s10811-012-9962-6>
- Neidhardt, J., Benemann, J.R., Zhang, L., Melis, A., 1998. Photosystem-II repair and chloroplast recovery from irradiance stress: relationship between chronic photoinhibition, light-harvesting chlorophyll antenna size and photosynthetic productivity in *Dunaliella salina* (green algae). *Photosynth. Res.* 56, 175–184.
- Ng, F.L., Phang, S.M., Lan, B.L., Kalavally, V., Thong, C.H., Chong, K.T., Periasamy, V., Chandrasekaran, K., kumar, G.G., Yunus, K., Fisher, A.C., 2020. Optimised spectral effects of programmable LED arrays (PLA)s on bioelectricity generation from algal-biophotovoltaic devices. *Sci. Rep.* 10, 16105. <https://doi.org/10.1038/s41598-020-72823-9>
- Ng, I.S., Tan, S.I., Kao, P.H., Chang, Y.K., Chang, J.S., 2017. Recent developments on genetic engineering of microalgae for biofuels and bio-based chemicals. *Biotechnol. J.* 12, 1600644. <https://doi.org/10.1002/biot.201600644>
- Nguyen, T.D.P., Nguyen, D.H., Lim, J.W., Chang, C.K., Leong, H.Y., Tran, T.N.T., Vu, T.B.H., Nguyen, T.T.C., Show, P.L., 2019. Investigation of the relationship between bacteria growth and lipid production cultivating of microalgae *Chlorella vulgaris* in seafood wastewater. *Energies* 12, 2282. <https://doi.org/10.3390/en12122282>
- Nguyen-Ngoc, H., Tran-Minh, C., 2007. Fluorescent biosensor using whole cells in an inorganic translucent matrix. *Anal. Chim. Acta* 583, 161–165. <https://doi.org/10.1016/j.aca.2006.10.005>
- Nielsen, M.W., Sternberg, C., Molin, S., Regenber, B., 2011. *Pseudomonas aeruginosa* and *Saccharomyces cerevisiae* biofilm in flow cells. *J. Vis. Exp.* 47, e2383. <https://doi.org/10.3791/2383>

- Nomura, K., Terwilliger, P., 2019. Study on the unsaturated hydrogen bond behavior of bio-based polyamide. *Spec. Matrices* 7, 23–31. <https://doi.org/10.1515/spma-2019-0001>
- Nordin, N., Yusof, N., Md Nadzir, S., Mohd Yusoff, M.Z., Hassan, M.A., 2019. Effect of photo-autotrophic cultural conditions on the biomass productivity and composition of *Chlorella vulgaris*. *Biofuels* 1–11. <https://doi.org/10.1080/17597269.2019.1652787>
- Nowack, E., 2005. The 96-Well twin-layer system: a novel approach in the cultivation of microalgae. *Protist* 156, 239–251. <https://doi.org/10.1016/j.protis.2005.04.003>
- Nymark, M., Valle, K.C., Brembu, T., Hancke, K., Winge, P., Andresen, K., Johnsen, G., Bones, A.M., 2009. An integrated analysis of molecular acclimation to high light in the marine diatom *Phaeodactylum tricorutum*. *PLoS ONE* 4, e7743. <https://doi.org/10.1371/journal.pone.0007743>
- O'Toole, G., Kaplan, H.B., Kolter, R., 2000. Biofilm formation as microbial development. *Annu. Rev. Microbiol.* 54, 49–79. <https://doi.org/10.1146/annurev.micro.54.1.49>
- Ozkan, A., Berberoglu, H., 2013a. Cell to substratum and cell to cell interactions of microalgae. *Colloids Surf. B Biointerfaces* 112, 302–309. <https://doi.org/10.1016/j.colsurfb.2013.08.007>
- Ozkan, A., Berberoglu, H., 2013b. Adhesion of algal cells to surfaces. *Biofouling* 29, 469–482. <https://doi.org/10.1080/08927014.2013.782397>
- Ozkan, A., Berberoglu, H., 2011. Adhesion of *Chlorella vulgaris* on hydrophilic and hydrophobic surfaces. Presented at the ASME International Mechanical Engineering Congress and Exposition, pp. 169–178. <https://doi.org/10.1115/IMECE2011-64133>
- Ozkan, A., Kinney, K., Katz, L., Berberoglu, H., 2012. Reduction of water and energy requirement of algae cultivation using an algae biofilm photobioreactor. *Bioresour. Technol.* 114, 542–548. <https://doi.org/10.1016/j.biortech.2012.03.055>
- Pacheco, M.M., Hoeltz, M., Moraes, M.S.A., 2015. Microalgae: Cultivation techniques and wastewater phycoremediation. *J. Environ. Sci. Health* 50, 585–601.
- Palmer, J., Flint, S., Brooks, J., 2007. Bacterial cell attachment, the beginning of a biofilm. *J. Ind. Microbiol. Biotechnol.* 34, 577–588. <https://doi.org/10.1007/s10295-007-0234-4>
- Pandey, L.K., 2020. In situ assessment of metal toxicity in riverine periphytic algae as a tool for biomonitoring of fluvial ecosystems. *Environ. Technol. Innov.* 18, 100675. <https://doi.org/10.1016/j.eti.2020.100675>
- Parikh, S.J., Chorover, J., 2006. ATR-FTIR spectroscopy reveals bond formation during bacterial adhesion to iron oxide. *Langmuir* 22, 8492–8500. <https://doi.org/10.1021/la061359p>
- Park, B.J., Abu-Lail, N.I., 2011. The role of the pH conditions of growth on the bioadhesion of individual and lawns of pathogenic *Listeria monocytogenes* cells. *J. Colloid Interface Sci.* 358, 611–620. <https://doi.org/10.1016/j.jcis.2011.03.025>
- Perkins, R., Underwood, G., Brotas, V., Snow, G., Jesus, B., Ribeiro, L., 2001. Responses of microphytobenthos to light: primary production and carbohydrate allocation over an emersion period. *Mar. Ecol. Prog. Ser.* 223, 101–112. <https://doi.org/10.3354/meps223101>
- Perkins, R.G., Kromkamp, J.C., Serôdio, J., Lavaud, J., Jesus, B., Mouget, J.L., Lefebvre, S., Forster, R.M., 2010. The application of variable chlorophyll fluorescence to microphytobenthic biofilms, in: *Chlorophyll a Fluorescence in Aquatic Sciences: Methods and Applications*. Springer, Dordrecht, pp. 237–275. https://doi.org/10.1007/978-90-481-9268-7_12
- Picioreanu, C., 2000. Effect of diffusive and convective substrate transport on biofilm structure formation: A two-dimensional modeling study. *Biotechnol. Bioeng.* 69,

- 504–515. [https://doi.org/10.1002/1097-0290\(20000905\)69:5<504::AID-BIT5>3.0.CO;2-S](https://doi.org/10.1002/1097-0290(20000905)69:5<504::AID-BIT5>3.0.CO;2-S)
- Pienkos, P.T., Darzins, A., 2009. The promise and challenges of microalgal-derived biofuels. *Biofuels Bioprod. Biorefining* 3, 431–440. <https://doi.org/10.1002/bbb.159>
- Podola, B., Li, T., Melkonian, M., 2017. Porous substrate bioreactors: a paradigm shift in microalgal biotechnology? *Trends Biotechnol.* 35, 121–132. <https://doi.org/10.1016/j.tibtech.2016.06.004>
- Post, A.F., Dubinsky, Z., Wyman, K., Falkowski, P.G., 1984. Kinetics of light-intensity adaptation in a marine planktonic diatom. *Mar. Biol.* 83, 231–238. <https://doi.org/10.1007/BF00397454>
- Pruvost, J., Le Borgne, F., Artu, A., Legrand, J., 2017. Development of a thin-film solar photobioreactor with high biomass volumetric productivity (AlgoFilm©) based on process intensification principles. *Algal Res.* 21, 120–137. <https://doi.org/10.1016/j.algal.2016.10.012>
- Qayyum, S., Sharma, D., Bisht, D., Khan, A.U., 2016. Protein translation machinery holds a key for transition of planktonic cells to biofilm state in *Enterococcus faecalis*: A proteomic approach. *Biochem. Biophys. Res. Commun.* 474, 652–659. <https://doi.org/10.1016/j.bbrc.2016.04.145>
- R Core Team, 2014. R: A language and environment for statistical computing.
- Rai, L.C., Gaur, J.P. (Eds.), 2001. *Algal adaptation to environmental stresses*. Springer Berlin Heidelberg, Berlin, Heidelberg. <https://doi.org/10.1007/978-3-642-59491-5>
- Rajendran, A., Hu, B., 2016. Mycoalgae biofilm: development of a novel platform technology using algae and fungal cultures. *Biotechnol. Biofuels* 9, 1–13. <https://doi.org/10.1186/s13068-016-0533-y>
- Ralph, P.J., Gademann, R., 2005. Rapid light curves: A powerful tool to assess photosynthetic activity. *Aquat. Bot.* 82, 222–237. <https://doi.org/10.1016/j.aquabot.2005.02.006>
- Ramus, J., 1981. The capture and transduction of light energy. In: *The Biology of Seaweeds Botanical Monographs*. Oxford.
- Raven, J.A., Geider, R.J., 2003. Adaptation, acclimation and regulation in algal photosynthesis, in: *Photosynthesis in Algae*. Springer, Dordrecht, pp. 385–412. https://doi.org/10.1007/978-94-007-1038-2_17
- Rayen, F., Behnam, T., Dominique, P., 2019. Optimization of a raceway pond system for wastewater treatment: a review. *Crit. Rev. Biotechnol.* 39, 422–435. <https://doi.org/10.1080/07388551.2019.1571007>
- Razzak, S.A., Ali, S.A.M., Hossain, M.M., deLasa, H., 2017. Biological CO₂ fixation with production of microalgae in wastewater – A review. *Renew. Sustain. Energy Rev.* 76, 379–390. <https://doi.org/10.1016/j.rser.2017.02.038>
- Renner, L.D., Weibel, D.B., 2011. Physicochemical regulation of biofilm formation. *MRS Bull.* 36, 347–355. <https://doi.org/10.1557/mrs.2011.65>
- Rincon, S.M., Romero, H.M., Aframehr, W.M., Beyenal, H., 2017. Biomass production in *Chlorella vulgaris* biofilm cultivated under mixotrophic growth conditions. *Algal Res.* 26, 153–160. <https://doi.org/10.1016/j.algal.2017.07.014>
- Rincon, S.M., Urrego, N.F., Avila, K.J., Romero, H.M., Beyenal, H., 2019. Photosynthetic activity assessment in mixotrophically cultured *Chlorella vulgaris* biofilms at various developmental stages. *Algal Res.* 38, 101408. <https://doi.org/10.1016/j.algal.2019.101408>
- Ritz, M., Thomas, J.C., Spilar, A., Etienne, A.L., 2000. Kinetics of photoacclimation in response to a shift to high light of the red alga *Rhodella violacea* adapted to low irradiance. *Plant Physiol.* 123, 1415–1426. <https://doi.org/10.1104/pp.123.4.1415>

- Roberts, S., Sabater, S., Beardall, J., 2004. Benthic microalgal colonization in streams of different riparian cover and light availability. *J. Phycol.* 40, 1004–1012. <https://doi.org/10.1111/j.1529-8817.2004.03333.x>
- Rochaix, J.D., 2011. Regulation of photosynthetic electron transport. *Biochim. Biophys. Acta BBA - Bioenerg.* 1807, 878–886. <https://doi.org/10.1016/j.bbabi.2011.05.009>
- Rodríguez-Palacio, M.C., Crisóstomo-Vázquez, L., Álvarez-Hernández, S., Lozano-Ramírez, C., 2012. Strains of toxic and harmful microalgae, from waste water, marine, brackish and fresh water. *Food Addit. Contam. Part A* 29, 304–313. <https://doi.org/10.1080/19440049.2011.596164>
- Romeu, M.J.L., Domínguez-Pérez, D., Almeida, D., Morais, J., Campos, A., Vasconcelos, V., Mergulhão, F.J.M., 2020. Characterization of planktonic and biofilm cells from two filamentous cyanobacteria using a shotgun proteomic approach. *Biofouling* 36, 631–645. <https://doi.org/10.1080/08927014.2020.1795141>
- Rooke, J.C., Léonard, A., Sarmiento, H., Meunier, C.F., Descy, J.P., Su, B.L., 2011. Novel photosynthetic CO₂ bioconvertor based on green algae entrapped in low-sodium silica gels. *J Mater Chem* 21, 951–959. <https://doi.org/10.1039/C0JM02712J>
- Roostaei, J., Zhang, Y., Gopalakrishnan, K., Ochocki, A.J., 2018. Mixotrophic microalgae biofilm: a novel algae cultivation strategy for improved productivity and cost-efficiency of biofuel feedstock production. *Sci. Rep.* 8, 1–10. <https://doi.org/10.1038/s41598-018-31016-1>
- Rosli, S.S., Amalina Kadir, W.N., Wong, C.Y., Han, F.Y., Lim, J.W., Lam, M.K., Yusup, S., Kiatkittipong, W., Kiatkittipong, K., Usman, A., 2020. Insight review of attached microalgae growth focusing on support material packed in photobioreactor for sustainable biodiesel production and wastewater bioremediation. *Renew. Sustain. Energy Rev.* 134, 110306. <https://doi.org/10.1016/j.rser.2020.110306>
- Rosli, S.S., Lim, J.W., Jumbri, K., Lam, M.K., Uemura, Y., Ho, C.D., Tan, W.N., Cheng, C.K., Kadir, W.N.A., 2019. Modeling to enhance attached microalgal biomass growth onto fluidized beds packed in nutrients-rich wastewater whilst simultaneously biofixing CO₂ into lipid for biodiesel production. *Energy Convers. Manag.* 185, 1–10. <https://doi.org/10.1016/j.enconman.2019.01.077>
- Ru, I.T.K., Sung, Y.Y., Jusoh, M., Wahid, M.E.A., Nagappan, T., 2020. *Chlorella vulgaris* : a perspective on its potential for combining high biomass with high value bioproducts. *Appl. Phycol.* 1, 2–11. <https://doi.org/10.1080/26388081.2020.1715256>
- Safi, C., Zebib, B., Merah, O., Pontalier, P.Y., Vaca-Garcia, C., 2014. Morphology, composition, production, processing and applications of *Chlorella vulgaris*: A review. *Renew. Sustain. Energy Rev.* 35, 265–278. <https://doi.org/10.1016/j.rser.2014.04.007>
- Sakarika, M., Kornaros, M., 2019. *Chlorella vulgaris* as a green biofuel factory: Comparison between biodiesel, biogas and combustible biomass production. *Bioresour. Technol.* 273, 237–243. <https://doi.org/10.1016/j.biortech.2018.11.017>
- Salvi, K.P., da Silva Oliveira, W., Horta, P.A., Rörig, L.R., de Oliveira Bastos, E., 2021. A new model of Algal Turf Scrubber for bioremediation and biomass production using seaweed aquaculture principles. *J. Appl. Phycol.* <https://doi.org/10.1007/s10811-021-02430-2>
- Sathananthan, S., Genin, S.N., Aitchison, J.S., Allen, D.G., 2013. Micro-structured surfaces for algal biofilm growth. Presented at the SPIE Micro/Nano Materials, Devices, and Applications, Melbourne, Victoria, Australia, p. 892350. <https://doi.org/10.1117/12.2033794>
- Scardino, A.J., Harvey, E., De Nys, R., 2006. Testing attachment point theory: diatom

- attachment on microtextured polyimide biomimics. *Biofouling* 22, 55–60. <https://doi.org/10.1080/08927010500506094>
- Schatz, D., Nagar, E., Sendersky, E., Parnasa, R., Zilberman, S., Carmeli, S., Mastai, Y., Shimoni, E., Klein, E., Yeger, O., Reich, Z., Schwarz, R., 2013. Self-suppression of biofilm formation in the cyanobacterium *Synechococcus elongatus*: Self-suppression of biofilm formation in a cyanobacterium. *Environ. Microbiol.* 15, 1786–1794. <https://doi.org/10.1111/1462-2920.12070>
- Schenk, P.M., Thomas-Hall, S.R., Stephens, E., Marx, U.C., Mussgnug, J.H., Posten, C., Kruse, O., Hankamer, B., 2008. Second generation biofuels: high-efficiency microalgae for biodiesel production. *BioEnergy Res.* 1, 20–43. <https://doi.org/10.1007/s12155-008-9008-8>
- Schilp, S., Kueller, A., Rosenhahn, A., Grunze, M., Pettitt, M.E., Callow, M.E., Callow, J.A., 2007. Settlement and adhesion of algal cells to hexa(ethylene glycol)-containing self-assembled monolayers with systematically changed wetting properties. *Biointerphases* 2, 143–150. <https://doi.org/10.1116/1.2806729>
- Schnurr, P.J., Allen, D.G., 2015. Factors affecting algae biofilm growth and lipid production: A review. *Renew. Sustain. Energy Rev.* 52, 418–429. <https://doi.org/10.1016/j.rser.2015.07.090>
- Schnurr, P.J., Espie, G.S., Allen, D.G., 2014. The effect of light direction and suspended cell concentrations on algal biofilm growth rates. *Appl. Microbiol. Biotechnol.* 98, 8553–8562. <https://doi.org/10.1007/s00253-014-5964-4>
- Schnurr, P.J., Espie, G.S., Allen, D.G., 2013. Algae biofilm growth and the potential to stimulate lipid accumulation through nutrient starvation. *Bioresour. Technol.* 136, 337–344. <https://doi.org/10.1016/j.biortech.2013.03.036>
- Schultze, L.K.P., Simon, M.V., Li, T., Langenbach, D., Podola, B., Melkonian, M., 2015. High light and carbon dioxide optimize surface productivity in a Twin-Layer biofilm photobioreactor. *Algal Res.* 8, 37–44. <https://doi.org/10.1016/j.algal.2015.01.007>
- Sciandra, A., Lazzara, L., Claustre, H., Babin, M., 2000. Responses of growth rate, pigment composition and optical properties of *Cryptomonas* sp. to light and nitrogen stresses. *Mar. Ecol. Prog. Ser.* 201, 107–120. <https://doi.org/10.3354/meps201107>
- Seabra, L.M.J., Pedrosa, L.F.C., 2010. Astaxanthin: structural and functional aspects. *Rev. Nutr.* 23, 1041–1050. <https://doi.org/10.1590/S1415-52732010000600010>
- Sebestyén, P., Blanken, W., Bacsá, I., Tóth, G., Martin, A., Bhajji, T., Dergez, Á., Kesserű, P., Koós, Á., Kiss, I., 2016. Upscale of a laboratory rotating disk biofilm reactor and evaluation of its performance over a half-year operation period in outdoor conditions. *Algal Res.* 18, 266–272. <https://doi.org/10.1016/j.algal.2016.06.024>
- Sekar, R., Venugopalan, V.P., Satpathy, K.K., Nair, K.V.K., Rao, V.N.R., 2004. Laboratory studies on adhesion of microalgae to hard substrates. Springer, Dordrecht.
- Senger, H., Bishop, N.I., 1966. The light-dependent formation of nucleic acids in cultures of synchronized *Chlorella*. *Plant Cell Physiol.* 7, 441–455. <https://doi.org/10.1093/oxfordjournals.pcp.a079195>
- Serôdio, J., Ezequiel, J., Barnett, A., Mouget, J., Méléder, V., Laviale, M., Lavaud, J., 2012. Efficiency of photoprotection in microphytobenthos: role of vertical migration and the xanthophyll cycle against photoinhibition. *Aquat. Microb. Ecol.* 67, 161–175. <https://doi.org/10.3354/ame01591>
- Setlik, I., 1984. The multiple fission cell reproductive patterns in algae. *Microb. Cell Cycle* 253–279.
- Šetlík, I., Ballin, E., Doucha, J., Kubín, Š., endlová, J., Zachleder, V., 1972. The coupling of synthetic and reproduction processes in *Scenedesmus quadricauda*. *Arch Hydrobiol Algal Stud* 7, 172–213.

- Severes, A., Hegde, S., D'Souza, L., Hegde, S., 2017. Use of light emitting diodes (LEDs) for enhanced lipid production in micro-algae based biofuels. *J. Photochem. Photobiol. B* 170, 235–240. <https://doi.org/10.1016/j.jphotobiol.2017.04.023>
- Shahzadi, L., Zeeshan, R., Yar, M., Qasim, S.B., Chaudhry, A.A., Khan, A.F., Muhammad, N., 2018. Biocompatibility through cell attachment and cell proliferation studies of nylon 6/chitosan/ha electrospun mats. *J. Polym. Environ.* 26, 2030–2038. <https://doi.org/10.1007/s10924-017-1100-8>
- Shalaby, S.M., Yasin, N.M.N., 2013. Quality characteristics of croissant stuffed with imitation processed cheese containing microalgae *Chlorella vulgaris* biomass. *World J. Dairy Food Sci.* 8, 58–66. <https://doi.org/10.5829/idosi.wjdfs.2013.8.1.1118>
- Sharif, D.I., Gallon, J., Smith, C.J., Dudley, E., 2008. Quorum sensing in Cyanobacteria: N-octanoyl-homoserine lactone release and response, by the epilithic colonial cyanobacterium *Gloeothoece PCC6909*. *ISME J.* 2, 1171–1182. <https://doi.org/10.1038/ismej.2008.68>
- Sharma, P.K., Saharia, M., Srivastava, R., Kumar, S., Sahoo, L., 2018. Tailoring microalgae for efficient biofuel production. *Front. Mar. Sci.* 5, 382. <https://doi.org/10.3389/fmars.2018.00382>
- Shen, Y., Xu, X., Zhao, Y., Lin, X., 2014. Influence of algae species, substrata and culture conditions on attached microalgal culture. *Bioprocess Biosyst. Eng.* 37, 441–450. <https://doi.org/10.1007/s00449-013-1011-6>
- Shen, Y., Yang, T., Zhu, W., Zhao, Y., 2017. Wastewater treatment and biofuel production through attached culture of *Chlorella vulgaris* in a porous substratum biofilm reactor. *J. Appl. Phycol.* 29, 833–841. <https://doi.org/10.1007/s10811-016-0981-6>
- Shen, Y., Zhang, H., Xu, X., Lin, X., 2015. Biofilm formation and lipid accumulation of attached culture of *Botryococcus braunii*. *Bioprocess Biosyst. Eng.* 38, 481–488. <https://doi.org/10.1007/s00449-014-1287-1>
- Sheng, G.P., Yu, H.Q., Li, X.Y., 2010. Extracellular polymeric substances (EPS) of microbial aggregates in biological wastewater treatment systems: A review. *Biotechnol. Adv.* 28, 882–894. <https://doi.org/10.1016/j.biotechadv.2010.08.001>
- Shetty, P., Gitau, M.M., Maróti, G., 2019. Salinity stress responses and adaptation mechanisms in eukaryotic green microalgae. *Cells* 8, 1657. <https://doi.org/10.3390/cells8121657>
- Shi, J., Podola, B., Melkonian, M., 2014. Application of a prototype-scale Twin-Layer photobioreactor for effective N and P removal from different process stages of municipal wastewater by immobilized microalgae. *Bioresour. Technol.* 154, 260–266. <https://doi.org/10.1016/j.biortech.2013.11.100>
- Shi, J., Podola, B., Melkonian, M., 2007. Removal of nitrogen and phosphorus from wastewater using microalgae immobilized on twin layers: an experimental study. *J. Appl. Phycol.* 19, 417–423. <https://doi.org/10.1007/s10811-006-9148-1>
- Shiratake, T., Sato, A., Minoda, A., Tsuzuki, M., Sato, N., 2013. Air-drying of cells, the novel conditions for stimulated synthesis of triacylglycerol in a green alga, *Chlorella kessleri*. *PLoS ONE* 8, e79630. <https://doi.org/10.1371/journal.pone.0079630>
- Sirakov, I., Velichkova, K., Stoyanova, S., Staykov, Y., 2015. The importance of microalgae for aquaculture industry. *Review. Int. J. Fish. Aquat. Stud.* 2, 81–84.
- Sirmerova, M., Prochazkova, G., Siristova, L., Kolska, Z., Branyik, T., 2013. Adhesion of *Chlorella vulgaris* to solid surfaces, as mediated by physicochemical interactions. *J. Appl. Phycol.* 25, 1687–1695. <https://doi.org/10.1007/s10811-013-0015-6>
- Skjånes, K., Aesoy, R., Herfindal, L., Skomedal, H., 2021. Bioactive peptides from microalgae: Focus on anti-cancer and immunomodulating activity. *Physiol. Plant. ppl.* 13472. <https://doi.org/10.1111/ppl.13472>

- Slaveykova, V.I., Wilkinson, K.J., 2002. Physicochemical aspects of lead bioaccumulation by *Chlorella vulgaris*. *Environ. Sci. Technol.* 36, 969–975. <https://doi.org/10.1021/es0101577>
- Song, F., Koo, H., Ren, D., 2015. Effects of material properties on bacterial adhesion and biofilm formation. *J. Dent. Res.* 94, 1027–1034. <https://doi.org/10.1177/0022034515587690>
- Sukačová, K., Trtílek, M., Rataj, T., 2015. Phosphorus removal using a microalgal biofilm in a new biofilm photobioreactor for tertiary wastewater treatment. *Water Res.* 71, 55–63. <https://doi.org/10.1016/j.watres.2014.12.049>
- Sukačová, K., Vicha, D., Dušek, J., 2020. Perspectives on microalgal biofilm systems with respect to integration into wastewater treatment technologies and phosphorus scarcity. *Water* 12, 2245. <https://doi.org/10.3390/w12082245>
- Sukenik, A., Bennett, J., Falkowski, P., 1987. Light-saturated photosynthesis - Limitation by electron transport or carbon fixation? *Biochim. Biophys. Acta BBA - Bioenerg.* 891, 205–215. [https://doi.org/10.1016/0005-2728\(87\)90216-7](https://doi.org/10.1016/0005-2728(87)90216-7)
- Sukenik, A., Bennett, J., Mortain-Bertrand, A., Falkowski, P.G., 1990. Adaptation of the photosynthetic apparatus to irradiance in *Dunaliella tertiolecta*: a kinetic study. *Plant Physiol.* 92, 891–898.
- Sutherland, I., 2001. The biofilm matrix - an immobilized but dynamic microbial environment. *Trends Microbiol.* 9, 222–227. [https://doi.org/10.1016/S0966-842X\(01\)02012-1](https://doi.org/10.1016/S0966-842X(01)02012-1)
- Tamiya, H., Iwamura, T., Shibata, K., Hase, E., Nihei, T., 1953. Correlation between photosynthesis and light-independent metabolism in the growth of *Chlorella*. *Biochim. Biophys. Acta* 12, 23–40. [https://doi.org/10.1016/0006-3002\(53\)90120-6](https://doi.org/10.1016/0006-3002(53)90120-6)
- Tan, J.S., Lee, S.Y., Chew, K.W., Lam, M.K., Lim, J.W., Ho, S.H., Show, P.L., 2020. A review on microalgae cultivation and harvesting, and their biomass extraction processing using ionic liquids. *Bioengineered* 11, 116–129. <https://doi.org/10.1080/21655979.2020.1711626>
- Tang, D., Han, W., Li, P., Miao, X., Zhong, J., 2011. CO₂ biofixation and fatty acid composition of *Scenedesmus obliquus* and *Chlorella pyrenoidosa* in response to different CO₂ levels. *Bioresour. Technol.* 102, 3071–3076. <https://doi.org/10.1016/j.biortech.2010.10.047>
- Tang, J., Liu, B., Gao, L., Wang, W., Liu, T., Su, G., 2021. Impacts of surface wettability and roughness of styrene-acrylic resin films on adhesion behavior of microalgae *Chlorella* sp. *Colloids Surf. B Biointerfaces* 199, 111522. <https://doi.org/10.1016/j.colsurfb.2020.111522>
- Tesson, S.V.M., Skjøth, C.A., Šantl-Temkiv, T., Löndahl, J., 2016. Airborne microalgae: insights, opportunities, and challenges. *Appl. Environ. Microbiol.* 82, 1978–1991. <https://doi.org/10.1128/AEM.03333-15>
- Tikkanen, M., Grieco, M., Nurmi, M., Rantala, M., Suorsa, M., Aro, E.M., 2012. Regulation of the photosynthetic apparatus under fluctuating growth light. *Philos. Trans. R. Soc. B Biol. Sci.* 367, 3486–3493. <https://doi.org/10.1098/rstb.2012.0067>
- Timoner, X., Buchaca, T., Acuña, V., Sabater, S., 2014. Photosynthetic pigment changes and adaptations in biofilms in response to flow intermittency. *Aquat. Sci.* 76, 565–578. <https://doi.org/10.1007/s00027-014-0355-6>
- Tolker-Nielsen, T., 2015. Biofilm Development. *Microbiol. Spectr.* 3, 1–12. <https://doi.org/10.1128/microbiolspec.MB-0001-2014>
- Toninelli, A.E., Wang, J., Liu, M., Wu, H., Liu, T., 2016. *Scenedesmus dimorphus* biofilm: Photoefficiency and biomass production under intermittent lighting. *Sci. Rep.* 6, 32305. <https://doi.org/10.1038/srep32305>

- Torzillo, G., Faraloni, C., Silva, A.M., Kopecký, J., Pilný, J., Masojídek, J., 2012. Photoacclimation of *Phaeodactylum tricornerutum* (Bacillariophyceae) cultures grown outdoors in photobioreactors and open ponds. *Eur. J. Phycol.* 47, 169–181. <https://doi.org/10.1080/09670262.2012.683202>
- Torzillo, G., Vonshak, A., 2013. Environmental stress physiology with reference to mass cultures, in: *Handbook of Microalgal Culture*. John Wiley & Sons, Ltd, Oxford, UK, pp. 90–113. <https://doi.org/10.1002/9781118567166.ch6>
- Tran, H.D., Do, T.T., Le, T.L., Nguyen, M.L.T., Pham, C.H., Melkonian, M., 2019. Cultivation of *Haematococcus pluvialis* for astaxanthin production on angled bench-scale and large-scale biofilm-based photobioreactors. *Vietnam J. Sci. Technol. Eng.* 61, 61–70. [https://doi.org/10.31276/VJSTE.61\(3\).61-70](https://doi.org/10.31276/VJSTE.61(3).61-70)
- Tsavatopoulou, V.D., Manariotis, I.D., 2020. The effect of surface properties on the formation of *Scenedesmus rubescens* biofilm. *Algal Res.* 52, 102095. <https://doi.org/10.1016/j.algal.2020.102095>
- Turpin, D.H., 1991. Effects of inorganic N availability on algal photosynthesis and carbon metabolism. *J. Phycol.* 27, 14–20.
- Uauy, R., Mena, P., Rojas, C., 2000. Essential fatty acids in early life: structural and functional role. *Proc. Nutr. Soc.* 59, 3–15. <https://doi.org/10.1017/S0029665100000021>
- Ugwu, C.U., Aoyagi, H., Uchiyama, H., 2008. Photobioreactors for mass cultivation of algae. *Bioresour. Technol.* 99, 4021–4028. <https://doi.org/10.1016/j.biortech.2007.01.046>
- Urabe, J., Kagami, M., 2001. Phytoplankton growth rate as a function of cell size: an experimental test in Lake Biwa. *Limnology* 2, 111–117. <https://doi.org/10.1007/s102010170006>
- van Leeuwe, M.A., Brotas, V., Consalvey, M., Gillespie, D., Jesus, B., Roggeveld, J., 2008. Photoacclimation in microphytobenthos and the role of xanthophyll pigments. *Eur. J. Phycol.* 43, 123–132.
- Venable, M.E., Podbielski, M.R., 2019. Impact of substrate material on algal biofilm biomass growth. *Environ. Sci. Pollut. Res.* 26, 7256–7262. <https://doi.org/10.1007/s11356-019-04148-8>
- Vert, M., Doi, Y., Hellwich, K.-H., Hess, M., Hodge, P., Kubisa, P., Rinaudo, M., Schué, F., 2012. Terminology for biorelated polymers and applications (IUPAC Recommendations 2012). *Pure Appl. Chem.* 84, 377–410. <https://doi.org/10.1351/PAC-REC-10-12-04>
- Vigeant, M.A.S., Ford, R.M., Wagner, M., Tamm, L.K., 2002. Reversible and irreversible adhesion of motile *Escherichia coli* cells analyzed by total internal reflection aqueous fluorescence microscopy. *Appl. Environ. Microbiol.* 68, 2794–2801. <https://doi.org/10.1128/AEM.68.6.2794-2801.2002>
- Vivier, B., Claquin, P., Lelong, C., Lesage, Q., Peccate, M., Hamel, B., Georges, M., Bourguiba, A., Sebaibi, N., Boutouil, M., Goux, D., Dauvin, J.C., Orvain, F., 2021. Influence of infrastructure material composition and microtopography on marine biofilm growth and photobiology. *Biofouling* 37, 740–756. <https://doi.org/10.1080/08927014.2021.1959918>
- Wagner, H., Jakob, T., Fanesi, A., Wilhelm, C., 2017. Towards an understanding of the molecular regulation of carbon allocation in diatoms: the interaction of energy and carbon allocation. *Philos. Trans. R. Soc. B Biol. Sci.* 372, 20160410. <https://doi.org/10.1098/rstb.2016.0410>
- Wagner, H., Jebsen, C., Wilhelm, C., 2019. Monitoring cellular C:N ratio in phytoplankton by means of FTIR -spectroscopy. *J. Phycol.* 55, 543–551. <https://doi.org/10.1111/jpy.12858>

- Wagner, M., Horn, H., 2017. Optical coherence tomography in biofilm research: A comprehensive review. *Biotechnol. Bioeng.* 114, 1386–1402. <https://doi.org/10.1002/bit.26283>
- Waite, R.D., Papakonstantinou, A., Littler, E., Curtis, M.A., 2005. Transcriptome analysis of *Pseudomonas aeruginosa* growth: comparison of gene expression in planktonic cultures and developing and mature biofilms. *J. Bacteriol.* 187, 6571–6576. <https://doi.org/10.1128/JB.187.18.6571-6576.2005>
- Walach, MarekR., Pirt, S.J., 1986. The growth and adhesion to glass of algal (*Chlorella*) cells: the effects of iron and other mineral nutrients. *Appl. Microbiol. Biotechnol.* 24, 468–470. <https://doi.org/10.1007/BF00250325>
- Wang, B., Lan, C.Q., Horsman, M., 2012. Closed photobioreactors for production of microalgal biomasses. *Biotechnol. Adv.* 30, 904–912. <https://doi.org/10.1016/j.biotechadv.2012.01.019>
- Wang, J., Liu, J., Liu, T., 2015. The difference in effective light penetration may explain the superiority in photosynthetic efficiency of attached cultivation over the conventional open pond for microalgae. *Biotechnol. Biofuels* 8, 1–12. <https://doi.org/10.1186/s13068-015-0240-0>
- Wang, J., Liu, W., Liu, T., 2017. Biofilm based attached cultivation technology for microalgal biorefineries - A review. *Bioresour. Technol.* 244, 1245–1253. <https://doi.org/10.1016/j.biortech.2017.05.136>
- Wang, Y., Jiang, Z., Lai, Z., Yuan, H., Zhang, Xinru, Jia, Y., Zhang, Xinxin, 2021. The self-adaptation capability of microalgal biofilm under different light intensities: Photosynthetic parameters and biofilm microstructures. *Algal Res.* 58, 102383. <https://doi.org/10.1016/j.algal.2021.102383>
- Webb, W.L., Newton, M., Starr, D., 1974. Carbon dioxide exchange of *Alnus rubra*. *Oecologia* 17, 281–291. <https://doi.org/10.1007/BF00345747>
- Wellburn, A.R., 1994. The spectral determination of chlorophylls *a* and *b*, as well as total carotenoids, using various solvents with spectrophotometers of different resolution. *J. Plant Physiol.* 144, 307–313. [https://doi.org/10.1016/S0176-1617\(11\)81192-2](https://doi.org/10.1016/S0176-1617(11)81192-2)
- Wollmann, F., Dietze, S., Ackermann, J., Bley, T., Walther, T., Steingroewer, J., Krujatz, F., 2019. Microalgae wastewater treatment: Biological and technological approaches. *Eng. Life Sci.* 19, 860–871. <https://doi.org/10.1002/elsc.201900071>
- Woods, D.C., Fletcher, R.L., 1991. Studies on the strength of adhesion of some common marine fouling diatoms. *Biofouling* 3, 287–303. <https://doi.org/10.1080/08927019109378183>
- Wykoff, D.D., Davies, J.P., Melis, A., Grossman, A.R., 1998. The regulation of photosynthetic electron transport during nutrient deprivation in *Chlamydomonas reinhardtii*. *Plant Physiol.* 117, 129–139. <https://doi.org/10.1104/pp.117.1.129>
- Xia, L., Li, H., Song, S., 2016. Cell surface characterization of some oleaginous green algae. *J. Appl. Phycol.* 28, 2323–2332. <https://doi.org/10.1007/s10811-015-0768-1>
- Xiang, Q., Wei, X., Yang, Z., Xie, T., Zhang, Y., Li, D., Pan, X., Liu, X., Zhang, X., Yao, C., 2021. Acclimation to a broad range of nitrate strength on a euryhaline marine microalga *Tetraselmis subcordiformis* for photosynthetic nitrate removal and high-quality biomass production. *Sci. Total Environ.* 781, 146687. <https://doi.org/10.1016/j.scitotenv.2021.146687>
- Xiao, R., Zheng, Y., 2016. Overview of microalgal extracellular polymeric substances (EPS) and their applications. *Biotechnol. Adv.* 34, 1225–1244. <https://doi.org/10.1016/j.biotechadv.2016.08.004>
- Xu, Y., Harvey, P.J., 2019. Carotenoid production by *Dunaliella salina* under red light. *Antioxidants* 8, 123. <https://doi.org/10.3390/antiox8050123>

- Yan, N., Fan, C., Chen, Y., Hu, Z., 2016. The potential for microalgae as bioreactors to produce pharmaceuticals. *Int. J. Mol. Sci.* 17, 962. <https://doi.org/10.3390/ijms17060962>
- Yang, X., Liu, L., Yin, Z., Wang, X., Wang, S., Ye, Z., 2020. Quantifying photosynthetic performance of phytoplankton based on photosynthesis–irradiance response models. *Environ. Sci. Eur.* 32, 1–13. <https://doi.org/10.1186/s12302-020-00306-9>
- Yarish, C., Redmond, S., Kim, J.K., 2012. *Gracilaria* culture handbook for new England.
- Yildiz, F.H., Visick, K.L., 2009. *Vibrio* biofilms: so much the same yet so different. *Trends Microbiol.* 17, 109–118. <https://doi.org/10.1016/j.tim.2008.12.004>
- Young, J.N., Schmidt, K., 2020. It's what's inside that matters: physiological adaptations of high-latitude marine microalgae to environmental change. *New Phytol.* 227, 1307–1318. <https://doi.org/10.1111/nph.16648>
- Yu, Z., Pei, H., Li, Y., Yang, Z., Xie, Z., Hou, Q., Nie, C., 2020. Inclined algal biofilm photobioreactor (IABPBR) for cost-effective cultivation of lipid-rich microalgae and treatment of seawater-diluted anaerobically digested effluent from kitchen waste with the aid of phytohormones. *Bioresour. Technol.* 315, 123761. <https://doi.org/10.1016/j.biortech.2020.123761>
- Yuan, H., Wang, Y., Lai, Z., Zhang, Xinru, Jiang, Z., Zhang, Xinxin, 2021. Analyzing microalgal biofilm structures formed under different light conditions by evaluating cell–cell interactions. *J. Colloid Interface Sci.* 583, 563–570. <https://doi.org/10.1016/j.jcis.2020.09.057>
- Yuan, H., Wang, Y., Xi, Y., Jiang, Z., Zhang, Xinru, Wang, X., Zhang, Xinxin, 2020a. Light-emitting diode power conversion capability and CO₂ fixation rate of microalgae biofilm cultured under different light spectra. *Energies* 13, 1536. <https://doi.org/10.3390/en13071536>
- Yuan, H., Zhang, Xinru, Jiang, Z., Wang, X., Chen, X., Cao, L., Zhang, Xinxin, 2019. Analyzing the effect of pH on microalgae adhesion by identifying the dominant interaction between cell and surface. *Colloids Surf. B Biointerfaces* 177, 479–486. <https://doi.org/10.1016/j.colsurfb.2019.02.023>
- Yuan, H., Zhang, Xinru, Jiang, Z., Wang, X., Wang, Y., Cao, L., Zhang, Xinxin, 2020b. Effect of light spectra on microalgal biofilm: Cell growth, photosynthetic property, and main organic composition. *Renew. Energy* 157, 83–89. <https://doi.org/10.1016/j.renene.2020.04.109>
- Yun, C.-J., Hwang, K.-O., Han, S.-S., Ri, H.-G., 2019. The effect of salinity stress on the biofuel production potential of freshwater microalgae *Chlorella vulgaris* YH703. *Biomass Bioenergy* 127, 105277. <https://doi.org/10.1016/j.biombioe.2019.105277>
- Zachleder, V., Bišová, K., Vítová, M., 2016. The Cell Cycle of Microalgae, in: *The Physiology of Microalgae*. Springer, Cham, pp. 3–46. https://doi.org/10.1007/978-3-319-24945-2_1
- Zachleder, V., Schlafli, O., Boschetti, A., 1997. Growth-controlled oscillation in activity of histone H1 kinase during the cell cycle of *Chlamydomonas reinhardtii* (Chlorophyta). *J. Phycol.* 33, 673–681. <https://doi.org/10.1111/j.0022-3646.1997.00673.x>
- Zachleder, V., Van Den Ende, H., 1992. Cell cycle events in the green alga *Chlamydomonas eugametos* and their control by environmental factors. *J. Cell Sci.* 102, 469–474.
- Zhang, L., Chen, L., Wang, J., Chen, Y., Gao, X., Zhang, Z., Liu, T., 2015. Attached cultivation for improving the biomass productivity of *Spirulina platensis*. *Bioresour. Technol.* 181, 136–142. <https://doi.org/10.1016/j.biortech.2015.01.025>
- Zhang, Q., Liu, C., Li, Y., Yu, Z., Chen, Z., Ye, T., Wang, X., Hu, Z., Liu, S., Xiao, B., Jin, S., 2017. Cultivation of algal biofilm using different lignocellulosic materials as carriers. *Biotechnol. Biofuels* 10, 1–16. <https://doi.org/10.1186/s13068-017-0799-8>

- Zhang, Q., Yu, Z., Jin, S., Liu, C., Li, Y., Guo, D., Hu, M., Ruan, R., Liu, Y., 2020. Role of surface roughness in the algal short-term cell adhesion and long-term biofilm cultivation under dynamic flow condition. *Algal Res.* 46, 101787. <https://doi.org/10.1016/j.algal.2019.101787>
- Zhang, Q., Yu, Z., Zhu, L., Ye, T., Zuo, J., Li, X., Xiao, B., Jin, S., 2018. Vertical-algal-biofilm enhanced raceway pond for cost-effective wastewater treatment and value-added products production. *Water Res.* 139, 144–157. <https://doi.org/10.1016/j.watres.2018.03.076>
- Zhang, W., Wang, Junfeng, Wang, Jialin, Liu, T., 2014. Attached cultivation of *Haematococcus pluvialis* for astaxanthin production. *Bioresour. Technol.* 158, 329–335. <https://doi.org/10.1016/j.biortech.2014.02.044>
- Zhang, X., Ma, Y., Ye, G., 2018. Morphological observation and comparative transcriptomic analysis of *Clostridium perfringens* biofilm and planktonic cells. *Curr. Microbiol.* 75, 1182–1189. <https://doi.org/10.1007/s00284-018-1507-z>
- Zhang, Xinru, Yuan, H., Guan, L., Wang, X., Wang, Y., Jiang, Z., Cao, L., Zhang, Xinxin, 2019. Influence of photoperiods on microalgae biofilm: photosynthetic performance, biomass yield, and cellular composition. *Energies* 12, 3724. <https://doi.org/10.3390/en12193724>
- Zhang, X., Yuan, H., Wang, Y., Guan, L., Zeng, Z., Jiang, Z., Zhang, Xinxin, 2020. Cell surface energy affects the structure of microalgal biofilm. *Langmuir* 36, 3057–3063. <https://doi.org/10.1021/acs.langmuir.0c00274>
- Zhao, R., Song, Y., Dai, Q., Kang, Y., Pan, J., Zhu, L., Zhang, L., Wang, Y., Shen, X., 2017. A starvation-induced regulator, RovM, acts as a switch for planktonic/biofilm state transition in *Yersinia pseudotuberculosis*. *Sci. Rep.* 7, 1–13. <https://doi.org/10.1038/s41598-017-00534-9>
- Zheng, Y., Huang, Y., Xia, A., Qian, F., Wei, C., 2019. A rapid inoculation method for microalgae biofilm cultivation based on microalgae-microalgae co-flocculation and zeta-potential adjustment. *Bioresour. Technol.* 278, 272–278. <https://doi.org/10.1016/j.biortech.2019.01.083>
- Zhuang, L.L., 2018. The characteristics and influencing factors of the attached microalgae cultivation: A review. *Renew. Sustain. Energy Rev.* 94, 1110–1119. <https://doi.org/10.1016/j.rser.2018.06.006>
- Zhuang, L.L., Azimi, Y., Yu, D., Wang, W.L., Wu, Y.H., Dao, G.H., Hu, H.Y., 2016. Enhanced attached growth of microalgae *Scenedusmus*. Lx1 through ambient bacterial pre-coating of cotton fiber carriers. *Bioresour. Technol.* 218, 643–649. <https://doi.org/10.1016/j.biortech.2016.07.013>
- Zhuang, L.L., Wang, J.H., Hu, H.Y., 2018. Differences between attached and suspended microalgal cells in ssPBR from the perspective of physiological properties. *J. Photochem. Photobiol. B* 181, 164–169. <https://doi.org/10.1016/j.jphotobiol.2018.03.014>
- Zippel, B., Rijstenbil, J., Neu, T.R., 2007. A flow-lane incubator for studying freshwater and marine phototrophic biofilms. *J. Microbiol. Methods* 70, 336–345. <https://doi.org/10.1016/j.mimet.2007.05.013>
- Zou, Y., Woo, J., Ahn, J., 2012. Cellular and molecular responses of *Salmonella typhimurium* to antimicrobial-induced stresses during the planktonic-to-biofilm transition: Antimicrobial-induced responses of foodborne pathogens. *Lett. Appl. Microbiol.* 55, 274–282. <https://doi.org/10.1111/j.1472-765X.2012.03288.x>